



<https://theses.gla.ac.uk/>

Theses Digitisation:

<https://www.gla.ac.uk/myglasgow/research/enlighten/theses/digitisation/>

This is a digitised version of the original print thesis.

Copyright and moral rights for this work are retained by the author

A copy can be downloaded for personal non-commercial research or study, without prior permission or charge

This work cannot be reproduced or quoted extensively from without first obtaining permission in writing from the author

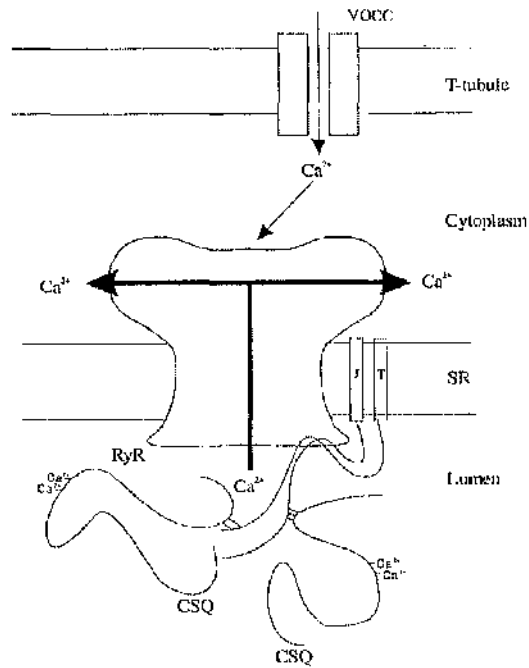
The content must not be changed in any way or sold commercially in any format or medium without the formal permission of the author

When referring to this work, full bibliographic details including the author, title, awarding institution and date of the thesis must be given

Enlighten: Theses

<https://theses.gla.ac.uk/>
research-enlighten@glasgow.ac.uk

Characteristics of Oxalate Supported Calcium Uptake and Release from the SR of Permeabilised Rabbit Ventricular Myocytes



A Thesis Presented for the Degree of

Doctor of Philosophy

To

University of Glasgow
Faculty of Medicine

by

Lorraine Bruce BSc (Hons)

Institute of Biomedical and Life Sciences
Department of Physiology
September 2003

ProQuest Number: 10390999

All rights reserved

INFORMATION TO ALL USERS

The quality of this reproduction is dependent upon the quality of the copy submitted.

In the unlikely event that the author did not send a complete manuscript and there are missing pages, these will be noted. Also, if material had to be removed, a note will indicate the deletion.



ProQuest 10390999

Published by ProQuest LLC (2017). Copyright of the Dissertation is held by the Author.

All rights reserved.

This work is protected against unauthorized copying under Title 17, United States Code
Microform Edition © ProQuest LLC.

ProQuest LLC.
789 East Eisenhower Parkway
P.O. Box 1346
Ann Arbor, MI 48106 – 1346

**GLASGOW
UNIVERSITY
LIBRARY:**

“Nothing ever materialises, out of thin air.
No matter how long, you sit and you stare.”

L. MacLeod

DECLARATION

The experimental work contained within this thesis was undertaken by me and has not been presented as part of any other degree. Some of the results have been published during the period of this study, details of which are listed on page xvii.

ACKNOWLEDGEMENTS

First of all, I would like to thank Aileen Rankin and Anne Ward. Technicians are the foundations of research; overlooked masterpieces and I will treasure the time we spent dissociating cells. The memories of the dark room, my home from home for 3 years; the lack of daylight and the digestive enzyme/EGTA/calcium debate will remain with me forever.

To my supervisor Professor Godfrey Smith, I am extremely grateful for all your help, input and patience. The never-ending story is finally ending and you will not be tortured with this thesis anymore, unless you decide to pick up on a few earth shattering discoveries unmasked by the hard work that went into every angle of this thesis.

To Susan Curry for her help with my protein assays, and to Professor Billy Martin for allowing me to use the lab's plate reader. I analysed so many protein samples I amazed myself at the accuracy of my readings, practice really does make perfect.

I have made a few absolutely fantastic friends over the years, the majority of whom never cease to amaze me with their love and support, especially throughout the excruciating writing years. You have made the long haul more bearable so thank you; Shona and Keith Robertson, Anna-Marie Loudon, Donna McGow, Audrey Brown, Louise Gourlay, Alison Prior, Alexis Duncan, Sarah Kettlewell, Debbie Reynolds, Four Star Mary (especially Tad Looney) and my 'sister' Tamara.

I would especially like to thank my mum and dad who are always there whenever I need them. To my brothers Brian and Stuart, whose constant ribbing lightened the whole situation, remembering my 'thesis-in-progress' phrases and learning to decipher the truth.

Finally to my husband Gary, you have been there for me through exams, University and a PhD. Giving me support at crucial, heart rendering moments but from now on, tear soaked shirts will be a thing of the past.

ABSTRACT

This thesis investigated the characteristics of sarcoplasmic reticulum (SR) calcium uptake and release from permeabilised cardiac myocytes: focusing on adenosine triphosphate calcium pump (Ca^{2+} -ATPase pump), the ryanodine receptor (RyR) and the non-specific SR leak. In order to do this, the following aims were investigated.

1. Cell viability: do balled-up cells contribute to total cell protein?
2. Is the rate of calcium uptake and leak affected by SR calcium load, RuR and by varying the oxalate concentration?
3. How sensitive is this preparation to stimulatory and inhibitory concentrations of ryanodine?
4. To what extent is the caffeine-mediated calcium leak blocked by ryanodine and ruthenium red (RuR)?
5. What are the characteristics of the RuR/ryanodine insensitive SR leak?

Method

Cardiac myocytes from New Zealand White, male rabbits were dissociated using the Langendorff retrograde perfusion system. The cells were permeabilized with $100\mu\text{g/ml}$ β -escin, and measurements of SR calcium uptake were made using the fluorescent indicator Fura-2 ($10\mu\text{M}$).

Calcium Uptake Versus protein Measurements

The protein measurements of permeabilised cardiac myocytes indicated that the haemocytometer was an accurate and consistent method of cell counting and that rod shaped myocytes did not influence the total protein concentration to a significant degree. Therefore, balled-up cells contribute to total cellular protein and may retain functional calcium pumps as a greater number of cells were observed to induce an increase in the calcium uptake rate constant, i.e. a greater number of cells give rise to more functional pumps available to sequester calcium.

Characteristics of Calcium Leak

A significant leak, referred to as the non specific leak, exists through the RyR at $1\mu\text{M}$ free calcium concentration and is independent of conventional RyR activity. In the absence of a calcium challenge, an SR calcium leak was not observed suggesting that the SR calcium content is negligible at the start of the experiment but with a single calcium challenge, a sufficient SR load was generated to sustain a leak. It was noted that 3 calcium challenges produced reproducible calcium transients, induced a large SR leak gradient in the presence of $5\mu\text{M}$ thapsigargin, as well as generating a large steady state calcium level in the presence of $10\mu\text{M}$ ionomycin. This suggests that the sequential additions of calcium to the cuvette system caused a progressive increase in the luminal free calcium concentration and SR calcium load. In this study, 10 or 20mM oxalate effectively clamped intracellular calcium concentration in order to facilitate calcium uptake into the SR. This was noted by a faster rate of decay, a lower SR leak gradient and a reduction in the amount of calcium available for release.

Ryanodine Mediated Calcium leak

In response to repeated calcium challenges in the absence of RuR or ryanodine, a gradual increase in the rate of uptake of the calcium transient was observed which could arise from the gradual phosphorylation of phospholamban.

Low concentrations of ryanodine ($0.3\mu\text{M}$ and $3\mu\text{M}$) were observed to induce a sustained increase in the SR calcium leak from the RyR. High concentrations of ryanodine ($30\mu\text{M}$, $300\mu\text{M}$ and 3mM) induced an increase in the calcium leak from the SR for a short period before a reduction in the SR leak was noted and, during the given time frame, oxalate supported cuvette based experiments favour a block with 3mM ryanodine. This is consistent with the literature that suggest high concentrations of ryanodine are required to decrease the opening probability of the RyR and that RyR possess two binding sites for ryanodine (a high affinity and a low affinity site). The leak produced in the presence of $0.3\mu\text{M}$ ryanodine was not inhibited with $5\mu\text{M}$ RuR and a slight slowing of the rate of uptake was observed with the addition of $5\mu\text{M}$ RuR in the presence of 3mM ryanodine. Therefore, $5\mu\text{M}$ RuR in the presence

of 3mM ryanodine or repeated calcium challenges may enhance the detrimental effects of SERCA2A noted by Kargacin & Kargacin (1998).

Caffeine Mediated Calcium Leak

In this study it was observed that caffeine mediated calcium release from the SR of permeabilised cardiac myocytes occurred in a dose dependent manner and that even in the presence of high concentrations of caffeine (up to 20mM), the SR accumulated a significant amount of calcium but only in the presence of ATP. At caffeine concentrations above 20mM, calcium reuptake was observed to be incomplete.

At low intracellular calcium concentration (in the absence of calcium challenges) 40mM was required to induce a significant release of calcium from the SR, a release that was greater than that produced with 20mM caffeine. However, in the presence of activating calcium concentrations, as low as 2mM caffeine was observed to induce an SR leak.

3mM ryanodine as well as 5 μ M RuR inhibited caffeine mediated calcium release and, varying the oxalate concentration did not significantly affect the ryanodine block of the caffeine mediated leak.

SR calcium Leak and Bastadin Mix

In isolated cardiac muscle preparations thapsigargin unmasks an SR calcium leak. A portion of this leak was blocked with the addition of 5 μ M RuR and 3mM ryanodine but only when the free calcium concentration exceeded 500nM. This indicates that the RyR contributes greatly to the SR leak under these conditions. Interestingly, the fraction of the SR leak that remained in the presence of blocking concentrations of RuR or ryanodine was inhibited by 20 μ M Bastadin mix (5-10 Bastadin Mix), therefore a component of the SR leak may be due to the RyR being in an open configuration that can be blocked by Bastadin.

In conclusion, balled-up cells were included in the cell count for the cuvette based uptake studies as they were deemed as viable cells and may retain functional pumps. The gradual increase in the rate of calcium uptake of the calcium transient observed in response to repeated calcium challenges could arise from the gradual phosphorylation of phospholamban. A substantial leak exists through the RyR under control conditions as 5 μ M was observed to

induce a significant increase in the rate of calcium uptake. The non specific leak unmasked by 5 μ M thapsigargin is RuR/ryanodine insensitive and is influenced by SR calcium load and oxalate concentration. The oxalate supported cuvette based experiments favour 3mM ryanodine and 5 μ M RuR in order to block the SR calcium leak observed in the presence of a calcium challenge as well as blocking caffeine mediated SR leak. The inhibition by 20 μ M Bastadin mix of the SR leak that remained in the presence of blocking concentrations of RuR or ryanodine indicated that a component of the SR leak may be due to the RyR being in an open configuration.

TABLE OF CONTENTS	PAGE
Declaration	iii
Acknowledgements	iv
Abstract.....	v
List of Contents.....	ix
List of Figures.....	xiii
List of Tables.....	xvi
List of Publications.....	xvii
Abbreviations.....	xviii
CHAPTER 1: INTRODUCTION.....	1
1.1 The Sarcoplasmic Reticulum Network.....	2
1.1.1. The Terminal Cisternae.....	3
1.1.2. The Calcium binding Protein: Calsequestrin.....	3
1.2. Excitation – Contraction Coupling.....	4
1.2.1. Voltage Dependent Calcium Channels.....	5
1.2.2. Calcium Induced Calcium release.....	5
1.3. The Calcium ATP - ase Pump: SERCA 2A.....	5
1.3.1. Structure of the Ca ²⁺ - ATPase Pump.....	5
1.3.2. Isoforms of the Ca ²⁺ - ATPase Pump.....	6
1.3.3. Regulation of SERCA 2 by PLB.....	7
1.3.4. Structure of PLB.....	9
1.4. Transport of Calcium Across the SR Membrane.....	11
1.4.1. Reaction Cycle.....	11
1.4.2. Calcium Binding and Dissociation Mechanisms.....	12
1.5. Calcium Efflux Mechanisms.....	13
1.5.1. The Ryanodine Receptor.....	14
1.5.1.1. Activation of SR Calcium Release via the DHPR.....	14
1.5.1.2 Stochastic and Coupled Gating.....	15
1.5.1.3 Ligand Modulation.....	16
1.5.1.4. Structure.....	18
1.5.1.5. Phosphorylation.....	19
1.5.1.6. Regulation by Intraluminal Calcium.....	19
1.5.1.7. Calcium Quarks, Sparks and Waves.....	20
1.5.1.8. FK506 Binding Protein.....	21
1.5.1.9. Bastadin.....	23

1.5.2. Ca ²⁺ -ATPase Pump Mediated Efflux Routes.....	25
1.5.2.1. Myocardial Ischemia: Increase in P _i	25
1.5.2.2. Calcium Phosphate Precipitation.....	26
1.5.2.3. Effects of P _i on the Cardiac RyR.....	26
1.5.2.4. Pump Reversal.....	26
1.5.2.5. Pump Channel Transition.....	28
CHAPTER 2: METHODS AND MATERIALS.....	36
2.1. Preparing Cells for Calcium Uptake Measurements	37
2.1.1. Rabbit Models: Coronary Artery Ligated, Sham and Control.....	37
2.1.2. Harvesting.....	37
2.1.3 Isolating Cardiac Myocytes.....	38
2.1.4. Chemical Skinning Procedure.....	39
2.1.4.1 β-escin Concentration Curve.....	39
2.1.4.2. Skinning of Dissociated Myocytes.....	40
2.2. Measuring Changes in Intracellular Calcium.....	40
2.2.1. Cuvette System.....	40
2.2.2. Fura-2.....	41
2.2.3. Oxalate	41
2.2.4. Calibration Curve for Fura-2 Measurement of Free Calcium.....	42
2.3. Measurement of Protein Concentration.....	43
2.3.1. Preparation for Protein Assay.....	43
2.3.2. Plating the Samples and Standards.....	43
2.4. Data Recording, Analysis and Curve Fitting.....	44
CHAPTER 3: Calcium Uptake Versus Protein Measurements.....	54
3.1. Relationship Between Total Protein and Yield of Rods.....	55
3.2. Relationship Between Total Calcium Uptake Rate, Cell Number and Percentage of Rods.....	55
3.3. Calcium Buffering.....	56
3.4. Discussion.....	57
CHAPTER 4: Characteristics of Calcium leak.....	65
4.1. Introduction.....	66
4.1.1. Ruthenium Red.....	66
4.1.2. Thapsigargin.....	67
4.1.3. Ionomycin.....	68
4.2. Methods.....	69

4.3. Results	69
4.3.1. Effects of RuR on SR Leak.....	69
4.3.2. SR Leak in the Presence and Absence of Calcium.....	70
4.3.3. Effects of Calcium Load on SR Leak.....	71
4.3.4. Effects of Changing Oxalate Concentrations on SR Leak.....	71
4.4. Discussion	72
CHAPTER 5: Ryanodine Mediated Calcium Leak	88
5.1. Introduction	89
5.2. Methods	89
5.3. Results	90
5.3.1. The Effects of RuR on SR Calcium leak.....	90
5.3.2. The Effects of Ryanodine on SR Calcium Leak.....	92
5.4. Discussion	95
5.4.1. The Effects of RuR on SR leak.....	95
5.4.1.1. Intrinsic Changes in SERCA2 Activity and the SR Calcium Leak	96
5.4.1.2. Changes in Solution Composition that Indirectly Affect SERCA2 and RyR Activity.....	98
5.4.2. The Effects of Ryanodine on SR Leak.....	99
CHAPTER 6. Caffeine Mediated Calcium leak	118
6.1. Introduction	119
6.2. Methods	121
6.3. Results	122
6.3.1. The Effects of Low Concentrations of Caffeine on SERCA 2A.....	122
6.3.2. Effect of Caffeine Concentration on SERCA 2A.....	123
6.3.3. RuR Inhibition of Caffeine Mediated Calcium Leak.....	124
6.3.4. Ryanodine Inhibition of Caffeine Mediated Calcium Leak.....	124
6.4. Discussion	125
CHAPTER 7. SR Calcium Leak and Bastadin	136
7.1. Introduction	137
7.2. Methods	137
7.3. Results	137
7.4. Discussion	140
7.5. Conclusions	141

CHAPTER 8. SUMMARY	148
8.1. Balling of Rod Shaped Cells	149
8.2. Effects of RuR on Permeabilised Myocytes	149
8.3. RuR/ryanodine insensitive leak	151
8.4. Intraluminal Calcium	152
References.....	154
Appendix.....	179

LIST OF FIGURES	PAGE
1.1. E-C Coupling mechanisms.....	29
1.2. The Reaction Cycle Diagram For SR Ca ²⁺ - ATPase.....	30
1.3. Representation of the Movement of Calcium Across the SR Membrane via Ca ²⁺ -ATPase.....	31
1.4. Simplified Diagram to Show the Calcium Efflux Routes in the SR	32
1.5. Interaction Between the RyR and the DHPR in Cardiac and Skeletal Muscle.....	33
1.6. The Proposed Theories to Induce Calcium Release in Striated Muscle.....	34
1.7. Coordinated SR Calcium Release via RyR clusters.....	35
2.1. The Effects of Increasing β -escin Concentrations in the Presence of 1nM and 10 μ M Calcium in Cardiac Myocytes.....	50
2.2. Diagram of the Cuvette System.....	51
2.3. Calibration Curve For the Protein Standards.....	52
2.4. Calibration Curves for Fura2, 3.3 μ M RuR and 13.3 μ M RuR.....	53
3.1. The Relationship Between Total Protein and Cell Number.....	58
3.2. The Relationship Between the Total Number of Cells per mg of Protein and the Percentage Yield of Rods.....	59
3.3. A Typical Experimental Trace Showing the Calcium Uptake Protocol.....	60
3.4. The Relationship Between the Rate Constant for Calcium Uptake and the Cell Number.....	61
3.5. The Relationship Between the Rate Constant for Calcium Uptake and Percentage Yield of Rods.....	62
3.6. The Relationship Between the Rate Constant for Calcium Uptake Against Total Protein.....	63
3.7. Calcium Buffering Diagram.....	64
4.1. Effect of RuR on SR Calcium Leak.....	76
4.2. SR Leak in the Presence and Absence of SR Calcium.....	77
4.3. Mean Data to Show the Effect of Calcium Load on SR Calcium Leak.....	78
4.4. Typical Experimental Traces to Display the Effects of Calcium Load on SR Leak Induced by Thapsigargin and Ionomycin.....	79
4.5. Effects of Calcium Load on SR Leak.....	80
4.6. Summary of the Mean Results of Calcium Load on Thapsigargin and Ionomycin Induced SR Leak.....	81
4.7. Typical Experimental Traces Produced by Various Oxalate Concentrations.....	83
4.8. Effects of Oxalate Concentration on SR Leak.....	85

4.9. Mean Data to Show the Effect of Various Oxalate Concentrations on SR Calcium Leak.....	87
5.1. Typical Experimental Trace For Early Addition of RuR.....	103
5.2. Typical Experimental Trace For Late Addition of RuR.....	104
5.3. Description of the Rate of Change (dCa^{2+}/dt) Analysis.....	105
5.4. Raw and Normalised Mean Rate of Decay for the Early Addition of RuR...	106
5.5. The Raw and Normalised Mean Rate of Decay for the Late Addition of RuR.....	107
5.6. The Raw and Normalised Mean Rate of Decay for the Early and Late Additions of RuR.....	108
5.7. Summary of the Raw and Normalized Mean Rate of Decay Produced in the Presence and in the Absence of RuR.....	109
5.8. The Effects of Ryanodine and RuR on the Rate of Decay of Successive Calcium Transients.....	110
5.9. The Effect of 0.3 μ M Ryanodine on the Rate of Decay for Successive Calcium Transients.....	112
5.10. Effects of 3 μ M Ryanodine on the Rate of Decay for Successive Calcium Transients.....	113
5.11. The Effects of 30 μ M Ryanodine on the Rate of Decay for Successive Calcium Transients.....	114
5.12. The Effects of 300 μ M Ryanodine on the Rate of Decay for Successive Calcium Transients.....	115
5.13. The Effects of 3mM Ryanodine on the Rate of Decay for Successive Calcium Transients.....	116
5.14. Summary of the Effects of Ryanodine on Calcium Transient Rate of Decay.....	117
6.1. The Effects of Ryanodine, RuR and Caffeine on the Rate of Decay of Successive Calcium Transients.....	128
6.2. The Mean Data for the Effects of Caffeine, Ryanodine and RuR on the Calcium Decay Time Constant (T_1).....	129
6.3. The Effect of Caffeine Concentration on T_1 and C_{ss} for Successive Calcium Transients.....	130
6.4. Effect of Caffeine Concentration on SR Calcium Leak.....	132
6.5. The Effect of RuR Inhibition of Caffeine Mediated Calcium Release.....	133
6.6. The Effect of Ryanodine Inhibition of Caffeine Mediated Calcium Release.....	134
6.7. The Mean Results of RuR and Ryanodine on 40mM Caffeine Mediated SR Calcium Release.....	135

7.1. Experimental Trace Showing the Effects of Thapsigargin, RuR and Ionomycin on SR Calcium Leak.....	142
7.2. The Effects of RuR on SR Leak Unmasked by Thapsigargin in the Presence of Calcium Concentrations Below and Above 500nM.....	143
7.3. Experimental Trace Showing the Effects of RuR on the Rate of Calcium Decay.....	144
7.4. The Effects of Bastadin Mix in the Presence and in the Absence of RuR and Low Calcium Concentrations.....	145
7.5. The Experimental Trace Displaying the Effects of Bastadin Mix in the Presence of Ryanodine on the SR Leak Unmasked by Thapsigargin.....	146
7.6. Experimental Trace Displaying the Effects of Bastadin mix on the Rate of Calcium Decay in the Presence of 3mM Ryanodine.....	147

LIST OF TABLES	PAGE
2.1. List of Drugs and Compounds Used In The Experimental Protocol.....	46
2.2. List of Chemicals Required to Make Ca ²⁺ Free Krebs.....	47
2.3. List of Chemicals Added to the Cuvette System.....	48
2.4. List of Chemicals Required to Make 10mM EGTA and 10mM CaEGTA Stock Solutions for Fura-2 Calibration Curve.....	48
2.5. Summarizes the Ratios and Volumes Required to Make Increasing Calcium Concentrations Using 10mM EGTA and 10mM CaEGTA Stock Solution.....	49
2.6. Values for the constants, R _{min} , R _{max} and K _D	49

LIST OF PUBLICATIONS

Copies of the published papers are inserted at the end of this thesis.

Smith G. L., Duncan A. M., Bruce L., Neary P. (1998) Inhibition of Ca²⁺ uptake by inorganic phosphate is accompanied by increased Ca²⁺ leak from the sarcoplasmic reticulum in permeabilised cardiac myocytes from rabbit. *Journal of Physiology*, 509P, P145-P146 (T).

Smith G.L., Bruce L. (1999) Bastadin mix reduces Ca²⁺ leak from the SR of permeabilised cardiac myocytes. *Biophysical Journal*, 76 (1 Pt2), A307 (P).

Smith, G.L., Bruce, L.(1999) Low ryanodine sensitivity of caffeine-induced Ca²⁺ release from rabbit SR. *Journal of Physiology*, 518P 45P (T).

Smith G. L., Duncan A. M., Bruce L., Neary P. (2000) P(i) inhibits the SR Ca(2+) pump and stimulates pump-mediated Ca(2+) leak in rabbit cardiac myocytes. *American Journal of Physiology - Heart & Circulatory Physiology*, 279(2), H577-H585.

Prestle, J., Janssen, P. M. L., Janssen, A. P., Zeitz, O., Lehnart, S. E., Bruce, L., Smith, G. L., Hasenfuss, G. (2001) Overexpression of FK506-binding protein FKBP12.6 in cardiomyocytes reduces ryanodine receptor-mediated Ca²⁺ leak from the sarcoplasmic reticulum and increases contractility. *Circulation Research*, 88(2), 188-194.

ABBREVIATIONS

ATP	Adenosine triphosphate
ATPase	Adenosine triphosphatase
ADP	Adenosine diphosphate
Ca ²⁺	Calcium
Ca ²⁺ -ATPase	SR calcium pump
Caff	Caffeine
CaM	Calmodulin
CaM-K	Calmodulin kinase
cAMP	Cyclic adenosine 3',5'-monophosphate
CCCP	Carbonyl cyanide m-chlorophenylhydrazone
cADP	Cyclic adenosine diphosphate
cGMP	Cyclic guanine 3',5' - monophosphate
CICR	Calcium induced calcium release
CRC	Calcium release channel
C _{ss}	Steady state calcium concentration
CSQ	Calsequestrin
CrP	Creatine phosphate
dCa ²⁺ /dt	Rate of decay
dH ₂ O	Distilled water
DHPR	Dihydropyridine receptor
DTT	Dithiothreitol
E-C coupling	Excitation-contraction coupling
EtOH	Ethanol
ER	Endoplasmic reticulum
EGTA	EthyleneGlycol-bis (β-aminoethyl Ether) N,N,N',N'- Tetraacetic Acid
FK506BP	FK506 binding protein
FKBP12	FK506 binding, 12kDa protein

FKBP12.6	FK 506 binding, 12.6kDa protein
H ⁺	Hydrogen ion
[³ H] ryanodine	Radiolabelled ryanodine
IP ₃ R	Inositol 1,4,5-trisphosphate receptor
K _d	Dissociation constant
KOH	Potassium hydroxide
K ₂ Oxalate	Potassium oxalate
MgATP	Magnesium adenosine trisphosphate
NaH ₂ PO ₄	Sodium hydrogen phosphate
PKA	Protein kinase A
PKC	Protein kinase C
PKG	Protein kinase G
PLB	Phospholamban
PP1	Protein phosphatase 1
PP2B	Protein Phosphatase 2B
Rotamase	cis-trans peptidyl-propyl isomerisation
Ry	Ryanodine
RyR	Ryanodine receptor
RyR1	Skeletal muscle ryanodine receptor
ryr1	Gene that encodes for skeletal muscle ryanodine receptor
RyR2	Cardiac muscle ryanodine receptor
ryr2	Gene that encodes for cardiac muscle ryanodine receptor
RyR3	Smooth muscle ryanodine receptor
ryr3	Gene that encodes for smooth muscle ryanodine receptor
RuR	Ruthenium red
Ox	Oxalate
P _i	Inorganic phosphate
P _o	RyR channel opening probability

SDS-page	Sodium dodecyl sulfate polyacrylamide gels
SERCA	Sarcoplasmic/endoplasmic reticulum calcium ATPase
SERCA 1	Fast twitch skeletal muscle sarcoplasmic-endoplasmic reticulum calcium pump
SERCA2a	Cardiac sarcoplasmic-endoplasmic reticulum calcium pump
SERCA2b	Smooth muscle and brain sarcoplasmic –endoplasmic reticulum calcium pump
SERCA 3	Large intestine, spleen, brain, stomach, Uterus, skeletal muscle and heart sarcoplasmic-endoplasmic reticulum calcium pump
SH	Thiol group
SL	Sarcolemma
SOFK	State of Filling Kinase
SR	Sarcoplasmic reticulum
TC	Terminal cisternae
T-Tubules	Transverse tubules
V _{max}	Maximum velocity
VOCC	L-type voltage operated calcium channels
w	With
w/o	Without

CHAPTER ONE

INTRODUCTION

1.1. THE SARCOPLASMIC RETICULUM NETWORK

The SR membrane, like all other biological membranes, consists of a phospholipid bilayer containing a number of intrinsic membrane proteins. The SR is a specialised form of the endoplasmic reticulum (ER) that pervades all cell types (Porter, 1956; Porter & Palade, 1957) and from its deposition in relation to the myofibrils (Bennett & Porter, 1953) indicates a functional role in muscle contractility (Franzini-Armstrong, 1999). The SR is a calcium reservoir which has two functions in imposing fast changes in intracellular calcium concentrations: accumulation of calcium drawn from the intracellular medium to induce muscle relaxation and calcium release to promote muscle contraction. Calcium release occurs through the RyR (Schneider & Chandler, 1973) whereas calcium uptake occurs through the Ca^{2+} -ATPase pump (MacLennan, 1970; Raeymaekers & Hasselbach, 1981; referred to from here on in as the SR calcium pump).

As reviewed in Bers 2003, the SR membrane consists of a closed set of anastomosing tubules coursing over the myofibrils and can be divided into two regions: the subsarcolemmal cisternae or terminal cisternae (TC). The TC are dilated extensions of the SR that expand into flattened sacs near the transverse tubular system (T-tubules) and contain the calcium channels through which calcium flows to initiate contraction. The second region is the much more extensive sarcotubular network that contains a densely packed array of calcium pumps. In the heart, TC are found beneath the plasma membrane and alongside the T-tubules, whereas the sarcotubular network surrounds the contractile proteins in the centre of the sarcomere. The T-tubules are invaginations of the sarcolemma (SL), extending into a series of fine transverse tubules that run into the cell's interior. The lumina of these tubules are continuous with the bulk interstitial fluid (Huxley, 1964) and in cardiac muscle play a key role in Excitation-Contraction coupling (E-C Coupling) by possessing essential features necessary to transmit the surface membrane depolarisation rapidly into the interior of the cell (Sun *et al.*, 1995). Membrane depolarization opens voltage operated calcium channels (VOCC) in the SL allowing the passage of calcium ions into the cell (Schneider & Chandler, 1973). However, the calcium ions entering the cell from the extracellular space are not sufficient to induce contraction of the myofibrils but serve as a trigger to release calcium from intracellular calcium

stores and together, these mechanisms activate the numerous myofibrils almost simultaneously (Fabiato, 1983).

1.1.1. The Terminal Cisternae

As reviewed in Bers 2003, the TC are dilated extensions of the SR that assume a flattened saccular shape near the T-tubules as well as the SL. The junction between these membrane systems is termed a dyad, as the T-tubule associate with a single TC in cardiac muscle. These dyads consist of two membrane proteins. The first protein is the L-type calcium channel of the plasma membrane and T-tubules, often referred to as the dihydropyridine receptor (DHPR). This protein acts as a voltage sensor as well as a calcium channel; the action of which is necessary for initiating calcium release from the SR. The other protein is the “foot” protein which projects from the TC into the space within the dyad, is termed the RyR and is the major route for calcium release from the SR to the cytoplasm.

1.1.2. Calcium Binding Protein: Calsequestrin

Calsequestrin (CSQ) is one of the major protein components of the SR and was first identified in 1971 by MacLennan and Wong (MacLennan & Wong *et al.*, 1971). It is located in the lumen of the junctional SR and acts by increasing the total capacity of the SR lumen for calcium while maintaining a relatively high free calcium concentration, thus allowing a large gradient in ionic calcium concentration between SR lumen and the myofibrils.

Extensive studies on its physiochemical properties have revealed it is a highly acidic (MacLennan *et al.*, 1971; Ikemoto *et al.*, 1974), water soluble protein with a molecular mass of 60kDa (Kawasaki & Kasai, 1994) and possesses calcium binding properties (MacLennan *et al.*, 1971; Meissener *et al.*, 1973; Ikemoto *et al.*, 1974) with a large capacity (~40mol/mol) and a relatively low affinity ($K_{\text{assoc}}=10^3\text{M}^{-1}$). CSQ is not accessible at the cytoplasmic membrane (Mickaluk *et al.*, 1980; Hidalgo & Ikemoto, 1977) but seems to be anchored to the internal surface of the membrane. Triadin and the structurally related protein junction also co-localise to the junctional region and therefore, it has been suggested that these integral proteins maybe required for physically coupling CSQ to the RyR (Zhang *et al.*, 1997).

CSQ has been linked to the regulation of the calcium release channel and Ikemoto *et al.*, (1989) demonstrated that calcium released from SR vesicles was abolished by selective depletion of CSQ; the amount and rate constant of calcium release was investigated as a function of the extent of calcium loading. It was found that the amount of calcium release increased monotonically in parallel to calcium loading, that the rate constant sharply increased at partial calcium loading, and that subsequent loading reduced the rate constant. Thus, the kinetic properties of induced calcium release show significant variation depending on the level of calcium bound to CSQ (Ikemoto *et al.*, 1989).

CSQ has been shown to be a target of Casein Kinase II and recent research links the phosphorylation state of the protein to SR calcium release. The results from this work showed that CSQ selectively controls the activity of the RyR at 1mM free luminal calcium concentration depending on its phosphorylation state. In its dephosphorylated state, CSQ enhanced the open probability (P_o) of the channel, thus implying that dephosphorylated CSQ can regulate calcium release from the SR. This correlates with the fact that CSQ has been found to exist in close proximity to the RyR and that the binding of calcium to CSQ leads to a conformational change in the RyR.

As CSQ exists mainly in the phosphorylated state in the SR (Szegedi *et al.*, 1999), this would imply that dephosphorylation of the protein by a phosphatase of CSQ is a means of physiological regulation of CSQ and may be part of an as yet unidentified calcium responsive signalling cascade within the SR.

1.2. EXCITATION-CONTRACTION COUPLING

Contraction of cardiac muscle is initiated through an increase of the intracellular calcium concentration. Two possible mechanisms have been suggested to contribute to this increase in intracellular calcium concentration; calcium entry via Voltage Dependent Calcium Channels and Calcium Induced Calcium Release (CICR) (Figure 1.1).

1.2.1. Voltage Dependent Calcium Channels

Calcium entry via voltage dependent calcium channels requires depolarization of the muscle membrane to open the VOCC (L-type channels). The spread of excitation is due to local electrical currents depolarizing the cellular membrane to threshold, thereby generating action potentials. These action potentials propagate along the T-tubule system in a unidirectional manner activating L-type calcium channels in the sarcolemma to release calcium into the cytoplasm of the cell. The rise in calcium through this method is insufficient to initiate contraction of the muscle but is amplified by the release of calcium from intracellular stores, such as the SR.

1.2.2. Calcium Induced Calcium Release

Cytoplasmic calcium binds to the RyR in the SR and exerts a positive feedback mechanism on the channel to release calcium from the internal store. The trigger for this release is calcium itself and is therefore termed CICR, the most widely accepted mechanism in cardiac muscle.

1.3. THE CALCIUM ATP-ase PUMP: SERCA 2

The SR calcium pump is responsible for rapidly lowering the cytoplasmic calcium concentration by pumping calcium into the lumen of the SR, and hence facilitates relaxation. Failure to refill the SR calcium pool would result in an inability of the cell to respond to repeated challenges (Grover *et al.*, 1992). The pump activity not only determines the rate and extent of relaxation, but also the rate and amplitude of contraction, since these are determined by the amount of calcium sequestered by the SR and the calcium gradient between the SR and the cytosol at the time calcium release occurs (Movsesian *et al.*, 1998).

1.3.1. Structure of the Ca²⁺-ATPase Pump

The Ca²⁺-ATPase pump (SR calcium pump) is a magnesium activated ATPase pump with a molecular mass of 110-115kDa and comprises of a unique polypeptide of 994 amino acids. The polypeptide contains 2-3 disulfide bonds, the reduction of which leads to virtually total inhibition of calcium uptake into the lumen of the SR (Mintz *et al.*, 1997) as well as possessing 24 Cysteine residues which react with thiol (SH) reagents. Of these 24 cysteine residues, nine are protected by

ATP and may be involved in the ATP binding site and ATP-induced conformational changes (Mintz *et al.*, 1997).

The proposed structure of the SR calcium pump contains a transmembrane domain and two large cytoplasmic domains (Läuger, 1991). The transmembrane region is formed by 10 α -helices joined by five luminal short loops and four cytoplasmic loops (Mintz *et al.*, 1997). The cytoplasmic domains of the molecule are connected to the transmembrane segments by a 'stalk' consisting of amphiphathic α -helices (Läuger, 1991). The total height of the SR calcium pump is 120Å and 70% of its mass can be located in the cytoplasmic domain, 25% in the membrane and 5% in the lumen (Tanford, 1984). The catalytic site, comprising the ATP binding site and the phosphorylation site, is located in the cytoplasmic part of the molecule whereas the transport sites (calcium binding sites) are thought to be buried in the membrane (Mintz *et al.*, 1997). The nucleotide binding domain and the calcium binding sites (separated by 40Å) interact at each step of the transport cycle to translocate two calcium ions into the lumen of the SR (Mintz *et al.*, 1997).

Although the calcium binding sites contain carboxyl groups, chemical studies have confirmed that they are hydrophobic in nature (Mintz *et al.*, 1997). Site-directed mutagenesis studies in the M4, M5 and M6 membrane regions have shown that Glu³⁰⁹, Glu⁷⁷¹, Asn⁷⁹⁶, Thr⁷⁹⁹ and Asp⁸⁰⁰ are essential for calcium transport, calcium-dependent phosphorylation by ATP as well as calcium occlusion. Alteration of these amino acid residues resulted in complete loss of calcium transport and of calcium dependent phosphorylation of ATP (Läuger, 1991; Mintz *et al.*, 1997). It was discovered that Glu³⁰⁹ and Asn⁷⁹⁶ are associated with one calcium binding site, whereas Glu⁷⁷¹ and Thr⁷⁹⁹ are associated with another, whilst Asp⁸⁰⁰ is associated with them both. This suggests that the two calcium binding sites are distinguishable and that M4, M5, M6 and M8 form the channel (Mintz *et al.*, 1997).

1.3.2. Isoforms of the SR Calcium Pump

Based on cloning and characterisation of cDNA and genomic DNA, there are several isoforms of the SR calcium pump, encoded for by three genes; SERCA1, SERCA2 and SERCA3 (Grover *et al.*, 1992). SERCA1 gene encodes the SR calcium pump isoforms expressed mainly in the fast twitch skeletal muscle; SERCA2 gene encodes the isoforms expressed in the slow twitch skeletal, cardiac

or smooth muscle, brain, stomach mucosa, liver, kidney and several other tissues (Grover *et al.*, 1992) and SERCA3 is expressed mainly in the large intestine and spleen at high levels; in brain, stomach, uterus, skeletal muscle and heart at intermediate levels and in several other tissues in lower levels (Grover *et al.*, 1992). All three isoforms contain the protein sequence for binding of ATP. SERCA1 and SERCA2 pump proteins can bind phospholamban, and SERCA3 protein has been reported to have potential sites for the cAMP-dependent protein kinase phosphorylation but it remains to be shown that it is phosphorylated and/or regulated in this manner (Grover *et al.*, 1992).

The cardiac muscle RNA is spliced alternatively to produce the isoforms SERCA2a or SERCA2b. These isoforms differ in their 3'-sequences such that the last four amino acids of SERCA2a are replaced by 49 different ones to give rise to SERCA2b and the 3'-noncoding regions are also different. From the cDNA data it is predicted that SERCA2a encodes a protein of 110kD, SERCA2b encodes a protein of 115kD and that the heart and the slow twitch skeletal muscle express mainly the isoform SERCA2a whereas smooth muscle, brain and most other tissues express SERCA2b.

1.3.3. Regulation of SERCA 2 by Phospholamban

Unlike calcium channels, the calcium pump can move calcium against its own electrochemical gradient by using the energy created from the hydrolysis of ATP; transporting two calcium ions into the lumen of the SR for every molecule of ATP consumed. The activity of the pump is regulated by the phosphoprotein phospholamban (PLB).

PLB was discovered in the early 1970's by Arnold Katz and is one of the major proteins phosphorylated upon adrenergic stimulation of cardiac myocytes. Katz demonstrated that phosphorylation of isolated cardiac SR membranes occurred mainly on a low molecular weight protein, named PLB from the Greek root words meaning "to receive phosphate". PLB is a small transmembrane phosphoprotein comprising 52 amino acid residues, with a molecular mass of 27kDa. In-vitro studies indicated that PLB is phosphorylated at three distinct sites by different protein kinases: serine 10 by protein kinase C; serine 16 by a cyclic adenosine 3',5'-monophosphate/cyclic guanine monophosphate -dependent protein kinase (cAMP/cGMP-dependent protein kinase) and threonine 17 by a calcium/calmodulin-dependent protein kinase

(Ca²⁺/CaM-dependent protein kinases) (Arkin *et al.*, 1997; Rapundalo, 1998; Koss *et al.*, 1996; Kadambi *et al.*, 1997, Simmerman & Jones, 1998). Phosphorylation by either one of these three protein kinases results in stimulation of the SR calcium pump activity, leading to an elevation in the rate of calcium uptake (Koss *et al.*, 1996). PLB is one of the few proteins to be phosphorylated by both cAMP-dependent and Ca²⁺/CaM-dependent protein kinase. These phosphorylations occur independently of one another to produce equivalent effects (Simmerman *et al.*, 1998; Rapundalo, 1998) and have been found to be adjacent on the same polypeptide (Simmerman *et al.*, 1998).

Phosphorylated PLB was thought to function as a stimulator for the SR calcium pump enzyme due to the observation that PLB phosphorylation induced an increase in calcium uptake into the lumen of the SR. In the late 1980s it was discovered that this was not the case, and that dephosphorylated PLB is actually an inhibitor of the cardiac calcium pump at low ionized calcium concentrations (Simmerman *et al.*, 1998). Upon phosphorylation, this inhibition is overcome (Jencks, 1989; Katz, 1996) leading to an increase in the enzymes apparent calcium affinity with little or no change in the maximum velocity (*V*_{max}) (Koss *et al.*, 1996, Simmerman *et al.*, 1998). The suppression of the pump by PLB was further investigated, looking into the effects of phosphorylation on the kinetic level (Tada, 1980). On phosphorylation of PLB by cAMP-dependent protein kinase, a marked increase occurred in the rate of calcium binding to the enzyme and the rate at which acylphosphoprotein intermediate was formed (Tada, 1980). Whether phosphorylation of PLB affected the calcium-binding affinity of the pump directly, or caused an increase in calcium affinity by accelerating a kinetic step was unknown. However, Inesi *et al.*, (1989) measured calcium binding to the pump in cardiac SR using monoclonal antibodies directed against PLB. Antibody binding removed the inhibitory effect of PLB and shifted the concentration dependence to the left with no effect on the calcium affinity of the ATPase. It was concluded that PLB affects the kinetics of enzyme activation by bound calcium rather than the actual calcium binding affinity (Cantilina, 1993). Inesi *et al.*, (1989) supported this theory further with the evidence that the calcium affinity of cardiac SERCA2a is identical to that of fast twitch skeletal SERCA1a (devoid of PLB). PLB does not alter this stoichiometry or the positive cooperativity of calcium binding to SERCA in both cardiac and skeletal SR vesicles (Cantilina, 1993). On the basis of these results it

was proposed that PLB acts by inhibiting the slow isomeric transition after binding of the first calcium to the pump, without changing the overall equilibrium constant for calcium binding and that phosphorylation greatly accelerates this slow transition.

In order for phosphorylation of PLB to play a physiological role in regulating cardiac SR function and thereby myocardial contraction and relaxation, mechanisms must exist to dephosphorylate the protein and return it to its role as a functional inhibitor of SERCA2. Such a mechanism is fulfilled by protein phosphatases which hydrolyse the phosphodiester bonds formed by protein kinases. These endogenous protein phosphatases have been shown to dephosphorylate the protein kinase A (PKA) sites on PLB resulting in a decrease in the degree of stimulation of calcium transport activity (Rapundalo, 1998). Three distinct types of protein phosphatases have now been demonstrated to dephosphorylate PLB. A 'PLB-specific' phosphatase, capable of dephosphorylating both PKA and Ca^{2+} /CaM-dependent protein kinase activated phosphorylation sites; protein phosphatase 1 (PP1) which is capable of dephosphorylating PLB when PLB has been phosphorylated by PKA but not Ca^{2+} /CaM-dependent protein kinase phosphorylation sites; and protein phosphatase 2B (PP2B) which is capable of dephosphorylating PKA-activated PLB under certain conditions (Rapundalo, 1998). With the discovery of these cardiac SR-associated endogenous protein phosphatases, PLB can function as a reversible inhibitor of SERCA2 (Rapundalo, 1998; Koss *et al.*, 1996).

1.3.4. Structure of PLB

Several models based on amino acid sequence of the tertiary structure of PLB have been proposed. The protein consists of two domains; a hydrophilic cytoplasmically orientated domain (amino acids 1-30) and a carboxy-terminal hydrophobic membrane spanning domain (amino acids 31-52) (Arkin *et al.*, 1997, Rapundalo, 1998; Koss *et al.*, 1996; Kadambi *et al.*, 1997; Simmerman, *et al.*, 1998). The cytoplasmic domain (domain 1) can be further divided into two sub-domains: domain 1a and domain 1b (Kadambi *et al.*, 1997). Domain 1a contains the three phosphorylation sites for the three protein kinases, has a higher preponderance of charged amino acids and has been suggested to exist in a helical conformation. Domain 1b (amino acids 21-30) is highly polar and is proposed to be unstructured (Kadambi *et al.*, 1997).

The hydrophobic domain (domain 2) anchors the protein into the SR membrane and holds the multiple subunits together (Koss *et al.*, 1996; Kadambi *et al.*, 1997; Simmerman *et al.*, 1998). It is proposed to have a helical structure but there is no evidence to suggest this domain interacts with the SERCA2 (Koss *et al.*, 1996). Despite this, it is thought to be just as important in mediating the regulatory effects as seen during co-expression studies with SR calcium pump, the results of which revealed the domain was capable of modifying the calcium affinity of SERCA2 (Kadambi *et al.*, 1997). Cysteine residues, C36, C41 and C46 (Arkin *et al.*, 1997) in the α -helical transmembrane domain provides for non-covalent interactions between monomeric forms and contribute to stabilisation of a pentameric structure of PLB (Arkin *et al.*, 1997). Domain 1 on the other hand mediates the regulatory effects of PLB on the SR calcium pump through protein-protein interaction. Specific residues among amino acids 2-18 in PLB interact with amino acids 336-412 (Koss *et al.*, 1996; Kadambi *et al.*, 1997) and 467-762 (Koss *et al.*, 1996) in SERCA2 for functional modification. Both the cytoplasmic and transmembrane regions of PLB are essential for normal calcium pump regulation (Simmerman *et al.*, 1998). The cytoplasmic domain of PLB by itself is not inhibitory but instead modulates the inhibitory interactions in the transmembrane domains through a long-range coupling process (Simmerman *et al.*, 1998).

The oligomeric structure of PLB has been proposed to exist as a pentamer in the SR membrane as detected by sodium dodecyl sulfate polyacrylamide gels (SDS-page). The most populated forms of PLB are those of monomer and pentamer, and upon phosphorylation of the pentamer, 10 phosphorylation levels were revealed indicating each monomer contained two phosphorylation sites (Arkin *et al.*, 1997). No oligomerisation is seen in a peptide corresponding to the cytoplasmic domain providing evidence that the pentamerization of PLB is solely a function of its transmembrane segment, Domain2 (Arkin *et al.*, 1997; Simmerman *et al.*, 1998). Equilibrium exists between monomeric and pentameric states of PLB but phosphorylation by protein kinases shifts the equilibrium in favour of the pentameric form (Kadambi *et al.*, 1997). Shifting the equilibrium in favour of the monomer form, using alanine scanning mutagenesis of the transmembrane domain 2, results in an increase in the inhibitory function (Kadambi *et al.*, 1997). As demonstrated by Autry *et al.* (1997), PLB monomers are more effective SERCA2 inhibitors thus

suggesting that the monomeric form of PLB is a more effective inhibitor than pentameric PLB. This dynamic equilibrium between PLB pentamers and monomers in the plane of the lipid membrane appears to be controlled by electrostatic interactions, and buffers of high ionic strength promote pentameric stability in the protein.

Electrostatic interactions have been shown to be an important factor in the ability of PLB to inhibit the pump. A change in surface membrane potential occurs after phosphorylation of PLB, and under high ionic strength conditions both the surface membrane potential and PLB phosphorylation effects on the apparent calcium affinity of the SR calcium pump are attenuated, supporting the idea that electrostatic interactions between cytoplasmic domain of PLB and the pump are involved in the regulatory mechanisms.

1.4. TRANSPORT OF CALCIUM ACROSS THE SR MEMBRANE

1.4.1. Reaction Cycle

In 1973, Makinose proposed a model for calcium transport and suggested that the pump can adopt two conformations during the calcium transport cycle: a theory that was later substantiated by De Meis *et al.* in 1979. The reaction cycle describes a scheme whereby the SR calcium pump is phosphorylated and dephosphorylated; and an interconversion of conformational states of the protein result in the transport of two calcium ions through the SR membrane, against its concentration gradient, and into the lumen of the SR for every molecule of ATP hydrolysed (Jäger, 1991; Mintz *et al.*, 1997; Ikemoto, 1982). An important feature of the SR calcium pump cycle is its total reversibility (Makinose, 1971; Makinose & Hasselbach, 1971). The ground state (which prevails in the absence of calcium) and the conformations distinguished by an external or internal calcium transport site denoted by E_1 and E_2 respectively, are the three conformational states in question (Ikemoto, 1982). E_1 (calcium state) and E_2 (magnesium state) are distinguished by the fact that the former has the ability to form EP from ATP but not from P_i , whereas E_2 can form EP from P_i but not ATP. The phosphorylation of the enzyme does not take place unless the enzyme changes from the ground state to E_1 or E_2 (Ikemoto, 1982) (Figure 1.2).

Step 1, the enzyme (E_1) binds two calcium ions sequentially at high affinity sites ($K_m \sim 1 \mu M$). The calcium binding sites have a cytoplasmic orientation (Läuger, 1991; Ikemoto, 1982) and after calcium binds, the pump becomes phosphorylated by ATP. The calcium-binding step is therefore the rate-limiting step of the cycle (Ikemoto, 1982).

Step 2, in the state $Ca_2 \bullet E_1 \bullet ATP$, the terminal phosphate group of the bound ATP is transferred in a rapid reaction to an aspartyl residue of the enzyme, forming an acid-stable acylphosphate.

Step 3, synchronously with the phosphorylation reaction, the two bound calcium ions become occluded, i.e. they are retained in the channel and unable to exchange with either the free calcium in the cytoplasm or with the calcium in the lumen.

Step 4, the phosphoenzyme is unstable and undergoes a conformational change to E_2 ; therefore the binding sites now face the lumen of the SR. In the E_2 state the affinity for calcium is strongly reduced ($K_m \sim 1 mM$) and permits the release of the bound calcium into the lumen of the SR.

Step 5, following the release of calcium, the phosphoenzyme $P-E_2$ is dephosphorylated. After transition back to conformation E_1 , a new transport cycle can be initiated.

1.4.2. Calcium Binding and Dissociation Mechanisms

Inesi *et al.*, (1980), proposed that calcium binding occurs as a two-step process, comprising fast binding of a first calcium followed by a slow conformational change which allows binding of a second calcium (Figure 1.3). A simple possibility for two sites being sequentially accessible from the cytoplasm is a narrow channel with a deep site (high affinity) and a superficial site (low affinity). In such a model the sites are not accessible simultaneously so that during the calcium-binding process the first ion that is bound to the superficial site induces a conformational change that increases the affinity of the site and reveals a second site of high affinity. Therefore the calcium ions are transported and released in an ordered and sequential fashion, whereby the binding of calcium to two high affinity sites is cooperative (Dupont, 1982).

In the absence of phosphorylation, the calcium ion bound to the superficial site can still exchange with the medium. The binding of the two calcium ions can be described as having three

substates of the calcium-uptake state (E_1). The first substate (the domain) is an open cavity and can bind only a single calcium ion. Once bound the cavity partially closes to generate a second calcium binding site (substate 2). Again, after the calcium ion binds to the site the cavity closes, leading to a state in which both ions are bound with high affinity (substate 3) (Lüger, 1991). Once the transport sites are saturated with calcium, ATPase becomes phosphorylatable by ATP and upon phosphorylation induces occlusion of the two bound calcium ions (Dupont, 1980). In this state, calcium cannot dissociate unless a slow conformational change occurs or reverse dephosphorylation is induced by ADP (Cantilina *et al.*, 1993).

Calcium occlusion in the phosphorylated ATPase occurs together with a change in the accessibility of the calcium sites that become inaccessible from the cytoplasmic side and accessible from the luminal side (Dupont, 1980). However, the occluded calcium ions are still bound to ATPase and not dissociated inside the vesicle, as both EGTA and ADP are required for rapid dephosphorylation to induce calcium release on the cytoplasmic side (Mintz *et al.*, 1997). Once the calcium sites have become accessible from the lumen, the affinity of calcium ions for the ATPase should decrease to allow their dissociation towards the SR lumen thus allowing the SR to store the calcium ions. It is thought that the calcium ion bound more deeply is the first to be released, whereas the superficial bound calcium ion is released more slowly (Lüger, 1991). This would be consistent with the idea of a narrow channel in the phosphoenzyme. Other theories have been developed that allow the occluded calcium ions to exchange positions, randomising the ions, allowing the first calcium ion bound to be the first or second to dissociate (Mintz *et al.*, 1997).

1.5. CALCIUM EFFLUX MECHANISMS

The SR must possess calcium efflux as well as calcium uptake mechanisms in order to regulate intracellular free calcium. Two families of calcium release channels have been extensively characterized: the RyR and the inositol 1,4,5-trisphosphate receptor (IP_3R). RyRs and IP_3R s are distantly related, sharing some structural properties and both exhibiting biphasic dependencies on cytosolic calcium, such that they are activated at low (nM- μ M ranges) calcium concentrations and inhibited at high calcium concentrations (mM) (Bezprozvanny *et al.*, 1991). However, RyRs are the

major calcium release channels in striated muscle and cardiac muscle possesses 50- to 100- fold more RyR than IP₃Rs (Moschella & Marks, 1993).

The SR calcium pump may also contribute to an SR calcium efflux route and under certain conditions induce the reversal of the pump or the transition of the pump into an efflux channel (Figure 1.4).

1.5.1. The Ryanodine Receptor

One of the SR calcium efflux mechanisms is termed the RyR on the basis of the ability of the protein to bind ryanodine, a plant alkaloid. Ryanodine is a natural product found in the stem and root of *Ryania speciosa*, that grows as shrubs or trees in several tropical locations in central and South America including Trinidad and the Amazon basin (Sutko *et al.*, 1997). The wood from trees in the *Ryania* genus is known to contain toxic components; the crude extracts of which were used as an insecticide to induce muscle paralysis in insects (Rogers *et al.*, 1948; DeVault, 1983).

In striated muscle, RyRs are high conductance calcium channels. They are located in the triadic junctions, projecting into the junctional gap between the TC and T-tubules (Fleischer *et al.*, 1985; Block *et al.*, 1988; Fleisher & Inui, 1989) and corresponds to the "feet" structures observed in electron microscope images within the triads (Figure 1.5). However, RyRs also have been identified in SR structures that do not lie in contiguity with the sarcolemma such as corbular and expanded junctional SR, as well as in intracellular membranes of other cells and tissues such as brain, smooth muscle, endothelium liver and fibroblasts (Franzini-Armstrong & Jorgensen, 1994; Meissner, 1994).

1.5.1.1. Activation of SR Calcium Release via the DHPR

In skeletal muscle, calcium can be released from the SR as a result of direct electrical stimulation. During depolarisation of the T-tubules, the DHPR undergoes a conformational change transmitted through the bulbous heads of the RyR to induce the release of calcium from the SR through RyRs (Figure 1.5). It is thought that the DHPR, a slow activating calcium channel in the surface membrane, is structurally linked to the RyR as postulated by Schneider and Chandler (1973). It acts as the voltage sensor and alternate arrays of RyR tetramers are associated and aligned with four

DHPR (tetrads), therefore there are two RyR for each DHPR tetrad in skeletal muscle (Franzini-Armstrong & Nunzi, 1983; Block *et al.*, 1988; Protasi *et al.*, 1997) and the interaction between DHPR and RyR, whether directly or indirectly, is required for the formation of tetrads (Sorrentino, 1995).

In cardiac muscle depolarisation of the transverse tubules activates the DHPR, initiating calcium influx into the dyadic space and activating the RyR via the process of CICR (Figure 1.5) thus contributing greatly to the rise in intracellular calcium concentration. The released calcium together with the calcium entering through the sarcolemma, increase the cytoplasmic concentration sufficiently to activate the contractile apparatus in myocytes.

In contrast to skeletal muscle, the cardiac muscle DHPRs are in close proximity of the RyR but have not been proven to have a direct link to the RyR, as they seem to lack the well ordered array of tetrads that are seen with skeletal muscle SR (Sun *et al.*, 1995; Protasi *et al.*, 1996; Franzini-Armstrong, 1999). From these findings, it is thought that the calcium flux through the DHPR diffuses into a restricted space to act as the activator of the immediate adjacent RyRs via CICR (Fabiato, 1983; Sham *et al.*, 1995; Santana *et al.*, 1996). Thus, entry of extracellular calcium through the DHPR is required for E-C coupling in cardiac muscle, whereas skeletal muscle contraction can occur in the absence of external calcium (Ashley *et al.*, 1991). Also, in cardiac muscle, there are many more RyR than there are DHPR (Bers & Stiffel, 1993) and thus four to ten RyR might be associated with a single L-type calcium channel (one tetrad); activating a whole cluster of RyR and the temporal and spatial summation of these events would lead to the production of a calcium spark (Niggli, 1999). Both skeletal and cardiac RyR are clustered into arrays on the junctional SR such that each channel physically contacts four of its neighbours (Saito *et al.*, 1988; Flutcher & Franzini-Armstrong, 1996; Franzini-Armstrong *et al.*, 1999), possibly near where the FKBP interacts with the RyR (Wagenknecht *et al.*, 1996).

1.5.1.2. Stochastic and Coupled Gating

The stochastic gating theory proposed that RyRs operate independently and the activation of one RyR may elevate local calcium levels sufficiently to activate neighbouring RyRs (Figure 1.6a). The

activation of neighbouring RyRs occur at different intrinsic latencies, and thus open and close randomly to generate a relatively slow, damped and irregular local calcium flux.

However, in contrast to the “stochastic gating” theory, Marx *et al.* (1998) proposed a theory termed “coupled gating”: a coordinated gating hypothesis where two or more RyR are mechanically linked and gate simultaneously (Figure 1.6b). Under these conditions, the RyRs open and close in a coordinated fashion, operating as functional units to generate large, fast local calcium release events. This concerted effect would speed the SR calcium release process but for this process to be physiologically important, clustering of RyR is critical. This mechanism also provides a method for simultaneously closing all the RyRs in the junctions thereby reducing the probability that individual RyRs channels will be reactivated stochastically by calcium fluxing through their neighbours (Marx *et al.*, 2001). This method of RyR inactivation is proposed to arise from a reduction in the SR content (due to calcium release via RyR) that signals the RyR to close, as the open probability of the channel (P_o) depends, in part, on luminal calcium concentrations (Gyorke & Gyorke, 1998). Therefore, when the first RyR closes, all the RyRs in the junction will close due to coupled gating.

The RyR is closely associated with a number of proteins in the TC including, triadin (Caswell *et al.*, 1991), calsequestrin (Collins *et al.*, 1990; Ikemoto *et al.*, 1989), calmodulin (Tripathy *et al.*, 1995), FKBP12 (Jayaraman *et al.*, 1992; Timmerman *et al.*, 1993) and the immunophilin FK-506-binding protein, all of which have been shown to modulate the release of calcium from the TC.

1.5.1.3. Ligand Modulation

The RyR is regulated by cytosolic calcium; the process of CICR. To date only calcium (Sitsapesan & Williams, 1994) and annexin VI (Diaz-Munoz *et al.*, 1990) are thought to act on the luminal side of the channel. Many other ligands alter the activity of the channel to stimulate or inhibit calcium release but calcium is the primary activating ligand; being effective in the absence of all other ligands (Sitsapesan & Williams, 1994a; Smith *et al.*, 1986). In the absence of calcium, the ligands will not be able to activate the channel or if they do, the channel will not work at its maximal level (Sitsapesan & Williams, 1994a). A few of the diverse array of ligands known to modulate the function of ryanodine-sensitive calcium channels are caffeine (mM) (Palade, 1987; Ashley &

Williams, 1988), cADP-ribose (mM)(Buck, 1992; Galione *et al.*, 1991), ATP (mM) (Meissner, 1986; Smith *et al.*, 1986; Meissner & Henderson, 1987) and ryanodine (<10 μ M) (Buck, 1992b, Ogawa, 1994; Meissner, 1986). They bind to specific sites on the cytosolic side of the RyR, increasing the P_o of the channel to release calcium from the store. The P_o of the channel is decreased by free magnesium (mM) (Ashley & Williams, 1990; Meissner *et al.*, 1986; Laver *et al.*, 1997), tetracaine or procaine (μ M), by RuR (μ M) (Ma, 1993), ryanodine (>100 μ M) (Buck, 1992b, Meissner, 1986; Rousseau *et al.*, 1987) and by a decrease in the pH (Rousseau & Pinkos, 1990).

Radioactive ryanodine binding ($[^3\text{H}]$ ryanodine) studies in skeletal and cardiac muscle have revealed the existence of two classes of sites, a low affinity and a high affinity binding sites. High concentrations of ryanodine (10 μ M-300 μ M) interact with a low affinity binding sites to lock the channel in the closed position thereby inhibiting calcium release from the SR. Low concentrations of ryanodine (0.01 μ M-10 μ M) interact with high affinity binding sites to lock the release channel in a semi-open state (Coronado *et al.*, 1994). This state produces an early rapid release of calcium until the stores are depleted. There is some controversy as to the ratio of high to low affinity binding sites although two groups have reported a ratio of 1:3 for high to low affinity binding sites (Pessah *et al.*, 1991; Meissner *et al.*, 1989). The mechanism by which bound ryanodine alters the activity of the calcium release channel is unknown, but tetrameric assembly is required for the binding of ryanodine at its high affinity site.

Another group of calcium releasing agents that affect ryanodine receptors are fatty acids and their metabolites. Glycolipid sphingosine has a dual effect, inducing release at high concentrations and inhibiting caffeine induced calcium release at low concentrations (Sabbadini *et al.*, 1992). Arachidonic acid (Dettbarn *et al.*, 1993) stearic acid (Cardoso & de Meis, 1993), and the fatty acid derivatives palmitoyl carnitine (El-Hayek *et al.*, 1993) and palmitoyl coenzyme A (Connelly *et al.*, 1994) stimulated calcium release from skeletal and cardiac muscle. It was observed that palmitoyl carnitine increased the SR calcium permeability in nM free calcium and mM magnesium suggesting that palmitoyl carnitine may generate a small calcium leak from the SR in resting muscle cells. This leak could influence the resting cytosolic calcium and serve to bring the calcium release channel to threshold for activation by voltage or other signals (El-Hayek *et al.*, 1993).

1.5.1.4. Structure

The massive size of the RyRs may make them physically the largest ion channel. It is not clear why RyRs have an unusually high molecular mass (2.3Mda) (Jayaraman *et al.*, 1992) although, it has been suggested that the reason for this might lie within the numerous endogenous modulatory ligands known to regulate the activity of the receptor and therefore the gigantic cytoplasmic domains of these ion channels are scaffolds for regulators of channel function (Marx *et al.*, 2000). The calcium release channel exists as a homotetramer; each monomer has a molecular weight of approximately 550kDa (Takeshima, 1989; Zorzato, 1990) and possesses over 5000 amino acids. The receptor comprises of two major components; the larger part is the N-terminus, forming the bulbous heads that project into the cytosol and comes into close contact with the T-tubular membrane. The second component is the C-terminus which is the smaller region and forms the calcium release channel (Berridge, 1993) often referred to as the "foot" region (Ferguson *et al.*, 1984), a term that was applied to the structure based on its appearance in electron micrographs of sectioned muscle before its molecular identity was known.

The RyR has been purified, cloned and sequenced from a variety of species and several isoforms have been identified, thus the RyR family is proving to be extensive. Three family members named RYR1-3 are encoded for by three separate genes, identified as *ryr1*, *ryr2* and *ryr3* respectively. The expression of these genes do not appear to be tissue specific but each was predominantly expressed in mammalian skeletal muscle, cardiac muscle and in the brain, and smooth muscle respectively (Marks *et al.*, 1989; Hakamata *et al.*, 1992; Otsu *et al.*, 1990). The gene for the RYR1 was specifically localised to region 19q13.1, on the long arm of human chromosome 19 whereas RYR2 gene was located to human chromosome 1 and RYR3 on chromosome 15 (Marks *et al.*, 1989).

Sequence homologs of the three mammalian RyR isoforms are expressed also in nonmammalian vertebrates and have been termed α (RYR1), β (RYR3) and cardiac (RYR2) (Airey *et al.*, 1990; Ogawa, 1994). In addition, two alternatively spliced variants of RYR1 and one variant of RYR2 have been identified (Sutko & Airey, 1996; Nakai *et al.*, 1990; Zorzato *et al.*, 1994; Futatsugi *et al.*, 1995). These variants are expressed in both a tissue- and a developmental stage-

specific manner, suggesting that they may have different functional properties and/or may be regulated in different ways (Futatsugi *et al.*, 1995).

1.5.1.5. Phosphorylation

RyR were found to be phosphorylated by exogenous calmodulin-dependent protein kinase, by exogenous catalytic subunit of cAMP-dependent protein kinase (PKA), and by guanine 3', 5'-cyclic monophosphate dependent protein kinase (PKG) (Seiler *et al.*, 1984). The phosphorylation rates for each of these kinases were similar, only that of protein kinase C-dependent phosphorylation occurred at a relatively slow rate (Takasago *et al.*, 1991). Phosphorylation of the cardiac receptor by PKA, PKG or protein kinase C (PKC) increased [³H]ryanodine binding by approximately 20% (Takasago *et al.*, 1991). In contrast CaM kinase dependent phosphorylation decreased [³H]ryanodine binding by approximately 40% (Takasago *et al.*, 1991). The altered ryanodine binding reflects different levels of channel activity since ryanodine can only bind to the channel once it is in the open state (Takasago *et al.*, 1991). It was observed that endogenous and exogenous CaM kinase reduced the activation of the cardiac receptor channel incorporated into lipid bilayers (Witcher *et al.*, 1991), whereas cAMP dependent phosphorylation of the cardiac ryanodine receptor may be involved in the positive inotropic effects of β -adrenergic agonists (Yoshida *et al.*, 1992).

1.5.1.6. Regulation by Intraluminal Calcium

Work carried out by Endo (1977) with skinned skeletal muscle fibres revealed that luminal calcium may play a role in regulating SR calcium release and that a loading threshold was required before calcium could be released. Fabiato & Fabiato (1979) later demonstrated that the magnitude of CICR in skinned cardiac cells was increased as the calcium loading of the SR was increased and that two types of CICR in skinned cardiac cells exist. The first one involves an increase of calcium concentration at the cytoplasmic side of the SR to trigger a time and calcium dependent activation. The second one involves the spontaneous release of calcium that requires calcium overload of the SR and may involve calcium binding to an intraluminal site (Fabiato, 1992) and since then luminal dependence of CICR has been shown in isolated SR vesicles (Sitsapesan & Williams, 1994).

It was initially thought that luminal calcium flowed through the pore of the RyR to act on the cytoplasmic calcium binding sites (Tripathy & Meissner, 1996; Hermann-Frank & Lehmann-Horn, 1996). However work carried out by Ching *et al.*, (2000) on cardiac RyR incorporated into bilayers proved otherwise by using the application of trypsin to digest binding sites exposed on the luminal side of the bilayer, thereby providing strong evidence for the existence of luminally located calcium activation and inhibition sites on the cardiac RyR channel itself or on a closely associated protein that regulates RyR gating. Thus luminal calcium was found not to flow through the channel pore and act on the cytosolic calcium binding sites (Sitsapesan & Williams, 1997; Lukyanenko *et al.*, 1996) but may bind to sites present within the channel pore or on the luminal face of the channel (Sitsapesan & Williams, 1997).

Another factor influencing luminal calcium content is calsequestrin. It is not known to what extent SR calcium is bound to this protein, nor at what stage the buffering capacity is reached and whether activation of RyR leads to a conformational change in calsequestrin thus leading to a rapid dissociation of calcium, that ultimately result in an increase in the calcium concentration at the luminal side of the RyR (Sitsapesan & Williams, 1997).

1.5.1.7. Calcium Sparks, Quarks and Waves

Calcium sparks is the term used to describe the localised transient rise of fluorescence observed in cardiac myocytes loaded with the dye fluo-3 first reported by Cheng *et al.*, 1993. Calcium sparks are localized, discrete SR calcium release events produced by the gating of RyRs and were first characterised in cardiac myocytes by Cheng *et al.*, (1993). It is thought that the electrically evoked calcium transients that activate contraction arise from the spatial and temporal summation of multiple sparks (Cheng *et al.*, 1993; Cannell *et al.*, 1994; Cannell *et al.*, 1995; Lopez-Lopez *et al.*, 1995) therefore, sparks represent the elementary event underlying E-C coupling (Cannell *et al.*, 1994). Sparks originate at the T-tubules probably at the dyadic junction and can arise spontaneously (although spontaneous calcium sparks do not occur in cardiac muscle under normal physiological conditions (Wier *et al.*, 1997)), as well as in response to electrical stimulation of the cell, triggered by local intracellular calcium concentrations which are first established in the region of the RyR by the opening of a single L-type calcium channel (Lopez-Lopez *et al.*, 1995; Santana *et al.*, 1996).

There is a great deal of uncertainty as to whether single or multiple RyRs (Stern *et al.*, 1997) are involved in the generation of a single calcium spark. Evidence based on anatomical data showed that RyRs generally occur in clusters in the dyadic junction (Bers, 1991). Marx *et al.*, (1998) demonstrated that coupled gating can exist between RyRs (Marx *et al.*, 1998) and Bers & Fill (1998) discussed the potential of coordinated gating between RyRs. These results together with the fact that the calcium flux through a single RyR (<0.5pA (Mejia-Alvarez *et al.*, 1998) is considerably smaller than the flux of calcium associated with a spark (3pA, Blatter *et al.* 1997; ~4pA, Cheng *et al.*, 1993), indicates that spark generation is more likely to be due to a cluster of RyR gating in concert, rather than through a single RyR (Figure 1.7A). A hypothesis stabilised by the discovery of smaller calcium release events termed "quarks" observed by Lipp & Niggli, (1996). Quarks represent the release of calcium from a single RyR thus implying that a number of RyRs must gate in concert to produce the larger calcium 'spark' however, it is unclear whether quarks occur during normal EC coupling.

Under normal cellular calcium loading conditions, sparks remain localized, random events but when the extracellular calcium concentration is elevated (as seen with calcium overload); sparks give rise to the initiation and propagation of calcium waves (Cheng *et al.*, 1996; Lukyanenko *et al.*, 1996, 1999; Figure 1.7B). During slow propagating waves or waves in the presence of EGTA (Lukyanenko & Gyorke, 1999), discrete calcium release events (similar to sparks) can be detected in the wave front. The discrete events appear to recruit other sparks in the wave front so that the wave progresses in a saltatory manner (Cheng *et al.*, 1996; Lukyanenko & Gyorke, 1999) and this saltatory manner is known as fire-diffuse (Keizer *et al.*, 1998).

1.5.1.8. FK506 Binding Protein

FK506 is a macrocyclic lactone used clinically as a potent immunosuppressant for the prevention of allograft rejection in organ transplantation (Spencer *et al.*, 1997). FK506 binds to the ubiquitous FK506 binding protein (FKBP), FKBP12. FKBP12 is a 12kDa soluble member of the immunophilin family (Marks, 1996b) and there are at least six members of the FKBP family that range from 12-52 kDa, all named according to their molecular masses (Lam *et al.*, 1995; Timerman *et al.*, 1996). All of the known FKBP family members display enzymatic activity, cis-trans peptidyl-

propyl isomerization (Rotamase), thought to be essential for protein folding during protein synthesis (Schmid, 1993). The enzymatic activity is unrelated to immunosuppression and is inhibited when FK506 or Rapamycin bind to the rotamase active site (Bierer, 1990). Thus far, only FKBP12 and FKBP12.6 were found in complex with the immunosuppressive drug to target calcineurin, a Ca^{2+} /CaM-dependent serine-threonine phosphatase (Marks, 1996; Lam *et al.*, 1995) in T-lymphocytes. Once bound, the complex inhibits calcineurin function, blocking IL-2 transcription thereby preventing T cell activation and consequent immune response (Thomson, *et al.*, 1995).

FKBP12 can be found in many cell types and is very well conserved from plants and yeast to humans (Kay, 1996), and participates in a variety of cellular processes such as, neurotransmitter release, nerve growth and calcium release from the RyR (Snyder *et al.*, 1998). In skeletal muscle, FKBP12 is physically associated with RyR1 (Jayaraman *et al.*, 1992; Marks *et al.*, 1990, 1989) whereas in cardiac muscle FKBP12.6 is physically associated with RyR2 (Timmerman *et al.*, 1994; Mchran, *et al.*, 1993) (Figure 1.5). Cardiac RyR2 binds FKBP12.6 with high specificity whereas skeletal RyR1 binds both FKBP12 and FKBP12.6 (Timmerman *et al.*, 1996). The two proteins copurify during sucrose density gradient centrifugation and co-localize to the TC of the SR (Jayaraman *et al.*, 1992). The association of FKBP12 with the calcium release channel suggests that FKBP12 may modulate the calcium channel; a distinct action from the ligand-activated immunosuppression and inhibition of proliferation.

FKBP12 was first cloned in 1994 and comprises of 108 amino acids. It was found to be closely related to FKBP12.6 as FKBP12.6 possesses 85% amino acid sequence identity to FKBP12. Both FKBP12 and FKBP12.6 have equal affinities for FK506 and are equipotent mediators of calcineurin inhibition by FK506. One molecule of FKBP12/12.6 is associated with each monomer of the RyR, giving rise to 4 molecules of FKBP12/12.6 per tetramer (Nakai *et al.*, 1990, Timmerman, *et al.*, 1993, Lam *et al.*, 1995). If FKBP is stripped from the receptor by addition of FK506, the channel displays a large number of subconductance states (Brillantes *et al.*, 1994). This increases both the mean open times and open probability of the channel causing the channel to become 'leaky' (Ahern *et al.*, 1994; Brillantes *et al.*, 1994; Mayrleitner *et al.*, 1994), reducing the net accumulation of calcium in the SR thus depleting the stores. FKBP12 also stabilises the interaction

between different RyRs thereby enhancing coupled gating of a cluster of RyR (Marks, 1996). As a result, releasing agents such as caffeine (Timerman *et al.*, 1993; Brillantes *et al.*, 1994) and calcium (Mayrleitner *et al.*, 1994; Timerman *et al.*, 1993) increase calcium flux at lower concentrations and higher concentrations of magnesium (Timerman *et al.*, 1993) are required for inactivation. These effects are reversed when FKBP12 is rebound to the RyR, and the channel can open to its full conductive state (Brillantes *et al.*, 1994) indicating FKBP12 enhances the cooperativity among the four subunits and is essential for stabilizing the native full conductance gating behaviour of the channel (Marks, 1996; Pessah *et al.*, 1997). However, studies using *Xenopus* oocytes revealed that recombinant RyR1 was capable of forming an intracellular calcium release channel that was activated by caffeine in the absence of FKBP12, suggesting that FKBP12 is not required for the tetrameric formation of the channel structure (Marks, 1996b).

The occurrence of subconductance states may not always be observed upon the removal of FKBP from the RyR. Work conducted by Timerman *et al.* (1996) found that the removal of FKBP from canine cardiac RyR with FK590 had no effect on channel function, whereas Barg *et al.* (1997) reported an increase in P_o of rabbit RyR 1 on the removal of FKBP, an effect reversed with the addition of FKBP12 or 12.6 however, no subconductance states were seen.

1.5.1.9. Bastadin

Bastadins are a class of macrocyclic bromotyrosine derivatives synthesized by the marine sponge *Ianthella basta* and were recently reported as novel modulators of RyR function (Mack *et al.*, 1994; Pessah *et al.*, 1997). A few different isoforms of bastadin (5, 7, 10 and 19) have been isolated and exhibit unprecedented activity towards skeletal muscle SR; the individual actions of which are highly dependent on the molecular structure.

The potency of bastadin 5 was noted to be 3-fold greater than that of bastadin 7 (Mack *et al.*, 1994) and in skeletal muscle, bastadin 5 and 7 behave as full agonists by enhancing the occupancy of [³H]Ryanodine with its high affinity sites and the concomitant decrease in the tendency for low affinity ryanodine binding (Mack *et al.*, 1994). Bastadin 19, on the other hand, is a weak partial agonist and can effectively diminish the actions of bastadin 5 (Mack *et al.*, 1994). The mechanism by which bastadins enhance the number of high affinity binding sites for [³H]Ryanodine on the SR

membrane is not fully understood, however equilibrium kinetic studies have revealed multiple high and low affinity binding sites for the alkaloid that appear to be allosterically coupled (Wang *et al.*, 1993) and maybe related to the subconductance behaviour of the channel (Buck *et al.*, 1992b). In bilayer lipid membrane studies, bastadin 5 dramatically slowed single channel gating kinetics without significantly altering unitary conductance or P_o (Chen *et al.*, 1999).

From work carried out by Chen *et al.*, (1999) it was discovered that bastadin 10 produces a concentration dependent (1-15 μ M) stimulation of calcium release from actively loaded SR vesicles in the absence of stimulatory concentrations of extravesicular calcium (Chen *et al.*, 1999), thus shortening closed dwell times and stabilizing the full open state of the channel. On addition of 10 μ M RuR and 10 μ M ryanodine, to a bastadin 10 modified channel, a block of the leak was observed with RuR and half conductance was observed with ryanodine. This suggests that bastadin 10 mediates its actions on channel gating through site distinct from ryanodine/RuR effector sites. Also, the effects of bastadin 10 are reversible, being abolished with the addition of FK506 or rapamycin and reconstituted by recombinant FKBP12.

It has been suggested that the actions of bastadin on SR channel function could be mediated either by a direct interaction with a site on FKBP or within the FKBP-RyR protein-protein boundary, since the effects of bastadin 5 were antagonised by FK506 (Pessah *et al.*, 1997). In contrast to FK506, bastadin 5 does not promote dissociation of the FKBP-RyR complex, but enhances the effect of FK506 to dissociate the FKBP from RyR. It stabilizes the full conductance gating transitions to significantly increase both the open and closed dwell times equally, whereas FK506 promotes subconducting gating behaviour. FK506 on its own enhances steady state loading capacity of SR vesicles which can be enhanced further with the addition of ryanodine channel blockers whereas bastadin 5 alone significantly reduces steady state loading capacity of the SR, but only in the presence of ryanodine channel blockers enhances calcium loading (Pessah *et al.*, 1997).

1.5.2. CALCIUM ATPase PUMP MEDIATED EFFLUX ROUTES

1.5.2.1. Myocardial Ischaemia: Increase in P_i

Myocardial ischaemia can be characterized by reduced blood flow depriving the heart of substrates leading to the accumulation of metabolites. Ischaemia is very difficult to study experimentally especially for preparations of cardiac tissue that have no blood supply, such as isolated cells which lack direct experimental equivalent to ischaemia. In this situation, anoxia is often used to observe the main mechanical features of ischaemia. This involves the removal of all or most of the oxygen in a perfused system supplying tissues, or using agents that inhibit oxidative phosphorylation such as cyanide (Allen *et al.*, 1989).

In the first few minutes of anoxia, inhibition of aerobic metabolism is accompanied by a pronounced decrease in contractile force (Allen & Orchard, 1987). During this phase, the intracellular concentration of ATP remains constant as ADP is rephosphorylated by creatine phosphate (CrP); a reaction catalysed by the enzyme creatine phosphokinase. The intracellular CrP concentration reduces rapidly from 15-20mM down to undetectable levels and simultaneously inorganic phosphate levels (P_i) increase from 2 to 20mM (Steele, McAnish & Smith, 1996). After depletion of CrP, ATP synthesis continues via anaerobic glycolysis, resulting in lactic acid production and an associated decrease in intracellular pH (Bailey *et al.*, 1981). With prolonged periods of anoxia, anaerobic glycolysis ceases and a further increase in intracellular P_i concentration occurs due to the net hydrolysis of ATP (Steele, McAnish & Smith, 1996).

Previous studies have shown that P_i decreases myofilament calcium sensitivity and maximum calcium-activated force (Kentish, 1986). More recent work on 'skinned' preparations suggests that increasing P_i may influence the regulation of calcium by the SR; that mM levels of P_i markedly reduce the amount of calcium available for release from the SR during systole (Smith & Steele, 1992; Steele, McAnish & Smith, 1995) and as a result the inhibitory action of P_i may be an important contributor to the rapid fall in contractility.

1.5.2.2. Calcium Phosphate Precipitation

Possible inhibitory actions of P_i on SR of skinned fibres involve actions within the SR lumen, on SR calcium channels or SR calcium pumps. Fryer *et al.*, (1995) have suggested that the decrease in releasable calcium may result from calcium phosphate precipitation within the SR. Like oxalate, P_i enters the SR by diffusion where precipitation of calcium phosphate occurs if the solubility product is exceeded (Makinose & Hasselbach, 1965). Precipitation reduces the free concentration of calcium within the SR, thereby increasing and prolonging calcium uptake from the surrounding medium. This process is limited only by the eventual rupture of the SR membrane during calcium phosphate crystallisation (Feher & Lipford, 1995). However, no evidence of precipitation occurred in experiments carried out on cardiac muscle, even at a concentration of P_i (60mM) exceeding that known to occur within the cytosol during prolonged anoxia (38-40mM) (Allen & Orchard, 1987). The absence of precipitation suggests some other action reduces intraluminal calcium to such an extent that the solubility product for calcium phosphate is not exceeded (Steele, McAnish & Smith, 1996).

1.5.2.3. Effects of P_i on Cardiac RyR

It was thought that P_i may also act on the cardiac RyR to increase calcium efflux via this route. Steele, McAnish & Smith, (1996) showed that this was not the case and in fact, on addition of ryanodine, P_i -induced calcium release from skinned fibres was unaffected. This suggests that P_i -induced calcium release does not result from direct activation of the SR calcium channel nor is it amplified by CICR mechanisms associated with the SR calcium release channels; although a ryanodine insensitive calcium efflux pathway cannot be ruled out.

1.5.2.4. Pump Reversal

Another inhibitory action of P_i on cardiac SR, to increase calcium efflux, could be mediated by the SR calcium pump. There are two mechanisms by which the pump can achieve this; pump reversal or pump channel transition. Reversal of the SR calcium pump would require mM levels of ADP as well as a calcium concentration gradient across the SR membrane in order to provide the energy required for ATP synthesis (Hasselbach, 1978). In the absence of an ATP regenerating system,

ADP concentrations would be expected to increase due to the presence of cellular ATPases. Micromolar levels of ADP have been shown to stimulate a rapid exchange between intra and extravesicular calcium (Waas & Hasselbach, 1981), but has little effect on the SR calcium content as calcium influx and efflux are increased to a similar extent in the presence of ADP alone (Waas & Hasselbach, 1981; Feher & Briggs, 1983; Soler *et al.*, 1990). However, calcium efflux was found to increase upon addition of millimolar levels of P_i and the concentration of ADP increased from $60\mu\text{M}$ (Smith & Steele, 1992), a level close to optimal levels for pump reversal (Barlogie *et al.*, 1971), to $120\mu\text{M}$. Similar values were measured in cardiac muscle during anoxia and ischaemia (Allen *et al.*, 1985). So the inhibitory effects of P_i may result from a dual action of P_i and ADP (produced by cellular ATPases) to induce a net calcium efflux via the SR calcium pump, rather than inhibition of calcium uptake per se (Steele, McAnish & Smith, 1995). This action helps explain why calcium phosphate precipitation was not observed even in the presence of 60mM P_i because as the concentration of P_i increases, the calcium content of the SR decreases so the solubility product is never exceeded.

Rephosphorylating ADP to ATP by phosphoenolpyruvate and pyruvate kinase can reduce P_i -induced calcium efflux of the SR. However, this provides unfavourable conditions for pump reversal because as ADP concentration decrease, this forces the pump to revert back to its original status of pumping two calcium into the lumen of the SR for every molecule of ATP utilised. Steele, McAnish & Smith (1995) have shown that creatine phosphokinase is retained after saponin treatment so even in the absence of these ATP regenerating systems, additions of creatine phosphate alone may interact with endogenous creatine phosphokinase to reduce the ADP concentration, thereby inhibiting P_i -induced calcium efflux via pump reversal. The effects of CrP have been shown to be due to reversal of the inhibitory actions of P_i and not as a result of increasing the calcium content of the SR by other means (Steele, McAnish & Smith, 1995). In preventing calcium efflux with the introduction of CrP, free luminal calcium concentrations will increase and if P_i concentration within the lumen is high, precipitation of calcium phosphate can occur. This will have no bearing in anoxia or ischaemia, since CrP concentrations fall as P_i concentrations increase.

1.5.2.5. Pump Channel Transition

Alternatively, some studies have suggested that under certain conditions, the SR calcium pump can mediate a fast efflux of calcium from the SR in an 'uncoupled' or substrate free state. Under these circumstances, the SR calcium pump acts as a channel and can mediate calcium leak from the SR. This mode of SR calcium pump is only seen in substrate free conditions or in presence of agents that inhibit substrate binding (e.g arsenate). Furthermore, P_i concentrations above 4mM appear to block the uncoupled mode of the calcium pump (De Meis & Inesi, 1992).

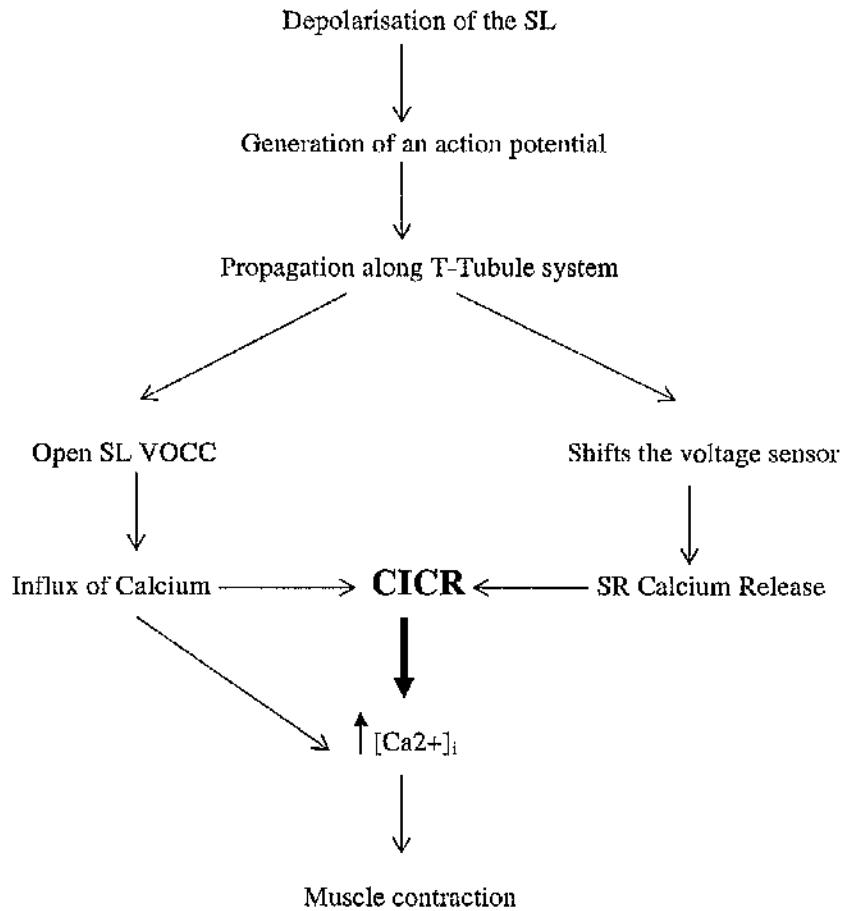


Figure 1.1: E-C Coupling Mechanisms. The intracellular calcium concentration is increased through two routes: voltage dependent calcium release pathway and CICR. Voltage dependent calcium release requires depolarisation of the cellular membrane to generate an action potential. The action potential propagates along the T-tubules, opening the VOCC to induce influx of calcium into the cytoplasm. This route also involves a direct link of the SL/T-tubule with the SR and depolarisation of the cellular membrane shifts the “voltage sensor” (DHPR) of the L-type calcium channel to allow influx of calcium into the cell. The second mechanism is CICR and involves the rise in intracellular calcium to induce the release of calcium from the SR via the RyR. All these mechanisms lead to muscle contraction.

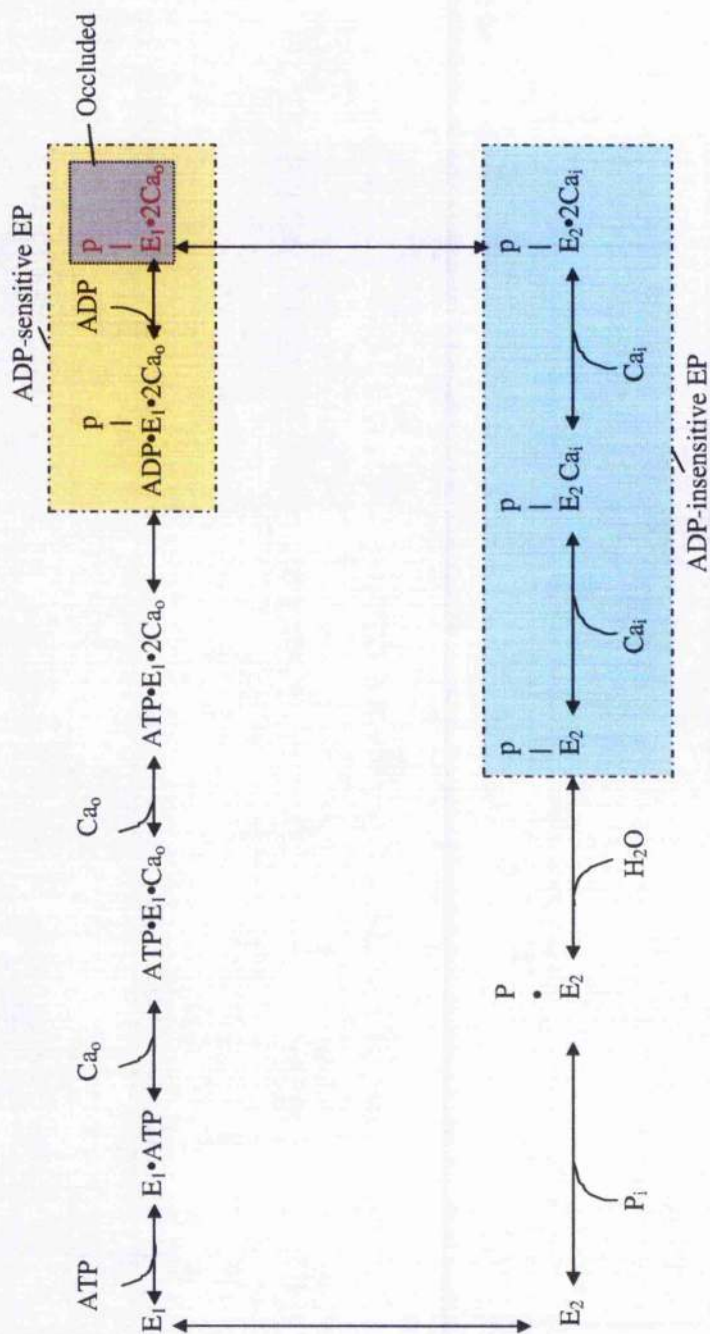


Figure 1.2: The reaction cycle diagram for SR Ca²⁺-ATPase. The calcium binding sites (E_1) are high affinity and are accessible from the cytoplasm (o); E_2 are of low affinity and are accessible from the lumen (i) whereas the binding sites in $E_1 \cdot P \cdot 2Ca_o$ are occluded. The ADP-sensitive components of E-P are $E_1 \cdot P \cdot ADP \cdot 2Ca_o$ and $E_1 \cdot P \cdot 2Ca_o$. The ADP-insensitive components of E-P are $E_2 \cdot P \cdot 2Ca_i$; $E_2 \cdot P \cdot Ca_i$; $E_2 \cdot P$.

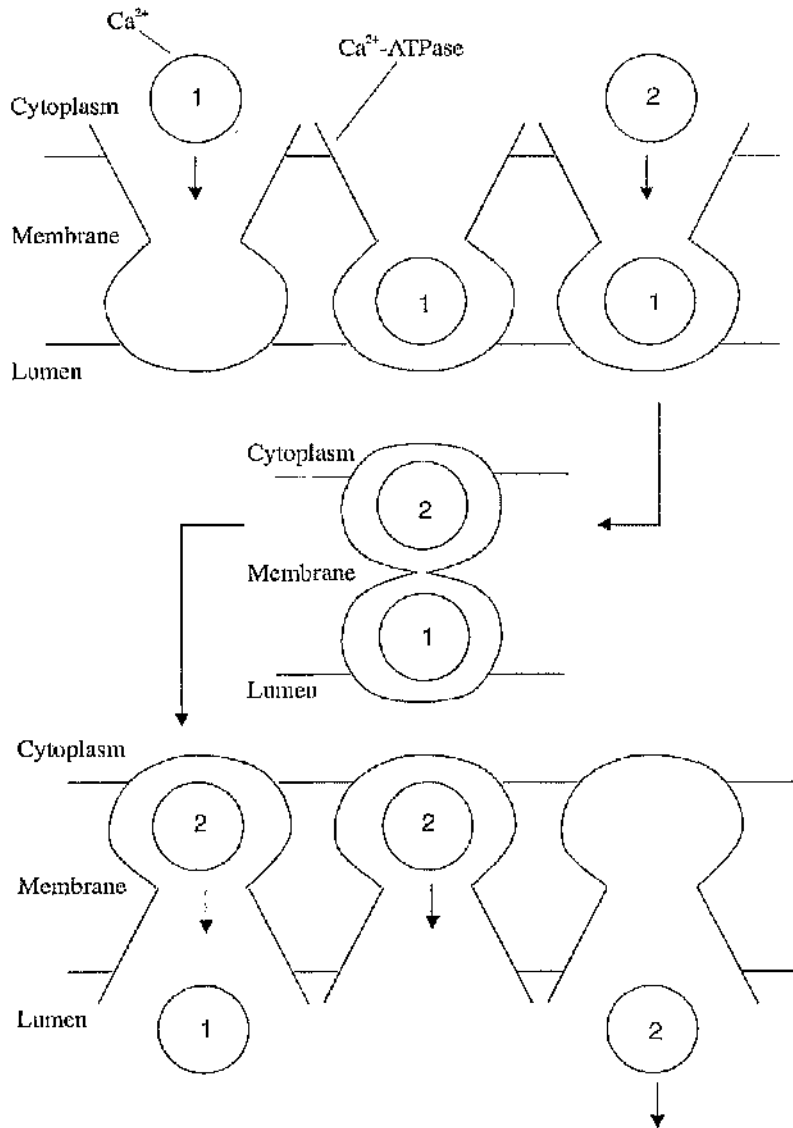


Figure 1.3: Representation of the movement of calcium across the SR membrane via the SR calcium pump. The calcium binding mechanism is a two step process: 1) the first calcium ion binds with high affinity to induce a conformational change of the protein and reveals the second binding site. 2) The second calcium ion binds with low affinity and is interchangeable with the medium until ATPase becomes phosphorylated. Once the ATPase is phosphorylated, both calcium ions are occluded, making them inaccessible. However, upon ATPase dephosphorylation, the binding sites can be accessed on the luminal side of the SR and the affinity for calcium is reduced, thus releasing calcium into the lumen of the SR.

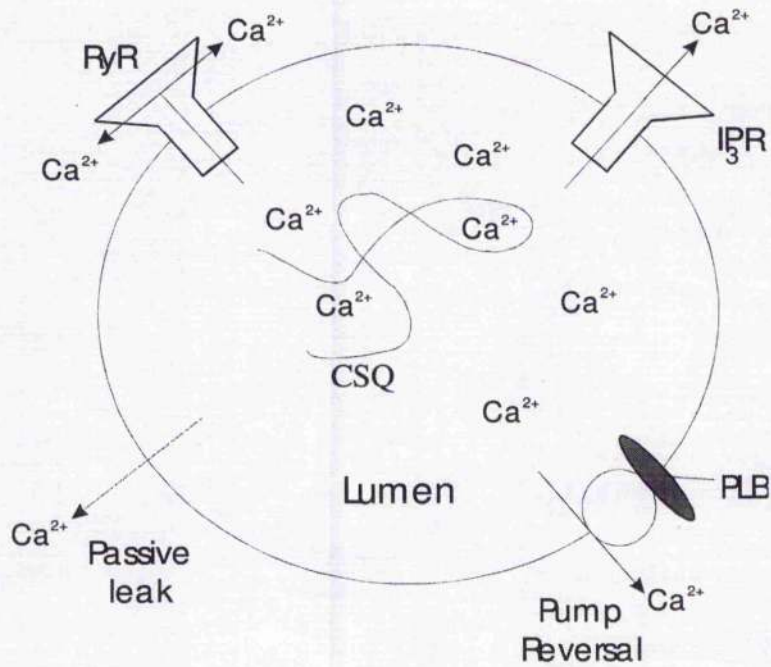


Figure 1.4: *Simplified diagram to show the calcium efflux routes in the SR.* It is essential that the calcium uptake and release mechanisms in the SR are tightly controlled. As the SR is the main calcium store, providing rapid calcium exchange with the cytosol to induce contraction and relaxation in cardiac muscle. The efflux mechanisms include; the ryanodine receptor (RyR); the inositol trisphosphate receptor (IP₃R); reversal of Ca²⁺-ATPase pump (under certain physiological conditions) and the passive SR leak. To buffer intraluminal calcium, the SR contains accessory proteins such as calsequestrin (CSQ).

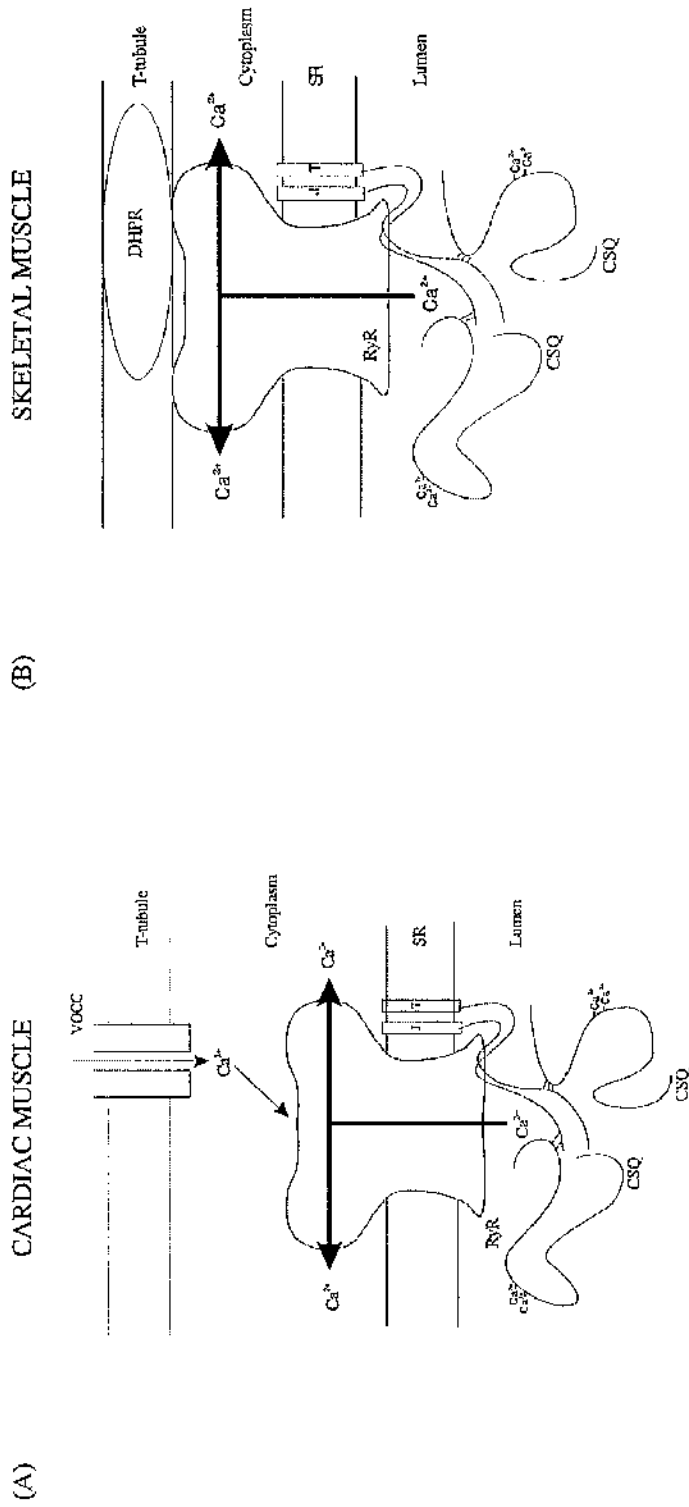
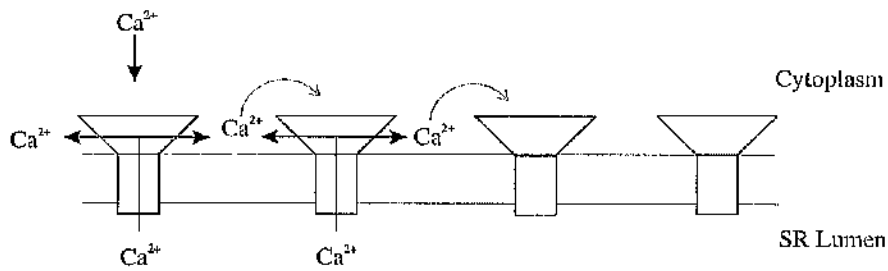


Figure 1.5: Interaction between the RyR and the DHPR in cardiac and skeletal muscle. The voltage operated calcium channel (DHPR) displays two types of contact with the RyR: indirect and direct. (A) In cardiac muscle, the indirect mechanism involves DHPR inducing an influx of calcium from the extracellular compartment. The influx of calcium then binds to the RyR to stimulate CICR. (B) In skeletal muscle, the direct mechanism involves DHPR acting as the voltage sensor and therefore when depolarisation of the t-tubule membrane occurs, the DHPR induces a conformational change in the RyR to calcium efflux from the SR.

(A)



(B)

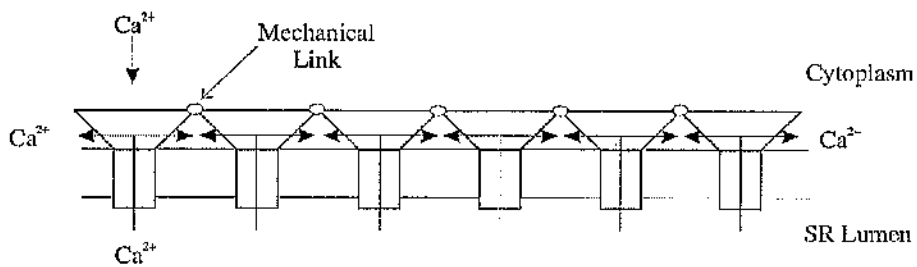
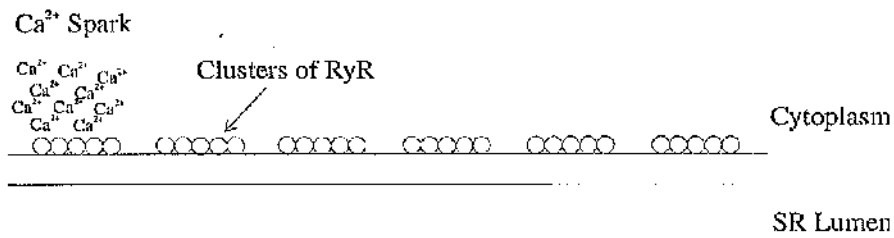


Figure 1.6: The proposed theories to induce calcium release in striated muscle. **A)** The stochastic gating theory proposes that the RyR operate independently of one another. The calcium released from one RyR increases the local calcium levels in the dyadic junction to stimulate the neighbouring RyR via CICR, thus the RyR open and close randomly. **B)** The coordinated-gating theory proposes that the RyR are mechanically linked to operate in a coordinated manner and thus give rise to fast local calcium release events.

(A)



(B)

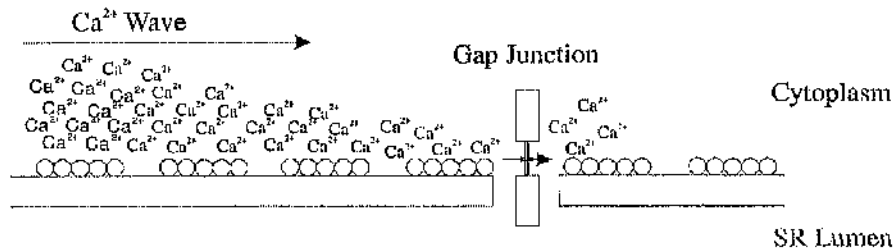


Figure 1.7: Coordinated SR calcium release via RyR clusters. A) Clusters of RyR are distributed along the SR and upon stimulation; small calcium release events called quarks summate to produce a calcium spark. B) When the cells are exposed to a maximal stimuli, calcium sparks summate to form a calcium wave and is then transmitted through the cell to induce the release of calcium neighbouring cells via CICR.

CHAPTER TWO

METHODS AND MATERIALS

2.1. PREPARING CELLS FOR CALCIUM UPTAKE MEASUREMENTS

2.1.1. Rabbit Models: Coronary Artery Ligated, Sham and Control

A coronary artery ligation model of left ventricular dysfunction was used in these studies as described by Pye et al., (1996). Experiments were undertaken in adult New Zealand White male rabbits (2.5-3kg) and the surgery was performed by technicians in the animal house at Glasgow Royal Infirmary. General anaesthesia was induced using Hypnorm and maintained with Halothane and Nitrous Oxide/Oxygen. After induction, a left thoracotomy was performed and the large circumflex branch of the left coronary artery was identified and occluded approximately midway between the left atrial appendage and the cardiac apex. This procedure gives rise to a large homogenous infarct in view of the minimal collateral circulation in the rabbit. Intravenous Quinidine was administered to minimise perioperative ventricular fibrillation. Post operative analgesia was provided and prophylactic antibiotics were administered. Animals were monitored for signs of distress and were withdrawn from the experimental protocol in cases of weight loss greater than 20% of baseline, evidence of overt infection or severe distress.

Sham operated animals were prepared in an identical manner, but the coronary artery was not tied. Following surgery, animals were allowed to recover for 8 weeks prior to being sacrificed for in vitro experimentation. Control animals were not subjected to an operation.

Prior to sacrifice, all animals underwent echocardiographic examination to assess the degree of left ventricular dysfunction produced by the experimental infarct. This was undertaken using a 5 MHz focused paediatric transducer under light sedation with Hypnorm. M-mode measurements of ventricular end diastolic diameter was made and area ejection fraction was calculated from 2-D measurements of end systolic and end diastolic dimensions in the short axis (Pye et al., 1996).

2.1.2. Harvesting

New Zealand White, adult, male rabbits (2.5-3kg) were subjected to deep anaesthesia via the marginal ear vein with an intravenous injection of 500U heparin together with a terminal overdose of sodium pentobarbitone (100mg/kg). The thoracic cavity was opened, the heart quickly excised then placed into a beaker of ice cold calcium free Krebs. These procedures were carried out by the

technicians Aileen Rankin and Anne Ward or me and unless otherwise stated, all the procedures after this point were carried out by me.

2.1.3. Isolating Cardiac Myocytes

To dissociate cardiac myocytes from an isolated whole heart, the excised heart was quickly mounted and tied via the aorta onto the cannula of a Langendorff retrograde perfusion system. The heart was trimmed removing fat and connective tissues. 200mls of calcium free Krebs (Table 2.2), maintained at 37°C and bubbled with 100% O₂, was perfused through the heart at a rate of 25mls/min to remove blood and calcium. The calcium free Krebs solution was made the previous day and the glucose was added on the day of the cell isolation. The heart was then perfused with an enzyme solution containing 3mg of protease (Type XIV) and 50mg of collagenase (Type 1), dissolved in 75mls of calcium free Krebs (Table 2.2). The enzyme was collected as it passed through the heart and then re-circulated once the initial volume of enzyme had been through. The recirculating enzyme was continued for 10 minutes to allow initial digestion of connective tissue until the left ventricular tissue became soft. The heart was then perfused with 100mls of 0.2% BSA solution (0.2% BSA, 10mM Creatine, 11.1mM Glucose, 20mM HEPES, 5.4mM KCl, 3.5mM MgCl₂, 120mM NaCl, 0.52mM NaH₂PO₄, 20mM Taurine) before the heart was cut down. The atria were discarded and the left and right ventricle were placed into a petri dish containing 10mM Ethylene bis[oxyethylenetriolo]tetraacetic acid (EGTA) solution (Table 2.2). The tissue was finely chopped into small sections before the myocytes were dissociated by lightly titrating the solution for about ten minutes. The cell suspension was filtered through 250µm nylon mesh before being spun gently for 2 minutes with a hand spinner. The supernatant was discarded and cell pellet resuspended in 10mM EGTA with 1mM ATP and 40mM CrP (Table 2.2) before being permeabilized with β-escin (Chapter 2.1.3). The cells were kept at room temperature (22°C) during the experiment.

In order to make comparative measurements of SR calcium uptake rates in myocytes, it was necessary to standardise the preparation as myocyte yield of rods varied between dissociations. The dissociation produces both rod shaped myocytes and myocytes that are balled-up. In our preparation both rods and balled-up cells were counted, as balled-up cells may retain functional SR material

(Chapter 3). The cells were counted using a haemocytometer where balled-up cells as well as rod shaped cells were counted. To obtain 1×10^6 cells total cells per ml (a standard concentration to provide valid comparison of calcium uptake rates) the suspension was either concentrated by centrifugation or diluted to give the desired concentration of cells. Then a recount took place to confirm myocytes concentration.

2.1.4. Chemical Skinning Procedure

β -escin is a saponin ester. Saponins are non-cardiac active alkaloids, some of which are extracted from plants and are available commercially (Sigma and BDH). At certain concentrations, saponins have been reported to selectively bind cholesterol residues in the sarcolemma (Ohtsuki *et al.*, 1978), causing the formation of 10-50nm holes (Seeman, 1967). β -escin has little or no effect on the membranes of intra-cellular organelles, thus permeabilised cells retain an active SR component (Endo & Iino, 1980). This is believed to be due to these internal membranes contain less cholesterol than the sarcolemma (Martinosi, 1968; Waku, Uda & Nakazawa 1971). The technique allows for the passage of substances through the sarcolemma membrane and into the interior of the cell thus allowing the regulation of the intracellular environment of the cardiac myocyte under these experimental conditions.

2.1.4.1. β -escin concentration curve

To ascertain the β -escin concentration required to 'skin' 100% of the cell population, the following protocol was carried out. 1×10^6 cells were bathed in 3mM EGTA (~ 1 nM calcium) at pH 7.0 then incubated in β -escin for 2 mins, increasing the β -escin concentration from 0-1000 μ g/ml. The cells were then spun down with a hand spinner, the supernatant was discarded and the pellet resuspended in 3mM EGTA. Counting the cells using a haemocytometer allowed for the determination of the percentage of rod shaped cells present after permeabilisation. In order to observe the effects of β -escin permeabilisation in the presence of a high calcium concentration, the same procedure was carried out but in the presence of 3mM CaEGTA (~ 10 μ M calcium). This level of calcium, if given access to the intracellular space, would cause a sustained contraction. Therefore the percentage of

cells forming hypercontracted balls, in the presence of 10 μ M calcium, reflect the cells that were rendered hyperpermeable by the β -escin treatment.

From figure 2.1, it was noted that increasing the calcium concentration from 1nM to 10 μ M in the presence of 0-1 μ g/ml β -escin, caused 50% of the myocytes to contract. This suggests that prior to β -escin treatment, the cells are hyperpermeable, possessing damaged membranes as a result of the isolation procedure. In the presence of 10 μ g/ml of β -escin, 80-90% of the cells hypercontracted indicating that a significant concentration of the cells were skinned, with 100% occurring in the presence of 100 μ g/ml and 1000 μ g/ml. However, 1000 μ g/ml of β -escin also induced 100% hypercontraction of the cells in the presence of the low calcium concentration solution. From this data we can conclude that 1000 μ g/ml of β -escin damages myocytes and therefore stimulates contraction of the cells in the absence of calcium.

2.1.4.2. Skinning of dissociated myocytes

Skinning the cells is achieved prior to each experiment. In this study, 100 μ g/ml of β -escin was used to achieve the skinning of close to 100% the cell population without damaging a significant proportion of the myocytes. 100 μ g β -escin was added to 1ml of cells, gently shaken for a minute then the cells were spun down with a hand spinner. The supernatant was discarded and the cells were resuspended in 0.05R (Table 2.2), before a last spin and resuspension in the final volume of 0.05R. This allows both β -escin and 10mM EGTA to be effectively removed from the solution.

2.2. MEASURING CHANGES IN INTRACELLULAR CALCIUM

2.2.1. Cuvette System

1 \times 10⁶ of the permeabilised cells were added to a closed cuvette system (Fig. 2.2), containing a mock intracellular solution mimicking the cell's intracellular environment (Table 2.2, 0.05R), along with the following drugs (Table 2.3). The cells suspension was constantly stirred at 20-22 $^{\circ}$ C to prevent cells settling and the stirrer speed was not changed between experiments. MgATP was added to supply the energy required for myofibril contraction; CrP to regenerate ATP from ADP; HEPES to maintain physiological environment and buffer H⁺; K₂Oxalate to maintain a low intraluminal

calcium concentration within the SR thus facilitating calcium uptake; K₂EGTA to reduce intracellular calcium concentration; Ruthenium Red (RuR) to inhibit calcium uptake/release by the mitochondria and to inhibit calcium induced calcium release from the ryanodine receptor (RyR); 0.033mM oligomycin and 0.01mM CCCP were used to inhibit mitochondrial activity.

2.2.2. Fura-2

The changes in the free intracellular calcium concentration were measured with the fluorescent indicator Fura-2 (10µM). The fluorescent ratio was produced due to excitation at 340nm and 380nm from a xenon arc light source and a spinning wheel system (Cairn Research Ltd, Kent, UK) at 30Hz. The fluorescence evoked was passed to a photomultiplier and the output signal correlated with the excitation filter using circuitry on the spectrophotometer (Cairn Research Ltd, Kent, UK). A ratiometric measurement of free calcium concentration was calculated from the fluorescence at 340 and 380nm and stored to disc using the program Newtape (Francis Burton, 1990) as well as to a chart recorder.

2.2.3. Oxalate

Oxalate was used to prevent the increase in free calcium concentration inside the SR (that would otherwise slow the rate of net uptake) by the precipitation of calcium-oxalate inside the SR (Madeira, 1982). A consequence of this is that the rate of SR calcium uptake can stay at the same rate determined by the free calcium in the suspension (rather than limited by high free calcium inside the SR). It has been shown that crystallization of calcium-oxalate inside the SR does not reach equilibrium at any time during calcium uptake (Feher & Briggs, 1980), and thus will continue to buffer intraluminal calcium. It is well documented that SR calcium leak depends on SR calcium content (Bassani, J. W. M. *et al.*, 1995; Smith & Steele, 1998; Shannon T.R. *et al.*, 2000) as well as the free calcium concentration in the mock intracellular solution (Ashley & Williams, 1988, 1989, 1990).

2.2.4. Calibration curve for Fura-2 measurement of free calcium

The relationship between calcium concentration and fluorescence ratio was established with a series of calibration experiments. The calibration experiments required a variety of solutions, containing increasing calcium concentrations (Table 2.5). These solutions were prepared from the stock solutions; 10mM EGTA (Table 2.4) and 10mM CaEGTA (Table 2.4). The calcium concentration in these solutions was calculated using the program React (Godfrey Smith 1990) with the binding constants for EGTA taken from Smith & Miller (1985) and the binding constants for ATP and CrP were taken from Fabiato & Fabiato (1975b).

The data for the calibration curve were produced by adding 1.5mls of the calcium solution (Table 2.5) to a cuvette together with 10 μ M Fura-2 and a stirrer bar. Each cuvette was then placed into the spectrophotometer and the fluorescence ratio produced at 340 and 380nm was noted. A calibration curve was then plotted for Fura-2 fluorescence ratio against the calcium concentration. The relationship was found to be sigmoidal and can be described by the following equation [1]:

$$[1] \quad \text{Ca}^{2+} = K_D \times [(R - R_{\min}) / (R_{\max} - R)]$$

Where 'R' is the measured Fura-2 ratio, 'R_{min}' is the ratio in calcium free solutions, 'R_{max}' is the ratio at saturating calcium concentrations and 'K' is constant (Grynkiewicz et al. 1985). A curve was then fitted to the data points using the equation [2]:

$$[2] \quad R = \frac{[([Ca^{2+}] / K_D) \times (R_{\max} + R_{\min})]}{(1 + X) \times K_D}$$

(Grynkiewicz et al. 1985)

Here R (Fura-2 ratio) is a function of the calcium concentration and dependent on the constants R_{max}, R_{min} and K_D. The curve was fitted by iterative variations of these constants until the best fit was found. This was achieved using the program Origin (Microcal Software). Utilising the constants calculated from this curve fitting, calcium concentrations could then be calculated from any given Fura-2 ratio using equation [1].

2.3. MEASUREMENT OF PROTEIN CONCENTRATION

The protein content for the cell solution after each experiment was determined using Coomassay dye and a 96 well plate.

2.3.1. Preparation for protein assay

An aliquot of the cell suspension solution was transferred from the cuvette into a 1.5ml Eppendorf tube and placed on ice to minimise protein degradation. If the cell suspensions were frozen with liquid nitrogen at the end of the experimental day, then the Eppendorfs were placed into a water bath and left to defrost.

The concentration of the standards required as a reference for the plate reader were made from a 2mg/ml BSA stock solution and deionised water (dH₂O) was used to dilute the BSA stock solution; the dilutions were as follows, 0.1mg/ml, 0.25mg/ml, 0.5mg/ml, 0.75mg/ml, 1mg/ml.

The protein samples were then diluted with dH₂O and two dilutions of the protein samples were made to make sure one of the readings measured was within the limits of the standards. The first dilution was in the ratio 1:1 (25 µl of sample was added to 25µl of dH₂O) and the second dilution was in the ratio 1:4 (10µl of the sample was added to 40µl of dH₂O). These dilutions were repeated for each new sample and a few samples were collected before the plate was run. If the colour change of the protein samples, upon addition of the dye, was out with the range of the standards then a more dilute protein sample was prepared.

2.3.2. Plating the samples and standards

10µl of the standards were plated out in triplicate into columns B through to C. In column A the background buffer was added to act as the blank. So in row 2, 0.1mg/ml of BSA was added in triplicate then in row 3, 0.25mg/ml of BSA, row 4 0.5mg/ml and so on. Once standards were plated, 200µl of the dye was introduced to the standards to make sure the triplicates were the same colour, if not then the plate had to be redone because it is important to get the standards as accurate as possible so that the sample reading would be accurately read. A standard curve for the protein standards was produced in order to calculate the protein concentration of the samples (Figure 2.3).

10 μ l of the samples were plated in triplicate and for the first few samples; 200 μ l of the dye was added to the wells, in order to check that the samples were within the standard range. If the colour change of the samples were within the colour range of the standards the rest of the samples were then plated out. If not, then a more diluted sample was prepared and plated for each new sample. Once all the samples were plated, 200 μ l of the dye was added to each well, making sure there were not any bubbles in the wells as this interferes with the plate reading. If bubbles were present, they were removed by bursting them with a clean needle. The plate was then read at 595nm, the computer automatically calculated the protein content and the results were printed out.

2.4. DATA RECORDING, ANALYSIS AND CURVE FITTING

During the experiment, the raw data was plotted in real time on chart paper, and the output voltage from the spectrophotometer for the individual wavelengths and the ratio were stored on hard disc for later analysis. The analysis of the digitised fluorescent ratio and wavelengths required the program QA (Francis Burton, 1990); the areas of interest within the data sets were selected for, and the digitised data was then converted into calcium concentrations using the parameters provided by the Fura-2 calibration curves. These values were plotted using the program Origin (Microcal software). Mono- and bi-exponential curves were fitted to the uptake time course using the inbuilt fitting routines, below 700nM calcium concentration and the best fit was provided by the Bi-exponential decay. From this plot, two time constants for each decay curve were calculated and noted as t_1 and t_2 ; t_1 was taken to reflect the fast phase of calcium uptake time course and t_2 was taken to reflect the slow phase of calcium uptake time course. However, only t_1 was utilised in the comparison of the calcium uptake rate between experiments as t_2 values were found to vary greatly within one experiment while the faster component, t_1 , was more consistent and represented the major component of calcium uptake under these conditions. Therefore only t_1 was used in the analysis.

The relationship of the ratio of Fura-2 fluorescence at 340nM and 380nM to calcium concentration was described in chapter 2.3.2. The relationship is sigmoidal (Figure 2.4) and depends on the constants R_{min} , R_{max} and K_d . These constants vary depending upon several properties of the system in use, in particular, the optical properties of the system and the presence of

other chemicals within the solution. For these reasons it was necessary to plot a calibration curve for these experiments. This was achieved as described previously in chapter 2.3.2, combining different ratios of 10mM EGTA and 10mM CaEGTA (individual solution composition, Table 2.4; Ratio mix, Table 2.5) to create a range of calcium concentrations before measuring the ratio of fluorescence at 340 and 380nm. The addition of high concentrations of RuR affected the fluorescence properties of Fura-2, quenching the fluorescent signal of both wavelengths. Therefore, when RuR concentration exceeded 5 μ M, a calibration curve was plotted in the presence and in the absence of RuR. The constants produced from the calibration curves were then used to compute the time constant (t_1) for the rate of calcium decay. Table 2.6 displays the constants produced from the Fura-2 and RuR calibration curves.

COMPOUND	SUPPLIER	SOLVENT
ATP (disodium salt)	Sigma	dH ₂ O
Bastadin mix(5-12)	Calbiochem	Methanol
β-escin	Sigma	dH ₂ O
BSA	Sigma	dH ₂ O
CaCl ₂	BDH	-
Caffeine	Sigma	dH ₂ O
CCCP	Calbiochem	EtOH
Collagenase (Type 1)	Worthing Chemicals	-
CrP (disodium salt)	Fluka	dH ₂ O
DTT	Sigma	EtOH
EGTA	Sigma	dH ₂ O
Fura-2	Molecular Probes	dH ₂ O
Glucose	Fischer	dH ₂ O
Heparin	-	-
Hepes	Sigma	dH ₂ O
Ionomycin	Calbiochem	DMSO
KCL	BDH	-
KH ₂ PO ₄	BDH	dH ₂ O
MgCl ₂	BDH	-
NaCl	BDH	-
NaHCO ₃	BDH	dH ₂ O
Oligomycin	Calbiochem	EtOH
Oxalate	Sigma	dH ₂ O
Phenobarbitone	-	-
Protease (Type XIV)	Sigma	dH ₂ O
Rapamycin	Calbiochem	-
RuR	Sigma	dH ₂ O
Thapsigargin	Calbiochem	DMSO

Table 2.1: List of drugs and compounds used in the experimental protocol.

Compound	Solution Composition			
	Ca ²⁺ Free Krebs (mM)	Ca ²⁺ Free Krebs + 10mM EGTA (mM)	0.05R (mM)	ATP + CrP (mM)
ATP	-	1	-	20
Creatine	10	-	-	-
CrP	-	4	-	40
EGTA	-	10	0.05	0.05
Glucose	11.1	11.1	-	-
HEPES	20	20	25	25
KCL	5.4	5.4	120	100
MgCl ₂ 6H ₂ O	3.5	7.0	1	19.75
NaCl	120	120	40	-
NaH ₂ PO ₄	0.52	0.52	-	-
Taurine	20	20	-	-

Table 2.2: List of chemicals required to make calcium free Krebs (pH 7.25 @ 37°C), 0.05R (pH 7 @ 22°C), 0.05R with ATP and CrP, and 10mM EGTA (pH 7 @ 22°C). The solvent used was distilled water (dH₂O).

COMPOUND	CONCENTRATION (mM)
Fura-2	0.01
Oxalate	0.02
RuR	0.005
ATP	5
CrP	15
DTT	0.1
CCCP	0.01
Oligomycin	0.033

Table 2.3: List of chemicals added to the cuvette system. The concentrations of the solutions listed were added to the cuvette system at the start of each experiment unless otherwise stated. Oxalate, RuR, ATP and CrP were all dissolved in dH₂O, pH to 7 using KOH, at 20-22°C.

COMPOUND	SOLUTION COMPOSITION (mM)	
	10mM EGTA	10mM CaEGTA
EGTA	10	-
CaEGTA	-	10
HEPES	25	25
KCL	120	120
NaCl	40	40
MgCl	1	1

Table 2.4: List of chemicals required to make 10mM EGTA and 10mM CaEGTA stock solutions for Fura-2 calibration curve. The final solution was pH to 7 using KOH, at 20-22°C and the solvent used was dH₂O.

RATIO of EGTA:CaEGTA	Volume (mls)		[Ca²⁺] (M)
1:0	5	-	0.2E-09
10:1	5	0.5	4.0E-08
3:1	3	1	1.2E-07
1:1	2	2	0.375E-06
1:3	1	3	1.12E-06
1:10	0.5	5	4E-06
0:1	-	5	6.0E-05

Table 2.5: Summarizes the ratios and volumes required to make up increasing calcium concentrations using 10mM EGTA and 10mM CaEGTA stock solution. The stock solutions were made prior to experiment, pH to 7 with KOH at 20-22°C.

Constants	No RuR	5µM RuR	13.3µM RuR
R_{min}	0.8µM ± 0.09	0.79µM ± 0.009	0.77µM ± 0.008
R_{max}	10.8µM ± 0.25	10.9µM ± 0.28	11.09µM ± 0.28
K_D	1.43µM ± 0.1	1.3µM ± 0.08	1.9µM ± 0.04

Table 2.6: Values for the constants, R_{min}, R_{max} and K_D produced from calibration curves in the absence, in the presence of 5µM RuR and in the presence of 13.3µM RuR.

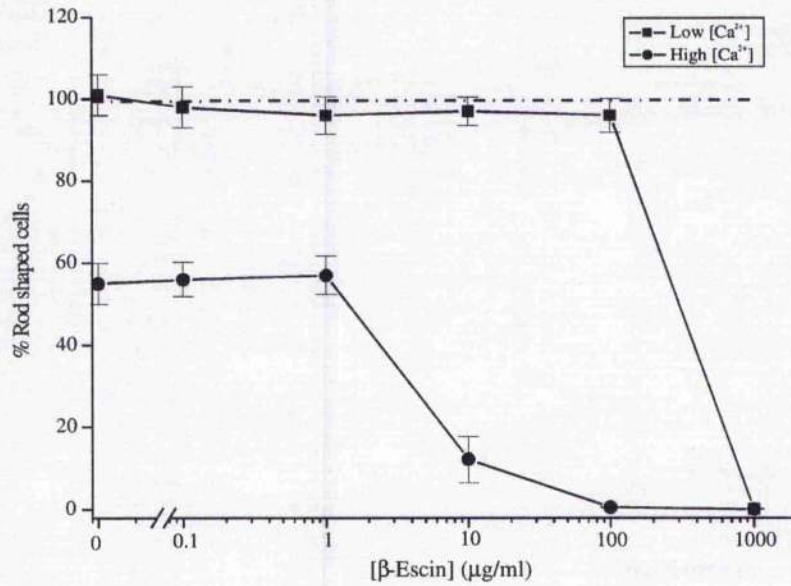


Figure 2.1: The effects of increasing β -escin concentrations in the presence of 1nM and 10 μ M calcium in cardiac myocytes. 1×10^6 cells were incubated in 3mM EGTA ($\sim 1\text{nM Ca}^{2+}$) then 3mM EGTA and β -escin for 2 minutes, [-■-] or 3M CaEGTA ($\sim 10\mu\text{M Ca}^{2+}$) and β -escin for 2 minutes, [-●-]. In the presence of 0 - 1 μ M/ml β -escin, increasing the calcium concentration from 1nM to 10 μ M caused 50% of the myocytes to contract, compared to 80 - 90 in 10 μ g/ml β -escin and 100% in the presence of 100 μ g/ml β -escin. No significant contraction occurred in 1nM calcium, until 1000 μ g/ml. The data was expressed as mean \pm s.e.m. (n = 13) and the difference was considered significant at $P < 0.05$. ANOVA with a Tukey post hoc test was used for multiple comparisons.

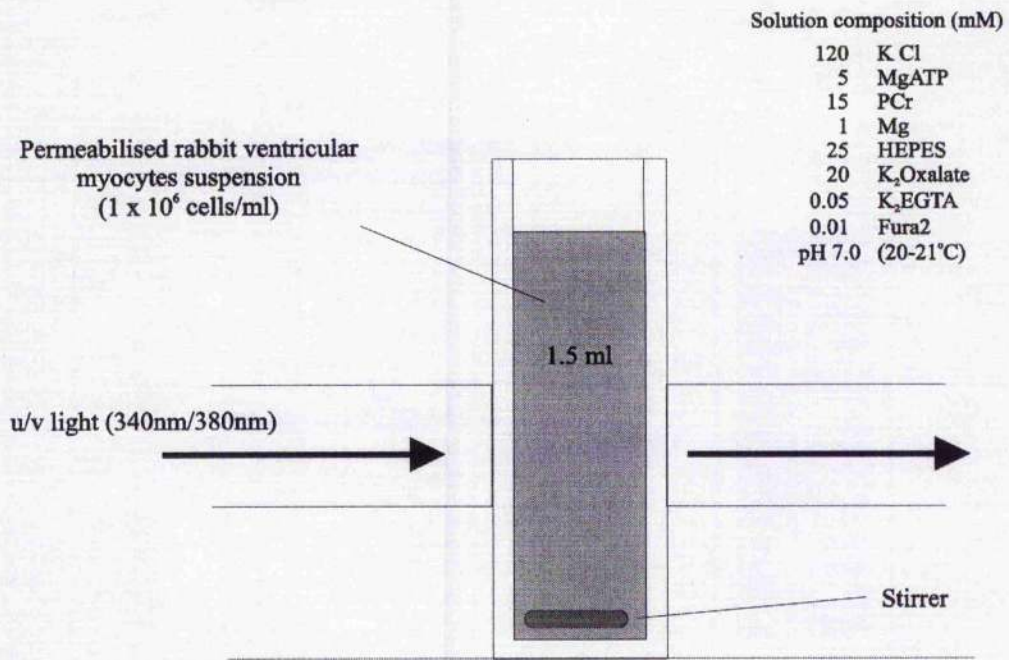


Figure 2.2: Diagram of the cuvette system. Apparatus used to measure changes in intracellular calcium concentrations of permeabilised cardiac myocyte cell suspension.

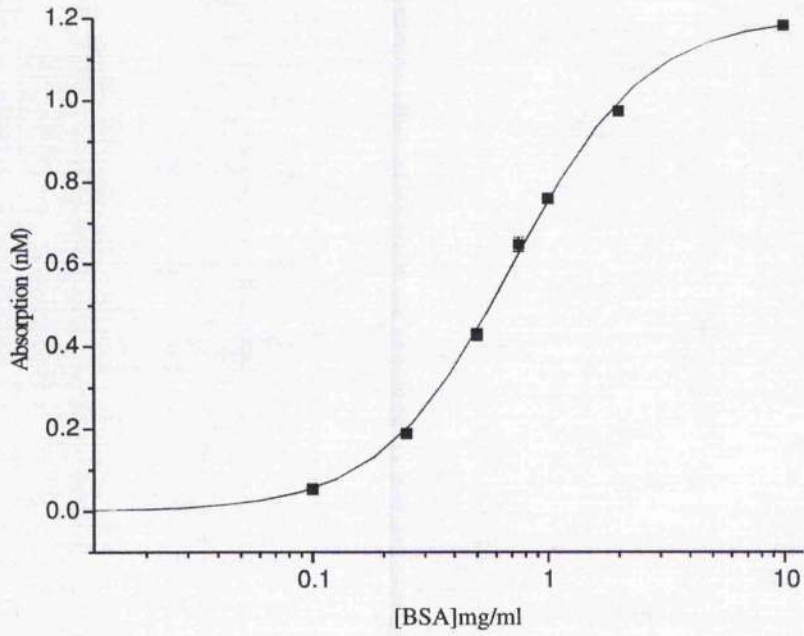


Figure 2.3: *Calibration curve for the protein standards.* Where Absorption (nm) is plotted against the Bovine Serum Albumin concentration ([BSA]) to give a sigmoidal relationship (mean \pm s.e.m., $n = 13$).

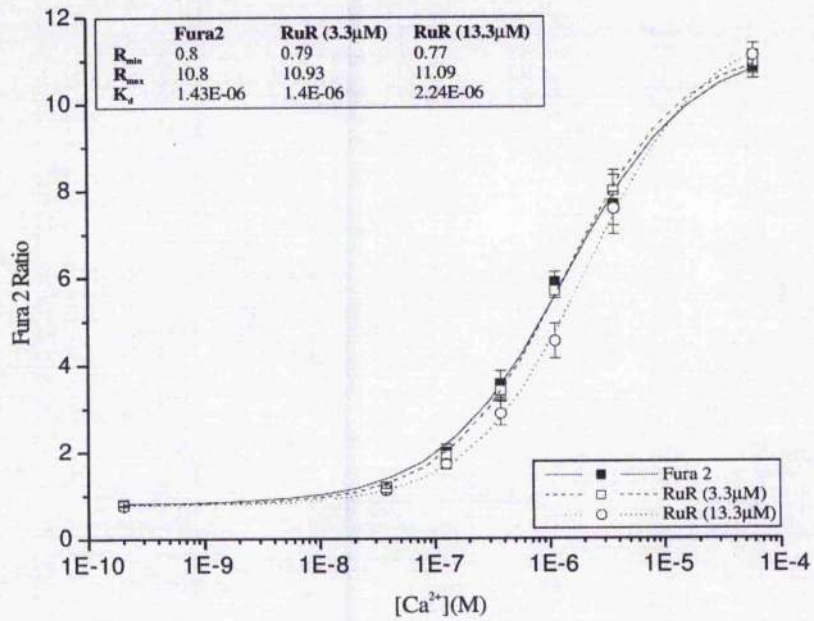


Figure 2.4: Calibration curves for Fura-2 (-■-), 3.3µM RuR (-□-) and 13.3µM RuR (-○-). The ratio of the Fura-2 fluorescence is plotted against the calcium concentration to give a sigmoidal relationship. The data was expressed as mean ± s.e.m. (n = 10) and the difference was considered significant at P<0.05. ANOVA with a Tukey post hoc test was used for multiple comparisons.

CHAPTER THREE

CALCIUM UPTAKE V PROTEIN MEASUREMENT

3.1 RELATIONSHIP BETWEEN TOTAL PROTEIN AND YIELD OF RODS

Figure 3.1 shows the linear relationship between total protein and cell number. No difference is observed between the three experimental groups, control, ligation and sham. Although more of a linear relationship occurred over the cell number range $5-15 \times 10^5$ producing a total protein level between 1-3mg. The yield of rods present ranged from 10-50 percent as seen in figure 3.2.

In Figure 3.2, the yield of rods ranged from 10-50% and no relationship was detectable between the total number of cells per mg of protein and the percentage yield of rods. Therefore, no protein degradation was observed as the percentage yield of rods decreased, indicating the rod cell count does not influence the total protein to a significant degree, whereas total cell number has a linear relationship with total protein, implying balled-up cells contribute to total protein. Overall, the yield of rods does not influence total protein, whereas total cell number does.

3.2 RELATIONSHIP BETWEEN CALCIUM UPTAKE RATE, CELL NUMBER AND YIELD OF RODS

Figure 3.3 is a typical experimental trace showing the calcium uptake protocol. Addition of an aliquot of calcium chloride (10 μ l of 10mM) increases the total calcium concentration within the cuvette by 67 μ M and causes a rapid increase of the free calcium concentration to approx. 1.6 μ M. Over the following 12 minutes, the calcium decayed below 100nM. This was repeated three times, noting the reproducibility of the transients. Addition of thapsigargin (5 μ M) caused an increase in the calcium concentration within the cuvette. This represents a linear calcium leak from the SR, since thapsigargin inhibits the calcium uptake processes. High concentrations of thapsigargin (5 μ M) were used to ensure effective inhibition of calcium pump activity. Assessing the calcium content of the SR with thapsigargin would not be practical since previous work (data not shown) has shown this would take over 3 hours so we increased calcium leak from the SR by the addition of Ionomycin (10 μ M), 15 minutes after the addition of thapsigargin.

Figure 3.4 shows a weak linear relationship between the rate constant (t_1) for calcium uptake and cell number and increasing the cell number produces an increase in rate constant. This could be explained in terms of calcium pumps; the more cells you have, the more functional pumps that would be present to take up calcium, thereby increasing the rate constant for calcium uptake into the SR.

Figure 3.5 displays the relationship between the rate constant (t_1) for calcium uptake and percentage yield of rods. From the figure, no relationship is observed suggesting that the increase in functional pumps observed in figure 3.4 is not due to an increase in the percentage yield of rods. As more rods would lead to an increase in rate constant, but no trend is observed.

Figure 3.6 shows the linear relationship between the rate constant for calcium uptake against total protein. Increasing the protein concentration increases the rate constant for calcium uptake. Similar results are displayed in figure 3.4, where the rate constant was plotted against cell number. However the relationship in figure 3.4 is not as good as that seen here. Figure 3.4 has a lower R value, of 0.683 where as here we have an R value of 0.85.

3.3 CALCIUM BUFFERING

This chapter concentrates on calcium buffering within the cuvette system in order to determine the calcium binding capacity of the solution containing the cardiac myocytes. Several studies have provided experimental information about the intracellular calcium buffering capacity and have thus shown that total calcium binding in some systems may be underestimated because of calcium binding to unknown sites, to the mitochondrial surface and to high affinity binding sites in the sarcolemma (Hove-Madsen & Bers, 1993; Fabiato, 1983). Measuring passive calcium buffering proves difficult in the presence of calcium uptake and calcium release from intracellular compartments. To inhibit these specific calcium regulatory mechanisms, $5\mu\text{M}$ thapsigargin was introduced to inhibit calcium uptake into the SR (Llopis *et al.*, 1991; Sagara & Inesi, 1991) and $5\mu\text{M}$ RuR to inhibit calcium release from the mitochondria as well as from the SR (McCormack *et al.*, 1989; Wimsatt *et al.*, 1990).

Figure 3.7 displays the relationship of bound and free calcium within the cuvette system. To assess whether calcium binds to non-specific sites within the cuvette, calcium was added in the presence of 50 μ M EGTA. This was referred to as the blank as the solution did not contain cardiac myocytes. It was noted that the calcium buffering in the presence of EGTA solution fitted that of the EGTA calcium binding curve model. Indicating little or no calcium binds to the apparatus used. On introduction of 20 μ M oxalate in the presence of 50 μ M EGTA, the measured free calcium increased rapidly to a concentration of 2 μ M then gradually plateaued in the presence of an increasing total calcium concentration where the curve superimposed the EGTA model up to 4 μ M free calcium. The absence of calcium saturation as seen with EGTA alone indicates a buffering mechanism was initiated, which was not significantly effected by increasing concentrations of cardiac myocytes until the free calcium concentration reached 3 μ M. Additional buffering was noted for 2x10⁶ cells/ml as the total calcium concentration increased above 3 μ M. However, in the cuvette system used in this investigation, the total free calcium concentration observed fell within the range 0-3 μ M and therefore no additional calculations had to be made to correct for calcium binding to unknown sites as all the graphs were superimposable below 3 μ M (Figure 3.7B).

3.4 DISCUSSION

Figures 3.1, 3.4 and 3.6, emphasize the point that cell number correlates well with protein concentration, whereas percentage yield of rods does not, figure 3.2 and 3.5. This implies, that amount of total protein does not depend on the yield of rod, so therefore balled cells must contribute to total protein. The fact that increasing cell number, or total protein can increase the rate of calcium uptake into the SR suggests more cells with functional pumps leads us to think about balled cells, and their calcium pumps. These data implies that balled cells may indeed have functional pumps, thus contribute to the total protein concentration.

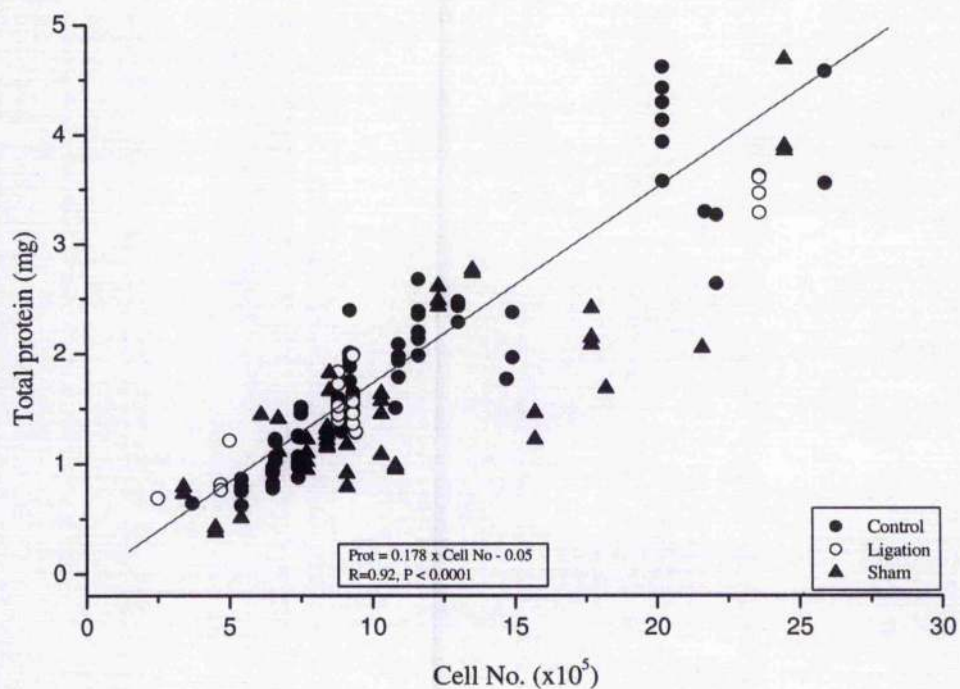


Figure 3.1: The relationship between total protein and cell number. The solution composition, bathing the cells during the experiment, is as follows; 0.05R (Table 2.2), 20mM Oxalate, 25 μ M RuR, 10 μ M Fura-2, 5mM ATP, 15mM CrP, 0.1 μ M DTT, 10 μ M CCCP and 33 μ M Oligomycin. The relationship was explained with the use of Linear Regression ($n = 100$).

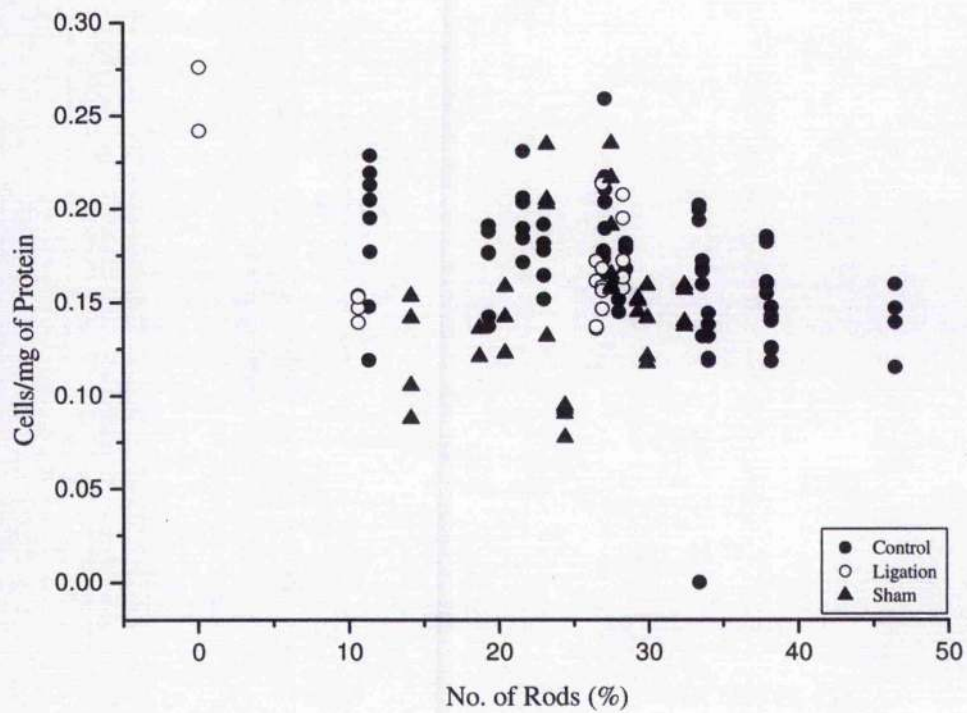


Figure 3.2: The relationship between the total number of cells per mg of protein and the percentage yield of rods. The solution composition, bathing the cells during the experiment, is as follows; 0.05R (table 2.2), 20mM Oxalate, 25 μ M RuR, 10 μ M Fura-2, 5mM ATP, 15mM CrP, 0.1 μ M DTT, 10 μ M CCCP and 33 μ M Oligomycin. (n = 134)

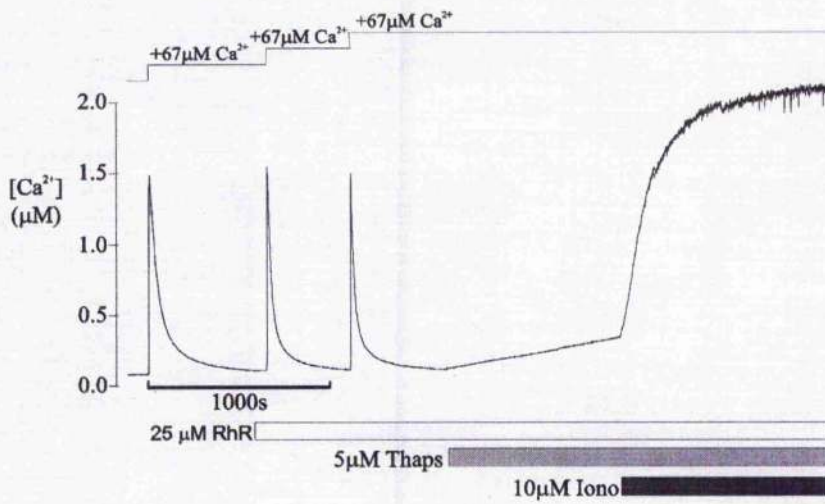


Figure 3.3: A typical experimental trace showing the calcium uptake protocol. An addition of an aliquot of calcium chloride ($67\mu M$) caused a rapid increase of the free calcium concentration to approx. $1.6\mu M$. Over the following 12 minutes, the calcium decayed below $100nM$. Another two aliquots of calcium were added in the presence of $25\mu M$ RuR, 12 minutes apart before the preparation was subjected to $5\mu M$ Thapsigargin. The leak induced with Thapsigargin was enhanced with $10\mu M$ ionomycin, both being incubated for 15 minutes. The solution composition, bathing the cells prior to the additions indicated in the figure, is as follows; $0.05R$ (table 2.2), $20mM$ Oxalate, $10\mu M$ Fura-2, $5mM$ ATP, $15mM$ CrP, $0.1\mu M$ DTT, $10\mu M$ CCCP and $33\mu M$ Oligomycin.

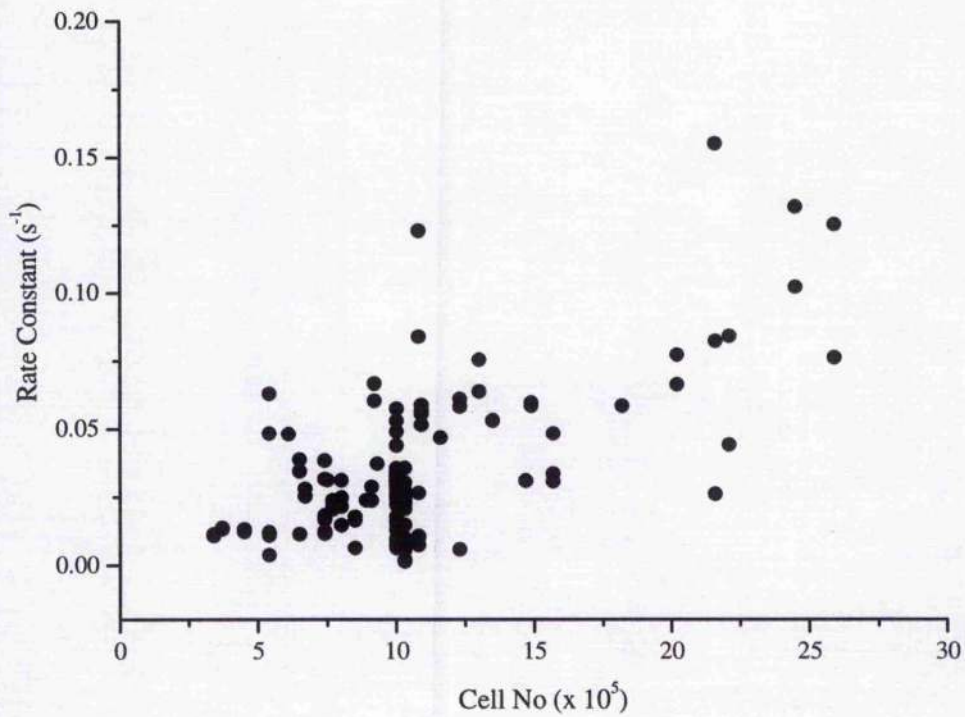


Figure 3.4: The relationship between the rate constant (t_1) for calcium uptake and the cell number. The solution composition, bathing the cells during the experiment, is as follows; 0.05R (table 2.2), 20mM Oxalate, 25 μ M RuR, 10 μ M Fura-2, 5mM ATP, 15mM CrP, 0.1 μ M DTT, 10 μ M CCCP and 33 μ M Oligomycin. (n = 124)

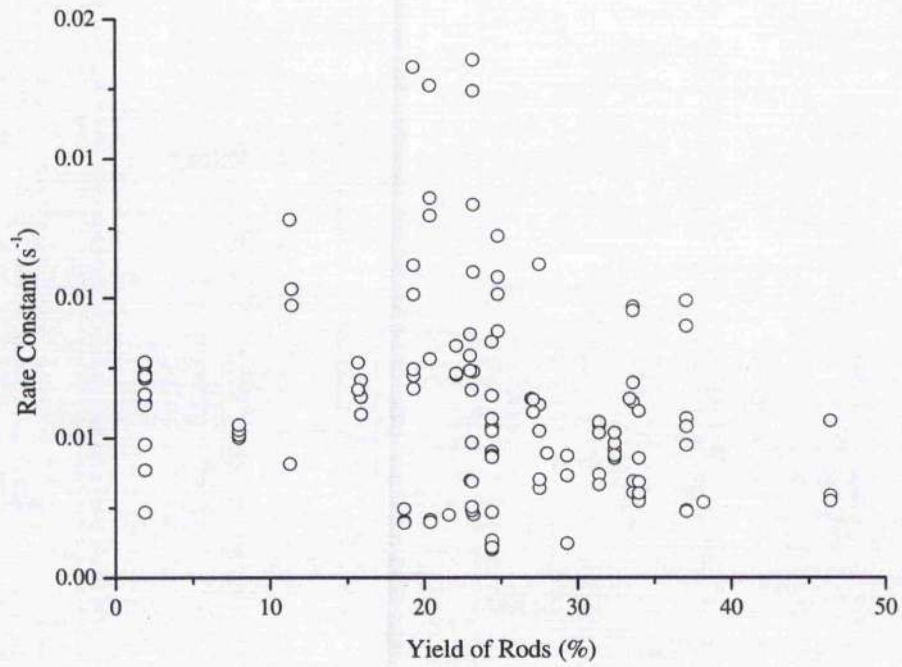


Figure 3.5: The relationship between the rate constant (t_1) for calcium uptake and percentage yield of rods. The solution composition bathing the cells during the experiment is as follows; 0.05R (table 2.2), 20mM Oxalate, 25 μ M RuR, 10 μ M Fura-2, 5mM ATP, 15mM CrP, 0.1 μ M DTT, 10 μ M CCCP and 33 μ M Oligomycin (n = 127).

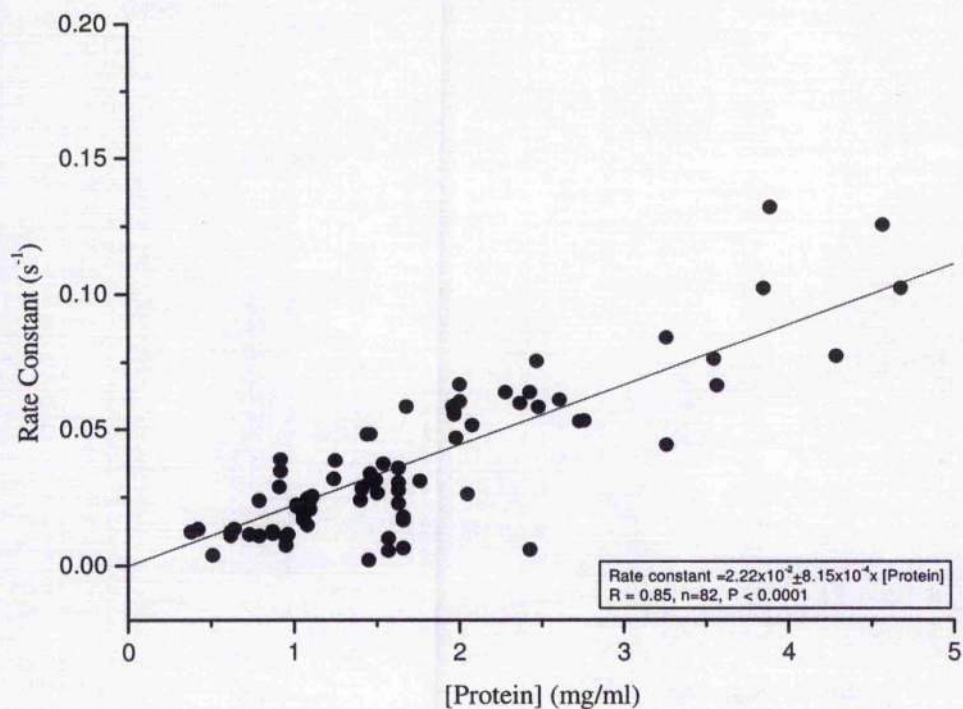
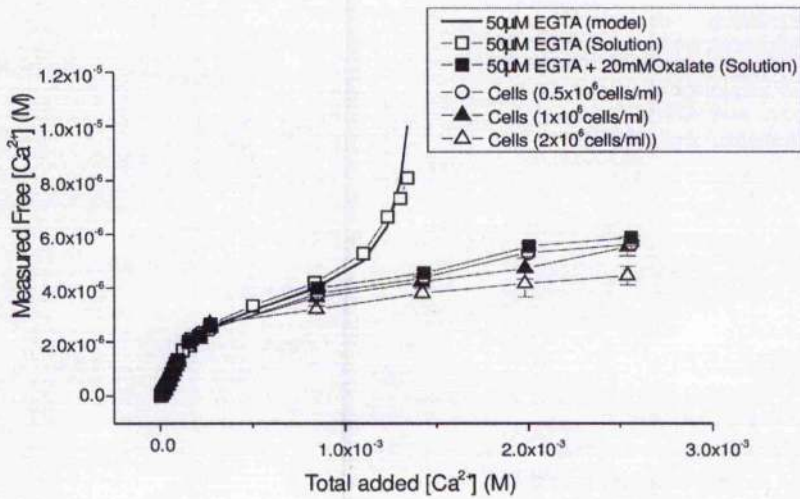


Figure 3.6: The relationship between the rate constant for calcium uptake against total protein. The solution composition bathing the cells during the experiment, is as follows; 0.05R (table 2.2), 20mM Oxalate, 25 μ M RuR, 10 μ M Fura-2, 5mM ATP, 15mM CrP, 0.1 μ M DTT, 10 μ M CCCP and 33 μ M Oligomycin. The relationship was explained with the use of Linear Regression (n = 82).

(A)



(B)

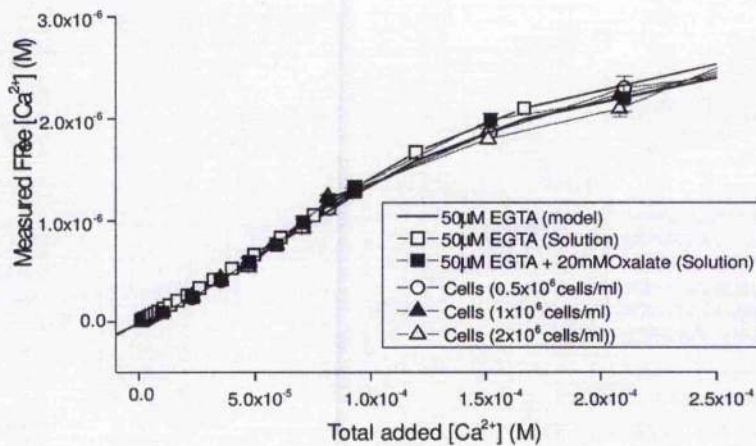


Figure 3.7: Displays the relationship of bound and free calcium within the cuvette system. (A) Aliquots of calcium were introduced to the system in the presence of 50µM EGTA, 5µM thapsigargin and 5µM RuR. It was noted that the calcium buffering in the presence of the EGTA solution, fitted that of the EGTA calcium binding curve model. On introduction of 20µM oxalate to the 50µM EGTA solution, the measured free calcium increased rapidly to a concentration of 2µM then gradually plateaued. It was also observed that the oxalate and EGTA curve superimposed the EGTA model up to 4µM free calcium. The absence of calcium saturation noted with EGTA alone, indicates a buffering mechanism was initiated with oxalate, which was not significantly affected by increasing concentrations of cardiac myocytes until the free calcium concentration reached 3µM. Additional buffering was noted for 2x10⁶ cells/ml as the total calcium concentration increased above 3µM. (B) Emphasise that all the graphs in 3.7A are superimposable below 3µM. (mean ± s.e.m., n = 5).

CHAPTER FOUR

CHARACTERISTICS OF SR CALCIUM LEAK

4.1. INTRODUCTION

As previously discussed (Chapter 1), there are only two recognised calcium release channels in the SR of striated muscle, the RyR2 and the IP₃R. However, the RyR is the major calcium release channel in skeletal and in ventricular cardiomyocytes. (Brilliantes *et al.*, 1992; Moschella & Marks, 1993)

The aim of this study involved investigating the characteristics of the calcium efflux from the SR of cardiac myocytes in the absence of RyR activity. The ability to study the properties of SR calcium leak was made available with the use of the drugs listed below, and the inhibition of SERCA by thapsigargin was used to determine whether the behaviour of the non-specific leak was consistent with the characteristics of a calcium channel.

4.1.1. Ruthenium Red

RuR is one of the most potent inhibitors of the calcium release channel (Zucchi & Ronca-Testoni, 1997). It decreases the rate of calcium release from the SR (Gyorke *et al.*, 1997) at concentrations ranging from 1nM to 20µM (Miyamoto & Racker, 1981; Palade, 1987; Meissner & Henderson, 1987; Kim *et al.*, 1983) and thereby induces an increase in the rate of calcium uptake. As well as having effects on the RyR, RuR also inhibits calcium uptake and release from the mitochondria (Gincel *et al.*, 2001; Bernardi, *et al.*, 1984), alters the calcium sensitivity of myofilaments (Zhu *et al.*, 1992) and changes the electrical properties of cell membranes (Zacharova *et al.*, 1990).

RuR is an inorganic polycationic dye with a linear structure consisting of three RuR atoms linked by two oxo-bridges, 14 amine groups and has a valence of 6 (see [1]). It is a highly charged molecule and therefore its permeation through membranes of intact cells is considered difficult but studies have revealed the molecule can diffuse slowly through intact papillary muscles (Tanaka *et al.*, 1997).



RuR is thought to block the calcium permeation through the RyR, but the mechanism for its action is unclear. Work carried out by Ma (1993), on the skeletal muscle calcium release channel

(CRC) reconstituted into planar lipid bilayers, proposed that multiple RuR molecules are involved in the inhibition of calcium release from the SR. A Hill Coefficient of -2 was obtained from the dose response curve of the RuR block on the RyR, suggesting that RuR binds to more than one site within the CRC conduction pore in a cooperative manner (Mai, 1994; Lai *et al.*, 1988). One RuR molecule was found to be sufficient to block the channel, but an additional molecule will ensure the channel remains in its closed state (Ma, 1993). The highly asymmetric nature of the block indicates that RuR is unlikely to permeate the open channel (*cis* to *trans*). *Trans* RuR has been observed to induce a similar affinity to that of *cis* but with a coefficient of 1, suggesting that a simple binding site can be approached from the luminal side of the CRC (Ma, 1993). The RuR block is also concentration and voltage dependent: a stronger block being observed with higher RuR concentrations and with large positive voltages (large positive voltages favour the movement of RuR molecules into the channel pore). However, work carried out on isolated channels suggests that RuR acts primarily by reducing the overall availability of the channels by inducing long closures (Rousseau & Meissner, 1989; Ashley & Williams, 1990).

It is unclear as to whether RuR competes with the calcium for the calcium activation sites on the RyR. Chen & MacLennan (1994) found that RuR binds to several calcium binding proteins, suggesting that RuR competes with calcium for the calcium activation sites. In support of this theory, the studies undertaken by Zimanyi & Pessah (1991) revealed that RuR decreases [3 H] ryanodine binding by competitive inhibition, as did Imagawa *et al.* (1987). Also, Alves & de Meis (1986) and Kargacin & Kargacin, (1998) found that RuR competes with calcium for the high affinity binding sites of the skeletal and cardiac muscle Ca^{2+} -ATPase respectively. While Xu *et al.* (1999) and Chu *et al.* (1990) favour the non-competitive inhibition.

4.1.2. Thapsigargin

Thapsigargin, a naturally occurring tumour promoting sesquiterpene lactone (Norregaard *et al.*, 1994) isolated from the plant *Thapsia garganica* (Christensen, 1988), is a highly specific inhibitor of the SR and ER Ca^{2+} -ATPase pumps (Thastrup *et al.*, 1990; Lytton, *et al.*, 1991). Its mode of action is to empty intracellular calcium stores as a consequence of inhibiting the uptake pathway (Thastrup

et al., 1990) without affecting sarcolemmal calcium currents (Kirby *et al.*, 1992) and thus it is utilised in calcium studies to define and manipulate intracellular calcium pools.

Thapsigargin inhibits SERCA 2A by binding to the low affinity state (E_2) of the enzyme. As discussed in Chapter 1.4.1, the reaction cycle describes a scheme where the pump is phosphorylated and dephosphorylated, and an interconversion of conformational states of the protein results in the transport of two calcium ions through the SR membrane against its concentration gradient, into the lumen of the SR for every molecule of ATP hydrolysed (Läuger, 1991; Mintz *et al.*, 1997; Ikemoto, 1982). Calcium binding occurs when the enzyme is in a high affinity state (E_1) and the release of calcium occurs when the enzyme is in a low affinity state (E_2). The shift in states from E_1 to E_2 is caused by the hydrolysis of ATP via the formation of a phosphorylated intermediate (EP). Thapsigargin acts to inhibit the enzyme in its high affinity state (E_2) (Kijima *et al.*, 1991). The sensitivity of the Ca^{2+} -ATPase to thapsigargin is lower in cardiac muscle than in skeletal muscle, however the sensitivity is increased in cardiac muscle by phosphorylation. Since PLB also binds to the E_2 form of SERCA 2A, and PLB is modulated by phosphorylation, it has been suggested that the binding sites of thapsigargin and phospholamban may occur in close proximity to each other on the enzyme (Kijima *et al.*, 1991).

4.1.3. Ionomycin

Ionomycin is a monocarboxylic acid ionophore. It is known as an ionophore due to its ability to complex and carry cations across lipophilic membranes (Pressman, 1976). Ionomycin is relatively nonselective, possessing the ability to transport several divalent and trivalent cations (Wang *et al.*, 1998; Liu & Hermann, 1978). One calcium ion is transported across membranes complexes to one ionomycin molecule and each calcium ion is exchanged for 2 protons so that the process is electroneutral (Stiles *et al.*, 1991; Toepfilitz *et al.*, 1979; Erdahl *et al.*, 1995). Thus avoiding ionomycin-mediated depolarisation of the membrane, which would affect voltage gated channels instead of ionomycin's actions being due to a direct elevation of cytosolic calcium concentrations per se. The driving force for transport is therefore a transmembrane calcium or proton gradient (Erdahl *et al.*, 1995).

A limited amount of experimental work has been published on the effect of ionomycin on cardiac myocytes however; low doses of ionomycin have been shown to cause the release of calcium from the SR in vascular smooth muscle (Smith *et al.*, 1989). The basis for the selective action of ionomycin at low doses is probably due to the relatively low affinity of ionomycin for calcium: higher calcium concentrations within the SR compared to extracellular concentrations, means the predominant effect of ionomycin is to transport calcium across the SR membranes rather than the sarcolemma.

4.2. METHODS

Cardiac myocytes were prepared for calcium leak studies as previously described in Chapter 2. 1×10^6 permeabilised cells suspended in 0.05R solution were transferred to the closed cuvette system and changes in the intracellular free calcium concentrations were detected using the fluorescent indicator Fura-2. Unless stated otherwise, the compounds listed in Table 2.3 were also introduced to the closed cuvette system. Following a three minute incubation to allow the cells to reach an equilibrium with the mock intracellular environment, the cells were then subjected to the following experimental protocols.

4.3. RESULTS

To investigate the involvement of the RuR insensitive SR leak under various conditions, the following studies were conducted on permeabilised cardiac myocytes. All the experiments discussed below are in the presence of $25 \mu\text{M}$ RuR unless otherwise stated.

4.3.1. Effect of RuR on SR Leak

Figure 4.1A, is a typical experimental trace to compare the time course of the calcium transients in the presence and in the absence of RuR. A control transient was established in the absence of RuR by adding a bolus of calcium ($67 \mu\text{M}$). This increased the free calcium to $\sim 3 \mu\text{M}$, before decaying back to the diastolic level in a 12 minute period. $25 \mu\text{M}$ RuR was then introduced to the preparation prior to a calcium bolus to assess the contribution of the RyR to the SR leak. In the presence of RuR the rate constant of decay is increased significantly (w/o RuR = $0.09 \text{s}^{-1} \pm 0.01$; with RuR =

$0.16\text{s}^{-1} \pm 0.03$; $P < 0.5$ (Fig. 4.1B). This suggests that a significant SR leak exists through the RyR under these circumstances.

4.3.2. SR Leak in the Presence and Absence of SR Calcium

Fig. 4.2 displays typical experimental traces to show the effects of $5\mu\text{M}$ thapsigargin in the presence and in the absence of a calcium challenge. In Fig. 4.2A, $5\mu\text{M}$ thapsigargin was introduced to the cuvette system in the absence of a calcium challenge. After 25 minutes, $10\mu\text{M}$ ionomycin was added and then incubated for 12 minutes. It was observed that a linear leak was not produced in the presence of $5\mu\text{M}$ thapsigargin or $10\mu\text{M}$ ionomycin, in the absence of calcium (Fig. 4.3A).

In Fig. 4.2B, the introduction of an aliquot of calcium increased the free calcium concentration to $1\mu\text{M}$ before decaying back to diastolic levels. After 12 minutes, $5\mu\text{M}$ thapsigargin was added to the preparation and left for 1hr. It was noted that in the presence of a calcium challenge, $5\mu\text{M}$ thapsigargin induces a significant SR leak compared to the gradient produced in the absence of a calcium challenge (w/o calcium, $m = 0.046\text{ nMs}^{-1} \pm 0.042$; single calcium challenge, $m = 0.77\text{ nM s}^{-1} \pm 0.18$; $P < 0.05$ (Fig 4.3A). The leak in the presence of a calcium challenge is resistant to RuR, as $25\mu\text{M}$ RuR was present in the cuvette. This indicates that the leak observed is not due to the passage of calcium through the RuR sensitive RyR.

Rather than waiting several hours for thapsigargin to induce a steady state SR calcium concentration (once the cytoplasmic and intra SR compartment had equilibrated), $10\mu\text{M}$ ionomycin was introduced to the preparation to enhance the equilibration process. Fig. 4.4A, is a typical experimental trace showing the effects of $5\mu\text{M}$ thapsigargin and $10\mu\text{M}$ ionomycin on SR leak after the introduction of a single calcium challenge. Once the calcium transient decayed to diastolic levels, $5\mu\text{M}$ thapsigargin was added to the preparation. After 12 minutes, $10\mu\text{M}$ ionomycin was introduced. It is observed that thapsigargin induced a calcium leak from the SR and was enhanced with the addition of ionomycin. The steady state calcium concentration (C_{ss}) produced in the presence of $10\mu\text{M}$ ionomycin was noted to increase significantly in the presence of a calcium challenge. (w/o calcium, leak $C_{ss} = 0.12\mu\text{M} \pm 0.005$; single calcium challenge, leak $C_{ss} = 0.37\mu\text{M} \pm 0.016$; $P < 0.05$ (Fig. 4.3B). This suggests that the calcium leak in the presence of the $5\mu\text{M}$

thapsigargin and 10 μ M ionomycin treatment, after the preparation has been subjected to a calcium challenge, is due to calcium loss from the SR.

4.3.3. Effects of Calcium Load on SR Leak

To assess if multiple calcium challenges increase the SR leak further, the same protocol as that described for Fig. 4.4A was followed but with two and three calcium challenges prior to the addition of 5 μ M thapsigargin and 10 μ M ionomycin. The experimental trace of 5 μ M thapsigargin and 10 μ M ionomycin in the presence of three calcium challenges is shown in Fig. 4.4B. Each calcium challenge was introduced at 12 minute intervals, allowing the transient to decay back to diastolic levels. 5 μ M Thapsigargin was added after the last calcium challenge and incubated for 12 minutes. 10 μ M ionomycin was introduced and incubated for the same amount of time. Under these circumstances it was noted that in the presence of three calcium challenges, 5 μ M thapsigargin and 10 μ M ionomycin induced a larger SR leak, increasing the gradient and the C_{ss} of the SR leak significantly more than that observed for a single calcium challenge. These differences are emphasised in Fig. 4.5B and 4.5C respectively.

Fig. 4.6 summaries the effects of calcium load on the RuR resistant SR leak. The leak gradient induced in the presence of 5 μ M thapsigargin increased significantly from 0 calcium to 1, 2 and 3 calcium challenges. However, calcium challenges 1 and 2 produced similar leak gradients whilst significantly increasing after 3 challenges. The leak C_{ss} induced with 10 μ M ionomycin follows a similar trend to that produced by the leak gradient and challenges 1 and 2 produced a non-significant increase in C_{ss} before significantly increasing to challenge 3.

4.3.4. The Effects of Changing Oxalate Concentrations on SR Leak

The subsequent figures (Fig 4.7A, B and C) are all typical experimental traces to show the effects of changing oxalate concentration on the RuR-insensitive SR leak. From previous data it was observed that three calcium challenges were sufficient to produce reproducible calcium transients as well as sufficiently loading up the SR. After the third transient decayed back to minimum calcium levels, 5 μ M thapsigargin was added to the cuvette system and incubated for 12 minutes before 10 μ M

ionomycin was introduced. The results of 5mM, 10mM and 20mM oxalate on SR leak can be noted in Fig. 4.7A, B and C respectively.

The calcium transient decays (for the third calcium challenges) produced in the presence of 5mM, 10mM and 20mM oxalate concentrations, were placed onto one graph (Fig. 4.8A). The leak gradients produced in the presence of the above oxalate concentrations were also cut and placed into onto a single graph (Fig. 4.8B) as with the leak C_{ss} (Fig. 4.9C) in order to emphasise the effects of various oxalate concentrations on SR leak. From Fig. 4.8A, it is observed that 20mM oxalate produced a transient that declines to minimum levels faster than either 5mM or 10mM oxalate. Also 5mM and 10mM oxalate produced similar calcium transient decays and the rate of decay for the calcium transients in the presence of various oxalate concentrations were calculated and displayed as a bar graph (Fig.4.9A). 5mM and 10mM oxalate produced similar rates of decay (5mM = $0.097\text{s}^{-1} \pm 0.02$; 10mM = $0.1\text{ s}^{-1} \pm 0.01$; $P > 0.05$ (Fig. 4.9A) where as 20mM oxalate produced a rate of decay significantly faster than 5mM and 10mM oxalate (20mM = $0.34\text{ s}^{-1} \pm 0.03$; $P < 0.05$ (Fig. 4.9A).

In Fig. 4.8B, 5mM oxalate induced a significant increase in the leak gradient compared with 20mM oxalate (5mM Ox = $2.9\text{nMs}^{-1} \pm 0.46$; 20mM Ox = $0.74\text{nMs}^{-1} \pm 0.19$; $P < 0.005$ (Fig. 4.9B) and from Fig 4.8C, 5mM induced a significant increase in the leak C_{ss} compared with 20mM oxalate (5mM Ox = $4.2\mu\text{M} \pm 1.25$; 20mM Ox = $0.68\mu\text{M} \pm 0.16$; $P < 0.05$ (Fig. 4.9C). Indicating a larger SR leak exists in the presence of low oxalate concentrations.

4.4 DISCUSSION

It is important for cells to regulate SR leak. Any abnormalities in leak, whether it is through the non-specific leak or through the RyR, can lead to altered SR calcium content. Diastolic calcium concentration is regulated by sarcolemma extrusion (i.e. mainly $\text{Na}^{2+}/\text{Ca}^{2+}$ exchanger) however an increase in the calcium leak from the SR during diastole can lead to a reduced SR calcium content and therefore reduced calcium transient and contraction.

From the data presented in this chapter, a significant SR leak exists in the presence of repeated calcium challenges. A component of this leak can be blocked by RuR; a potent inhibitor of

the CRC (Zucchi & Ronca-Testoni, 1997). However, a significant leak remains in the presence of RuR, suggesting that a leak pathway exists in cardiac muscle SR that is independent of RyR activity. Little is known about this non-specific leak although a few theories have arisen and will be discussed in more detail later in this thesis (Chapter 7).

In this preparation a concentration of 25 μ M RuR was used to ensure maximal inhibition of calcium leak via the RyR as well as inhibiting calcium sequestration via the mitochondria (Hove-Madsen & Bers, 1993). The concentration of RuR utilised in other studies varied between 0.08-20 μ M, depending on the experimental technique [$>20\mu$ M in homogenates in skeletal and cardiac muscle (Feher *et al.*, 1988); 10 μ M in SR vesicle work in skeletal and cardiac muscle (Xu *et al.*, 1999); 20 μ M in heavy fraction vesicles (Kim, 1983); 12 μ M in purified SR cardiac vesicles (Chamberlain *et al.*, 1984); 1 μ M RuR blocked RyR calcium release, 5 μ M blocked caffeine induced calcium release from rabbit skeletal SR fractions (Palade, 1987); 25 μ M permeabilised ventricular myocytes (Hove-Madsen & Bers, 1993)].

It was discovered that high concentrations of RuR might slow SR calcium uptake causing a decrease in rate of calcium uptake (Kargacin & Kargacin, 1998). This study showed that RuR acted by altering the calcium sensitivity of the SR calcium uptake with no detectable effect on the Hill coefficient or maximum uptake rate (Kargacin & Kargacin, 1998). This effect is likely to arise from direct action of RuR on SR Ca²⁺-ATPase and would occur independently of any effects of RuR on the RyR (Kargacin & Kargacin, 1998). A direct action of RuR was reported by Alves de Meis (1986) who found that RuR competes with calcium for the high affinity binding sites on the skeletal muscle SR Ca²⁺-ATPase as well as inhibiting calcium binding to calcium binding proteins. With this in mind, the RuR concentration in this study was reduced to avoid this detrimental effect on SERCA 2A. However, as discussed above, the level of RuR used would be expected to fully (>99%) inhibit RyR activity. Therefore it is unlikely that the remaining calcium leak pathway is via conventional RyR2.

In addition to RuR influencing SR leak: calcium load and oxalate concentration both affect the characteristics of calcium leak. Oxalate was used to prevent the increase in free calcium

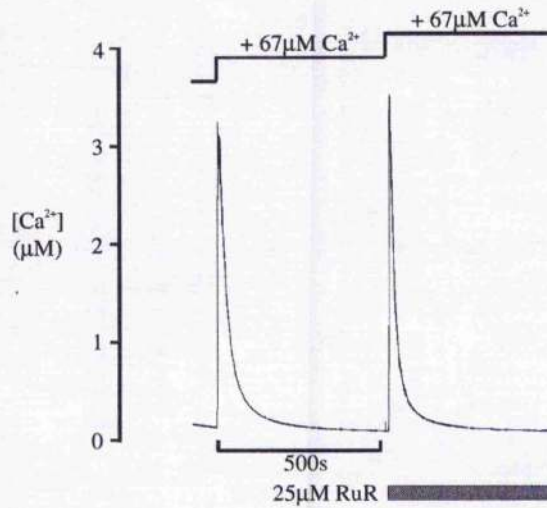
concentration inside the SR (that would otherwise slow the rate of net uptake) by the precipitation of calcium-oxalate inside the SR (Madeira, 1982). A consequence of this is that the rate of SR calcium uptake can stay at the same rate determined by the free calcium in the suspension (rather than limited by high free calcium inside the SR). It has been shown that crystallization of calcium-oxalate inside the SR does not reach equilibrium at any time during calcium uptake (Feher & Briggs, 1980), and thus will continue to buffer luminal calcium. It is well documented that SR calcium leak depends on SR calcium content (Bassani *et al.*, 1995; Smith & Steele, 1998; Shannon *et al.*, 2000) as well as the free calcium concentration in the mock intracellular solution. If the SR luminal calcium concentration was low (due to oxalate precipitation of calcium) then a calcium leak from the SR would be low, due to the lowered calcium concentration gradient across the SR membrane. The reduced calcium leak at higher oxalate concentrations could account for the faster rate of uptake (Fig. 4.9A). Therefore, the calcium concentration within the lumen of the SR plays a vital role in calcium regulation and evidence to suggest that lumen calcium influences the CRC has been published (Fabiato, 1992; Sitsapesan & Williams, 1994; Bassani *et al.*, 1995; Lukyanenko *et al.*, 1996; Gyorke *et al.*, 1997; Gyorke & Gyorke, 1998) and state that the loading of the SR directly alters the gain of the EC Coupling and therefore a higher SR calcium content leads to a greater release of calcium for any given calcium trigger (Bassani *et al.*, 1995; Lukyanenko, *et al.*, 1996). The effect of luminal calcium on calcium release from the RyR is discussed in more detail in Chapter 5.4.1.1.

It was discovered that calcium leak was not detectable in this preparation without the addition of calcium to the system, suggesting that at the start of the experiment, the SR calcium content was negligible. However, with the addition of only one bolus of calcium, sufficient SR load was generated to sustain a calcium leak. The rate of leak and C_{ss} are influenced by the number of calcium challenges added to the system (calcium load): rate of calcium leak being higher than the three separate calcium challenges (Fig. 4.6A & B). The most likely explanation for these results is that sequential additions of calcium to the system cause a progressive increase in the luminal free calcium concentration and total SR load. Increased free calcium within the SR will increase the calcium concentration gradient across the leak pathway and increased total calcium in the SR will

result in a higher C_{ss} . The increase in the rate constant with progressive calcium challenges is discussed in more detail in Chapter 5 (section 5.4.1.1).

It was interesting to note the pronounced effects of oxalate concentration on SR the calcium leak rate. This would suggest that the influence of oxalate on the rate of calcium uptake and the steady state calcium concentration is not simply due to the stimulation of SERCA but a reduced leak of calcium would also contribute to the change in the net calcium uptake rate.

(A)



(B)

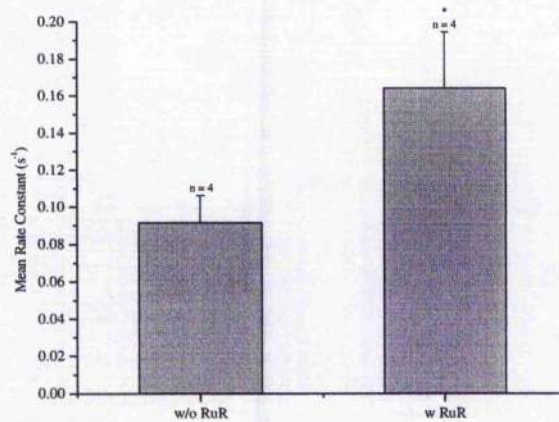
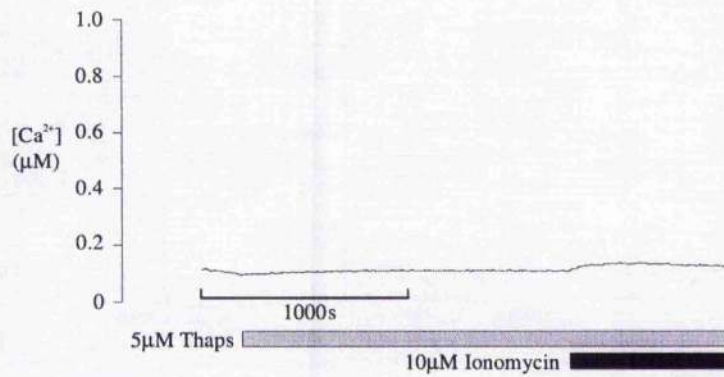


Figure 4.1: Effect of RuR on SR calcium leak. (A) Typical experimental trace displaying the calcium transient in the presence and in the absence of 25 μM RuR. Where a control transient was established before the addition of RuR, added after a 12 minute interval. The solution composition, bathing the cells prior to the additions indicated in the figure, is as follows; 0.05R (table 2.2), 20mM Oxalate, 10 μM Fura-2, 5mM ATP, 15mM CrP, 0.1 μM DTT, 10 μM CCCP and 33 μM Oligomycin. (B) The mean data for the effect of RuR on the rate constant of decay of the calcium transient. (mean \pm s.e.m., n = 4, * denotes $P < 0.05$). Significance was tested using a paired students t-test.

(A)



(B)

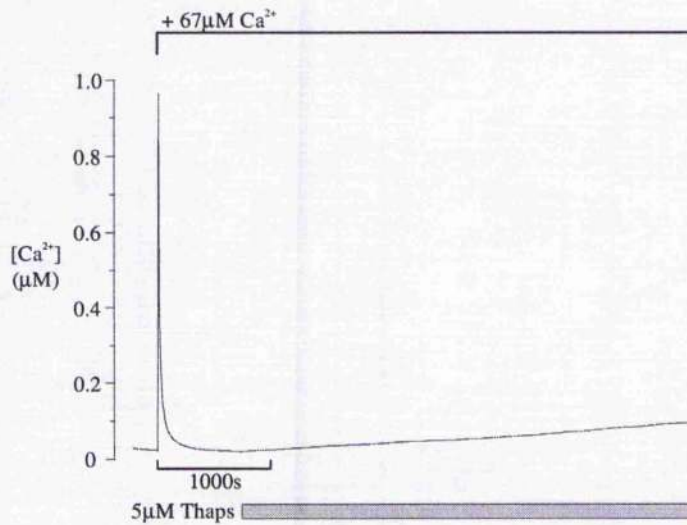
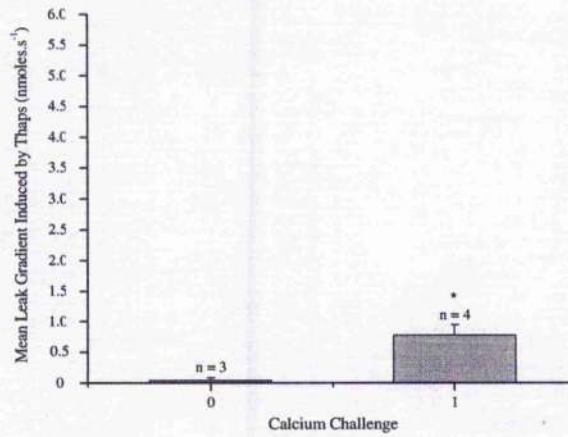


Figure 4.2: SR leak in the presence and absence of SR calcium. (A) Typical experimental trace to show the effects of 5 μM thapsigargin and 10 μM ionomycin in the presence of diastolic calcium concentrations. 5 μM Thapsigargin was introduced to the preparation in the absence of a calcium challenge. After 12 minutes, 10 μM ionomycin was added. (B) A typical experimental trace to show the effects of 5 μM thapsigargin in the presence of a calcium challenge. The calcium challenge increased the free calcium concentration to 1 μM before decaying back to diastolic levels before 5 μM thapsigargin was introduced. The solution composition, bathing the cells prior to the additions indicated in the figure, is as follows; 0.05R (table 2.2), 20mM Oxalate, 10 μM Fura-2, 25 μM RuR, 5mM ATP, 15mM CrP, 0.1 μM DTT, 10 μM CCCP and 33 μM Oligomycin.

(A)



(B)

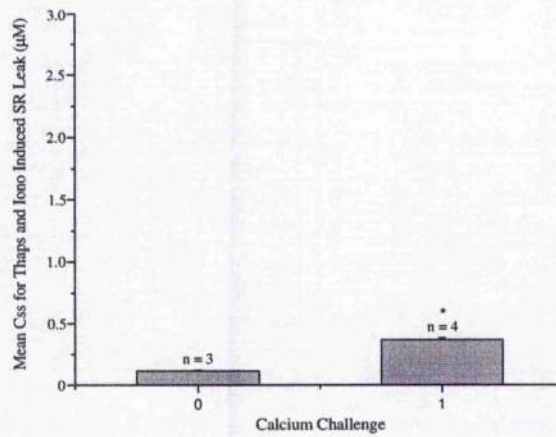
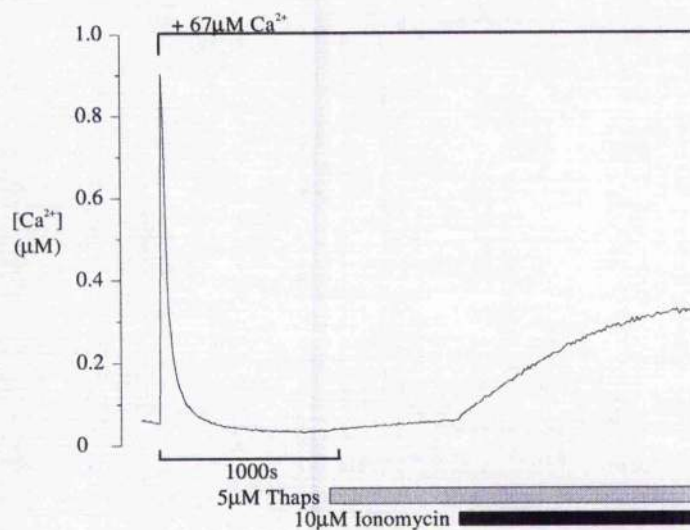


Figure 4.3: Mean data to show the effect of calcium load on SR calcium leak. (A) The following bar graph displays the gradient of thapsigargin-induced leak in the presence and absence of calcium load. (B) Displays the mean steady state calcium concentration (C_{ss}) induced by 10µM ionomycin and 5µM Thapsigargin in the presence and absence of a calcium load (mean ± s.e.m; n = 3 (0 calcium challenge), n = 4 (1 calcium challenge); * denotes p<0.05). Significance was tested using an unpaired students t-test.

(A)



(B)

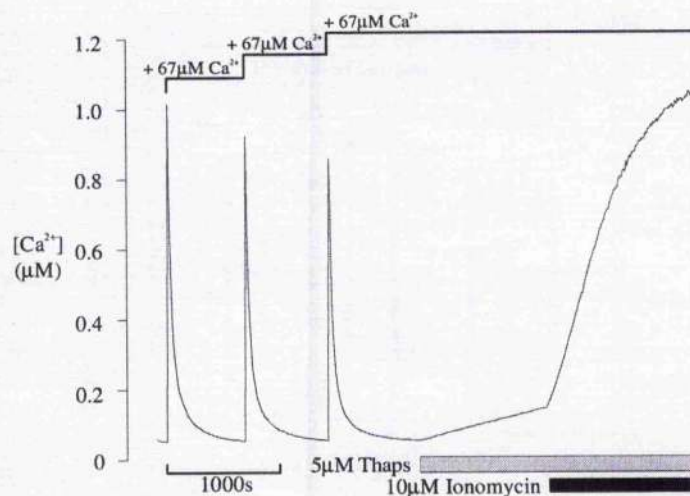
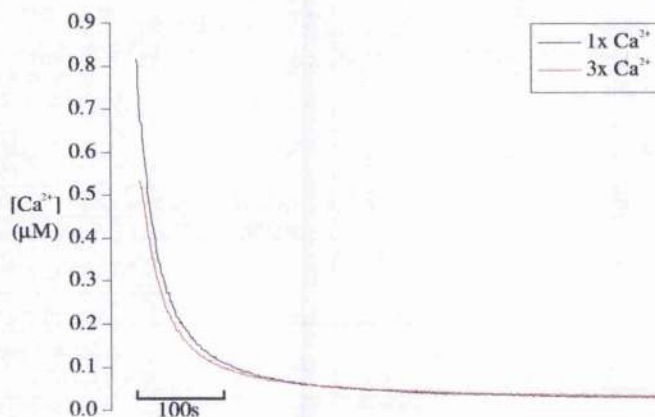
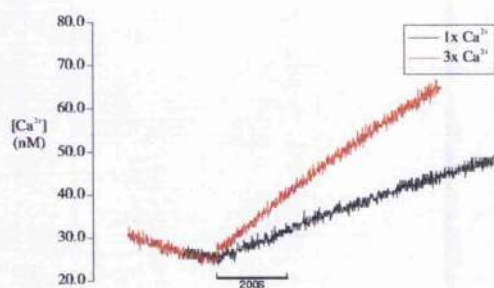


Figure 4.4: Typical experimental traces to display the effects of calcium load on SR leak induced by thapsigargin and ionomycin. (A) A single calcium challenge was added prior to $5 \mu M$ thapsigargin. $10 \mu M$ ionomycin was introduced after 12 minutes, to enhance the equilibration process (time taken for intra luminal and cytoplasmic calcium to reach a steady state calcium concentration). (B) Same protocol as (A) was followed except three calcium challenges were introduced to the preparation, 12 minutes apart prior to $5 \mu M$ thapsigargin and $10 \mu M$ ionomycin. The solution composition, bathing the cells prior to the additions indicated in the figure, is as follows; $0.05R$ (table 2.2), $20mM$ Oxalate, $10 \mu M$ Fura-2, $25 \mu M$ RuR, $5mM$ ATP, $15mM$ CrP, $0.1 \mu M$ DTT, $10 \mu M$ CCCP and $33 \mu M$ Oligomycin.

(A)



(B)



(C)

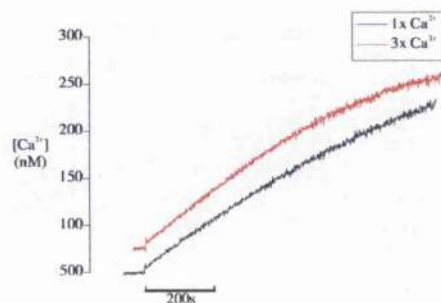
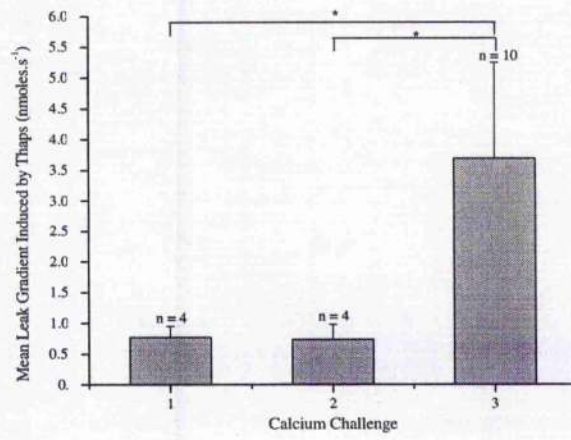
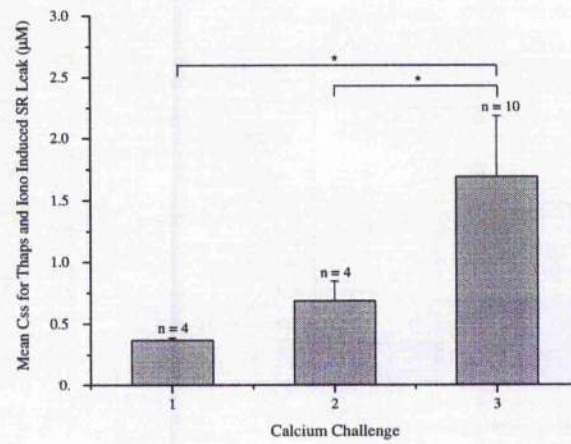


Figure 4.5: Effects of calcium load on SR leak. The solution composition, bathing the cells prior to the additions stated below, is as follows; 0.05R (table 2.2), 20mM Oxalate, 10 μM Fura-2, 25 μM RuR, 5mM ATP, 15mM CrP, 0.1 μM DTT, 10 μM CCCP and 33 μM Oligomycin. (A) Displays the calcium transient decays for 1 (—) and 3 (—) calcium challenges prior to thapsigargin addition. (B) The gradients for the calcium leak produced after the injection of 5 μM thapsigargin in the presence of 1 (—) and 3 (—) calcium challenges. (C) 10 μM ionomycin enhanced the Thapsigargin-induced leak, in the presence of 1 (—) and 3 (—) calcium challenges. Where the leak reached a steady state calcium concentration after about 12 minutes.

(A)



(B)



(C)

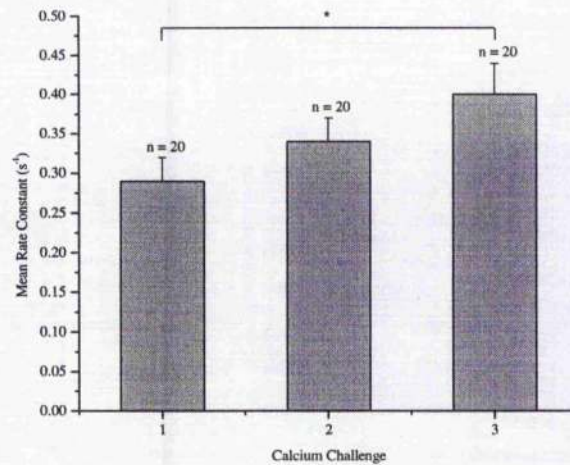
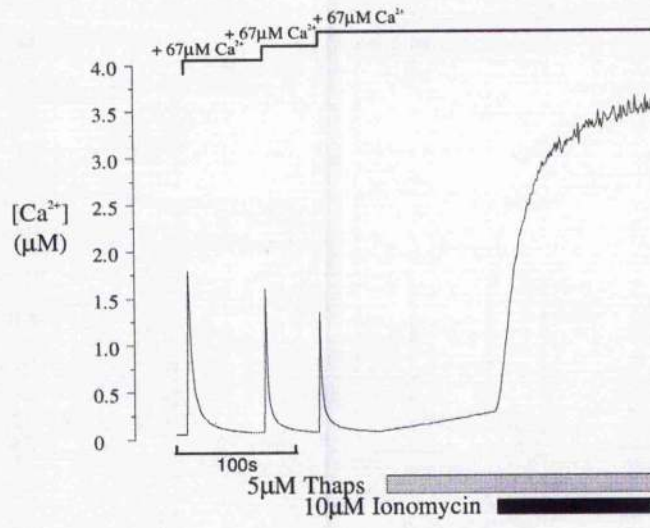
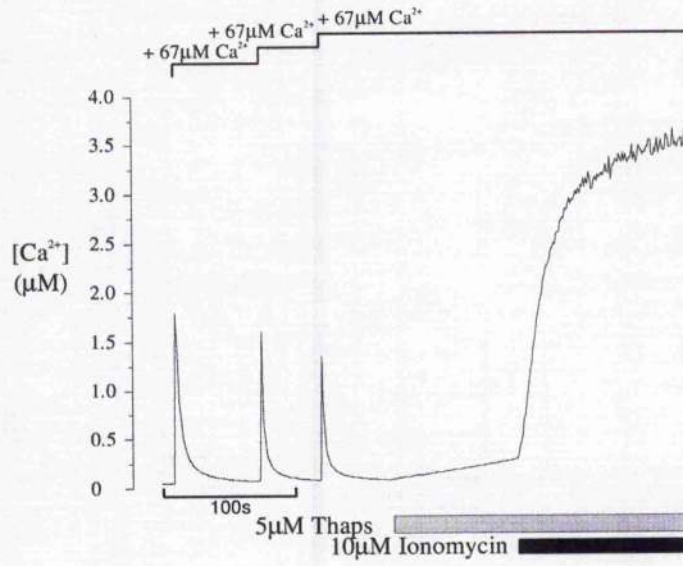


Figure 4.6: Summary of the mean results of calcium load on thapsigargin and ionomycin induced SR leak. (A) Displays the mean leak gradient induced by 5 μ M Thapsigargin after 1, 2 & 3 calcium challenges. (B) Displays the mean C_{ss} induced by 5 μ M Thapsigargin and 10 μ M ionomycin after 1, 2 & 3 calcium challenges. (mean \pm s.e.m; n = 4 (1 & 2 calcium challenges), n = 10 (3 calcium challenges); * denotes p<0.05, ** denotes p<0.005). (C) The mean rate constant for the transients after the addition of 1, 2 and 3 calcium challenges. (mean \pm s.e.m; n = 20; * denotes p<0.05). Significance was using an ANOVA with a Tukey post hoc test.

(A)



(B)



(C)

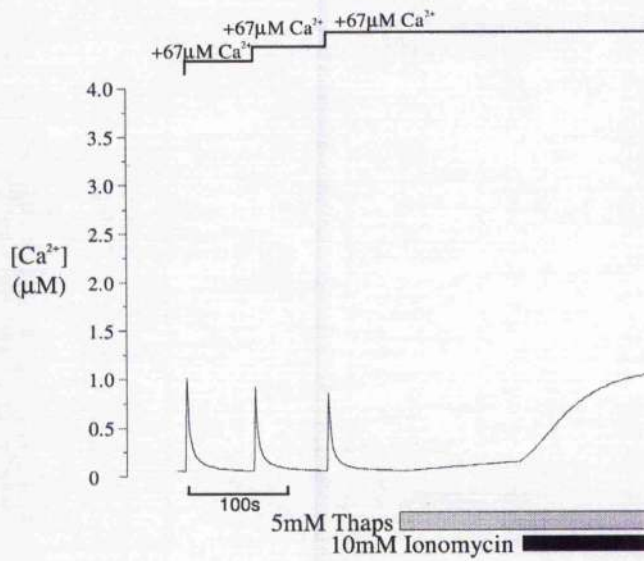
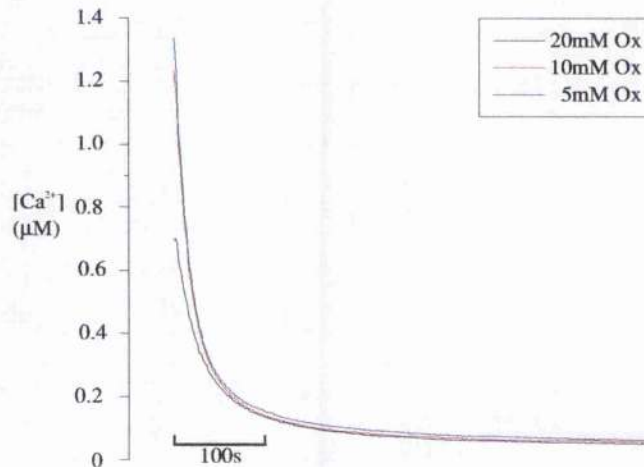
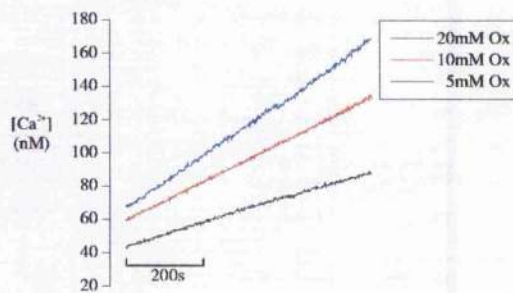


Figure 4.7: Typical experimental traces produced by various oxalate concentration The solution composition, bathing the cells prior to the additions stated below, is as follows; 0.05R (table 2.2), $10 \mu M$ Fura-2, $25 \mu M$ RuR, $5mM$ ATP, $15mM$ CrP, $0.1 \mu M$ DTT, $10 \mu M$ CCCP and $33 \mu M$ Oligomycin. Three calcium transients induced reproducible calcium transients prior to assessing the SR leak with thapsigargin and ionomycin. After the control transient was established, $5 \mu M$ thapsigargin was introduced to the preparation and left to incubate for 12 minutes before $10 \mu M$ ionomycin was added: in the presence of $5mM$ oxalate (A); $10mM$ oxalate (B); and $20mM$ oxalate (C).

(A)



(B)



(C)

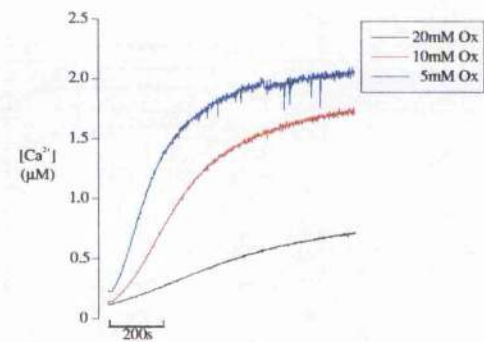
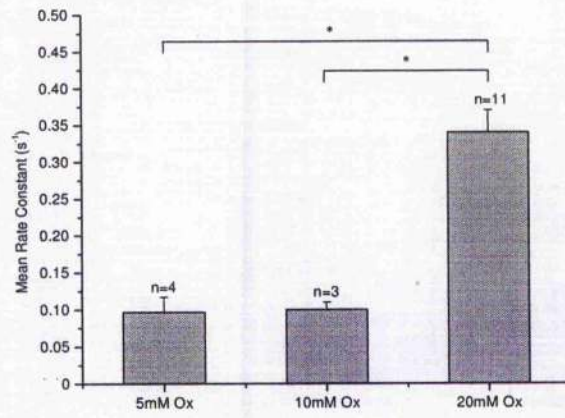
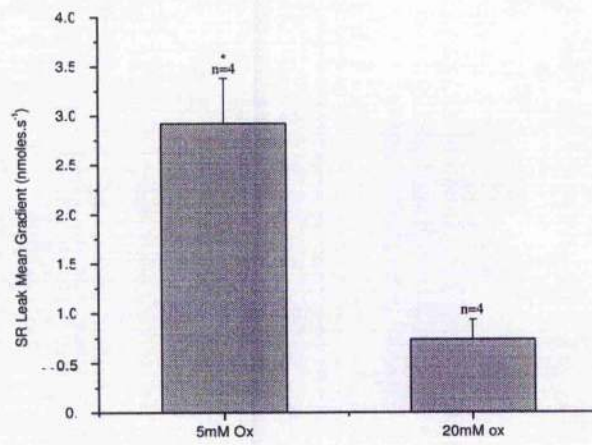


Figure 4.8: Effects of oxalate concentration on SR leak. The solution composition, bathing the cells prior to the additions stated below, is as follows; 0.05R (table 2.2), 10 μM Fura-2, 25 μM RuR, 5mM ATP, 15mM CrP, 0.1 μM DTT, 10 μM CCCP and 33 μM Oligomycin. (A) Displays the calcium transient decays in the presence of 20mM (—); 10mM (—) and 5mM oxalate (—) prior to thapsigargin addition. (B) The gradients for the calcium leak produced after the injection of 5 μM thapsigargin in the presence of 20mM (—); 10mM (—) and 5mM oxalate (—). (C) 10 μM ionomycin enhanced the thapsigargin-induced leak in the presence of 20mM (—); 10mM (—) and 5mM oxalate (—) and the leak reached a steady state calcium concentration after about 12 minutes.

(A)



(B)



(C)

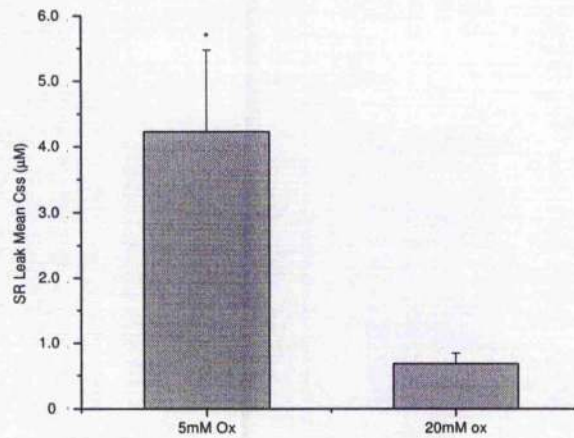


Figure 4.9: Mean data to show the effect of various oxalate concentration on SR calcium leak. (A) The mean data for the effect of 5mM, 10mM and 2mM oxalate on the rate constant for calcium decay (mean \pm s.e.m; n = 6 (5mM oxalate), n = 3 (10mM oxalate), n=11 (20mM oxalate)). (B) The following bar graph displays the mean thapsigargin-induced SR leak gradient for 5mM, 10mM and 20mM oxalate (mean \pm s.e.m; n = 4). (C) The bar graph shows the steady state calcium concentration (C_{ss}) of the thapsigargin leak, enhanced by the addition of 10 μ M ionomycin in the presence of 5mM, 10mM and 20mM oxalate (mean \pm s.e.m; n = 4; * denotes p<0.05). Significance was using an ANOVA with a Tukey post hoc test.

CHAPTER FIVE

RYANODINE MEDIATED CALCIUM LEAK

5.1. INTRODUCTION

The complex regulation and gating characteristics of the RyR are very important to the function of this SR calcium release channel. A great deal of information on the RyR has been gathered from work carried out on controlled environments such as SR vesicles (Meissner & Henderson, 1987; Bers, 1991) and the reconstitution of the RyR into lipid bilayers (Meissner, 1986; Rousseau & Meissner, 1989; Rousseau *et al.*, 1987; Gyorko & Fill, 1993; Valdivia *et al.*, 1995; Schiefer, *et al.*, 1995) and the most frequent isoforms studied at the single channel level include the cardiac RyR (RyR2) and the skeletal muscle RyR (RyR1). However, it is also important to study this channel under normal physiological conditions as the RyR is clearly regulated by a variety of agents and is highly sensitive to environmental changes such as pH, ionic strength, temperature, membrane potential and phosphorylation.

In this chapter permeabilised ventricular myocyte preparations were used to examine the properties of the calcium leak from the SR. The effects were interpreted with reference to previous work carried out on SR vesicles and isolated RyR2.

5.2. METHODS

Cardiac myocytes were prepared for calcium leak studies as previously described in Chapter 2. 1×10^6 permeabilised cells were transferred to the closed cuvette system where changes in the mock intracellular free calcium concentrations were detected using the fluorescent indicator Fura-2. Following a three minute incubation, to allow the cells to reach an equilibrium with the mock intracellular solution surrounding the myocytes, 3 aliquots of 8-10 μ l of 10mM calcium chloride were added in the presence of 20mM oxalate, to raise the free calcium concentration to 1-2 μ M which decayed in an exponential fashion back to minimum calcium level (~100nM). Three aliquots introduced at 12 minutes apart, were found to be adequate to generate reproducible calcium transient decays.

The experiments investigating the effect of RuR on SR calcium leak (5.3.1), required the addition of 5 μ M RuR at an early interval of the experiment, noted as calcium challenge #1 (figure 5.1) and at a late interval of the experiment, noted as calcium challenge #4 (figure 5.2). The action of RuR was studied by calculating the rate of change of the calcium transients and normalising them to the control transient. These responses were then compared with the responses from experiments in the absence of RuR.

The experiments investigating the effect of ryanodine on SR calcium leak (5.3.2) required the addition of ryanodine after a control transient was established. The action of ryanodine (0.3 μ M, 3 μ M, 30 μ M, 300 μ M and 3mM) was studied by monitoring the response to four further calcium challenges and in the presence of 5 μ M RuR prior to the last calcium challenge. The protocol was repeated for the full range of ryanodine concentrations. The action of ryanodine was studied by calculating the rate of change of the calcium transients and normalising them to the control transient. These responses were then compared with the responses from experiments in the absence of ryanodine.

5.3. RESULTS

5.3.1. The Effects of Ruthenium Red on SR Calcium Leak

To investigate the effects of increasing concentrations of ryanodine on SR calcium leak, control experiments were established in order to normalise the experimental data allowing a valid comparison to be made. Control experiments consisted of the addition of 5 aliquots of calcium (12 minutes apart) to the permeabilised muscle preparation after sufficiently loading the SR. This was repeated in the presence of 5 μ M RuR to assess SR leak under normal conditions as well as investigating the extent of the RuR block at various points in the experiment.

Figure 5.1 is a typical experimental trace showing the calcium uptake protocol for this chapter in the presence of an early addition of RuR. After the control transient decayed back to minimum calcium levels, 5 μ M RuR was introduced to the preparation followed by a bolus of

calcium then another 4 calcium additions were introduced at 12 minute intervals.

Figure 5.2 is a typical experimental trace showing the calcium uptake protocol in the presence of a late addition of RuR. The same protocol was followed as that described for figure 5.1, the only difference being, RuR was added before the last calcium transient instead of after the control.

Figure 5.3 describes the rate of change of calcium concentration (dCa^{2+}/dt) analysis carried out for this chapter. The digitised traces were converted into calcium concentrations as previously described in Chapter 2.5 (Panel A). Once converted, dCa^{2+}/dt was measured at each time interval and plotted against the corresponding calcium concentration (Panel B) using the program Origin (Microcal software). The value of dCa^{2+}/dt at $\sim 1\mu M$ ($\pm 0.2\mu M$) was used as a measure of the calcium flux through the RyR.

The subsequent figures illustrate the mean changes in dCa^{2+}/dt (here after referred to as the rate of decay) for the control, as well as for the effects of the early and late additions of $5\mu M$ RuR on permeabilised cardiac myocyte preparations. The results are displayed as a line graph with the rate of decay plotted against the cumulative calcium challenges. In the upper panel (A), the raw (uncorrected) changes in the rate of decay are shown. In the lower panel (B), the changes in the rate of decay are corrected for the changes observed under control conditions.

From figure 5.4(A), it is observed that the rate of decay for the control progressively increased from 0.76 to 1.06 during the first four challenges (# -2 to # 1), peaking at 1.06 for challenge #1 before decreasing over the remaining three challenges (#2 to #4) but to a lesser degree. The graph for the early addition of RuR follows a similar trend to that observed for the control over the challenges # -2 to #0. Then at challenge #1, $5\mu M$ RuR was introduced to the cuvette system resulting in a significant increase in the rate of decay above control levels due to the inhibition of RyR mediated calcium leak from the SR. Thereafter the changes in rate of decay almost parallel those seen in the control from #1 to #3. After #4, the rate of decay decreases sharply from 1.21 to 1.09. In figure 5.4(B), $5\mu M$ RuR significantly increases the rate of decay $\sim 20\%$ above the control

value as seen with the raw data. The subsequent calcium challenges induce an 11% increase in the rate (#2 and #3) before declining 20% with the last calcium challenge.

Figure 5.5 displays the results for the late addition of RuR. The graphs follow a similar trend to the control over the first 6 challenges (# -2 to #3). Then at challenge #4, 5 μ M RuR was introduced to the preparation. The rate of decay increased significantly above control levels, to a value similar to that observed when RuR was added at challenge #1 (figure 5.4). In figure 5.5(B) the addition of 5 μ M RuR significantly increased the rate of decay for the normalised data ~35% above the control value.

Figure 5.6 displays the results for early and late addition of RuR. Where 5 μ M RuR was introduced after the challenge #1 as well as after challenge #4. This diagram follows a similar trend to figure 5.4 for both the raw and the normalised data over the first 6 challenges (# -2 to #3) however, the rate of decay after the addition of RuR at challenge #4 induced a slight slowing of the rate of decay.

5.3.2 Effects of Ryanodine on SR Calcium Leak

From the results discussed on early and late additions of RuR, it was discovered that high concentrations of RuR might slow calcium uptake into the SR causing a decrease in the rate of decay (Kargacin & Kargacin, 1998). With this in mind, investigating increasing concentrations of ryanodine on the rate of calcium decay over subsequent calcium challenges in the permeabilised cardiac myocyte preparation would not only allow the observation of the individual effects over a set period of time but would determine the concentration of ryanodine best suited to replace RuR. Therefore the desired concentration would exert a full block on the RyR within a relatively fast time frame.

Figures 5.8A, B and C are typical experimental traces displaying the effects of ryanodine on the rate of decay in permeabilised cardiac myocytes. An aliquot of calcium increases the total calcium concentration in the cuvette by 67 μ M and causes a rapid increase in the free calcium to approximately 2.5 μ M. Another two aliquots of calcium were introduced to the preparation to allow

reproducible calcium transients before ryanodine was added.

In figure 5.8A, 3 μ M ryanodine caused an immediate slowing of the rate of decay, thus failing to block the RyR but instead produced an opening of the RyR with a slow time course of the calcium transient resulting in an increased leak from the SR, and an elevation in the minimum calcium level. An additional calcium challenge in the presence of 3 μ M ryanodine induced a further decrease in the rate of decay to produce an elevation of the minimum calcium level with each additional calcium challenge. 5 μ M RuR was introduced to the cuvette system at the end of the protocol. This caused a pronounced increase in the rate of calcium decay, consistent with a RuR blocking action on the RyR. However, upon the introduction of an aliquot of calcium, the rate of decay was still much slower than the control. The protocol described above, was repeated for the full range of ryanodine concentrations (30, 300 μ M and 3mM) but only the experimental traces for 3 μ M, 300 μ M and 3mM ryanodine are shown.

In figure 5.8B, 300 μ M ryanodine produced a decrease in the rate of decay in the presence of a calcium challenge thus stimulating calcium release from the SR, resulting in an elevated minimum calcium level. However, subsequent aliquots of calcium produced a progressive increase in the rate of decay suggesting that a gradual block of the RyR took place. Even in the presence of a gradual block, 300 μ M failed to bring the minimum calcium concentration down to the control level but instead produced a new steady state level that was slightly decreased in the presence of 5 μ M RuR. It was also noted that 5 μ M RuR increased the rate of decay of the calcium transient, suggesting that 300 μ M did not produce a full block on SR leak.

3mM ryanodine (figure 5.8C) induced a decline in the rate of calcium decay but to a lesser degree than that observed in 300 μ M ryanodine. However, it was noted that the calcium transient decayed back to control levels and on subsequent additions of calcium, the rate of decay increased. This suggests that a block on the RyR occurred with 3mM ryanodine. The introduction of 5 μ M RuR to the cuvette system failed to significantly increase the rate of decay further. Indicating that 3mM sufficiently blocked the RyR mediated calcium leak from the SR.

The following diagrams illustrate the mean changes in the rate of decay for the increasing concentrations of ryanodine (0.3 μ M, 3 μ M, 30 μ M, 300 μ M and 3mM). The results are presented as a line graph with the rate of decay of the calcium transient plotted against cumulative calcium challenges. In the upper panel (A) the raw (uncorrected) changes in the rate of decay (dCa^{2+}/dt) are shown. In the lower panels (B) the changes in the rate of decay were corrected for the changes observed under control conditions.

Figure 5.9 illustrates the mean results for the cumulative calcium challenges in the presence of 0.3 μ M ryanodine. It is observed that the rate of decay for 0.3 μ M ryanodine followed a similar trend to that of the control over the challenges #0 to #2, increasing by 5% during challenge #1 and then decreased by 3% during challenge #2. Thereafter, as the number of calcium challenge increased, the rate of decay decreased by 35% in the presence of 0.3 μ M ryanodine due to ryanodine increasing the P_o of the RyR. During challenge #4, 5 μ M RuR was introduced to the cuvette system but failed to exert a block on the RyR medicated leak under these conditions, as noted by the continued decline in the rate of decay. In figure 5.9(B), the changes in the rates of decay for 0.3 μ M ryanodine were normalised to the control and followed a similar trend as that seen for the raw data. However, an initial increase in the rate of decay above control levels was observed in the presence of 0.3 μ M ryanodine after the first challenge. This effect was not significant and thereafter the rate of decay declined by 43%. As seen in figure 5.9(A), 5 μ M RuR did not reduce the rate of decay and therefore failed to exert a block on the RyR in the presence of the large SR leak.

Figure 5.10 displays the mean results for 3 μ M ryanodine on SR leak in the presence of cumulative challenges of calcium. It was observed that 3 μ M ryanodine induced a significant decline in the rate of decay after the first calcium challenge (~40% of the control) and to a lesser degree after #1. 5 μ M RuR was introduced to the preparation at challenge #4, resulting in an increase in the rate of decay by ~16%. A value approximately the same as that seen after challenge #1. In figure 5.10(B), the normalised data follow a similar trend as that seen with the raw data although the decline seen with challenge #2 and #3 is less marked (uncorrected 16%, normalised 8.6%).

The mean effect of 30 μ M ryanodine in the presence of cumulative calcium challenges is displayed in figure 5.11. The normalised data produced a similar trend to that of the raw data and on addition of 30 μ M ryanodine, a ~34% decline in the rate of decay occurred. This decline was less marked after challenges #2 and then increased ~20% over challenges #3 and #4. The increase in the rate of decay after the introduction of 5 μ M RuR at #4 suggests a significant SR leak still exists in this preparation.

Figure 5.12 illustrates the mean results for 300 μ M ryanodine in the presence of cumulative calcium challenges. It was noted that 300 μ M ryanodine induced a ~62% decline in the rate of decay after the first calcium challenge. Thereafter the successive calcium challenges induced a gradual blocking effect on the RyR that was more pronounced than with 30 μ M ryanodine (Fig 5.11). The rate of decay increased by 23% from challenge #1 to #2; by 17% from #2 to #3 and then by ~20% in the presence of 5 μ M RuR. This suggests that 300 μ M ryanodine increases the P_o of the RyR before a gradual blocking effect can occur. Although within this time period, 300 μ M failed to exert a full block on the RyR as a slight increase in the rate of decay was noted in 5 μ M RuR.

Figure 5.13 displays the results for 3mM ryanodine in the presence of cumulative calcium challenges. 3mM ryanodine produced a 45% decline in the rate of decay before successive calcium challenges induced a rapid block on SR calcium release via the RyR. Challenge #2 induced a 34% increase in the rate of decay and after #3 the rate of decay increased back to control levels. In the presence of 5 μ M RuR the rate of decay declined by 9% to a rate similar to that produced by #2.

5.4 DISCUSSION

5.4.1. The Effects of RuR on SR Leak

The results for the mean changes in the rate decay for the control, as well as for the effects of the early and late additions of 5 μ M RuR on permeabilised cardiac myocyte preparations are summarised in figure 5.7. The early addition of RuR induced a rapid increase in the rate of decay

suggesting that under control conditions a significant leak exists through the RyR at $1\mu\text{M}$ calcium. Thereafter, subsequent changes in the rate of decay paralleled those seen in control conditions (Fig. 5.7, panel A). This suggests that the slow progressive decrease in the rate of decay over the time course of the experiment was not due to changes in RyR activity under control conditions. The late addition of RuR induced a rapid increase in the rate of decay to a value similar to that seen with the early RuR addition suggesting that the RyR activity is not affected during this protocol. The effects of RuR on the rate of decay can be seen more clearly when the values are normalised for the changes that occur under these conditions (Fig. 5.7, panel B). From the normalised data it appears that the continued presence of RuR causes a progressive decrease in the rate of decay. This was not due to increased RyR activity since additional RuR did not reverse this effect. It is suspected that this result arose from a progressive effect of RuR on SERCA2 (Kargacin & Kargacin, 1998). This is supported by the observation that higher concentrations of RuR ($25\mu\text{M}$) introduced to the preparation after the $5\mu\text{M}$ block, in the presence of subsequent calcium challenges, depressed the rate of decay further and was therefore more effective at slowing calcium uptake (data not shown). Although with a subsequent late addition of RuR in the presence of an early addition in the same preparation (Fig. 5.6), no significant decrease in the rate of decay was observed when compared to the preparation where a late addition of RuR was absent (Fig. 5.4). This suggests that $5\mu\text{M}$ RuR does not produce a significant effect on SERCA2a. However, as stated above, higher concentrations of RuR did produce a decline in the rate of decay. For this reason, lower concentrations of RuR were used in this study to minimise the side effects on SERCA.

The cause of the progressive increase and decrease in the rate of decay seen in figure 5.4A (control) is not known but some theories include

- a) intrinsic changes in SERCA2 activity and the SR calcium leak.
- b) Changes in the solution composition that indirectly affects these proteins.

5.4.1.1. Intrinsic changes in SERCA2 activity and the SR calcium leak

The successive calcium challenges (#-2 to #1) observed in the control (Fig. 5.4A) lead to an initial

increase in the rate of decay of the calcium transient. This progressive increase could arise from the gradual phosphorylation of PLB: the phosphoprotein regulating the activity of SERCA2. Inactivation of the RyR could also account for an increase in the rate of decay, shifting the equilibrium in favour of calcium uptake via Ca^{2+} -ATPase pump due to the loss of competition of the leak through the RyR. However, upon addition of $5\mu\text{M}$ RuR a substantial increase in the rate of decay was observed indicating an SR leak exists in the presence of $1\mu\text{M}$ calcium in this skinned cardiac muscle preparation. If inactivation did occur, a less pronounced blocking effect with $5\mu\text{M}$ RuR would have been expected to ensue. As previously stated, this muscle preparation requires at least 3 aliquots of calcium before reproducible time courses occurred and it is well documented that SR calcium leak depends on SR calcium content (Bassani *et al.*, 1995; Smith & Steele, 1998; Shannon *et al.*, 2000) as well as the free calcium concentration in the mock intracellular solution (Williams & Ashley, 1988). If the SR luminal calcium concentration was low (due to oxalate precipitation of calcium) then a calcium leak from the SR would be slight, thus giving rise to an increase in calcium uptake noted by a faster rate of decay upon initial calcium challenges, which is what was observed in this study. Therefore, phosphorylation of phospholamban seems a likely candidate for the increase in the rate of decay shown in figure 5.4, giving rise to a larger SR calcium pool available for release.

There is mounting evidence to suggest that calcium release channels in the SR can be influenced by luminal calcium (Fabiato, 1992; Sitsapesan & Williams, 1994; Bassani *et al.*, 1995; Lukyanenko *et al.*, 1996; Gyorke *et al.*, 1997; Gyorke & Gyorke, 1998) and that the loading of the SR directly alters the gain of the EC Coupling and therefore a higher SR calcium content leads to a greater release of calcium for any given calcium trigger (Bassani *et al.*, 1995; Lukyanenko, *et al.*, 1996). An increased luminal calcium content leads to the generation of calcium sparks and the propagation of calcium waves; a calcium waves arises from the spatial and temporal summation of sparks (Cannell *et al.*, 1994; Lopez-Lopez *et al.*, 1995; Cheng *et al.*, 1996). Under normal conditions, almost all sparks remain localised and die out without inducing the release of calcium in adjacent release sites (Cheng *et al.*, 1993; Lukyanenko *et al.*, 1996). However, under conditions of

increased cellular calcium load, sparks increase in amplitude and frequency to become the initiation sites for calcium wave propagation (Cheng *et al.*, 1993; Cheng *et al.*, 1996; Lukyanenko *et al.*, 1996; Satoh *et al.*, 1997). An increased resting calcium level and an elevated intraluminal calcium can induce a calcium spark from a local release site.

Calcium sequestered into the SR by the calcium pump can act at an intraluminal calcium binding site(s) (Takamatsu & Wier, 1990; Fabiato, 1992). Sitsapesan & Williams (1994) have shown that calcium acting on an intraluminal site of the RyR can induce calcium release in lipid bilayers (Sitsapesan & Williams, 1997; Lukyanenko *et al.*, 1996). The precise locations for the luminal activation and inhibition binding sites have yet to be located; they could be situated on the RyR or on a protein associated with the receptor. However, as demonstrated in chapter 4, the use of 20mM oxalate would reduce the luminal calcium concentration to ~6 μ M. Under these conditions luminal regulation would not be considered an important factor determining the activity of RyR on addition of RuR or ryanodine. So therefore, in our preparation, oxalate would prevent the initiation of calcium sparks and calcium induced waves in cardiac myocytes under these conditions.

5.4.1.2 Changes in solution composition that indirectly affect SERCA2 and RyR activity

The changes in solution chemistry may be linked to changes associated with the metabolic activity of the cells. A decrease in rate of decay of calcium uptake via SERCA2 could be explained by a fall in CrP levels within the preparation.

An elevation of the intracellular calcium concentration, whether through sarcolemma calcium channels or release from intracellular stores, activates the SR calcium pump. The pump transports two calcium ions into the lumen of the SR for every ATP consumed in the reaction. ATP levels are buffered with the addition of CrP to the preparation thus providing a source of ATP regeneration. If CrP levels were to fall, inorganic phosphate (Pi) levels would increase. Under these circumstances, insufficient ATP regeneration would ensue leading to a decrease in ATP concentration and therefore decreased pump activity. To test this hypothesis, 10mM CrP was introduced at the end of the protocol. If the preparation had an insufficient concentration of CrP, on

its addition an increase in the rate of decay would have been expected to occur. However, no change in the calcium uptake rate was observed (data not shown). Thus it is unlikely that this metabolic change can account for the fall in the rate of decay seen in figure 5.4A.

Other candidates influencing the rate of calcium uptake are H^+ ions and P_i (Smith *et al.*, 2000; Smith & Steele, 1998). The breakdown of MgATP to MgADP and P_i is accompanied by the release of protons. During the breakdown of MgATP, ~ 0.7 moles H^+ ions are released at neutral pH (Wilkie, 1979). CrP breakdown absorbs ~ 0.4 moles H^+ ions (Moisescu & Theileczek, 1978) and thus the net effect of ATP breakdown is that of a slight acidosis where the presence of 25mM Heps should be sufficient to buffer the pH and prevent large changes. However, measurements are required to confirm this.

5.4.2. The Effects of Ryanodine on SR Leak

The results for the normalised and raw relative changes in the rate decay for the effects of the individual ryanodine concentrations on permeabilised cardiac myocyte are summarised figure 5.14. In this preparation, low concentrations of ryanodine (0.3 μ M, 3 μ M) induced a sustained increase in SR calcium leak from the RyR and it was observed that 0.3 μ M did not exert an effect till after the second calcium challenge. High concentrations (30 μ M, 300 μ M and 3mM) increased the P_o of the ryanodine receptor for a short period before a reduction in the SR calcium leak was noted. Interestingly 3 μ M and 3mM exerted similar rates of decay after the first calcium challenge, whereas 30 μ M and 300 μ M induced a slowing in the rate of decay which was 20% more than that observed with 3 μ M or 3mM. A relatively fast block on SR occurred with 3mM whereas 300 μ M failed to block the SR leak in the given time frame for the oxalate supported experiments and also failed to reduce the calcium level back to the minimal level. Thus the preparation used in this study favoured a block with 3mM ryanodine whereas the literature states that 300 μ M ryanodine (Ma, 1993) blocks the calcium release channel. In support of our studies, that higher ryanodine concentrations are required to induce a block on the RyR, study carried out by Masumiya *et al.*, 2001 on RyR incorporated into lipid bilayers noted that 500 μ M ryanodine was unable to induce a

complete block of calcium release from the RyR. Therefore, the effect of ryanodine depends on a variety of factors including the method used (SR vesicles maybe more sensitive to ryanodine and therefore requires a lower concentration of ryanodine), the animal species as well as the length of time of ryanodine incubation and temperature.

The slow time course of the calcium transient produced during the effects of ryanodine on calcium uptake are consistent with the slow binding of ryanodine to the RyR at this temperature (22°C) (Smith *et al.*, 1988).

These results compliment the literature suggesting the RyR possess two binding sites for ryanodine: a low affinity and a high affinity binding site (Lai *et al.*, 1989; McCrew *et al.*, 1989; Meissner, Rousseau & Lai, 1989; Pessah & Zimanyi, 1991; Wang *et al.*, 1993). Low concentrations of ryanodine bind to the high affinity binding site to induce a long lived open state. High concentrations of ryanodine bind to the low affinity binding site to exert a block on SR leak. Lai *et al.* (1989) demonstrated that there is one high affinity and three low affinity binding sites per tetramer of the RyR. The binding of ryanodine to the RyR is very slow. Consequently the effects of ryanodine are slow to develop (Bers & Perez-Reyes, 1999; Alderston & Feher, 1987). The high affinity binding site is only accessible when the channel site is in an open configuration and thus led to the suggestion that this binding region is located in the pore of the channel (Tanna *et al.*, 2000). Recent investigations have demonstrated that mutations of residues located in the trans membrane regions of the RyR modify the ability of the receptor to bind ryanodine (Zhao *et al.*, 1999; Gao *et al.*, 2000). The effects of ryanodine require an active RyR either by increased calcium concentrations, decreased Mg^{2+} , ATP or caffeine.

In this study, the RyR activity was noted in the presence of 1mM Mg^{2+} . It is thought that physiological concentrations of Mg^{2+} cause a reduction in the open probability of all isoforms of the RyR to inhibit calcium release (Tinker & Williams, 1992). In order for Mg^{2+} to induce inhibition, it competes with calcium for the calcium activation/inhibition sites (Ashley & Williams, 1990; Meissner *et al.*, 1986; Laver *et al.*, 1997). The affinity and efficacy of Mg^{2+} for the calcium inhibition site is much greater than that for the activation site, thus Mg^{2+} binds to the high affinity

binding site to inhibit calcium release (Du *et al.*, 2000). However in this preparation, the presence of activating calcium levels as well as a ligand can stimulate the RyR even in the presence of 1mM Mg^{2+} .

It was observed that 5 μ M RuR failed to block the large SR leak induced by 0.3 μ M ryanodine. The reason for this is unknown; the leak could be so large that 5 μ M RuR may be ineffective thus higher concentrations of RuR maybe required. However, higher concentrations of RuR were not used in this study because, as stated previously, Kargacin & Kargacin (1998) proposed that high concentrations of RuR have a detrimental effect on SERCA2A, altering the calcium sensitivity of the SR calcium uptake with no detectable effect on the Hill coefficient or maximum uptake rate (Kargacin & Kargacin, 1998) and that the effect of RuR on SERCA2A is likely to arise from direct action of RuR on SR Ca^{2+} -ATP-ase and would occur independently of any effects of RuR on the RyR. A direct action of RuR was reported by Alves de Meis (1986) who found that RuR competes with calcium for the high affinity binding sites on the skeletal muscle SR Ca^{2+} -ATPase as well as inhibiting calcium binding to calcium binding proteins. However, as discussed in chapter 5.3.3.1, 5 μ M RuR did not produce a significant effect on SERCA2A. The results in this chapter suggest that RuR can have a blocking effect on RyR in the presence of 3 μ M, 30 μ M and 300 μ M ryanodine but no further block was observed in the presence of 3mM ryanodine, in fact the results suggest a slight increase in calcium release (not significant). It is unlikely that RuR displaces ryanodine from the RyR since the affinity of the RyR for ryanodine is very high. However, there are other pathways through which RuR may mediate an effect. Netticadan *et al.*, (1996) have shown that RuR exerts a concentration dependent inhibition of the phosphorylation of the RyR by both endogenous and exogenous CaM-K, whereas low concentrations of ryanodine (0.25 - 1 μ M) stimulate CaM-K mediated phosphorylation. RuR can act by binding to multiple sites located in the conduction pore of the calcium release channel. This block is cooperative with a Hill Coefficient of 2; one molecule is sufficient to block the channel and additional binding of RuR keeps the channel in a closed state (Ma, 1993). Thus RuR occludes the calcium release channel to induce closure and in doing so produces a conformation change in the protein thus rendering the CaM-K

phosphorylation site inaccessible (Netticadan, 1996). Under these circumstances 5 μ M RuR, in the presence of 3mM ryanodine and repeated calcium challenges, may enhance the detrimental effects on SERCA2A as discussed previously. Further work is required to determine the details of the interaction between RuR and ryanodine at the RyR.

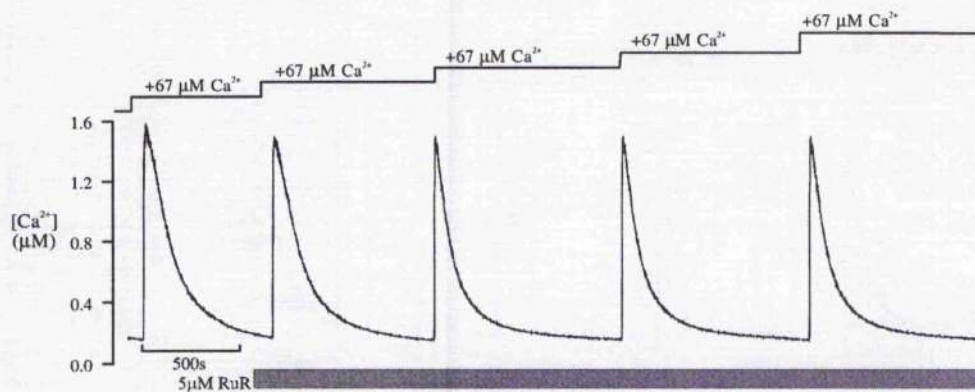


Fig 5.1: A typical experimental trace for an early addition of RuR. After a control transient was established, $5 \mu M$ RuR was introduced to the preparation prior to a calcium bolus ($67 \mu M$). The free calcium in the cuvette increased to $1.6 \mu M$ and then decayed back to diastolic levels before another 3 calcium challenges were added at 12 minute intervals. The solution composition, bathing the cells prior to the additions indicated in the figure, is as follows; $0.05R$ (table 2.2), $20mM$ Oxalate, $10 \mu M$ Fura-2, $5mM$ ATP, $15mM$ CrP, $0.1 \mu M$ DTT, $10 \mu M$ CCCP and $33 \mu M$ Oligomycin.

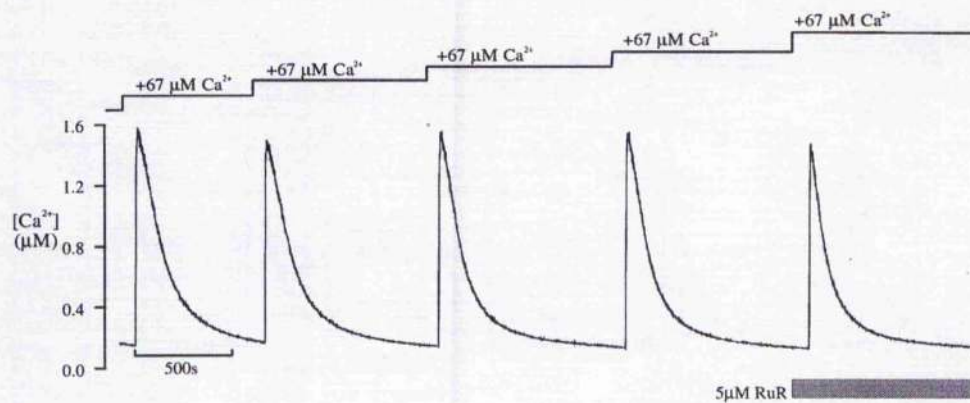
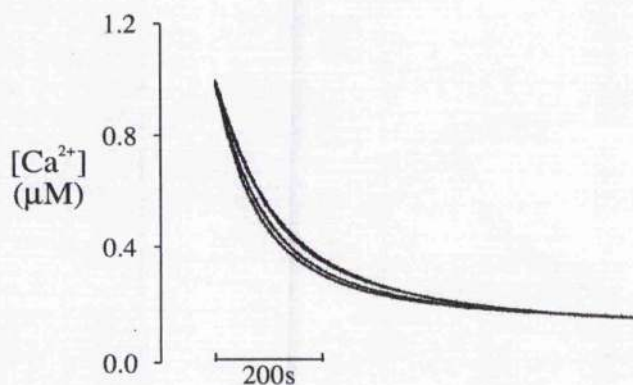


Figure 5.2: *Typical experimental trace for a late addition of RuR.* After a control transient was established, 3 successive calcium challenges were added at 12 minute intervals before $5 \mu M RuR$ was introduced to the preparation prior to a calcium bolus ($67 \mu M$). The solution composition, bathing the cells prior to the additions indicated in the figure, is as follows; 0.05R (table 2.2), 20mM Oxalate, $10 \mu M$ Fura-2, 5mM ATP, 15mM CrP, $0.1 \mu M$ DTT, $10 \mu M$ CCCP and $33 \mu M$ Oligomycin.

(A)



(B)

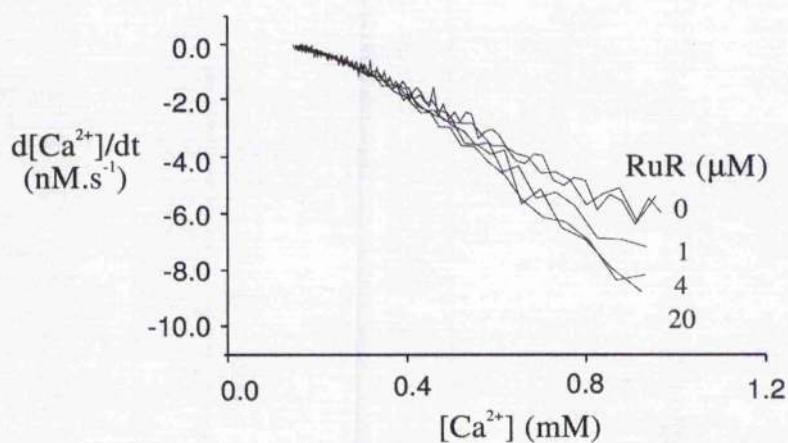
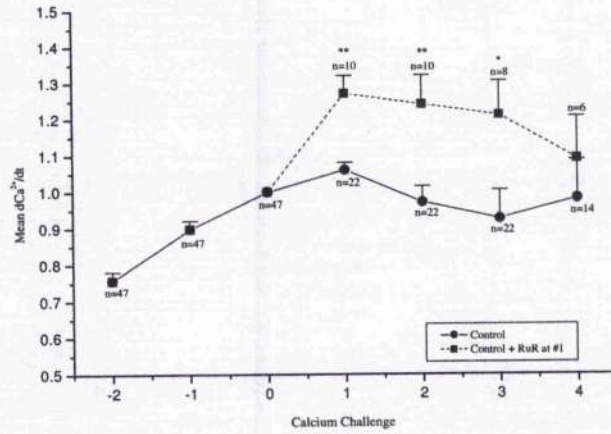


Figure 5.3: Description of the dCa^{2+}/dt analysis. (A) The digitised traces converted into calcium concentrations using the parameters provided by the Fura-2 calibration curves. These values were plotted using the program Origin (Microcal software), where a bi-exponential curve was fitted below 700nM calcium concentration. (B) The plot of the rate of change of calcium at each calcium concentration (dCa^{2+}/dt), derived from the curve shown in panel A. The value of dCa^{2+}/dt at $\sim 1\mu M$ ($\pm 0.2\mu M$) was used as a measure of flux through the RyR. The solution composition, bathing the cells prior to the RuR addition indicated in the figure, is as follows; 0.05R (table 2.2), 20mM Oxalate, 10 μM Fura-2, 5mM ATP, 15mM CrP, 0.1 μM DTT, 10 μM CCCP and 33 μM Oligomycin.

(A)



(B)

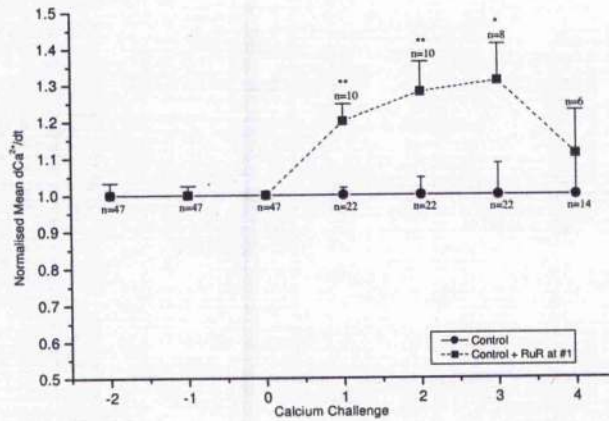
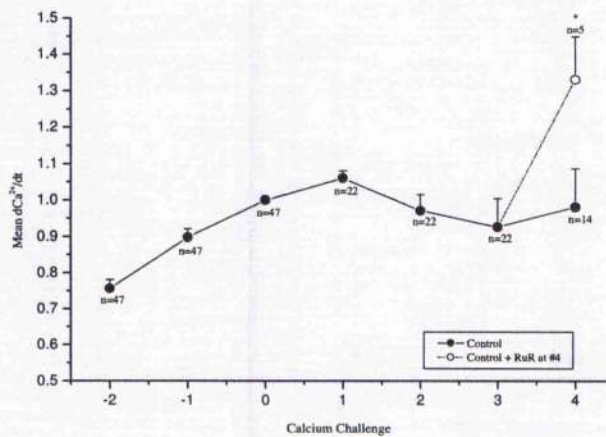


Figure 5.4: The raw and normalised mean rate of decay for the early addition of RuR. (A) Displays the raw mean data for the rate of decay in the presence (---■---) and in the absence (---●---) of $5\mu\text{M}$ RuR, plotted against the increasing calcium challenges. $5\mu\text{M}$ RuR was added at calcium challenge #1. (B) Displays the normalised mean data for the rate of decay in the presence (---■---) and in the absence (---●---) of $5\mu\text{M}$ RuR, plotted against the increasing calcium challenges. $5\mu\text{M}$ RuR was added at calcium challenge #1. (mean \pm s.e.m., * denotes $P < 0.05$, ** denotes $P < 0.005$). ANOVA with a Tukey post hoc test was used for multiple comparisons. The solution composition, bathing the cells prior to the RuR addition indicated in the figure, is as follows; 0.05R (table 2.2), 20mM Oxalate, $10\mu\text{M}$ Fura-2, 5mM ATP, 15mM CrP, $0.1\mu\text{M}$ DTT, $10\mu\text{M}$ CCCP and $33\mu\text{M}$ Oligomycin.

(A)



(B)

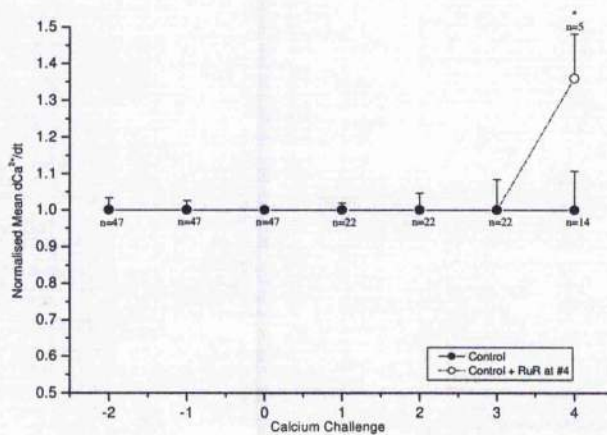
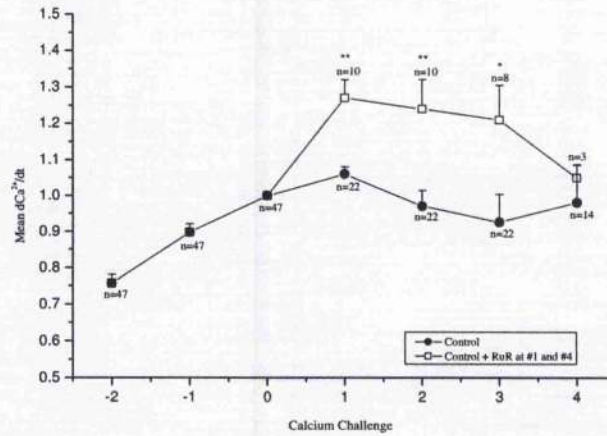


Figure 5.5: The raw and normalised mean rate of decay for the late addition of RuR. (A) Displays the raw mean data for the rate of decay in the presence (\circ) and in the absence (\bullet) of $5\mu\text{M}$ RuR, plotted against the increasing calcium challenges. $5\mu\text{M}$ RuR was introduced to the cuvette system at calcium challenge #4. (B) Displays the normalised mean data for the rate of decay in the presence (\circ) and in the absence (\bullet) of $5\mu\text{M}$ RuR, plotted against the increasing calcium challenges. $5\mu\text{M}$ RuR was added after #4. (mean \pm s.e.m., * denotes $P < 0.05$). Significance was tested using a students unpaired t-test. The solution composition, bathing the cells prior to the RuR addition indicated in the figure, is as follows; 0.05R (table 2.2), 20mM Oxalate, 10 μM Fura-2, 5mM ATP, 15mM CrP, 0.1 μM DTT, 10 μM CCCP and 33 μM Oligomycin.

(A)



(B)

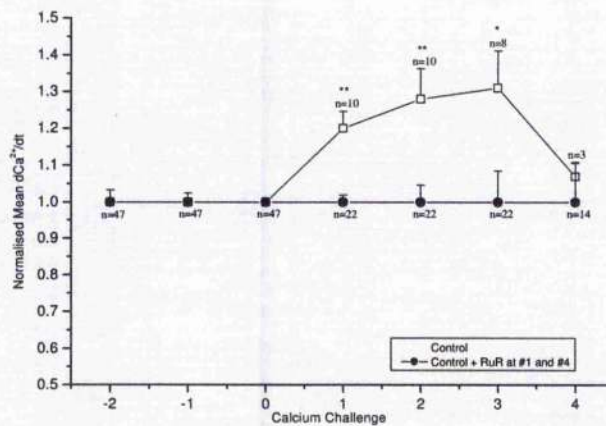
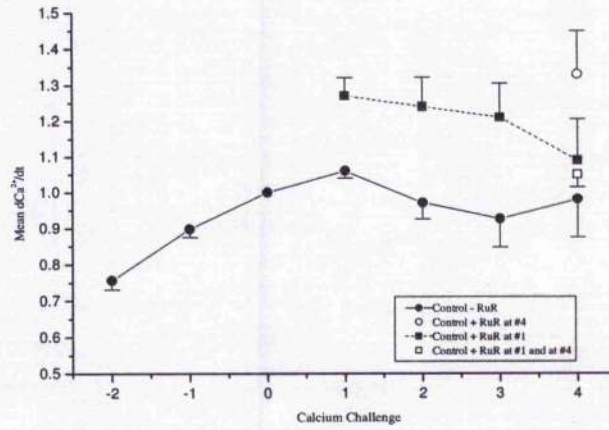


Figure 5.6: The raw and normalised mean rate of decay for the early and late additions of RuR. (A) Displays the raw mean data for the rate of decay in the presence ($-\square-$) and in the absence ($-\bullet-$) of $5\mu\text{M}$ RuR, plotted against the increasing calcium challenges. $5\mu\text{M}$ RuR was introduced to the cuvette system at calcium challenges #1 and #4. (B) Displays the normalised mean data for the rate of decay in the presence ($-\square-$) and in the absence ($-\bullet-$) of $5\mu\text{M}$ RuR, plotted against the increasing calcium challenges. $5\mu\text{M}$ RuR was added after #1 and #4. (mean \pm s.e.m., * denotes $P < 0.05$, ** denotes $P < 0.005$). ANOVA with a Tukey post hoc test was used for multiple comparisons. The solution composition, bathing the cells prior to the RuR addition indicated in the figure, is as follows; 0.05R (table 2.2), 20mM Oxalate, 10 μM Fura-2, 5mM ATP, 15mM CrP, 0.1 μM DTT, 10 μM CCCP and 33 μM Oligomycin.

(A)



(B)

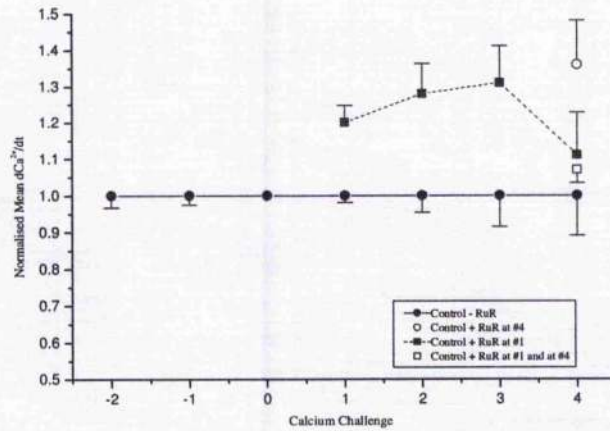
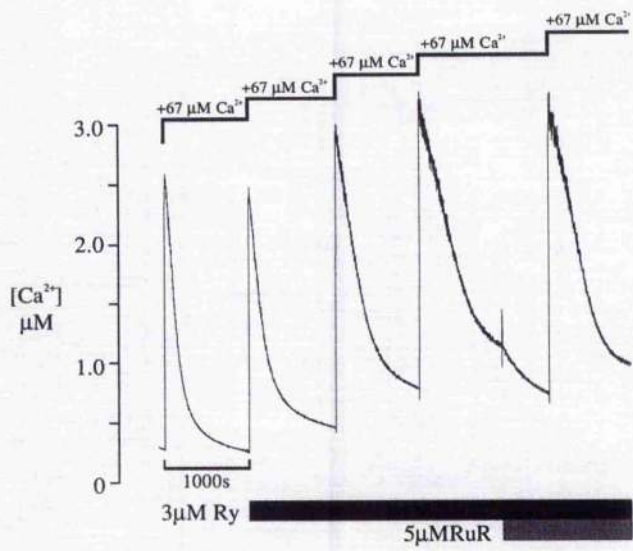
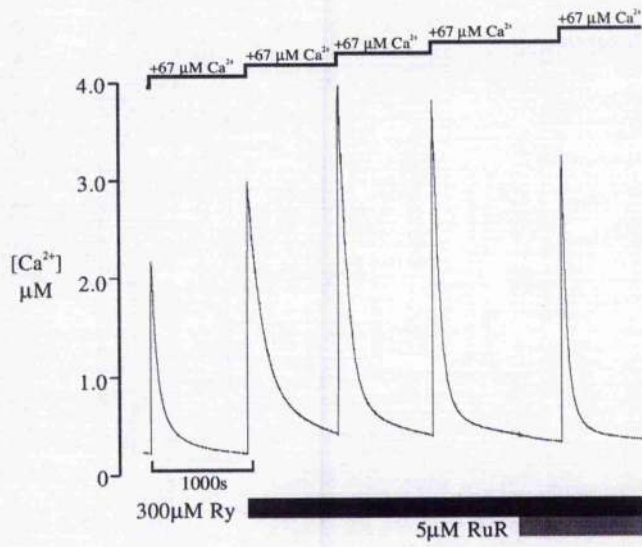


Figure 5.7: Summary of the raw and normalized mean rate of decay produced in the presence and in the absence of RuR. (A) Shows the raw mean data for the rate of decay. (B) Displays the mean normalized data for the rate of decay. Both in the absence (\bullet) and in the presence of $5\mu M$ RuR. $5\mu M$ RuR was added at #1 only (\blacksquare), at #4 only (\circ) and at #1 and #4 in the same preparation (\square). The solution composition, bathing the cells prior to the RuR addition indicated in the figure, is as follows; $0.05R$ (table 2.2), $20mM$ Oxalate, $10\mu M$ Fura-2, $5mM$ ATP, $15mM$ CrP, $0.1\mu M$ DTT, $10\mu M$ CCCP and $33\mu M$ Oligomycin.

(A)



(B)



(C)

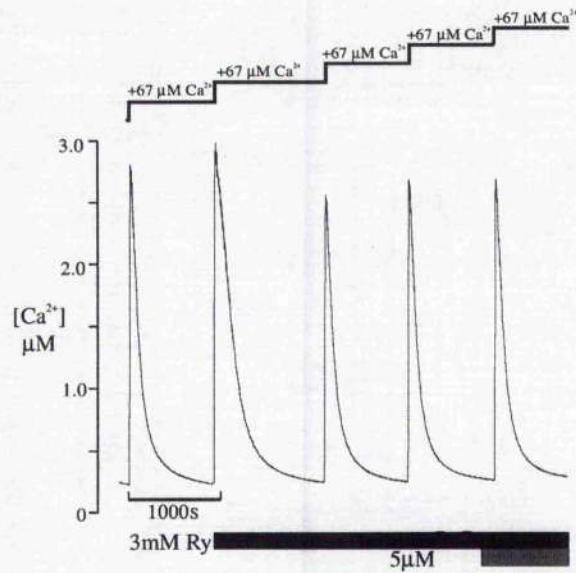
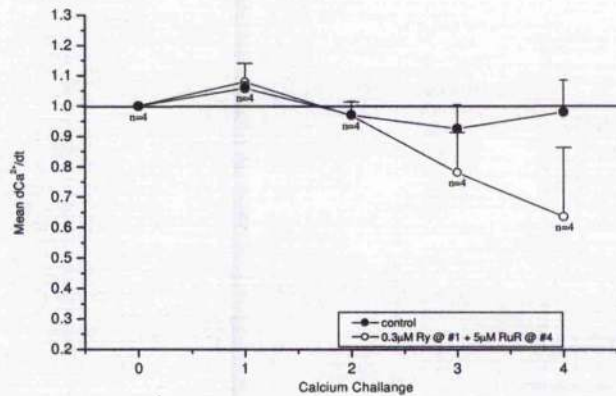


Figure 5.8: *The effects of ryanodine and RuR on the rate of decay of successive calcium transients.* (A) A typical experimental trace to show the effects of 3 μ M Ry and 5 μ M RuR on the rate of decay of the calcium transients. After a control transient was established, 3 μ M Ry was introduced to the preparation. Then 5 μ M RuR was added after the fourth calcium boli to assess the SR leak induced with Ry. (B) A typical experimental trace to display the effects of 300 μ M Ry and 5 μ M RuR on the rate of decay of the calcium transients. (C) A typical experimental trace showing the effects of 3mM Ry and 5 μ M RuR on the rate of decay of the calcium transients. The solution composition, bathing the cells prior to the Ryanodine and RuR additions indicated in the figure, is as follows; 0.05R (table 2.2), 20mM Oxalate, 10 μ M Fura-2, 5mM ATP, 15mM CrP, 0.1 μ M DTT, 10 μ M CCCP and 33 μ M Oligomycin.

(A)



(B)

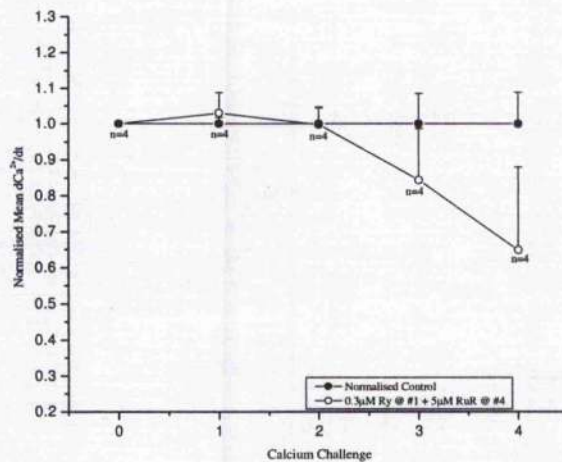
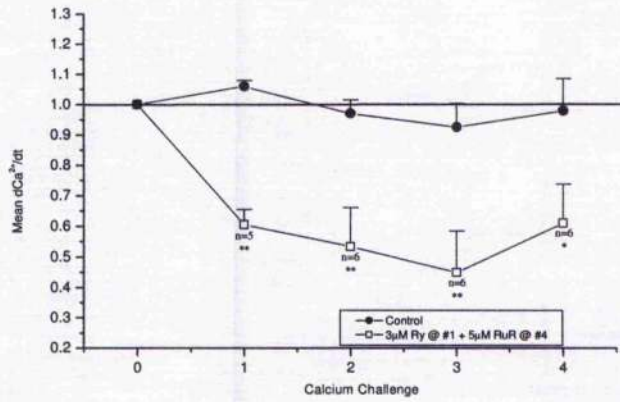


Figure 5.9: The effect of 0.3µM ryanodine on the rate of decay for successive calcium transients.

(A) Displays the mean raw (uncorrected) data for the rate of decay in the absence (—●—) and in the presence of 0.3µM Ry (—○—), plotted against successive calcium challenges. (B) Displays the normalised mean data for the rate of decay in the absence (—●—) and in the presence of 0.3µM Ry (○), where Ry was added at #1 and 5µM RuR was added at #4 (—○—). The mean rates of decay were normalised to the control. (mean ± s.e.m., n=4). ANOVA with a Tukey post hoc test was used for multiple comparisons. The solution composition, bathing the cells prior to the Ryanodine and RuR additions indicated in the figure, is as follows; 0.05R (table 2.2), 20mM Oxalate, 10µM Fura-2, 5mM ATP, 15mM CrP, 0.1µM DTT, 10µM CCCP and 33µM Oligomycin.

(A)



(B)

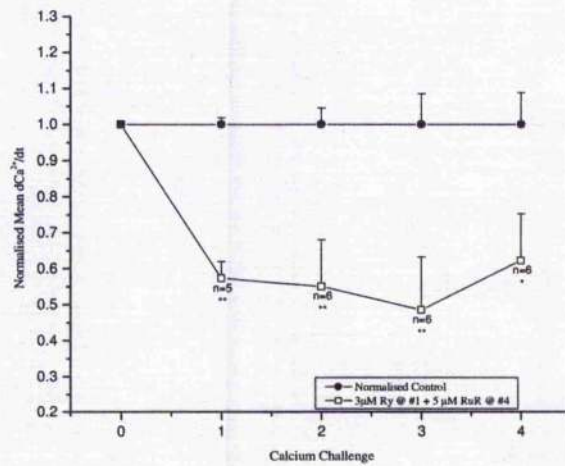
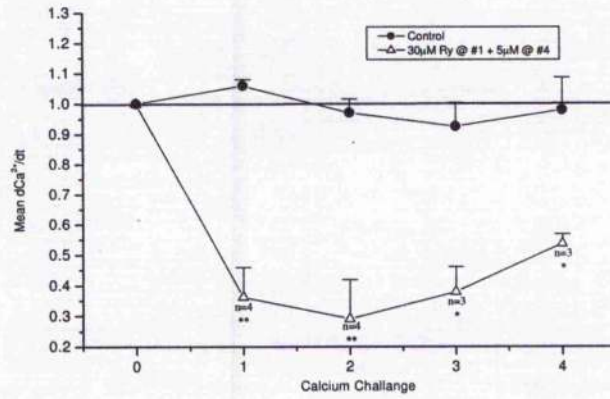


Figure 5.10: The effects of 3 μ M ryanodine on the rate of decay for successive calcium transients. (A) Displays the mean raw data for the rate of decay in the absence (—●—) and in the presence of 3 μ M Ry (—□—), where Ry was introduced at #1 and 5 μ M RuR at #4. (B) Displays the normalised mean data for the rate of decay in the absence (—●—) and in the presence of 3 μ M Ry (□). Ry was added at #1 and 5 μ M RuR at #4 (—□—). (mean \pm s.e.m., * denotes $P < 0.05$, ** denotes $P < 0.005$). ANOVA with a Tukey post hoc test was used for multiple comparisons. The solution composition, bathing the cells prior to the Ryanodine and RuR additions indicated in the figure, is as follows; 0.05R (table 2.2), 20mM Oxalate, 10 μ M Fura-2, 5mM ATP, 15mM CrP, 0.1 μ M DTT, 10 μ M CCCP and 33 μ M Oligomycin.

(A)



(B)

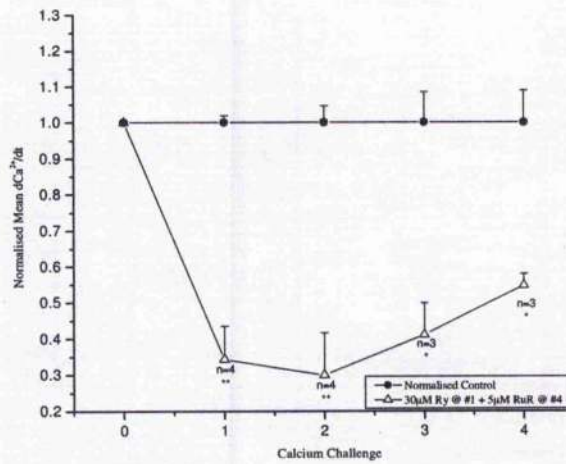
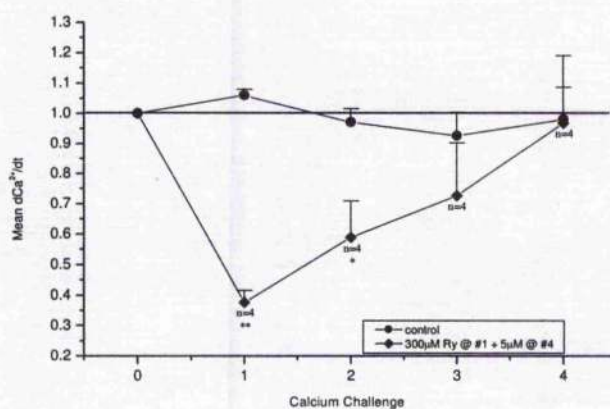


Figure 5.11: The effects of 30 μ M ryanodine on the rate of decay for successive calcium transients. (A) Displays the mean raw data for the rate of decay in the absence (\bullet) and in the presence of 30 μ M Ry (\square); Ry was introduced at #1 and 5 μ M RuR at #4. (B) Displays the normalised mean data for the rate of decay in the absence (\bullet) and in the presence of 30 μ M Ry (Δ); Ry was added at #1 and 5 μ M RuR at #4. (mean \pm s.e.m, * denotes $P < 0.05$, ** denotes $P < 0.005$). ANOVA with a Tukey post hoc test was used for multiple comparisons. The solution composition, bathing the cells prior to the Ryanodine and RuR additions indicated in the figure, is as follows; 0.05R (table 2.2), 20mM Oxalate, 10 μ M Fura-2, 5mM ATP, 15mM CrP, 0.1 μ M DTT, 10 μ M CCCP and 33 μ M Oligomycin.

(A)



(B)

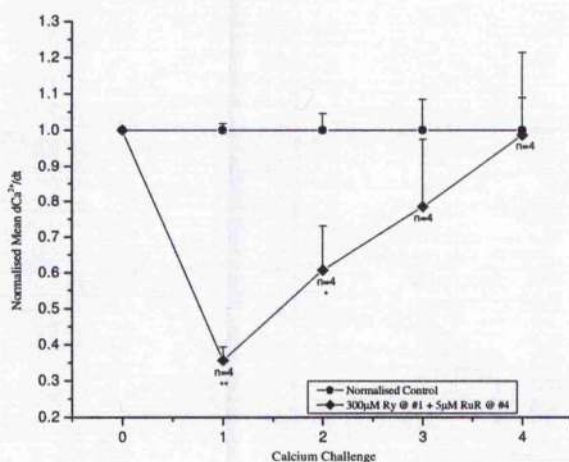
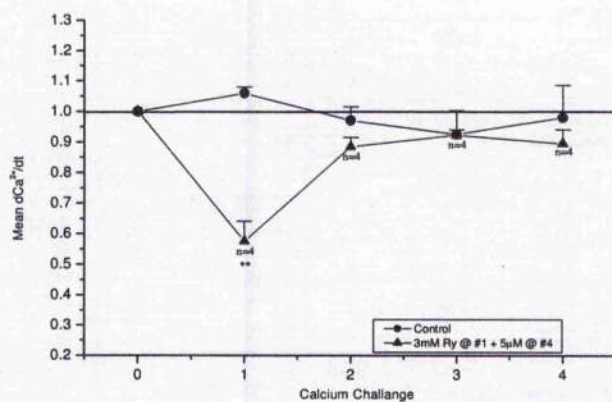


Figure 5.12: The effects of 300 μM ryanodine on the rate of decay for successive calcium transients. (A) Displays the mean raw data for the rate of decay in the absence (—●—) and in the presence of 300 μM Ry (—◆—); Ry was introduced at #1 and 5 μM RuR at #4. (B) Displays the normalised mean data for the rate of decay in the absence (—●—) and in the presence of 300 μM Ry (—◆—); Ry was added at #1 and 5 μM RuR at #4 (—◆—). (mean \pm s.e.m. * denotes $P < 0.05$, ** denotes $P < 0.005$). ANOVA with a Tukey post hoc test was used for multiple comparisons. The solution composition, bathing the cells prior to the Ryanodine and RuR additions indicated in the figure, is as follows; 0.05R (table 2.2), 20mM Oxalate, 10 μM Fura-2, 5mM ATP, 15mM CrP, 0.1 μM DTT, 10 μM CCCP and 33 μM Oligomycin.

(A)



(B)

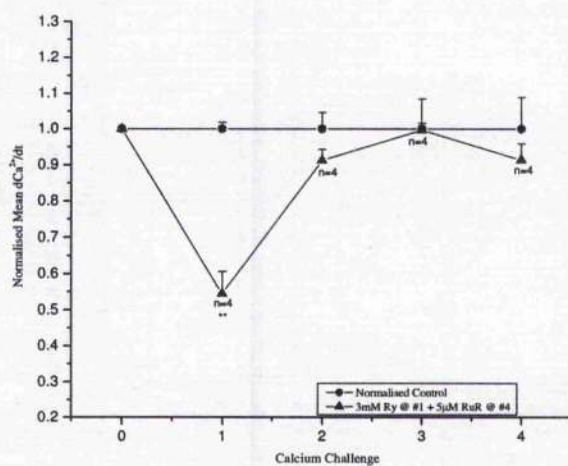
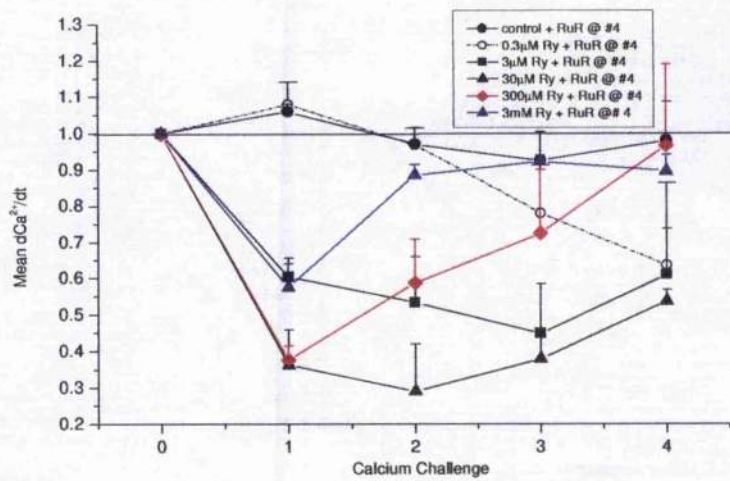


Figure 5.13: The effects of 3mM ryanodine on the rate of decay for successive calcium transients. (A) Displays the mean raw data for the rate of decay in the absence (●) and in the presence of 3mM Ry (▲); Ry was introduced at #1 and 5µM RuR at #4. (B) Displays the normalised mean data for the rate of decay in the absence (●) and in the presence of 3µM Ry (▲); Ry was added at #1 and 5µM RuR at #4. (mean \pm s.e.m., * denotes $P < 0.05$, ** denotes $P < 0.005$). ANOVA with a Tukey post hoc test was used for multiple comparisons. The solution composition, bathing the cells prior to the Ryanodine and RuR additions indicated in the figure, is as follows; 0.05R (table 2.2), 20mM Oxalate, 10µM Fura-2, 5mM ATP, 15mM CrP, 0.1µM DTT, 10µM CCCP and 33µM Oligomycin.

(A)



(B)

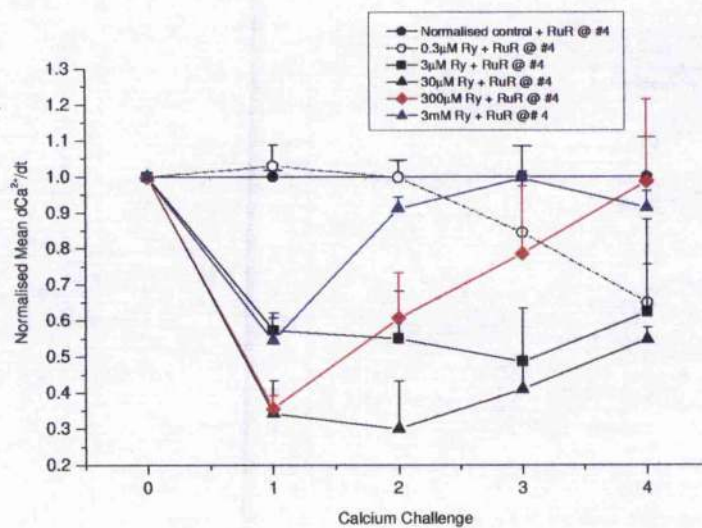


Figure 5.14: Summary of the effects of ryanodine on calcium transient rate of decay. (A) The mean raw rates of decay produced by the introduction of 0.3 μ M, 3 μ M, 30 μ M, 300 μ M and 3mM ryanodine at #1 and 5 μ M RuR at #4. (B) The normalised mean rates of decay for the above ryanodine concentrations.

CHAPTER SIX

CAFFEINE MEDIATED CALCIUM LEAK

6.1. INTRODUCTION

Caffeine has been widely used as a pharmacological tool for releasing calcium from intracellular stores to study the role of the sarcoplasmic reticulum during excitation contraction coupling. The exact mechanism by which caffeine exerts its action is not fully understood. However, studies so far have shown caffeine to possess several actions: it releases calcium ions from the SR (Weber & Herz, 1968); it sensitises the contractile machinery to intracellular calcium concentrations (Wendt & Stephenson, 1983; Eiscner & Valdecomillos, 1985); and acts to inhibit phosphodiesterase activity (Butcher & Sutherland, 1962; Robison *et al.*, 1968).

Caffeine induces calcium release from the SR by binding to a specific site on the cytosolic side of the RyR. Thus, increasing the apparent affinity of the calcium activation site for calcium causing a cooperative interaction between these sites, in a reversible manner (Rousseau *et al.*, 1989; Sitsapean & Williams, 1990; Meissner *et al.*, 1997) and markedly increases the P_o of the channel with no effect on single channel conductance. The P_o of the channel is primarily regulated by free cytosolic calcium concentrations (Ashley & Williams, 1990; Williams & Ashley, 1989) but can be further increased in the presence of ATP, and reduced by magnesium and RuR (Ashley & Williams, 1990; Williams & Ashley, 1989).

Cardiac muscle SR can accumulate a significant amount of calcium in the presence of ATP and high concentrations of caffeine (up to 20mM) and when caffeine is added in the absence of ATP, thus inhibiting the Ca^{2+} -ATPase pump, a sustained calcium release occurs increasing towards a maximal level (Feher & Briggs, 1982). This leak pathway is independent of the RyR due to the receptor being inhibited in the absence of ATP (Alpert *et al.*, 1989) and under these circumstances the total calcium released from the SR can be quantified and used to calculate the calcium content of the SR accessed by caffeine. (Varro *et al.*, 1993; Bers, 1987; Smith & Steele, 1998).

Ritter *et al.*, (2000) hypothesised that caffeine induced calcium release from cardiac myocytes (especially when intracellular caffeine concentrations are low) may commence with events that resemble calcium sparks. Calcium sparks are local increases in intracellular calcium concentrations and the spatial and temporal summation of which have been suggested to contribute to E-C

coupling (Cheng *et al.*, 1993; Cannell *et al.*, 1994). Spontaneous release of calcium occurs once a threshold level of SR calcium is reached (Díaz *et al.*, 1997) and the frequency at which spontaneous release occurs depends on the rate at which calcium pumped out of the cell is replenished (Díaz *et al.*, 1997).

Sparks have been ascribed to RyR openings induced by influx of calcium from the L-type calcium channels or by spontaneous RyR openings. In the presence of caffeine, calcium release occurs at lower levels of SR calcium suggesting that caffeine lowers the critical level of SR calcium content at which spontaneous calcium is released (Trafford *et al.*, 2000b). Ritter *et al.*, (2000) found that caffeine induced sparks are independent of the activation of the L-type calcium channel. This confirmed previous observations made by Cheng *et al.*, (1993) that initiation of sparks does not require calcium influx via the calcium channel and that the initiation is dependent on, the time to expose the cell to caffeine as well as diffusion of caffeine to the RyR. After the diffusion of caffeine, sparks first appeared close to the cell surface membrane before summation to produce a whole cell calcium transient. From these findings, Ritter suggested that caffeine induced calcium sparks originate from a cluster of RyR openings (Ritter *et al.*, 2000).

Work carried out by Sitsapesan and Williams (1990), showed that at least two distinct modes of action were responsible for caffeine induced calcium release from the SR: a calcium dependent mechanism seen with relatively low concentrations of caffeine (0.5-2.0mM) which can activate the SR calcium release channel by increasing the frequency of channel opening without significantly effecting the duration of open events; and a calcium independent mechanism requiring higher (>5mM) concentrations. Low doses of caffeine (0.5-2mM) have no effect on calcium induced calcium release when the cytosolic calcium level is below 80pm (Rousseau *et al.*, 1986). However, in the presence of high caffeine concentrations (>5mM) a second calcium independent activation of the RyR is revealed.

Sustained application of caffeine causes a concentration dependent release of calcium from the RyR where the ability of the SR to re-accumulate calcium is inversely proportional to the caffeine concentration applied in the range 5-40mM (Smith & Steele, 1998). High concentrations of caffeine will therefore deplete the SR of calcium since the rate of calcium release is greater than the

maximal rate of SERCA 2A mediated calcium re-uptake. The degree of calcium re-uptake in the presence of caffeine will depend on the cytosolic calcium concentration and the characteristics of the calcium pump (Smith & Steele, 1998). Where as sustained applications of low concentrations of caffeine are thought to stimulate calcium release without inhibiting the ability of the SR to re-accumulate calcium during diastole. Inesi & de Meis (1989) reported that a reduced luminal SR calcium content (as described above with the addition of low concentrations of caffeine) is known to stimulate SERCA 2A mediated calcium uptake (Inesi & de Meis, 1989; Weber, 1971). Decreasing luminal calcium concentrations as well as stimulating SR calcium uptake could prove to be an important modulator of calcium cycling and force development during excitation contraction coupling of cardiac muscle.

To date, the site(s) on the RyR responsible for the caffeine effect have not been elucidated, however studies conducted by Bhat *et al.*, (1997c) observed that caffeine induced release of calcium in a dose dependent manner from cells expressing the full length RyR. Therefore, the caffeine binding site(s) have been suggested to reside within the amino-terminal foot region of the RyR.

It is not clear from previous publications the extent to which caffeine mediated calcium leak is blocked by ryanodine and RuR. The purpose of this chapter is to describe experiments designed to study this in permeabilised rabbit cardiac myocytes preparations.

6.2 METHODS

Cardiac myocytes were prepared for calcium uptake/leak studies as previously described in chapter 2. 1×10^6 permeabilised cells were transferred to the closed cuvette system where changes in the intracellular free calcium concentrations were detected using the fluorescent indicator fura-2. Following a 3minute incubation, allowing the cells to reach an equilibrium with the mock intracellular environment, a few boluses of 8-12 μ l 10mM calcium chloride were added to raise the free calcium concentration to 1-2 μ M which decayed in an exponential fashion. Three boluses, introduced at 12minute intervals, were found to be adequate for producing reproducible calcium transients.

The analysis of the uptake time course was conducted in two ways: (1) The rate of decay at a set calcium concentration was used to assess the SR calcium uptake rate. (2) An exponential was fitted to the calcium decay and the time constant used as a measure of the rate of decay. This latter method was used in situations where the maximum and minimum calcium varied (e.g. in the presence of various caffeine concentrations). Under these circumstances, a single calcium concentration measurement was not reliable.

6.3 RESULTS

6.3.1. The Effects of Low Concentrations of Caffeine on SERCA2A

Figure 6.1A is a typical experimental trace to display the effects of 300 μ M Ryanodine and 5 μ M RuR on calcium uptake in the presence of 2mM caffeine. Once a control transient was established and decayed back to diastolic levels, 2mM caffeine was introduced prior to a bolus of calcium (67 μ M) thus increasing the calcium leak from the SR. This was noted by a slower T_1 compared with the control (2mM caffeine: Mean normalised T_1 = 483% of the control. (Fig. 6.2A). After 15 minutes, 300 μ M ryanodine was introduced prior to a calcium bolus resulting in an increase in T_1 (Mean normalised T_1 = 515% of the control. (Fig. 6.2A). 300 μ M ryanodine did not induce a block on the caffeine mediated SR leak but was observed to enhance the SR leak to a level similar to that produced by caffeine. Indicating that 2mM caffeine was insufficient to maximally stimulate an SR leak and that both caffeine and ryanodine have additive effects. On addition of 5 μ M RuR, at a 15minute interval, a significant block on this leak was observed (5 μ M RuR: Mean normalised T_1 = 233% of control. (Fig. 6.2A). However, this block failed to decrease the T_1 back to control levels, indicating that 5 μ M RuR did not completely block the SR leak under these conditions.

Figure 6.1B is a typical experimental trace to display the effects of 5 μ M RuR on 300 μ M ryanodine mediated leak and to investigate the effects of 2mM caffeine once the SR leak was blocked with 5 μ M RuR. After the established control decayed to diastolic levels, 300 μ M ryanodine, 5 μ M RuR and 2mM caffeine were introduced to the preparation at 15minute intervals, prior to a

calcium bolus ($67\mu\text{M}$). $300\mu\text{M}$ ryanodine induced a significant slowing of T_1 compared to the control ($300\mu\text{M}$ Ryanodine: Mean normalised $T_1 = 150\%$ of the control. (Fig. 6.2B), indicating that $300\mu\text{M}$ Ryanodine increased the open probability of the RyR leading to an elevated SR leak. $5\mu\text{M}$ RuR significantly increased the rate of decay, noted by a T_1 that was faster than the control ($5\mu\text{M}$ RuR: Mean normalised $T_1 = 84\%$ of the control), suggesting a substantial block of the RyR occurred and that an SR leak exists in the absence of RuR. 2mM caffeine did not significantly affect T_1 in the presence of $5\mu\text{M}$ RuR (2mM Caffeine: Mean normalised $T_1 = 97\%$ of control). Indicating that $5\mu\text{M}$ RuR was sufficient to block the ryanodine mediated SR leak as no further leak was observed in the presence of 2mM caffeine. It was also apparent that caffeine did not reverse the effects of the RuR block under these conditions.

6.3.2. Effects of Increasing Caffeine Concentrations on SERCA2A

From the previous results, 2mM caffeine alone has been shown to be insufficient at stimulating a sustained calcium leak from the SR and that calcium uptake was not impaired. The next step in this chapter involved investigating the effects of higher caffeine concentrations on SR calcium leak.

Figure 6.3A, shows a typical experimental trace for studying the effects of increasing caffeine concentrations on SR leak and how an increased leak affects SERCA2A. 5mM , 10mM , 20mM and 40mM caffeine were injected into the preparation at 15minute intervals, prior to a calcium bolus ($67\mu\text{M}$) to increase the free calcium to $1\mu\text{M}$. Even although the increasing caffeine concentrations produced a slowing of T_1 compared to the control (Fig. 6.3B) they did not produce a significant difference when compared with each other. Due to the non-significance of the T_1 results, the steady state (C_{ss}) for each transient was calculated, normalised to the control and then an average was taken (Fig. 6.3C). A general trend of increasing C_{ss} with increasing caffeine concentrations was observed. Where the increase in C_{ss} levels between 5mM and 10mM as well as between 20mM and 40mM were non-significant under these conditions.

These results were repeated in the presence of low calcium concentrations ($\sim 100\text{nM}$) to assess whether caffeine can induce a leak at resting calcium levels within permabilised cardiac myocytes (Fig. 6.4A). After a control transient was established, increasing caffeine concentrations

(5mM, 10mM, 20mM and 40mM caffeine) were introduced to the cuvette system at 15minute intervals in the absence of additional boli of calcium. From the mean normalised data displayed in Fig 6.5B, it was noted that the caffeine mediated calcium release was not apparent in our preparation until 20mM caffeine. Also, a substantial leak was only observed in the presence of 40mM caffeine. These results suggest that in this preparation, 20mM caffeine is insufficient to maximally stimulate calcium release from the SR and that significant reuptake of calcium occurs in the presence of caffeine concentrations less than 20mM.

6.3.3. RuR Inhibition of Caffeine Mediated Calcium Leak

From previous results, 40mM caffeine was found to stimulate a substantial calcium leak from the SR in the absence of additional calcium boli. In some preparations, this caffeine mediated leak increased to such high levels that calcium uptake was impaired (Figure 6.3A). In figure 6.5A, 40mM caffeine was introduced to the preparation after the control transient was established. Caffeine was noted to increase the calcium leak with a steady state being reached after about 10 minutes. Increasing concentrations of RuR (0.03, 0.3, 1, 2 and 5 μ M) were added at 15minute intervals. RuR had no apparent effect until 1 μ M, with a substantial block occurring in the presence of 5 μ M (Fig. 6.7). Once a steady state calcium level was reached in 5 μ M RuR, a bolus of calcium was introduced to the preparation to assess the rate of decay after the RuR block on the caffeine mediated calcium release from the SR. Another bolus was added in the presence of 25 μ M, to determine whether a further block of the calcium release channel occurred. The rate of decay was plotted against calcium concentration for the control, 5 μ M RuR and 25 μ M RuR (Figure 6.5B). Compared to the control, 5 μ M RuR (in the presence of 40mM caffeine) increased the rate of decay where as no further increase was observed with 25 μ M (in the presence of 40mM caffeine). This concludes that 5 μ M RuR was sufficient to exert a full block on the caffeine mediated calcium leak from the SR.

6.3.4. Ryanodine Inhibition of Caffeine Mediated Calcium Leak

Following the same protocol as previously described in 6.3.3, replacing increasing concentrations of RuR with Ryanodine (Figure 6.6A). It was observed that 40mM caffeine induced calcium release

from the SR with a steady state being reached after about 10 minutes. Increasing concentrations of Ryanodine (0.3 μ M, 3 μ M, 30 μ M, 300 μ M and 3mM) were added at 15minute intervals to assess ryanodine inhibition on the caffeine mediated SR calcium leak. Ryanodine has a slight effect at 3 μ M and 300 μ M but the most pronounced block occurred in the presence of 3mM ryanodine (Fig. 6.7). Where 3mM lowered the cytoplasmic calcium concentration back to basal levels. This suggests that 3mM ryanodine induced a full block on the caffeine mediated calcium leak from the SR.

Once a steady state calcium level was reached in the presence of 3mM ryanodine, a bolus of calcium was added to assess the rate of decay after the ryanodine inhibition on the caffeine mediated SR calcium release. After 15minutes another bolus of calcium was added in the presence of 5 μ M RuR, to determine whether a further block of the calcium leak occurred. The rate of decay was calculated for the control, 3mM ryanodine (in the presence of 40mM caffeine) and 5 μ M RuR (in the presence of 3mM ryanodine and 40mM caffeine). The results were plotted against calcium concentration (Figure 6.4B). Compared with the control, 3mM Ryanodine (in the presence of 40mM caffeine) increased the rate of decay where as no further increase was observed with 5 μ M RuR (in the presence of 3mM ryanodine and 40mM caffeine). This suggests that an SR leak exists in the absence of a ryanodine blocker. Also, 3mM Ryanodine was sufficient to block the caffeine mediated calcium release from the SR.

This experiment was repeated in the presence of 5mM oxalate (Fig 6.7) where 5mM oxalate produced a similar dose response curve to 20mM oxalate, thus indicating that oxalate did not significantly alter the ryanodine effects on caffeine mediated calcium leak.

6.4 DISCUSSION

As described in the introduction to this chapter, caffeine is widely used as a pharmacological tool for assessing calcium induced calcium release from the RyR. The effects exerted by caffeine are dose dependent. High concentrations of caffeine (40mM) deplete the SR of calcium and are thus used to assay the SR calcium content. Low concentrations of caffeine (<0.5-2mM) have been hypothesised to stimulate SR calcium recycling, thus increasing calcium uptake as well as release.

The reduced luminal calcium associated with an increase SR leak, in this case caffeine mediated SR leak, stimulates SERCA 2A activity which in turn increases SR calcium uptake (Inesi & de Meis, 1989).

In this study it was observed that caffeine mediated calcium release from the SR of permeabilised cardiac myocytes occurred in a dose dependent manner. Despite activation of the RyR by caffeine, the SR could still lower calcium in the cuvette to levels $<100\text{nM}$ via calcium uptake. The ability of the SR to sequester significant amounts of calcium in the presence of 10-20mM caffeine and $\sim 100\text{nM}$ calcium was observed in permeabilised rat myocytes by Smith & Steele (1998). This suggests that the results seen in this study are unlikely to be species dependent. Only at caffeine concentrations above 20mM was calcium reuptake incomplete, where the maximum concentration of 40mM caffeine appeared to cause additional leak at cytosolic calcium concentration of $\sim 1\text{-}2\mu\text{M}$. The caffeine mediated calcium leak was further enhanced by $300\mu\text{M}$ ryanodine but completely blocked by $5\mu\text{M}$ RuR (Fig. 6.1A). Since $5\mu\text{M}$ RuR was previously shown to maximally block the ryanodine receptor (chapter 5), the caffeine rate of decay after a RuR addition would have been expected to be similar to the rate of decay produced by RuR. However, the effect of 2mM caffeine after the RuR addition is small and not significant. Thus caffeine does not relieve the RuR block on calcium induced calcium release from the SR under these conditions. Also, the reagents added to the system do not appear to show order dependence.

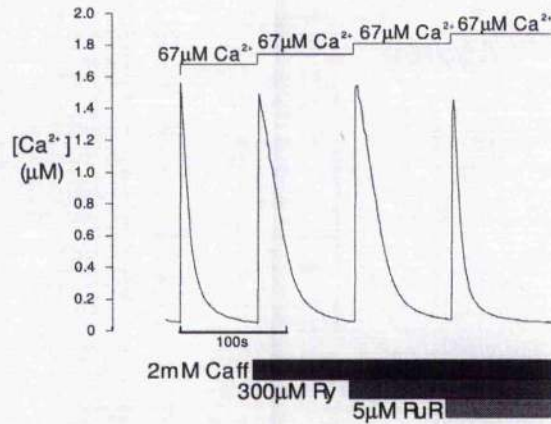
When caffeine was added at a resting calcium concentration of $\sim 100\text{nM}$ an increase in steady state calcium was not evident until the addition of 40mM caffeine. This suggests that SR leak was not significantly affected until 40mM caffeine. However, in the presence of activating calcium a slower rate of decay from $1.5\mu\text{M}$ calcium was noted in the presence of 2mM caffeine where the SR was able to re-establish a low resting calcium concentration. This latter result suggests that as little as 2mM caffeine can activate the RyR in the presence of $\sim 1\mu\text{M}$ calcium. The higher sensitivity to caffeine at $1\mu\text{M}$ calcium can be explained by calcium and caffeine acting together to activate the RyR. The very low sensitivity of the RyR to caffeine in the presence of $\sim 100\text{nM}$ calcium is consistent with the work on isolated RyR in lipid bilayers. Sitsapesan & Williams (1990) work, carried out on SR incorporated into lipid bilayer showed that there is

calcium dependent as well as a calcium independent mechanism for caffeine induced calcium release from the SR. Where the calcium independent mechanism requires high concentrations of caffeine ($>0.5\text{mM}$) to induce calcium release while the calcium dependent mechanism can release calcium from relatively low concentrations of caffeine ($0.5\text{-}2\text{mM}$). In this study 10mM caffeine only partially activates the RyR where as at 40mM caffeine induces a substantial release of calcium from the SR.

In the presence of 20mM oxalate, the sensitivity of calcium leak to caffeine was very much lower than that observed in intact cells (O'Neill & Eisner, 1990). The reason for this is unknown. Interestingly the caffeine sensitivity of the isolated RyR channels in lipid bilayer work has a similarly low sensitivity to caffeine (Rousseau & Meissner, 1989; Williams & Sitsapesan, 1990)

Another significant result of this work is the apparent low sensitivity of the SR calcium leak to ryanodine. Previous work on isolated channels suggest that $\sim 30\mu\text{M}$ is sufficient to block the RyR but in this study 3mM was required. The reason for this discrepancy is unknown. Isolated channel experiments have revealed that the slow binding of ryanodine to the RyR is very temperature sensitive and depends on the holding potential (Smith *et al.*, 1988). These variables may explain some aspects of the apparently low ryanodine sensitivity observed in this study.

(A)



(B)

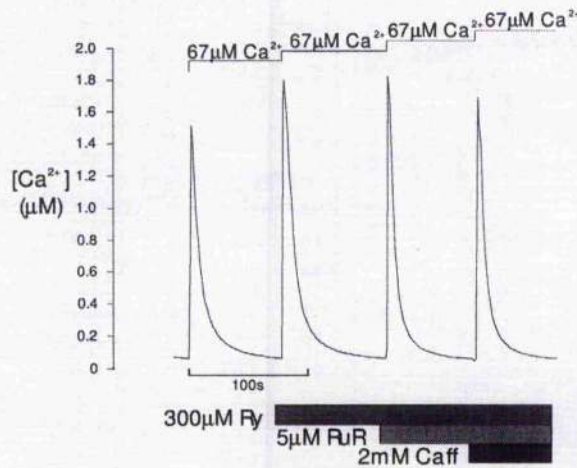
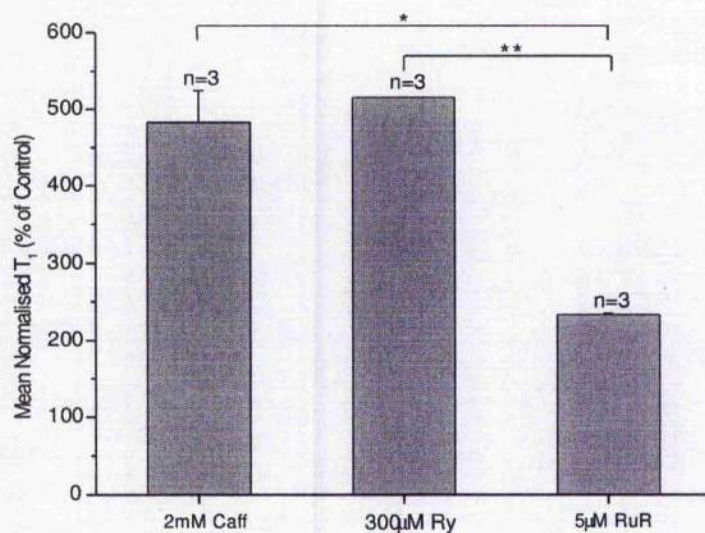


Figure 6.1: The effects of ryanodine, RuR and caffeine on the rate of decay of successive calcium transients. (A) A typical experimental trace displaying the effects of $300\mu M$ ryanodine (Ry) and $5\mu M$ RuR in the presence of $2mM$ caffeine (Caff) on the rate of decay of the calcium transients. A control was established before $2mM$ Caff, $300\mu M$ Ry and $5\mu M$ RuR were introduced at 12minute intervals, prior to a bolus of calcium chloride ($67\mu M$). (B) A typical experimental trace to show the effect $300\mu M$ Ry and $5\mu M$ RuR have on the rate of decay of the calcium transient and to assess if $2mM$ Caff can induce an SR leak in the presence of a RuR block. The solution composition, bathing the cells prior to the additions of ryanodine, RuR and caffeine as indicated in the figure, is as follows; $0.05R$ (table 2.2), $20mM$ Oxalate, $10\mu M$ Fura-2, $5mM$ ATP, $15mM$ CrP, $0.1\mu M$ DTT, $10\mu M$ CCCP and $33\mu M$ Oligomycin.

(A)



(B)

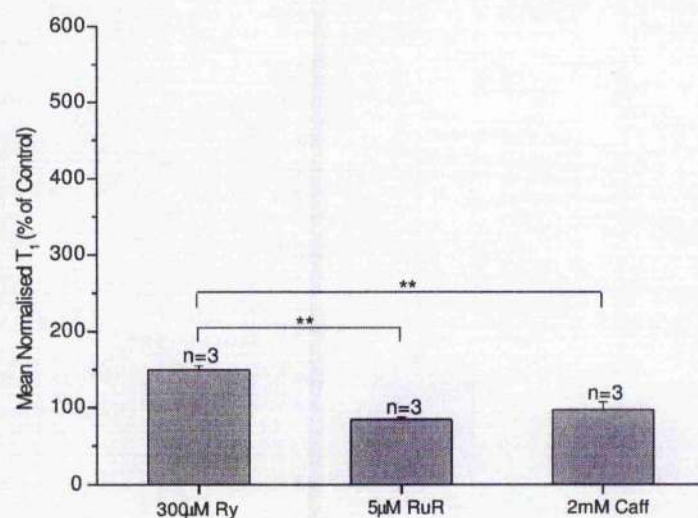
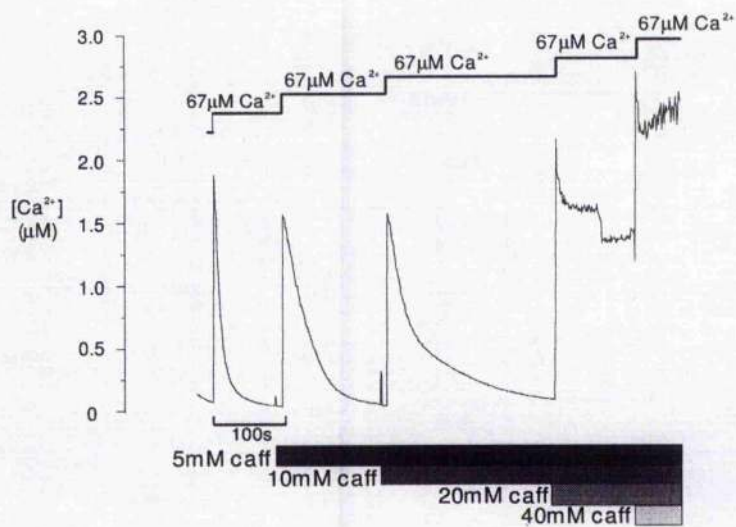
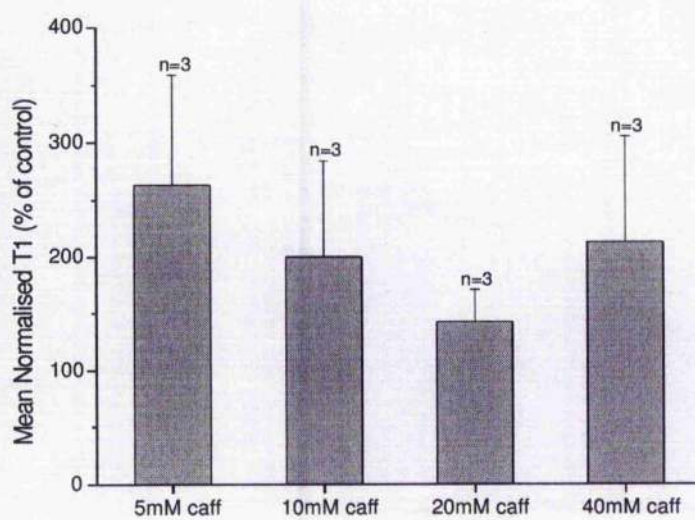


Figure 6.2: The mean data for the effects of caffeine, ryanodine and RuR on the calcium decay time constant (T_1). (A) A bar graph showing the mean normalised data for T_1 , influenced by 300µM Ry and 5µM RuR in the presence of 2mM Caff (mean \pm s.e.m., n=3, * denotes $P < 0.002$, ** denotes $P < 0.001$). (B) Shows a bar graph of the mean normalised data for T_1 influenced by 300µM Ry, 5µM RuR and 2mM Caff (mean \pm s.e.m., n=3, ** denotes $P < 0.005$). Significance was tested using an unpaired students t-test.

(A)



(B)



(C)

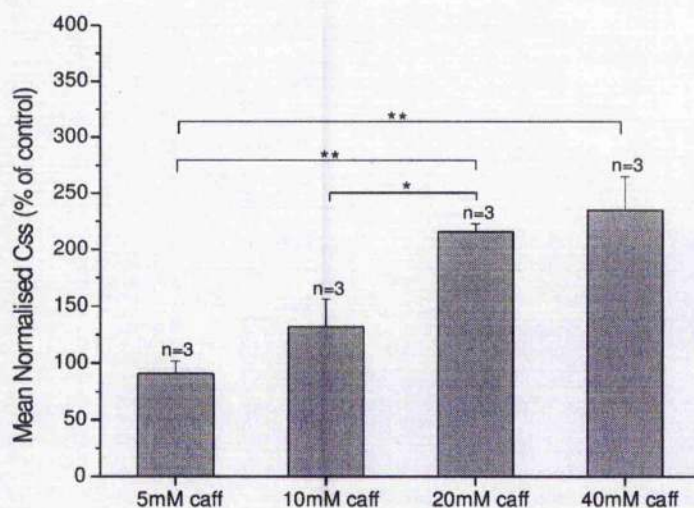
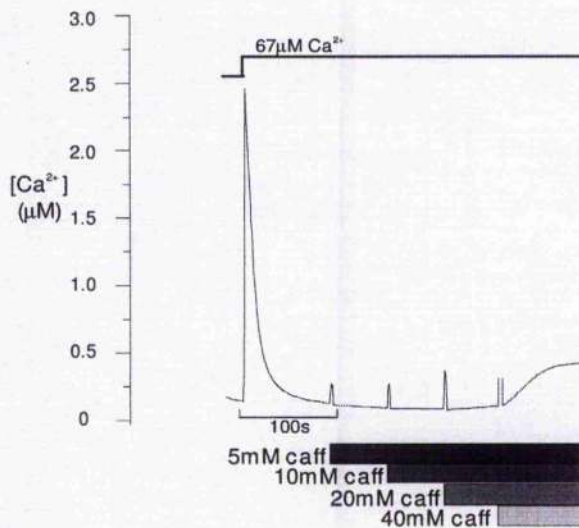


Figure 6.3: The effect of caffeine concentration on T_1 and C_{ss} during successive calcium transients. (A) A typical experimental trace displaying the effects of caffeine (caff) (5mM, 10mM, 20mM and 40mM) in the presence of repeated calcium challenges, to assess the ability of the SR to sequester calcium in the presence of an elevated SR calcium leak. Caffeine was introduced at 12minute intervals, prior to an aliquot of calcium chloride (67 μ M). Thus increasing the free calcium concentration in the preparation, which decayed exponentially. (B) A bar graph displaying the mean normalised data for the calcium decay time constant (T_1) produced with 5mM, 10mM, 20mM and 40mM caffeine additions prior to a calcium boli (67 μ M) as shown in the typical experimental trace (A) (mean \pm s.e.m., n=3, $P>0.05$). (C) The following bar graph displays the mean normalised steady state (C_{ss}) produced after each transient decayed in the presence of increasing caffeine concentrations (mean \pm s.e.m., n=3, ** denotes $P<0.01$, * denotes $P<0.05$). Significance was tested using an unpaired students t-test. The solution composition, bathing the cells prior to the additions of caffeine as indicated in the figure, is as follows; 0.05R (table 2.2), 20mM Oxalate, 10 μ M Fura-2, 5mM ATP, 15mM CrP, 0.1 μ M DTT, 10 μ M CCCP and 33 μ M Oligomycin.

(A)



(B)

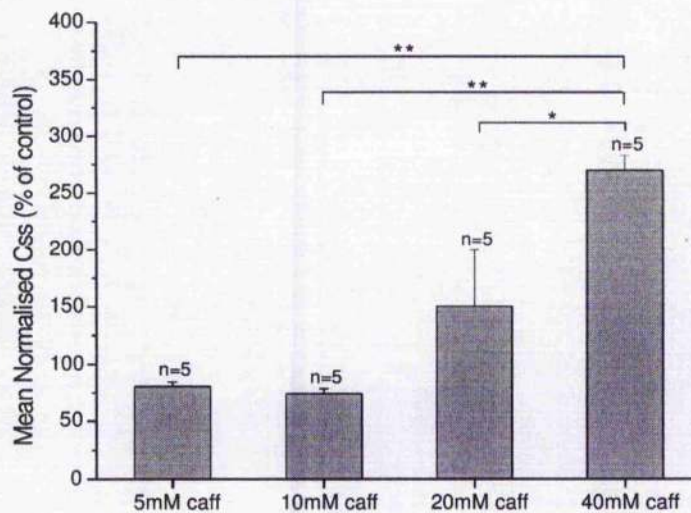
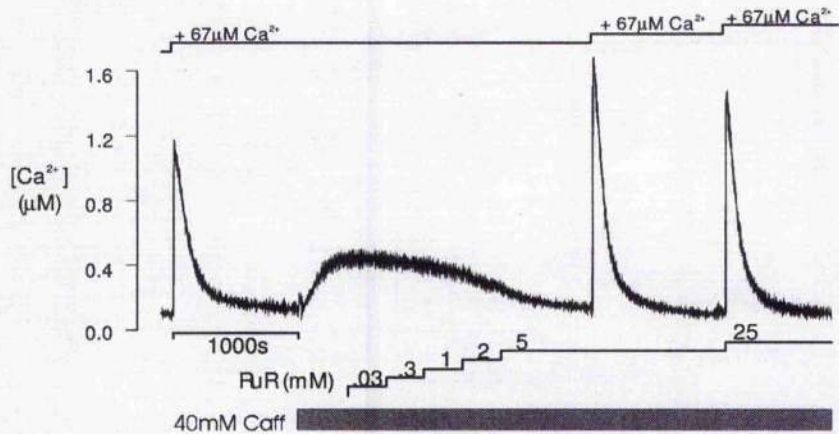


Figure 6.4: Effects of caffeine concentration on SR calcium leak. (A) A typical experimental trace displaying the effects of caffeine concentration (5mM, 10mM, 20mM and 40mM) introduced to the preparation at 12minute intervals (in the absence of successive calcium boli) in order to induce a maximal release of calcium from the SR. (B) The following bar graph displays the mean normalised data for the steady state (C_{ss}) produced after each caffeine addition (mean \pm s.e.m., $n=5$, ** denotes $P<0.001$, * denotes $P<0.05$). Significance was tested using an unpaired students t-test. The solution composition, bathing the cells prior to the additions of caffeine as indicated in the figure, is as follows; 0.05R (table 2.2), 20mM Oxalate, 10 μM Fura-2, 5mM ATP, 15mM CrP, 0.1 μM DTT, 10 μM CCCP and 33 μM Oligomycin.

(A)



(B)

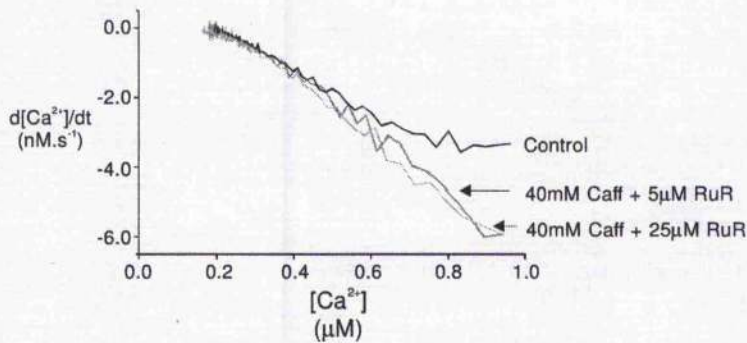
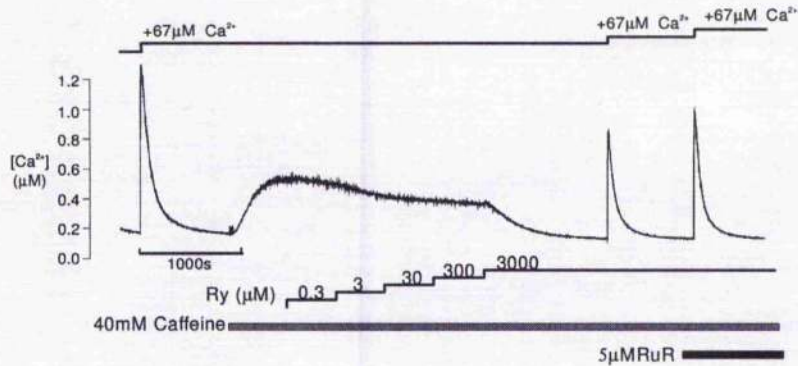


Figure 6.5: The Effect of RuR inhibition of caffeine mediated calcium release. (A) A control transient was established with the addition of a bolus of calcium ($67\mu\text{M}$). 40mM caffeine induced a maximal release of calcium from the SR, which was subsequently subjected to increasing RuR concentrations ($0.03\mu\text{M}$, $0.3\mu\text{M}$, $1\mu\text{M}$, $2\mu\text{M}$). Then $5\mu\text{M}$ and $25\mu\text{M}$ RuR were added prior to a calcium bolus to assess the extent of the block on the caffeine mediated SR calcium release. (B) Displays the rate of change of calcium uptake against calcium concentration for the control, $5\mu\text{M}$ RuR and $25\mu\text{M}$ RuR in the presence of 40mM caffeine. The solution composition, bathing the cells prior to the additions of caffeine and RuR as indicated in the figure, is as follows; 0.05R (table 2.2), 20mM Oxalate, $10\mu\text{M}$ Fura-2, 5mM ATP, 15mM CrP, $0.1\mu\text{M}$ DTT, $10\mu\text{M}$ CCCP and $33\mu\text{M}$ Oligomycin.

(A)



(B)

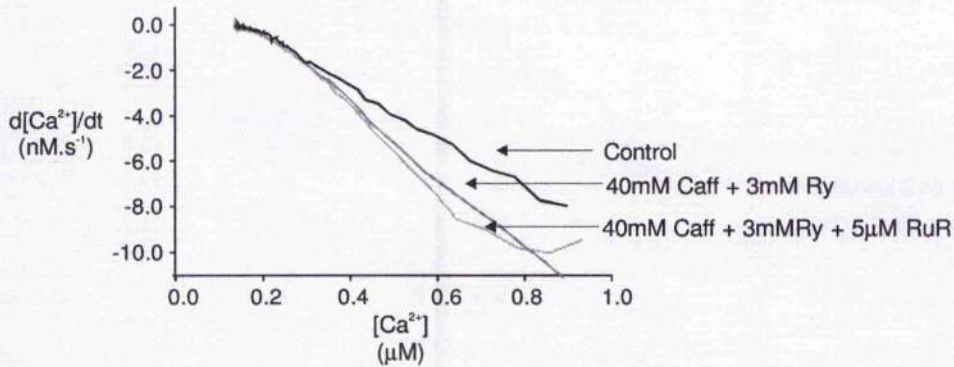


Figure 6.6: The effect of ryanodine inhibition of caffeine mediated calcium release. (A) A control transient was established with the addition of a bolus of calcium ($67\mu\text{M}$). 40mM Caff induced a maximal release of calcium from the SR, which was subsequently subjected to increasing Ry concentrations (0.3 , 3 , 30 , 300 , $3000\mu\text{M}$). Then a bolus of calcium was added in the presence of 3mM Ry, which decayed back to diastolic levels before another bolus was added in the presence of $5\mu\text{M}$ RuR. (B) Displays the rate of change of calcium uptake against calcium concentration for the control along with 40mM Caff and 3mM Ry in the presence and in the absence of $5\mu\text{M}$ RuR. The solution composition, bathing the cells prior to the additions of ryanodine, caffeine and RuR as indicated in the figure, is as follows; 0.05R (table 2.2), 20mM Oxalate, $10\mu\text{M}$ Fura-2, 5mM ATP, 15mM CrP, $0.1\mu\text{M}$ DTT, $10\mu\text{M}$ CCCP and $33\mu\text{M}$ Oligomycin.

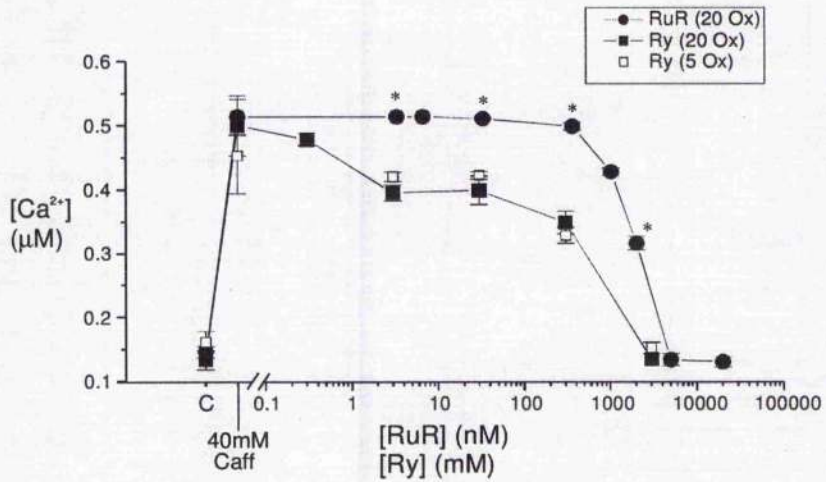


Figure 6.7: The mean results of RuR and Ryanodine on 40mM caffeine mediated SR calcium release. The control transient (C) displays the calcium level prior to the addition of Caff and RuR (or Ry). 40mM Caff produced a significant calcium leak from the SR, which was subsequently inhibited with increasing concentrations of RuR (—●—) and Ry (—■—). The Ry inhibition of caffeine mediated SR leak was repeated in the presence of 5mM oxalate (□) (mean ± s.e.m., n=7, * denotes P<0.05). Significance was tested using an unpaired students t-test.

CHAPTER SEVEN

SR CALCIUM LEAK AND BASTADIN

7.1. INTRODUCTION

As previously shown (Chapter 4), even in the presence of SERCA2 blockade, a calcium efflux from the SR occurs. The source of this remaining leak is unknown at present but one such theory arose from the work carried out with bastadin (*Pessah, et al. 1997*), a class of compounds that appear to affect SR calcium leak in skeletal muscle (Chapter 1). This chapter investigates the nature of the SR calcium leak in permeabilised cardiac myocyte preparations by observing the actions of RyR blockers, ryanodine and RuR in the absence and presence of bastadin mix (Bastadins 5-10), in order to assess the contribution of the RyR to the non-specific leak unmasked by thapsigargin.

7.2 METHODS

Cardiac myocytes were prepared for calcium leak studies as previously described in Chapter 2. 1×10^6 permeabilised cells were transferred to the closed cuvette system and changes in the intracellular free calcium concentrations were detected using the fluorescent indicator Fura-2. Following a three minute incubation to allow the cells to reach an equilibrium with the mock intracellular environment, 3 aliquots of 8-10 μ l of 10mM calcium chloride were added to raise the intracellular free calcium concentration to 1-2 μ M which decayed in an exponential fashion back to diastolic levels (~100nM). Three aliquots introduced at 12 minutes apart were found to be adequate to generate reproducible rates of calcium decay.

7.3. RESULTS

Figure 7.1 is a typical experimental trace showing the calcium uptake protocol. Three calcium transients were introduced at 12 minute intervals before 5 μ M Thapsigargin was added to the preparation. As stated in 4.1.2, thapsigargin allows the study of calcium leak from the SR by inhibiting the Ca²⁺-ATPase pump, thus after its addition a slow increase in the intracellular calcium concentration ensues and in this preparation represents the linear leak from the SR. The thapsigargin induced leak plateaued after about 3 hours (data not included), a time course that was considered unsuitable for this study and therefore 10 μ M ionomycin was introduced to induce a rapid elevation in the calcium concentration that reached a steady state at approximately 2 μ M.

From Figure 7.2 (A) it was observed that in the presence of low intracellular calcium (80-160nM) the SR leak is not affected by the addition of 5 μ M RuR (a known blocker of the RyR). This indicates that the RyR activity could not be detected at these low levels and that the majority of the leak could be the result of a non-specific leak rather than through the RyR. The dashed box represented in figure 7.1 was expanded (figure 7.2, panel A) to emphasise the point made earlier that the RyR does not significantly contribute to the SR calcium leak over this calcium concentration range. However, in the presence of a higher calcium concentration (>500nM) and in the presence of 5 μ M RuR, a marked reduction of the calcium leak was observed (figure 7.2, panel B), indicating that the RyR activity greatly contributes to the SR calcium leak under these conditions.

Another method for examining calcium leak involves comparing the time course of decay for the individual calcium transients. The rate of the decay is influenced by calcium uptake (via the SERCA pump) as well as leak through the RyR and the non-specific leak. Figure 7.3 shows a typical experimental trace displaying the effects of RuR on the time course of the calcium transients. As described previously an aliquot of calcium was introduced to the preparation, increasing the total calcium concentration in the cuvette by 67 μ M. This caused a rapid increase in free calcium concentration to approximately 3 μ M that decayed back to diastolic levels after 10 minutes. The second aliquot of calcium was added in the presence of 600nM RuR. The rate of decay reaching diastolic levels after 10 minutes and the third aliquot of calcium was injected in the presence of 5 μ M RuR. The rate of decay for the calcium transient was significantly faster in the presence of RuR, where 5 μ M exerted the largest block on the RyR (Figure 7.3, panel A). To emphasise these differences more clearly, the decays were superimposed onto one diagram (Figure 7.3, panel B). The control possessed the less steep gradient that corresponds to a slower rate of decay. This rate of decay significantly increased with exposure to increasing RuR concentrations, the fastest rate occurring in the presence of 5 μ M RuR. This increase is due to the inhibiting of the calcium leak from RyR. RuR reduces the competition between pump and leak, favouring uptake and therefore, the pump becomes more efficient at transporting calcium into the lumen of the SR thus lowering intracellular calcium levels within the cell. Below 500nM the three transients are

superimposable (Figure 7.3, panel B) suggesting that RuR failed to exert an increase in the rate of decay even at a concentration of $5\mu\text{M}$, indicating that the RyR remains inactive at these low calcium levels. This strengthens the point made earlier that the RyR activity does not significantly contribute to the SR calcium leak during calcium levels below 500nM .

This ryanodine/RuR insensitive calcium leak unmasked by thapsigargin was found to be blocked by bastadin mix (Bastadin 5-12) but only in the presence of RuR or ryanodine. Figure 7.4 displays the bastadin effects on SR leak both in the presence and in the absence of RuR over the calcium range $80\text{-}160\text{nM}$. In panel B, $20\mu\text{M}$ bastadin mix had no significant effect on SR calcium leak in the presence of thapsigargin when compared to the control ($98 \pm 2\%$, $n=4$). However, in panel A, when bastadin mix was introduced to the preparation in the presence of $5\mu\text{M}$ RuR and thapsigargin (leak rate = $120 \pm 10\text{nM}\cdot 10^3 \text{ s}^{-1}\cdot 10^6 \text{ cells}$; $n=5$), the calcium leak plateaued and thus reduced the calcium leak to $66 \pm 2\%$ ($n=4$).

Figure 7.5 (panel A), displays the effect of bastadin mix (Bastadins 5-10) on SR calcium leak after treatment with ryanodine. To investigate the effect of bastadin mix in presence of ryanodine, the calcium level was increased to 500nM . As discussed previously the RyR is inactive at calcium concentrations below 500nM so in order to activate this system the calcium levels were elevated. Two aliquots of calcium were introduced to the preparation in order to produce reproducible transients. Thapsigargin inhibited the SERCA pump and after 8 minutes 300nM of calcium was added to increase the calcium concentration within the cuvette. On addition of 3mM ryanodine a transient increase in the rate of calcium leak was observed, increasing the calcium from 500nM to approximately $1\mu\text{M}$ before plateauing. After 10 minutes, $20\mu\text{M}$ bastadin mix (Bastadins 5-10) was introduced to the cuvette and was observed to induce a further significant decrease in the rate of calcium leak from the SR. To emphasise the blocking effects of bastadin mix, the dashed line in panel A was amplified (Panel B). The solid line represents the rate of rise of calcium concentration before ryanodine addition and the dotted lines represent the rate of rise of calcium concentration after ryanodine addition. These results clearly suggest that ryanodine blocks the RyR after an initial phase of increased RyR activity and that this block was further increased with the addition of bastadin mix (Bastadins 5-10).

As described previously, another method for examining calcium leak involves comparing the time courses of decay for the individual calcium transients. The rate of the decay is influenced by calcium uptake (via the SERCA pump) as well as leak through the RyR and the non-specific leak. Figure 7.6 displays the effects of bastadin mix (Bastadins 5-10) on the time course of decay after treatment with 3mM ryanodine. Initially 3mM ryanodine decreases the rate of decay due to an initial opening of the RyR before a subsequent block on the addition of a second aliquot of calcium, where the rate of uptake is enhanced indicating a block on the RyR. Further additions of calcium gave rise to superimposable transient decays. 20µM bastadin mix (Bastadins 5-10) was introduced to the preparation after the ryanodine block. It was observed that bastadin mix (Bastadins 5-10) did not produce an increase in the rate of decay until an additional bolus of calcium was added. Panel B emphasises the point that bastadin mix (Bastadins 5-10) increases the rate of decay.

7.4 DISCUSSION

It was observed that even in the presence of SERCA2A blockers, calcium efflux from the SR occurred. The source of this leak is unknown at present but one such explanation came from the work with class of compounds called Bastadins.

Pessah *et al.*, (1997) speculated that the RyR may be stuck in an open configuration even in the presence of RuR or high concentrations of ryanodine, therefore releasing calcium from the internal calcium stores and is observed as a linear leak in the calcium uptake preparations. To investigate this theory 5µM RuR was introduced to the cuvette system in the presence of thapsigargin. At low intracellular calcium concentrations the leak is unaffected by RuR indicating that the RyR activity cannot be detected at these low levels, that the majority of the leak could be the result of the non-specific leak rather than through the RyR and that the RyR does not significantly contribute to the SR calcium leak over this calcium concentration range. However, RuR added in presence of calcium concentrations greater than 500nM caused a marked reduction on calcium leak, suggesting that the RyR activity greatly contributes to the SR calcium leak under these conditions. Similar results occurred with 3mM Ryanodine, where increasing the basal calcium levels above 500nM induced a block on the RyR after an initial increase in calcium leak.

RuR in the presence of 20 μ M bastadin mix (Bastadins 5-10) was observed to induce a block on the SR leak that was previously shown to be insensitive to RuR. Bastadin mix (Bastadins 5-10) also enhanced the 3mM ryanodine block in the presence of a calcium concentration >500nM. However, adding bastadin mix (Bastadins 5-10) alone did not exert a block on the SR leak. This is consistent with the suggestion that a component of the SR leak maybe be due to the RyR being in an open configuration (Pessah *et al.*, 1997) and only after binding of bastadin can these blockers induce an effect on the fraction of the SR calcium leak that remains in the presence of a RuR or a ryanodine block.

The earlier studies on bastadin suggest that they act on FKBP 12.0-RyR1 interaction in skeletal muscle SR (Pessah *et al.*, 1997), but this study has not been confirmed by other groups. Furthermore FKBP12.0 is not thought to bind to cardiac RyR (RyR2), instead the isomer FKBP12.6 is thought to be involved (Timerman *et al.*, 1994). Therefore it would be interesting to examine whether FKBP12.6 modulates the effects of bastadin in cardiac muscle SR.

7.4 CONCLUSIONS

In isolated cardiac muscle preparations, thapsigargin unmasks an SR calcium leak. This leak is insensitive to blocks on the RyR at calcium concentrations below 500nM but is attenuated by 3mM ryanodine and 5 μ M RuR at calcium concentrations above 500nM. (Fig. 7.2 & Fig. 7.5). This was confirmed by measurements of calcium uptake where SERCA2 is active and thus a blocking effect was only observed at calcium concentrations above 500nM (Fig. 7.3).

Bastadin mix (Bastadins 5-10) have no effect on thapsigargin mediated SR calcium leak in the absence of RuR or ryanodine (Fig 7.4A) but have a prominent effect on SR leak after the addition of 5 μ M RuR (Fig. 7.4B) and after a complete block with 3mM ryanodine (Fig. 7.5). Its actions are still present during SERCA2 activity (Fig. 7.6).

A fraction of the SR calcium leak that remains after blocking with RuR and ryanodine is blocked by bastadin mix (Bastadins 5-10). This suggests that a component of the SR leak is due to the RyR being in an open configuration that can be blocked by bastadin (Pessah *et al.*, 1997). However, further work is required to confirm these preliminary observations on the action of bastadin on SR calcium leak.

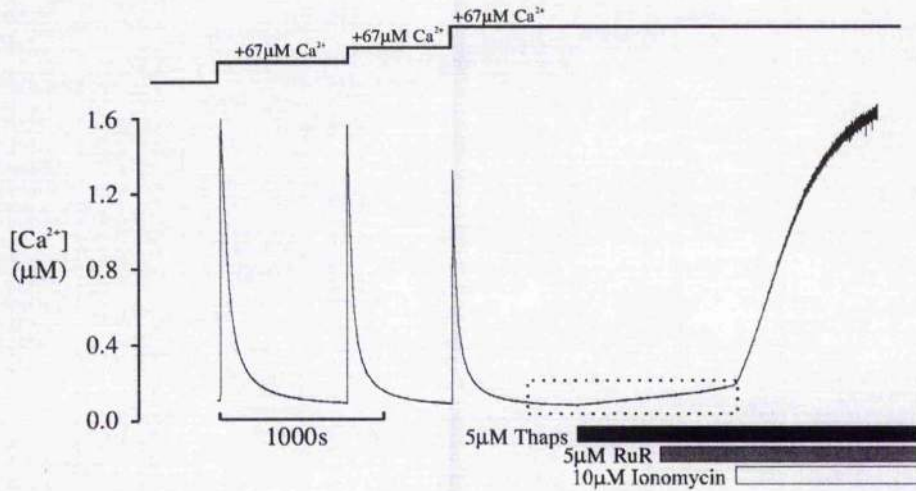
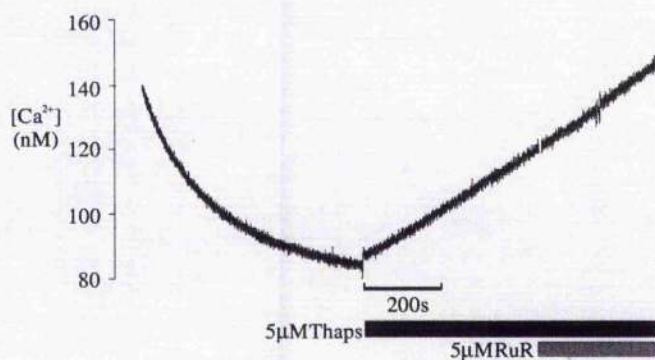


Figure 7.1: *Experimental trace showing the effects of thapsigargin, RuR and Ionomycin on SR calcium leak.* After three successive calcium challenges, 5µM thapsigargin (thaps) was introduced to the cuvette system, producing a linear leak from the SR. To test whether RyR activity is detectable at calcium concentrations below 500nM, 5µM RuR was added 5 mins after thapsigargin. 10µM ionomycin increased SR calcium leak, which increased diastolic calcium levels until an equilibrium with the intraluminal SR was reached. The solution composition, bathing the cells prior to the additions of thapsigargin, RuR and ionomycin as indicated in the figure, is as follows; 0.05R (table 2.2), 20mM Oxalate, 10µM Fura-2, 5mM ATP, 15mM CrP, 0.1µM DTT, 10µM CCCP and 33µM Oligomycin.

(A)



(B)

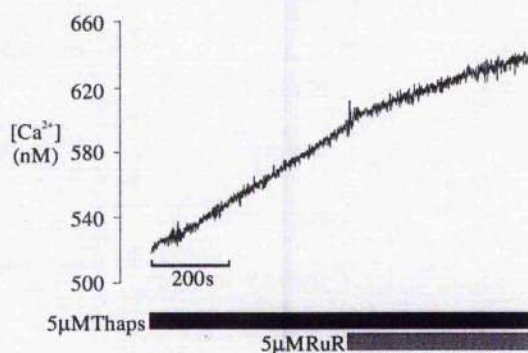
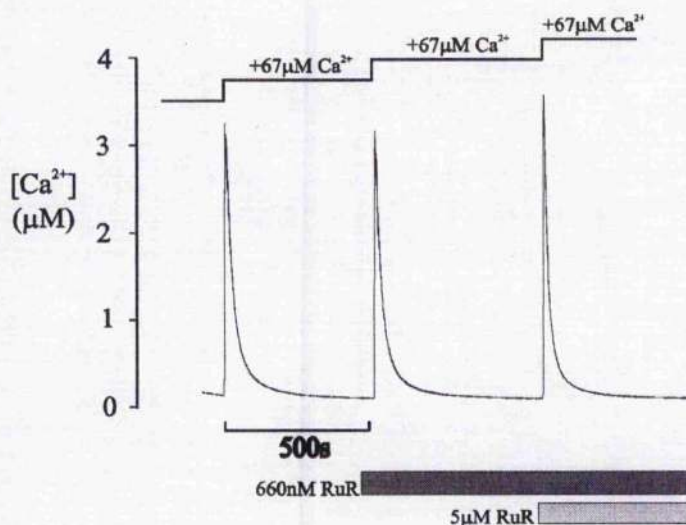


Figure 7.2: The effects of RuR on SR leak unmasked by thapsigargin in the presence of calcium concentrations below and above 500nM. (A) 5 μ M RuR was added in the presence of 5 μ M thapsigargin during calcium concentrations below 500nM. No detectable blocking effect was observed under these conditions. (B) 5 μ M RuR was added in the presence of thapsigargin during calcium concentration above 500nM. Under these conditions, RuR decreased the SR leak unmasked by thapsigargin. The solution composition, bathing the cells prior to the additions of thapsigargin and RuR as indicated in the figure, is as follows; 0.05R (table 2.2), 20mM Oxalate, 10 μ M Fura-2, 5mM ATP, 15mM CrP, 0.1 μ M DTT, 10 μ M CCCP and 33 μ M Oligomycin.

(A)



(B)

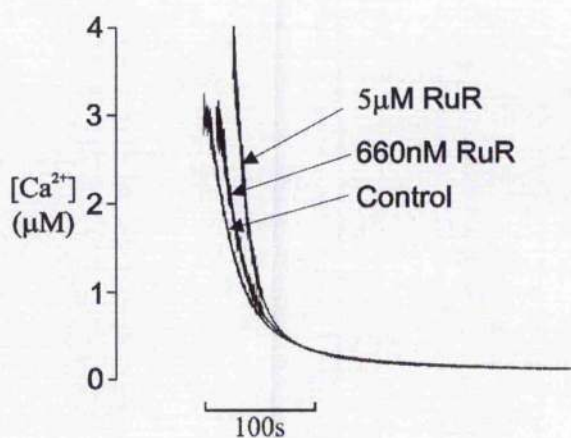
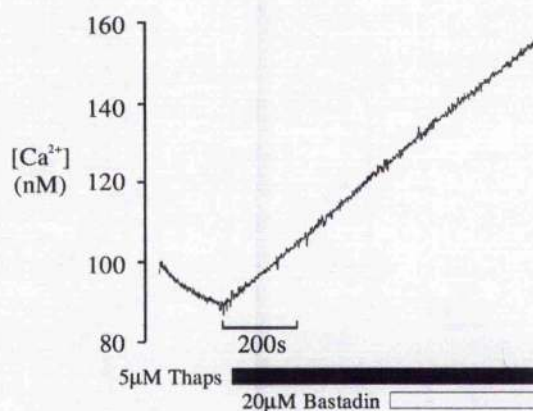


Figure 7.3: Experimental trace showing the effects of RuR on the rate of calcium decay. (A) $660nM RuR$ and $3.3\mu M RuR$ were introduced 8 minutes apart to the cuvette system in the presence of separate calcium challenges to assess the RuR block on the SR leak. **(B)** Compares the rates of decay for the calcium challenges in the presence and in the absence of RuR. $3.3\mu M RuR$ induced the fastest rate of decay, indicating a significant block of the SR leak occurred. The solution composition, bathing the cells prior to the additions of RuR as indicated in the figure, is as follows; $0.05R$ (table 2.2), $20mM Oxalate$, $10\mu M Fura-2$, $5mM ATP$, $15mM CrP$, $0.1\mu M DTT$, $10\mu M CCCP$ and $33\mu M Oligomycin$.

(A)



(B)

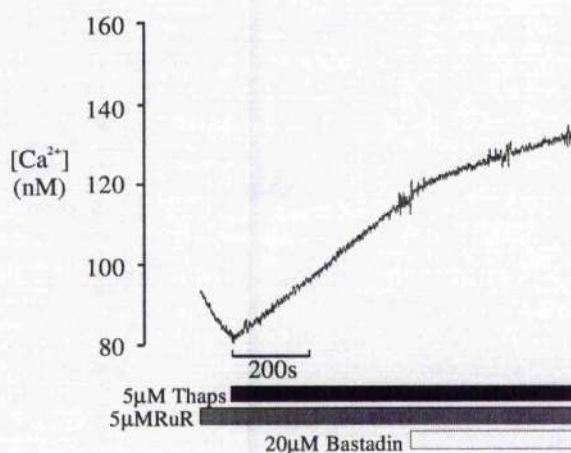
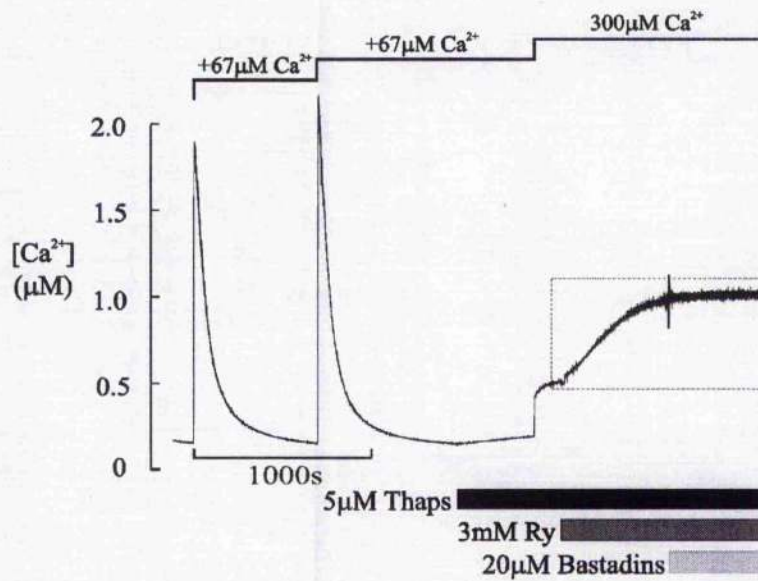


Figure 7.4: The effects of Bastadin mix in the presence and in the absence of RuR and low calcium concentrations. (A) 20 μ M Bastadin mix (Bastadins 5-10) was added in the presence of 5 μ M thapsigargin during low calcium concentrations. Showing Bastadin mix has no effect on the SR leak unmasked by thapsigargin. (B) 20 μ M Bastadin mix was added in the presence of 5 μ M RuR and thapsigargin. It was noted that an SR leak exists even in the presence of RyR blockers such as RuR and that Bastadin mix reduced this leak in the presence of RuR. The solution composition, bathing the cells prior to the additions indicated in the figure, is as follows; 0.05R (table 2.2), 20mM Oxalate, 10 μ M Fura-2, 5mM ATP, 15mM CrP, 0.1 μ M DTT, 10 μ M CCCP and 33 μ M Oligomycin.

(A)



(B)

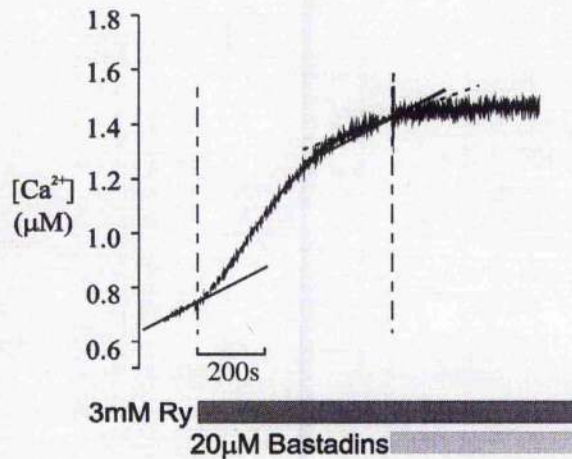
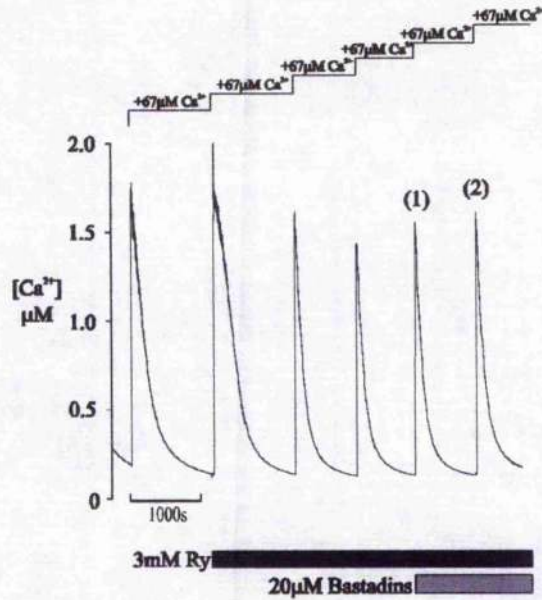


Figure 7.5: The experimental trace displaying the effects of Bastadin mix in the presence of ryanodine on the SR leak unmasked by thapsigargin. (A) 300µM calcium chloride was used to raise the calcium concentration above 500nM. Once a steady state was reached, 3mM ryanodine was introduced to the thapsigargin mediated leak. 20µM Bastadin mix (Bastadins 5-10) further decreased this leak. (B) The dashed line in panel A was amplified. The solid line represents the rate of rise of calcium concentration before ryanodine where as the dotted line represents the rate of rise of calcium concentration after ryanodine. The solution composition, bathing the cells prior to the drug additions indicated in the figure, is as follows; 0.05R (table 2.2), 20mM Oxalate, 10µM Fura-2, 5mM ATP, 15mM CrP, 0.1µM DTT, 10µM CCCP and 33µM Oligomycin.

(A)



(B)

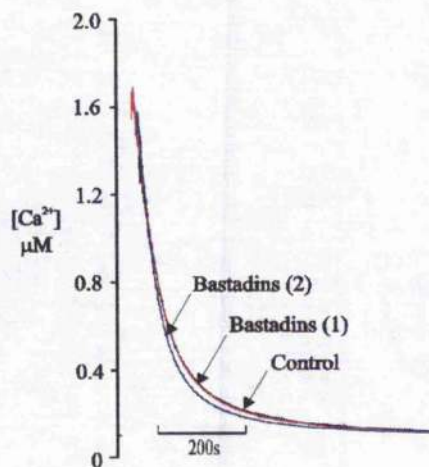


Figure 7.6: Experimental trace displaying the effects of Bastadin mix on the rate of calcium decay in the presence of 3mM Ryanodine. (A) Ryanodine was introduced after a control transient was established. $20 \mu M$ Bastadin mix (Bastadins 5-10) was added after a block on SR leak occurred with ryanodine. Once the transient decayed to minimum levels another calcium challenge was introduced in the presence of Bastadin mix. (B) Comparing the rates of decay before and after Bastadin mix. A control was established in the presence of ryanodine block; Bastadin 1 represents the rate of decay after the first calcium challenge in the presence of Bastadin mix, and Bastadin 2 represents the rate of decay after the second calcium challenge in the presence of Bastadin mix. The solution composition bathing the cells prior to the drug additions as indicated in the figure is as follows; $0.05R$ (table 2.2), $20mM$ Oxalate, $10 \mu M$ $10 \mu M$ Fura-2, $5mM$ ATP, $15mM$ CrP, $0.1 \mu M$ DTT, $10 \mu M$ CCCP and $33 \mu M$ Oligomycin.

CHAPTER EIGHT

SUMMARY

8.1. Balling of Rod Shaped Cells

Balled-up cells are rod shaped cells that are balled-up. The mechanism by which they become contracted is uncertain but may reflect calcium overload and hypercontracture due to membrane damage during dissociation that can ultimately lead to apoptosis and programmed cell death.

From the findings of this study it was revealed that balled cells may contribute to SR regulation and were therefore included in the experiment as viable cells. From the protein measurements we noted that the method of counting cells using a haemocytometer was accurate and consistent throughout the experimental protocols and that balled cells contributed to the protein content in this study. The rod cell count does not influence the total protein concentration to a significant degree, but that the total cell number has a linear relationship with total protein. This implies that balled-up cells contribute to the total protein concentration. Overall, the yield of rods does not influence total protein, where as total cell number does: therefore the number of balled cells was taken into consideration during cell counting.

A higher number of cells within an experimental preparation lead to an increase in the rate constant for calcium uptake. Therefore the greater the number of cells within a preparation, the greater the amount of functional pumps available to take up calcium, thereby increasing the rate constant for calcium uptake into the SR. However, no relationship was detected between total number of rods and the rate of calcium uptake, thus the increase in the rate constant observed was not due to an increase in the number of rod shaped myocytes within the preparation.

From the evidence in this study, balled-up cells contribute to total protein and increasing the total cell number leads to an increase in the rate of calcium uptake which suggests that balled-up cells may contain functional pumps, and will therefore contribute to SR regulation and can be considered as viable cells within this preparation.

8.2. Effects of RuR on Permeabilised Myocytes

In permeabilised cardiac myocytes, 5 μ M RuR induced a rapid increase in the rate of calcium decay (i.e. greater sequestration of calcium into the SR lumen) regardless of when it was introduced to the preparation, suggesting that under control conditions a significant leak exists through the RyR at

1 μ M calcium. 5 μ M RuR was observed to have a maximal inhibition on the CRC as a further block was not observed with higher concentrations of RuR (Fig. 6.5A) and was not reversed with 2mM caffeine (Fig. 6.2). This is emphasized in the results taken from chapter 5.3.1; where the late addition of RuR induced a rapid increase in the rate of decay to a value similar to that seen with the early RuR addition suggesting that the RyR activity is not significantly affected during this protocol.

However, the continued presence of 5 μ M RuR, during increasing calcium challenges, caused a progressive decrease in the rate of decay especially after the last calcium challenge (Fig 5.4A) and in the presence of a ryanodine block (Fig. 5.13B). This was not due to increased RyR activity since additional RuR did not reverse this effect. It is suspected that this result arose from a progressive effect of RuR on SERCA2 (Kargacin & Kargacin, 1998). This is supported by the observation that higher concentrations of RuR (25 μ M) introduced to the preparation after the 5 μ M block, in the presence of ryanodine, depressed the rate of decay further and was therefore more effective at slowing calcium uptake (data not shown). Although with a subsequent late addition of RuR in the presence of an early addition in the same preparation (Fig. 5.6), no significant decrease in the rate of decay was observed when compared to the preparation where a late addition of RuR was absent (Fig. 5.4). This suggests that 5 μ M RuR does not produce a significant effect on SERCA2A. However, as stated above, higher concentrations of RuR did produce a decline in the rate of decay. For this reason, lower concentrations of RuR were used in this study to minimise the side effects on SERCA.

It was also observed that successive calcium challenges in the absence of RuR led to an initial increase in the rate of decay of the calcium transient. This progressive increase could arise from the gradual phosphorylation of PLB and as discussed in chapter 1, PLB is the phosphoprotein that regulates the activity of SERCA2. In its dephosphorylated state, PLB is an inhibitor of the cardiac SR calcium pump (Simmerman *et al.*, 1998) but upon phosphorylation, this inhibition is overcome (Jencks, 1989; Katz, 1996) thereby stimulating calcium uptake into the lumen of the SR. Bhogal & Colyer (1998) reported that an enzyme capable of sensing the luminal calcium concentration can regulate the phosphorylation of PLB in response to changes in calcium load. This

enzyme is called a state of filling kinase (SOF kinase). The phosphorylation of PLB in response to the depletion of the luminal calcium concentration (store depletion) would accelerate calcium uptake into the SR (Colyer & Wang, 1991) to facilitate store refilling. Upon loading of the SR, a burst of phosphorylation of PLB was observed at low intraluminal calcium concentrations but as the SR reached C_{ss} , a gradual decline in PLB phosphorylation occurred. This is consistent with the activation of the SOF kinase activity during low luminal calcium concentrations ($<2.5\mu\text{M}$) and the inhibition at high luminal calcium concentrations ($35\mu\text{M}$). Suggesting a direct link between SR luminal calcium concentration and the phosphorylation of PLB and that SOF is regulated by the luminal calcium concentration in the SR. This is consistent with the findings in this study observed in chapter 4 and 5, of the gradual increase in the rate of decay occurring over the three successive calcium challenges before declining over the remaining challenges. Therefore a SOF kinase could be regulating the phosphorylation of PLB via luminal calcium concentrations in this preparation.

8.3. RuR/ryanodine insensitive leak

In this preparation, a significant SR leak exists in the presence of an SR calcium load and that three calcium challenges were sufficient to produce reproducible calcium transients as well as sufficiently loading up the SR. A component of this leak can be blocked by RuR although a significant leak remains, suggesting that there exists a leak pathway in cardiac muscle SR that is independent of conventional RyR activity. Little is known about this RuR/ryanodine insensitive leak unmasked by thapsigargin, although a few theories have arisen. It was discovered that in this preparation, RyR activity was not detected at low calcium concentrations ($<500\text{nM}$) but on addition of calcium, increasing calcium level $>500\text{nM}$, RuR/ryanodine caused a marked reduction of calcium leak. Therefore, the RyR activity greatly contributes to the SR calcium leak under these conditions.

Interestingly, a compound called Bastadin was found to induce a block on the SR leak that was previously shown to be insensitive to RuR/ryanodine. Adding Bastadin mix alone did not exert a block on the SR leak which suggests that a component of the SR leak maybe due to the RyR being in an open configuration (Pessah *et al.*, 1997), thus releasing calcium from the internal calcium stores and seen as a linear leak in the calcium uptake preparations. This RyR configuration is insensitive to RyR blockers and only in the presence of Bastadin can these blockers induce an effect

on the fraction of the SR calcium leak that remains in the presence of a RuR or a ryanodine block. This mechanism is complementary to work carried out by Pessah *et al.*, (1997), stating that through the modulatory actions of Bastadin on FKBP12-RyR1 complex, it converts the RuR/ryanodine insensitive leak unmasked by thapsigargin into a state that is recognized RuR/ryanodine in order to induce a block on the leak. Therefore, it would be interesting to examine whether FKBP12.6 modulates the effects of Bastadin in cardiac muscle SR.

8.4. Intraluminal Calcium

The calcium concentration within the lumen of the SR plays a vital role in calcium regulation (Bassani *et al.*, 1995; Sitsapesan & Williams, 1994; Lukyanenko *et al.*, 1996; Gyorke *et al.*, 1997; Gyorke & Gyorke, 1998). In uptake experiments, oxalate effectively clamps intraluminal calcium concentrations to facilitate SR calcium uptake that would otherwise slow the rate of net uptake, as crystallization of calcium-oxalate inside the SR does not reach equilibrium at any time during calcium uptake (Fcher & Briggs, 1980), and will thus continue to buffer intraluminal calcium. In this preparation it was noted that 10mM and 20mM oxalate sufficiently clamped luminal calcium in this preparation and that 3 calcium challenges were sufficient to load the SR resulting in reproducible calcium transients.

Caffeine has been widely used as a pharmacological tool for releasing calcium from intracellular stores to study the role of the sarcoplasmic reticulum during excitation contraction coupling. In agreement with the literature, high concentrations of caffeine (40mM) deplete the SR of calcium and are thus used to assay the SR calcium content. Low concentrations of caffeine (<0.5-2mM) have been hypothesised to stimulate SR calcium recycling, thus increasing calcium uptake as well as release. In this study it was observed that caffeine mediated calcium release from the SR of permeabilised cardiac myocytes occurred in a dose dependent manner and that even in the presence of high concentrations of caffeine (up to 20mM) the SR accumulated a significant amount of calcium but only in the presence of ATP. At caffeine concentrations above 20mM calcium reuptake was observed to be incomplete.

At low intracellular calcium concentration (in the absence of calcium challenges) 40mM was required to induce a significant release of calcium from the SR, a release that was greater than

that produced with 20mM caffeine. However, in the presence of activating calcium concentrations, as low as 2mM caffeine was observed to induce an SR leak, indicating that the effects of caffeine are dependent on calcium concentration and that calcium and caffeine act together to activate the RyR under these conditions.

3mM ryanodine and 5 μ M RuR have been observed to block caffeine mediated SR leak in this preparation and that varying the oxalate concentration had no effect on the ryanodine block of the caffeine mediated leak. This indicates that a similar blocking effect occurs independent of the intraluminal calcium concentration.

In this study 0.3 μ M-30 μ M ryanodine induced the release of calcium from the RyR and that 3mM ryanodine was found to inhibit calcium leak from the SR. This is consistent with ryanodine increasing the P_o of the RyR at lower concentrations where as 3mM ryanodine induced a Use-dependent block of calcium release. The requirement of such high concentrations of ryanodine suggest that the sensitivity of RyR for ryanodine was lower than that observed in SR vesicle preparations although the results in this study complement the literature with RyR possessing two binding sites for ryanodine, a high affinity and a low affinity binding site. However, the sensitivity of permeabilised cells to RuR was comparable to that observed in SR vesicles. Further work is required to determine whether the RyR activity in this preparation is significantly different to that observed in SR vesicles and isolated channel studies.

REFERENCES

- Ahern, G.P., Junankar, P.R. and Dulhunty, A.F. (1994) Single channel activity of the ryanodine receptor calcium release channel is modulated by FK-506. *FEBS Letters* **352**, 369-374.
- Airey, J.A., Beck, C.F., Murakami, K., Tanksley, S.J., Deerinck, T.J., Ellisman, M.H. and Sutko, J.L. (1990) Identification and localization of two triad junctional foot protein isoforms in mature avian fast twitch skeletal muscle. *J.Biol.Chem.* **265**, 14187-14194.
- Alderston, B.H. and Feher, J.J. (1987) The interaction of calcium and ryanodine with cardiac sarcoplasmic reticulum. *Biochem.Biophys.Acta* **900**, 221-229.
- Allen, D.G., Eisner, D.A., Pirolo, J.S. and Smith, G.L. (1985) The relationship between intracellular calcium and contraction in calcium-overloaded ferret papillary muscles. *J.Physiol* **364**, 169-182.
- Allen, D.G. and Orchard, C.H. (1987) Myocardial Function During Ischemia and Hypoxia. *Circ.Res.* **60**, 153-168.
- Allen, D.G., Lee, J.A. and Smith, G.L. (1989) The Consequences of stimulated ischemia on intracellular calcium and tension in isolated ferret ventricular muscle. *J.Physiol.* **410**, 297-323.
- Alpert, N.R., Blanchard, E.M. and Mulieri, L.A. (1989) Genetic and non-genetic control of myocardial calcium. *J.Physiol.* **414**, 433-453.
- Alves, E.W. and De Meis, L. (1986) Effect of compound 48/80 and ruthenium red on the Ca²⁺ - ATPase of sarcoplasmic reticulum. *J.Biol.Chem.* **261**, 16854-16859.
- Arkin, I.T., Adams, P.D., Brünger, A.T., Smith, S.O. and Engelman, D.M. (1997) Structural Perspectives of Phospholamban, A Helical Transmembrane Pentamer. *Ann.Rev.Biophys.Biomol.Struct.* **26**, 157-179.
- Ashley, R.H. and Williams, A.J. (1988) Some effects of calcium and magnesium on the gating of the Ca release channel of sheep heart sarcoplasmic reticulum. *J.Physiol.* **406**, 89π
- Ashley, R.H. and Williams, A.J. (1990) Divalent cation activation and inhibition of single calcium release channels from sheep cardiac sarcoplasmic reticulum. *J.Gen.Physiol.* **95**, 981-1005.
- Autry, J.M. and Jones, L.R. (1997) Functional co-expression of the canine cardiac Ca²⁺ pump and phospholamban in *Spodoptera frugiperda* (Sf21) cells reveals new insights on ATPase regulation. *J.Biol.Chem.* **272**, 15872-15880.

- Bailey, I.A., Williams, S.R., Radda, G.K. and Gadian, D.G. (1981) Activity of phosphatase in total global ischemia in the rat heart. *Biochem.J.* **196**, 171-178.
- Barg, S., Copello, J. A. and Fleischer, S. (1997) Different interactions of cardiac and skeletal muscle ryanodine receptors with FK-506 binding protein isoforms. *Am J Physiol.* **272**(5 Pt 1), C1726-1733.
- Barlogie, B., Hasselbach, W. and Makinose, M. (1971) Activation of calcium efflux by ADP and inorganic phosphate. *FEBS Letters* **12**, 267-268.
- Bassani, J.W.M., Yuan, W. and Bers, D.M. (1995) Fractional SR Ca Release is Regulated by Trigger Ca and SR Ca Content in Cardiac Myocytes. *Am.J.Physiol.* **268**, C1313-C1329.
- Bennett, H. S., and Porter, K. R. (1953) An electron microscope study of sectioned breast muscle of the domestic fowl. *Am. J. Anat.* **159**, 61-73.
- Berlin, J.R., Cannell, M.B. and Lederer, W.J. (1989) Cellular origins of the transient inward current in cardiac myocytes. Role of fluctuations and waves of elevated intracellular calcium. *Circ.Res.* **65**, 115-126.
- Bernardi, P., Paradisi, V., Pozzan, T. and Azzone, G.F. (1984) Pathway for uncoupler-induced calcium efflux in rat liver mitochondria: inhibition by Ruthenium Red. *Biochemistry* **23**, 1645-1651.
- Berridge, M.J. (1993) Inositol Trisphosphate and Calcium Signalling. *Nature* **361**, 315-325.
- Bers, D.M. (1987) Ryanodine and the calcium content of cardiac SR assessed by caffeine and rapid cooling contractures. *Am.J.Physiol.* **253**, C408-C415
- Bers, D.M. (1991) Ca regulation in cardiac muscle. *Med Sci Sports Exercise* **23**, 1157-1162.
- Bers, D. M. (1993) Excitation-contraction coupling and cardiac contractile force. Eds. Kluwer Academic Publishers, Dordrecht.
- Bers, D.M. and Stiffel, V.M. (1993) Ratio of ryanodine to dihydropyridine receptors in cardiac and skeletal muscle and implications for E-C coupling. *Am.J.Physiol.* **264**, C1587-C1593
- Bers, D.M. and Fill, M. (1998) Coordinated Feet and the Dance of Ryanodine Receptors. *Science* **281**, 790-791.

- Bers, D.M. and Perez-Reyes, E. (1999) Ca Channels in Cardiac Myocytes: Structure and Function in Ca Influx and Intracellular Ca release. *Cardiovascular Research* **42**, 339-360.
- Bezprozvanny, I., Watras, J. and Ehrlich, B.E. (1991) Bell-shaped calcium-response curves of Ins(1,4,5)P₃- and calcium-gated channels from endoplasmic reticulum of cerebellum. *Nature* **351**, 751-754.
- Bhat, M.B., Ma, J., Zhao, J.Y., Hayek, S., Freeman, E.C. and Takeshima, H. (1997) (a) Deletion of amino acids 1641-2437 from the foot region of skeletal muscle ryanodine receptor alters the conduction properties of the Ca release channel. *Biophys.J.* **73**, 1320-1328.
- Bhat, M.B., Zhao, J.Y., Takeshima, H. and Ma, J. (1997) (b) Functional calcium release channel formed by the carboxyl-terminal portion of ryanodine receptor. *Biophys.J.* **73**, 1329-1336.
- Bhat, M.B., Zhao, J., Zang, W., Balke, C. W., Takeshima, H., Wier, W. G. and Ma, J. (1997) (c) Caffeine-induced release of intracellular calcium from Chinese Hamster Ovary cells expressing skeletal muscle ryanodine receptor. Effects on full-length and carboxy terminal portion of calcium release channels. *J. Gen. Physiol.* **110**, 749-762.
- Bierer, B.E. (1990) Probing Immunosuppressant Action With a Nonnatural Immunophilin ligand. *Science* **250**, 556-559.
- Blatter, L.A., Hüser, J. and Ríos, E. (1997) Sarcoplasmic reticulum Ca²⁺ release flux underlying Ca²⁺ sparks in cardiac muscle. *Proc.Natl.Acad.Sci.* **94**, 4176-4181.
- Block, B.A., Imagawa, T., Campbell, K.P. and Franzini-Armstrong, C. (1988) Structural evidence for direct interaction between the molecular components of the transverse tubule/sarcoplasmic reticulum junction in skeletal muscle. *J.Cell Biology* **107**, 2587-2600.
- Brillantes, A.B., Ondrias, K., Scott, A., Ondriasova, E., Moschella, M.C., Jayaraman, T., Landers, M., Ehrlich, B.E. and Marks, A.R. (1994) Stabilization of calcium release channel (ryanodine receptor) function by FK506-binding protein. *Cell* **77**, 513-523.
- Buck, W. R., Rakow, T. L. and Shen, S. S. (1992) Synergistic release of calcium in sea urchin eggs by caffeine and ryanodine. *Exp Cell Res.* **202**(1), 59-66.
- Buck, E., Zimanyi, I., Abramson, J. J. and Pessah, I. N. (1992b) Ryanodine stabilizes multiple conformational states of the skeletal muscle calcium release channel. *J Biol Chem.* **267**(33), 23560-23567.

- Butcher, R.W. and Sutherland, E.W. (1962) Adenosine 3',5'-phosphate in biological materials. I. Purification and properties of cyclic 3',5'-nucleotide phosphodiesterase and use of this enzyme to characterize adenosine 3',5'-phosphate in human urine. *J.Biol.Chem.* **237**, 1244-1250.
- Cannell, M.B., Cheng, H. and Lederer, W.J. (1994) Spatial non-uniformities in $[Ca^{2+}]_i$ during excitation-contraction coupling in cardiac myocytes. *Biophys.J.* **67**, 1942-1956.
- Cannell, M.B., Cheng, H. and Lederer, W.J. (1995) The control of calcium release in heart muscle. *Science* **268**, 1045-1049.
- Cantilina, T., Sagara, Y., Inesi, G. and Jones, L.R. (1993) Comparative Studies of cardiac and Skeletal Sarcoplasmic Reticulum ATPase: Effects of a Phospholamban Antibody on Enzyme Activation by Calcium. *J.Biol.Chem.* **268**, 17018-17025.
- Cardoso, C. M. and De Meis, L. (1993) Modulation by fatty acids of Ca^{2+} fluxes in sarcoplasmic-reticulum vesicles. *Biochem J.* **296**, 49-52.
- Caswell, A.H., Brandt, A.R., Brunschwig, J.P. and Purkerson, S. (1991) Localization and partial characterization of the oligomeric disulfide-linked molecular weight 95,000 protein (triadin) which binds the ryanodine and dihydropyridine receptors in skeletal muscle triadic vesicles. *Biochemistry* **30**, 7507-7513.
- Chamberlain, B.K., Volpe, P. and Fleischer, S. (1984) Inhibition of calcium-induced calcium release from purified cardiac sarcoplasmic reticulum vesicles. *J.Biol.Chem.* **259**, 7547-7553.
- Chen, L., Molinski, T. F. and Pessah, I. N. (1999) Bastadin 10 stabilizes the open configuration of the ryanodine-sensitive Ca^{2+} channel in an FKBP12-dependent manner. *J. Biol. Chem.* **274**, 32603-32612.
- Chen, S.R. and MacLennan, D.H. (1994) Asymmetrical blockade of the Ca^{2+} release channel (ryanodine receptor) by 12-kDa FK506 binding protein. *Proc.Natl.Acad.Sci.USA* **91**, 11953-11957.
- Cheng, H., Lederer, W.J. and Cannell, M.B. (1993) Calcium sparks: elementary events underlying excitation-contraction coupling in heart muscle. *Science* **262**, 740-744.
- Cheng, H., Lederer, M.R., Lederer, W.J. and Cannell, M.B. (1996) Calcium sparks and $[Ca^{2+}]_i$ waves in cardiac myocytes. *Am.J.Physiol.(Cell Physiol)* **270**, X148-X159

- Ching, L.L., Williams, A.J. and Sitsapesan, R. (2000) Evidence of Ca²⁺ Activation and Inactivation Sites on the Luminal Side of the Cardiac Ryanodine Receptor Complex. *Circ.Res.* **87**, 201-206.
- Christensen, S.B. (1988) *Acta Chem.Scand.* **B42**, 623-628.
- Chu, A., Díaz-Munro, M., Hawkes, M.J., Brush, K. and Hamilton, S.L. (1990) Ryanodine as a probe for the functional state of the skeletal muscle sarcoplasmic reticulum calcium release channel. *Molecular Pharmacology* **37**, 735-741.
- Collins, J.H., Tarcsafalvi, A. and Ikemoto, N. (1990) Identification of a region of calsequestrin that binds to the junctional face membrane of sarcoplasmic reticulum. *Biochem.Biophys.Res.Commun.* **167**, 189-193.
- Connelly, T., Ahern, C., Sukhareva, M. and Coronado, R. (1994) Removal of Mg²⁺ inhibition of cardiac ryanodine receptor by palmitoyl coenzyme A. *FEBS Lett.* **352**(3), 285-290.
- Coronado, R., Morrissette, J., Sukhareva, M. and Vaughan, D.M. (1994) Structure and Function of Ryanodine Receptors. *Am.J.Physiol.* **266** (Cell Physiol. **35**), C1485-C1504.
- de Meis, L. and Vianna, A.L. (1979) Energy interconversion by the Ca²⁺-dependent ATPase of the sarcoplasmic reticulum. *Annu.Rev.Biochem.* **48**, 275-292.
- de Meis, L. and Inesi, G. (1992) Functional evidence of a transmembrane channel within the Ca²⁺ transport ATPase of sarcoplasmic reticulum. *FEBS* **299**, 33-35.
- Dettbarn, C. and Palade, P. (1993) Arachidonic acid-induced Ca²⁺ release from isolated sarcoplasmic reticulum. *Biochem Pharmacol.* **45**(6), 1301-1309.
- DeVault, G. (1983) The return of RYANIA. *New farm (Μαψ/θύπε)*:25-27.
- Díaz-Munoz, M., Hamilton, S.L., Kactzel, M. A., Hazarika, P. and Dedman, J. R. (1990) Modulation of Ca²⁺ release channel activity from sarcoplasmic reticulum by annexin VI (67-kDa calcimedin). *J. Biol. Chem.* **265**, 15894-15899.
- Du, G.G., Khanna, V.K. and MacLennan, D.H. (2000) Mutation of divergent region 1 alters caffeine and Ca(2+) sensitivity of the skeletal muscle Ca(2+) release channel (ryanodine receptor). *J.Biol.Chem.* **275**, 11778-11783.

- Dupont, Y. (1980) Occlusion of divalent cations in the phosphorylated calcium pump of sarcoplasmic reticulum. *Eur.J.Biochem.* **109**, 231-238.
- Dupont, Y. (1982) Low-temperature studies of the sarcoplasmic reticulum calcium pump. Mechanisms of calcium binding. *Biochem.Biophys.Acta* **688**, 75-87.
- El-Hayek, R., Valdivia, C., Valdivia, H. H., Hogan, K. and Coronado, R. (1993) Activation of the Ca²⁺ release channel of skeletal muscle sarcoplasmic reticulum by palmitoyl carnitine. *Biophys J.* **65**(2), 779-789.
- Endo, M. (1977) Calcium release from the sarcoplasmic reticulum. *Physiol.Rev.* **57**, 71-108.
- Endo, M. and Lino, M. (1980) Specific perforation of muscle cell membranes with preserved SR functions by saponin treatment. *J.Muscle Res.Cell Mot.* **1**, 89-100.
- Erdahl, W.L., Chapman, C.J., Taylor, R.W. and Pfeiffer, D.R. (1995) Effects of pH conditions on Ca²⁺ transport catalysed by ionophores A23187, 4-BrA23187 and Ionomycin suggests problems with common applications of these compounds in biological systems. *Biophys.J.* **69**, 2350-2363.
- Fabiato, A. and Fabiato, F. (1979) Use of chlorotetracycline fluorescence to demonstrate Ca²⁺-induced release of Ca²⁺ from the sarcoplasmic reticulum of skinned cardiac cells. *Nature* **281**, 146-148.
- Fabiato, A. and Fabiato, F. (1979b) Calculator programs for computing the composition of the solutions containing multiple metals and ligands used for experiments in skinned muscle cells. *J Physiol (Paris)*. **75**, 463-505.
- Fabiato, A. (1983) Calcium-induced release of calcium from the cardiac sarcoplasmic reticulum. *Am.J.Physiol.* **245**, C1-C14
- Fabiato, A. (1992) Two kinds of calcium-induced release of calcium from the sarcoplasmic reticulum of skinned cardiac cells. *Adv.Exp.Med.Biol.* **311**, 245-262.
- Feher, J.J. and Briggs, F.N. (1980) Characterization of cardiac sarcoplasmic reticulum from ischemic myocardium: comparison of isolated sarcoplasmic reticulum with unfractionated homogenates. *J.Mol.Cell.Cardiol.* **12**, 427-432.
- Feher, J.J. and Briggs, F.N. (1983) Determinants of calcium loading at steady state in sarcoplasmic reticulum. *Biochem.Biophys.Acta* **727**, 389-402.

- Feher, J.J., Manson, N.H. and Poland, J.L. (1988) The Rate and Capacity of Calcium Uptake by Sarcoplasmic Reticulum in Fast, Slow and Cardiac Muscle: Effects of Ryanodine and Ruthenium Red. *Arch.Biochem.Biophys.* **265**, 171-182.
- Feher, J.J. and Lipford, G.B. (1995) Calcium oxalate and calcium phosphate capacities of cardiac sarcoplasmic reticulum. *Biochem.Biophys.Acta* **818**, 373-385.
- Ferguson, D. G., Schwartz, H. W. and Franzini-Armstrong, C. (1984) Subunit structure of junctional feet in triads of skeletal muscle: a freeze-drying, rotary-shadowing study. *J Cell Biol.* **99**(5), 1735-42.
- Fleischer, S., Ogunbunmi, E.M., Dixon, M.C. and Fleer, E.A.M. (1985) Localization of Ca²⁺ release channels with ryanodine in junctional terminal cisternae of sarcoplasmic reticulum of fast skeletal muscle. *Proc.Natl.Acad.Sci.USA* **82**, 7256-7259.
- Fleischer, S. and Inui, M. (1989) Biochemistry and biophysics of excitation-contraction coupling. *Annu Rev Biophys Biophys Chem.* **18**, 333-364.
- Fletcher, J.M., Greenfield, B.F., Scargill, H.D. and Woodhead, J.L. (1961) Ruthenium Red. *J.Chemical Society* 2000-2006.
- Flutcher, B.E. and Franzini-Armstrong, C. (1996) Formation of junctions involved in excitation-contraction coupling in skeletal and cardiac muscle. *Proc.Natl.Acad.Sci.USA* **93**, 8101-8106.
- Franzini-Armstrong, C. and Nunzi, G. (1983) Junctional feet and particles in the triads of a fast-twitch muscle fibre. *J.Muscle Res.Cell Mot.* **4**, 233-252.
- Franzini-Armstrong, C. and Jorgensen, A.O. (1994) Structure and development of E-C coupling units in skeletal muscle. *Ann.Rev.Physiol.* **56**, 509-534.
- Franzini-Armstrong, C. (1995) Ultrastructural Studies on Feet/Ryanodine Receptors. In: Sorrentino, V., (Ed.) *Ryanodine Receptors*, pp. 1-16. London: CRC Press Inc.]
- Franzini-Armstrong, C. (1999) The Sarcoplasmic Reticulum and the Control of Muscle Contraction. *FASEB J.* **13**, S266-S270
- Fryer, M.W., Owen, V.J., Lamb, G.D. and Stephenson, D.G. (1995) Effects of creatine phosphate and P(i) on Ca²⁺ movements and tension development in rat skinned skeletal muscle fibres. *J.Physiol.* **482**, 123-140.

- Futatsugi, A., Kuwajima, G. and Mikoshiba, K. (1995) Tissue-specific and developmentally regulated alternative splicing in mouse skeletal muscle ryanodine receptor mRNA. *Biochem.J.* **305**, 373-378.
- Galione, A., Lee, H. C. and Busa, W. B. (1991) Ca²⁺-induced Ca²⁺ release in sea urchin egg homogenates: modulation by cyclic ADP-ribose. *Science*. **253**(5024), 1143-6.
- Gao, L., Balshaw, D., Xu, L., Tripathy, A., Xin, C. and Meissner, G. (2000) Evidence for a Role of the Luminal M3-M4 Loop in Skeletal Muscle Ca²⁺ Release Channel (Ryanodine Receptor) Activity and Conductance. *Biophys.J.* **79**, 828-840.
- Gilchrist, J.S., Belcastro, A.N. and Katz, S. (1992) Intraluminal Ca²⁺ dependence of Ca²⁺ and ryanodine-mediated regulation of skeletal muscle sarcoplasmic reticulum Ca²⁺ release. *J.Biol.Chem.* **267**, 20850-20856.
- Gincel, D., Zaid, H. and Shoshan-Barmatz, V. (2001) Calcium binding and translocation by the voltage-dependent anion channel: a possible regulatory mechanism in mitochondrial function. *Biochem.J.* **358**, 147-155.
- Grover, A.K. and Khan, I. (1992) Calcium Pump Isoforms: Diversity, Selectivity and Plasticity. *Cell Calcium* **13**, 9-17.
- Grynkiewicz, G., Poenie, M. and Tsien, R.Y. (1985) A new generation of Ca²⁺ indicators with greatly improved fluorescence properties. *J.Biol.Chem.* **260**, 3440-3450.
- Györke, I. and Györke, S. (1998) Regulation of the Cardiac Ryanodine Receptors Channel by Luminal Ca²⁺ Involves Luminal Ca²⁺ Sensing Sites. *Biophys.J.* **75**, 2801-2810.
- Györke, S. and Fill, M. (1993) Ryanodine Receptor Adaptation: Control Mechanism of Ca²⁺-Induced Ca²⁺ Release in Heart. *Science* **260**, 807-809.
- Gyorke, S., Lukyanenko, V. and Gyorke, I. (1997) Dual effects of tetracaine on spontaneous calcium release in rat ventricular myocytes. *J.Physiol.* **500**, 297-309.
- Hakamata, Y., Nakai, J., Takeshima, H. and Imoto, K. (1992) Primary structure and distribution of a novel ryanodine receptor/calcium release channel from rabbit brain. *FEBS Lett.* **312**, 229-235.
- Hasselbach, W. (1978) The Reversibility of the Sarcoplasmic Calcium Pump. *Biochem.Biophys.Acta* **515**, 23-53.

- Herrmann-Frank, A. and Lehmann-Horn, F. (1996) Regulation of the purified Ca²⁺ release channel/ryanodine receptor complex of skeletal muscle sarcoplasmic reticulum by luminal calcium. *Pflugers Arch.* **432**, 155-157.
- Hidalgo, C. and Ikemoto, N. (1977) Disposition of proteins and aminophospholipids in the sarcoplasmic reticulum membrane. *J.Biol.Chem.* **252**, 8446-8454.
- Hove-Madsen, L. and Bers, D.M. (1993) Sarcoplasmic Reticulum Ca²⁺ Uptake and Thapsigargin Sensitivity in Permeabilized Rabbit and Rat Ventricular Myocytes. *Circ.Res.* **73**, 820-828.
- Huxley, H. E. (1964) Evidence for continuity between central elements of the triad and extracellular space in frog sartorius. *Nature* **202**, 10676-10771.
- Ikemoto, N., Nagy, B., Bhatnagar, G.M. and Gergely, J. (1974) Studies on a metal-binding protein of the sarcoplasmic reticulum. *J.Biol.Chem.* **249**, 2357-2365.
- Ikemoto, N. (1982) Structure and Function of the Calcium Pump Protein of Sarcoplasmic Reticulum. *Ann.Rev.Physiol.* **44**, 297-317.
- Ikemoto, N., Ronjat, M., Meszaros, L.G. and Koshita, M. (1989) Postulated role of calsequestrin in the regulation of calcium release from sarcoplasmic reticulum. *Biochemistry* **28**, 6764-6771.
- Imagawa, T., Smith, J.S., Coronado, R. and Campbell, K.P. (1987) Purified ryanodine receptor from skeletal muscle sarcoplasmic reticulum is the Ca²⁺-permeable pore of the calcium release channel. *J.Biol.Chem.* **262**, 16636-16643.
- Inesi, G. and de Meis, L. (1989) Regulation of steady state filling in sarcoplasmic reticulum. Roles of back-inhibition, leakage, and slippage of the calcium pump. *J.Biol.Chem.* **264**, 5929-5936.
- Inesi, G., Kurzmack, M., Coan, C. and Lewis, D.E. (1980) Cooperative calcium binding and ATPase activation in sarcoplasmic reticulum vesicles. *J.Biol.Chem.* **255**, 3025-3031.
- Ishide, N. (1996) Intracellular calcium modulators for cardiac muscle in pathological conditions. *Japanese Heart J.* **37**, 1-17.
- Jayaraman, T., Brillantes, A.-M., Timmerman, A.P., Fleischer, S., Erdjument-Bromage, H., Tempst, P. and Marks, A.R. (1992) FK506 binding protein associated with the calcium release channel (ryanodine receptor). *J.Biol.Chem.* **267**, 9474-9477.

- Jencks, W.P. (1989) How Does a Calcium Pump Pump Calcium. *J.Biol.Chem.* **264**, 18855-18858.
- Kadambi, V.J. and Kranias, E.G. (1997) Phospholamban: A protein Coming of Age. *Biochem.Biophys.Res.Commun.* **239**, 1-5.
- Kargacin, G.J. and Kargacin, M.E. (1998) Ruthenium Red Reduces the Ca²⁺ Sensitivity of Ca²⁺ Uptake into Cardiac sarcoplasmic Reticulum. *Pflügers Arch.-Eur.J.Physiol.* **436**, 338-342.
- Katz, A.M. (1996) Calcium Channel Diversity in the Cardiovascular System. *J.Amer.Coll.Card.* **28**, 522-529.
- Kawasaki, T. and Kasai, M. (1994) Regulation of calcium channel in sarcoplasmic reticulum by calsequestrin. *Biochem Biophys Res Commun* **199**, 1120-1127.
- Kay, J.E. (1996) Structure-function relationships in the FK506-binding protein (FKBP) family of peptidylprolyl cis-trans isomerases. *Biochem.J.* **314**, 361-385.
- Keizer, J., Smith, G.D., Ponce-Dawson, S. and Pearson, J.E. (1998) Saltatory propagation of ca²⁺ waves by ca²⁺ sparks. *Biophys.J* **75**, 595-600.
- Kentish, J.C. and Allen, D.G. (1986) Is Force Production in the Myocardium Directly Dependent Upon the Free Energy Change of ATP Hydrolysis. *J.Mol.Cell Cardiol.* **18**, 879-882.
- Kijima, Y., Ogunbunmi, E. and Fleischer, S. (1991) Drug Action of Thapsigargin on the Ca²⁺ Pump Protein of sarcoplasmic Reticulum. *J.Biol.Chem.* **266(34)**, 22912-22918.
- Kim, D.H., Ohnishi, S.T. and Ikemoto, N. (1983) Kinetic studies of calcium release from sarcoplasmic reticulum in vitro. *J.Biol.Chem.* **258**, 9662-9668.
- Kirby, M.S., Sagara, Y., Gaa, S., Inesi, G., Lederer, W.J. and Rogers, T.B. (1992) Thapsigargin Inhibits Contraction and Ca²⁺ Transient in Cardiac Cells by Specific Inhibition of the Sarcoplasmic Reticulum Ca²⁺ Pump. *J.Biol.Chem.* **267**, 12545-12551.
- Koss, K.L. and Kranias, E.G. (1996) Phospholamban: A Prominent Regulator of Myocardial Contractility. *Circ.Res.* **79**, 1059-1063.
- Läuger, P. (1991) *Electrogenic Ion Pump*, Sinauer Associates Inc.

- Lai, F.A., Erickson, H.P., Rousseau, E., Liu, Q.L. and Meissner, G. (1988) Purification and reconstitution of the calcium release channel from skeletal muscle. *Nature* **331**, 315-319.
- Lai, F.A. and Meissner, G. (1989) The muscle ryanodine receptor and its intrinsic Ca²⁺ channel activity. *J Bioenerg Biomembr.* **21**, 227-246.
- Lakatta, E.G. (1992) Functional Implications of Spontaneous Sarcoplasmic Reticulum Ca²⁺ Release in the Heart. *Cardiovascular Research* **26**, 193-214.
- Lam, E., Martin, M.M., Timmerman, A.P., Sabers, C., Fleischer, S., Lukas, T., Abraham, R.T., O'Keefe, S.J., O'Neill, E.A. and Wiederrecht, G.J. (1995) A Novel FK506 Binding Protein Can Mediate the Immunosuppressive Effects of FK506 and Is Associated with the Cardiac Ryanodine Receptor. *J.Biol.Chem.* **270**, 26511-26522.
- Laver, D. R., Baynes, T. M. and Dulhunty, A. F. (1997) Magnesium inhibition of ryanodine-receptor calcium channels: Evidence for two independent mechanisms. *J. Membr. Biol.* **156**, 213-229.
- Lipp, P. and Niggli, E. (1996) Submicroscopic calcium signals as fundamental events of excitation-contraction coupling in guinea-pig cardiac myocytes. *J.Physiol.* **492**, 31-38.
- Liu, C.-M. and Herman, T.E. (1978) Characterization of Ionomycin as a Calcium Ionophore. *J.Biol.Chem.* **253**, 5892-5894.
- Llopis, J., Chow, S.B., Kass, G.E., Gahn, A. and Orrenius, S. (1991) Comparison between the effects of the microsomal Ca(2+)-translocase inhibitors thapsigargin and 2,5-di-(t-butyl)-1,4-benzohydroquinone on cellular calcium fluxes. *Biochem.J.* **277**, 553-556.
- Lopez-Lopez, J.R., Shacklock, P.S., Balke, C.W. and Wier, W.G. (1995) Local calcium transients triggered by single L-type calcium channel currents in cardiac cells. *Science* **268**, 1042-1045.
- Loughrey, C.M., MacEachern, K.E., Neary, P., Smith, G.L. (2003) The relationship between intracellular [Ca²⁺] and Ca²⁺ wave characteristics in permeabilised cardiomyocytes from the rabbit. *J. Physiol.* **543.3**, 859-870.
- Lukyanenko, V., Györke, I. and Györke, S. (1996) Regulation of calcium release by calcium inside the sarcoplasmic reticulum in ventricular myocytes. *Pflugers Arch.* **432**, 1047-1054.

- Lukyanenko, V. and Györke, S. (1999) Ca^{2+} Sparks and Ca^{2+} Waves in Saponin-Permeabilized Rat Ventricular Myocytes. *J.Physiol.* **521**,3, 575-585.
- Lytton, J., Westlin, M. and Hanley, M.R. (1991) Thapsigargin inhibits the sarcoplasmic or endoplasmic reticulum Ca-ATPase family of calcium pumps*. *J.Biol.Chem.* **266**, 17067-17071.
- Ma, J. (1993) Block by Ruthenium Red of the Ryanodine-activated Calcium Release Channel of Skeletal Muscle. *J.Gen.Physiol.* **102**, 1031-1056.
- Mack, M.M., Molinski, T.F., Buck, E.D. and Pessah, I.N. (1994) Novel Modulators of Skeletal Muscle FKBP12/Calcium Channel Complex from *Ianthella basta*. *J.Biol.Chem.* **269**, 23236-23249.
- Mack, W.M., Zimanyi, I. and Pessah, I.N. (1992) Discrimination of multiple binding sites for antagonists of the calcium release channel complex of skeletal and cardiac sarcoplasmic reticulum. *J Pharmacol Exp Ther.* **262**, 1028-1037.
- MacLennan, D.H., Seeman, P., Iles, G.H. and Yip, C.C. (1971) Membrane formation by the adenosine triphosphate of sarcoplasmic reticulum. *J.Biol.Chem.* **246**, 2702-2710.
- Madeira, V.M. (1982) Oxalate transfer across the membranes of sarcoplasmic reticulum during the uptake of Ca^{++} . *Cell Calcium* **3**, 67-79.
- Makinose, M. and Hasselbach, W. (1965) The Influence of oxalate on calcium transport of isolated sarcoplasmic reticular vesicles. *Biochemische Zeitschrift* **343**, 360-382.
- Makinose, M. (1971) Calcium efflux dependent formation of ATP from ADP and orthophosphate by the membranes of the sarcoplasmic vesicles. *FEBS Letters* **12**, 269-270.
- Makinose, M. and Hasselbach, W. (1971) ATP synthesis by the reverse of the sarcoplasmic calcium pump. *FEBS Letters* **12**, 271-272.
- Makinose, M. (1973) Possible functional states of the enzyme of the sarcoplasmic calcium pump. *FEBS Letters* **37**, 140-143.
- Marks, A.R., Tempst, P., Hwang, K.S., Taubman, M.B., Inui, M., Chadwick, C., Fleischer, S. and Nadal-Ginard, B. (1989) Molecular cloning and characterization of the ryanodine receptor/junctional channel complex cDNA from skeletal muscle sarcoplasmic reticulum. *Proc.Natl.Acad.Sci.USA* **86**, 8683-8687.

- Marks, A.R., Fleischer, S. and Tempst, P. (1990) Surface topography analysis of the ryanodine receptor/junctional channel complex based on proteolysis sensitivity mapping. *J.Biol.Chem.* **265**, 13143-13149.
- Marks, A.R. (1996) Cellular Functions of Immunophilins. *Physiol.Rev.* **76**, 631-649.
- Marks, A. R. (1996b) Immunophilin modulation of calcium channel gating. *METHODS: A Companion to Methods in Enzymology.* **9**, 177-187
- Martonosi, A. (1968) Sarcoplasmic reticulum versus the structure of sarcoplasmic reticulum membranes. *Biochimica et Biophysica Acta* **150**, 694-704.
- Marx, S.O., Ondrias, K. and Marks, A.R. (1998) Coupled Gating Between Individual Skeletal Muscle Ca²⁺ Release Channels (Ryanodine receptor). *Science* **281**, 818-821.
- Marx, S.O., Reiken, S., Hisamatsu, Y., Jayaraman, T., Burkhoff, D., Rosemblyt, N. and Marks, A.R. (2000) PKA phosphorylation dissociates FKBP12.6 from the calcium release channel (ryanodine receptor): defective regulation in failing hearts. *Cell* **101**, 365-376.
- Marx, S.O., Gaburjakova, J., Gaburjakova, M., Henrikson, C., Ondrias, K. and Marks, A.R. (2001) Coupled Gating Between Cardiac Calcium Release Channels (Ryanodine receptor). *Circ.Res.* **88**, 1151-1158.
- Masumiya, H., Li, P., Zhang, L. and Chen, S.R.W. (2001) Ryanodine sensitizes the Ca²⁺ release channel (ryanodine receptor) to Ca²⁺ activation. *J.Biol.Chem.* **276**, 39727-39735.
- Mayrleitner, M., Timmerman, A.P., Wiederrecht, G. and Fleischer, S. (1994) The calcium release channel of sarcoplasmic reticulum is modulated by FK-506 binding protein: effect of FKBP-12 on single channel activity of the skeletal muscle ryanodine receptor. *Cell Calcium* **15**, 99-108.
- McCormack, J.G., Browne, H.M. and Dawes, N.J. (1989) Studies on mitochondrial Ca²⁺-transport and matrix Ca²⁺ using fura-2-loaded rat heart mitochondria. *Biochem.Biophys.Acta* **973**, 420-427.
- McCrew, S.G., Wolleben, C., Siegl, P., Inui, M. and Fleischer, S. (1989) Positive cooperativity of ryanodine binding to the calcium release channel of sarcoplasmic reticulum from heart and skeletal muscle. *Biochemistry* **28**, 1686-1691.
- McLennan, D. H. (1970) Purification and properties of an adenosine triphosphatase from sarcoplasmic reticulum. *J. Biol. Chem.* **245**, 4508-4518.

- Mehran, R., Brillantes, A., Jayaraman, T., Kobrinsky, E. and Marks, A. (1993) *Circulation* **88**, 1624
- Meissner, G., Conner, G.E. and Fleischer, S. (1973) Isolation of sarcoplasmic reticulum by zonal centrifugation and purification of Ca²⁺-pump and Ca²⁺-binding proteins. *Biochem.Biophys.Acta* **298**, 246-269.
- Meissner, G. (1986) Ryanodine activation and inhibition of the Ca²⁺ release channel of sarcoplasmic reticulum. *J.Biol.Chem.* **261**, 6300-6306.
- Meissner, G., Darling, E. and Eveleth, J. (1986) Kinetics of rapid Ca²⁺ release by sarcoplasmic reticulum. Effects of Ca²⁺, Mg²⁺ and adenine nucleotides. *Biochemistry* **25**, 236-244.
- Meissner, G. and Henderson, J.S. (1987) Rapid calcium release from cardiac sarcoplasmic reticulum vesicles is dependent on Ca²⁺ and is modulated by Mg²⁺, adenine nucleotide, and calmodulin. *J.Biol.Chem.* **262**, 3065-3073.
- Meissner, G., Rousseau, E. and Lai, F.A. (1989) Structural and functional correlation of the trypsin-digested Ca²⁺ release channel of skeletal muscle sarcoplasmic reticulum. *J.Biol.Chem.* **264**, 1715-1722.
- Meissner, G. (1994) Ryanodine receptor/Ca²⁺ release channels and their regulation by endogenous effectors. *Ann.Rev.Physiol.* **56**, 508
- Meissner, G., Rios, E., Tripathy, A. and Pasek, D.A. (1997) Regulation of skeletal muscle Ca²⁺ release channel (ryanodine receptor) by Ca²⁺ and monovalent cations and anions. *J.Biol.Chem.* **272**, 1628-1638.
- Mejia-Alvarez, R., Kettlun, C., Ríos, E., Stern, M. and Fill, M. (1998) Unitary calcium currents through cardiac ryanodine receptor under physiological conditions. *Biophys.J.* **74**, A58
- Michalak, M., Campbell, K.P. and MacLennan, D.H. (1980) Localization of the high affinity calcium binding protein and an intrinsic glycoprotein in sarcoplasmic reticulum membranes. *J.Biol.Chem.* **255**, 1317-1326.
- Mintz, E. and Guillain, F. (1997) Ca²⁺ Transport by the Sarcoplasmic Reticulum ATPase. *Biochem.Biophys.Acta* **1318**, 52-70.

- Miyamoto, H. and Racker, E. (1981) Calcium induced calcium release at terminal cisternae of skeletal sarcoplasmic reticulum. *FEBS Letters* **133**, 235-238.
- Moisesescu, D.G. and Theileczek, R. (1978) Calcium and strontium concentration changes within skinned muscle preparations following a change in the external bathing solutions. *J.Physiol.* **275**, 241-262.
- Moschella, M.C. and Marks, A.R. (1993) Inositol 1,4,5-trisphosphate receptor expression in cardiac myocytes. *J.Cell Biology* **120**, 1137-1146.
- Movsesian, M.A. and Schwinger, R.H.G. (1998) Calcium Sequestration by the Sarcoplasmic Reticulum in Heart Failure. *Cardiovascular Research* **37**, 352-359.
- Nakai, J., Imagawa, T., Hakamat, Y., Shigekawa, M., Takeshima, H. and Numa, S. (1990) Primary structure and functional expression from cDNA of the cardiac ryanodine receptor/calcium release channel. *FEBS Letters* **271**, 169-177.
- Nelson, T.E. and Nelson, K.E. (1990) Intra- and extraluminal sarcoplasmic reticulum membrane regulatory sites for Ca²⁺-induced Ca²⁺ release. *FEBS Letters* **263**, 292-294.
- Netticadan, T., Xu, A. and Narayanan, N. (1996) Divergent Effects of Ruthenium Red and Ryanodine on Ca²⁺/Calmodulin-Dependent Phosphorylation of the Ca²⁺ Release Channel (Ryanodine Receptor) in Cardiac Sarcoplasmic Reticulum. *Arch.Biochem.Biophys.* **333**, 368-376.
- Niggli, E. (1999) Localized Intracellular Calcium Signalling in Muscle: Calcium Sparks and Calcium Quarks. *Ann.Rev.Physiol.* **61**, 311-335.
- Norregaard, A., Vilsen, B. and Andersen, J.P. (1994) Transmembrane segment M3 is essential to thapsigargin sensitivity of the sarcoplasmic reticulum Ca(2+)-ATPase. *J.Biol.Chem.* **264**, 26598-26601.
- Ogawa, Y. (1994) Role Of Ryanodine Receptors. *Crit.Rev.Biochem.Mol.Biol.* **29**, 229-274.
- Otsu, K., Willard, H. F., Khanna, V. K., Zorzato, F., Green, N.M. and MacLennan, D. H. (1990) Molecular cloning of cDNA encoding the Ca²⁺ release channel (ryanodine receptor) of rabbit cardiac muscle sarcoplasmic reticulum. *J Biol Chem.* **265**,13472-13483.
- Ohtsuki, I., Manzi, R.M., Palade, G.E. and Jamieson, J.D. (1978) Entry of marmolecular tracers into cells fixed with low concentrations of aldehydes. *Biologie Cellulaire* **31**, 119-126.

- Overend, C.L., Eisner, D.A. and O'Neill, S.C. (1997) The effect of tetracaine on spontaneous Ca²⁺ release and sarcoplasmic reticulum calcium content in rat ventricular myocytes. *J.Physiol.* **502**, 471-479.
- Overend, C.L., Eisner, D.A. and O'Neill, S.C. (2001) Altered cardiac sarcoplasmic reticulum function of intact myocyte of rat ventricular metabolic inhibition. *Circ.Res.* **88**, 181-187.
- Palade, P. (1987) Drug induced calcium release from isolated saroplasmic reticulum. *J.Biol.Chem.* **262**, 6135-6141.
- Pessah, I.N. and Zimanyi, I. (1991) Characterization of multiple [3H]ryanodine binding sites on the Ca²⁺ release channel of sarcoplasmic reticulum from skeletal and cardiac muscle: evidence for a sequential mechanism in ryanodine action. *Molecular Pharmacology* **39**, 679-689.
- Pessah, I.N., Molinski, T.F., Meloy, T.D., Wong, P., Buck, E.D., Allen, P.D., Mohr, F.C. and Mack, M.M. (1997) Bastadins Relate Ryanodine-Sensitive and -Insensitive Ca²⁺ Efflux Pathways in Skeletal SR and BC₃H1 cells. *Am.J.Physiol.* **272 (Cell Physiol. 41)**, C601-C614.
- Porter, K. R. (1956) The sarcoplasmic reticulum in muscle cells of *Amblystoma* larvae. *J. Biophys. Biochem. Cytol.* **2**, 163-170.
- Porter, K.R., and Palade, G. E. (1957) Studies on the endoplasmic reticulum. III. Its form and distribution in striated muscle cells. *J. Biophys. Biochem. Cytol.* **3**, 269-300.
- Pressman, B.C. (1976) Biological Applications of Ionophores. *Annu.Rev.Biochem.* **45**, 501-530.
- Protasi, F., Sun, X.H. and Franzini-Armstrong, C. (1996) Formation and maturation of the calcium release apparatus in developing and adult avian myocardium. *Developmental Biology* **173**, 265-278.
- Protasi, F., Franzini-Armstrong, C. and Flutcher, B.E. (1997) Coordinated incorporation of skeletal muscle dihydropyridine receptors and ryanodine receptors in peripheral couplings of BC₃H1 cells. *J.Cell Biology* **137**, 859-870.
- Ríos, E. and Stern, M.D. (1997) Calcium in Close Quarters: Microdomain Feedback in Excitation-Contraction Coupling and Other Cell Biological Phenomena. *Ann.Rev.Biophys.Biomol.Struct.* **26**, 47-82.

- Raeymaekers, L., & Hasselbach, W. (1981) Ca²⁺ uptake, Ca²⁺-ATPase activity, phosphoprotein formation and phosphate turnover in a microsomal fraction of smooth muscle. *Eur J Biochem.* **116**, 373-8.
- Rapundalo, S.T. (1998) Cardiac Protein Phosphorylation: Function and Pathophysiological Correlates. *Cardiovascular Research* **38**, 559-588.
- Robison, G.A., Butcher, K.W. and Sutherland, E.W. (1968) Cyclic AMP. *Annu.Rev.Biochem.* **37**, 149-174.
- Rogers, E.F. (1948) Plant Insecticides. I. Ryanodine: A new alkaloid from *Ryania speciosa* Vahl. *J.Am.Chem.Soc.* **70**, 3086-3088.
- Rousseau, E., Smith, J.S., Henderson, J.S. and Meissner, G. (1986) Single channel and ⁴⁵Ca²⁺ flux measurements of the cardiac sarcoplasmic reticulum calcium channel. *Biophys.J.* **50**, 1009-1014.
- Rousseau, E., Smith, J.S. and Meissner, G. (1987) Ryanodine Modifies Conductance and Gating Behaviour of Single Ca²⁺ Release Channel. *Am.J.Physiol.(Cell Physiol)* **253**, C364-C368
- Rousseau, E. and Meissner, G. (1989) Single Cardiac Sarcoplasmic Reticulum Ca²⁺ - Release Channel: Activation by Caffeine. *Am.J.Physiol.(Heart Circ.Physiol.)* **256**, H328-H333.
- Rousseau E. and Pinkos, J. (1990) pH modulates conducting and gating behaviour of single calcium release channels. *Pflugers Arch.* **415(5)**, 645-647.
- Sabbadini, R. A., Betto, R., Teresi, A., Fachechi-Cassano, G. and Salviati G. (1992) The effects of sphingosine on sarcoplasmic reticulum membrane calcium release. *J Biol Chem.* **267(22)**, 15475-15484.
- Sagara, Y. and Inesi, G. (1991) Inhibition of the sarcoplasmic reticulum Ca²⁺ transport ATPase by thapsigargin at subnanomolar concentrations. *J.Biol.Chem.* **266**, 13503-13506.
- Saito, A., Inui, M., Radermacher, M., Frank, J. and Fleischer, S. (1988) Ultrastructure of the calcium release channel of sarcoplasmic reticulum. *J.Cell Biology* **107**, 211-219.
- Santana, L.F., Cheng, H., Gómez, A.M., Cannell, M.B. and Lederer, W.J. (1996) Relation between the sarcolemmal Ca²⁺ current and Ca²⁺ sparks and local control theories for cardiac excitation-contraction coupling. *Circ.Res.* **78**, 166-171.

- Satoh, H., Blatter, L.A. and Bers, D.M. (1997) Effects of $[Ca^{2+}]_i$, SR Ca^{2+} load, and rest on Ca^{2+} spark frequency in ventricular myocytes. *Am.J.Physiol.* **272**, H657-H668
- Schiefer, A., Meissner, G. and Isenberg, G. (1995) Ca^{2+} activation and Ca^{2+} inactivation of canine reconstituted cardiac sarcoplasmic reticulum Ca^{2+} -release channels. *J.Physiol.* **498**, 337-348.
- Schmid, F.X. (1993) Prolyl isomerase: enzymatic catalysis of slow protein-folding reactions. *Annu Rev Biophys Biomol Struct.* **22**, 123-142.
- Schneider, M.F. and Chandler, W.K. (1973) Voltage dependent charge movement of skeletal muscle: a possible step in excitation-contraction coupling. *Nature* **242**, 244-246.
- Seeman, P. (1967) Transient holes in the erythrocyte membrane during hypotonic hemolysis and stable holes in the membrane after lysis by saponin and lysolecithin. *J.Cell Biology* **32**, 55-70.
- Sham, J.S., Cleemann, L. and Morad, M. (1995) Functional coupling of Ca^{2+} channels and ryanodine receptors in cardiac myocytes. *Proc.Natl.Acad.Sci.USA* **92**, 121-125.
- Shannon, T.R., Ginsburg, K.S. and Bers, D.M. (2000) Reverse mode of the sarcoplasmic reticulum calcium pump and load-dependent cytosolic calcium decline in voltage-clamped cardiac ventricular myocytes. *Biophys.J* **78**, 322-333.
- Simmerman, H.K.B. and Jones, L.R. (1998) Phospholamban: Protein Structure, Mechanism of Action, and Role in Cardiac Function. *Physiol.Rev.* **78**, 921-947.
- Sitsapesan, R. and Williams, A.J. (1994a) Gating of the native and purified cardiac SR Ca^{2+} - release channel with monovalent cations as permeant species. *Biophys. J.* **67**, 1484-1494.
- Sitsapesan, R. and Williams, A.J. (1994) Regulation of the gating of the sheep cardiac sarcoplasmic reticulum Ca^{2+} -release channel by luminal Ca^{2+} . *J.Membrane Biol.* **137**, 215-226.
- Sitsapesan, R., McGarry, S.J. and Williams, A.J. (1995) Cyclic ADP-Ribose, The Ryanodine Receptor and Ca^{2+} Release. *TIPS* **16**, 386-391.
- Sitsapesan, R. and Williams, A.J. (1997) Regulation of Current Flow Through Ryanodine Receptors by Luminal Ca^{2+} . *J.Membrane Biol.* **159**, 179-185.

- Smith, G. L. and Miller, D. J. (1985) Potentiometric measurements of stoichiometric and apparent affinity constants of EGTA for protons and divalent ions including calcium. *Biochim Biophys Acta*. **839**, 287-299.
- Smith, G.L. and Steele, D.S. (1992) Inorganic Phosphate Decreases Ca²⁺ Content of the Sarcoplasmic Reticulum in Saponin-Treated Rat Cardiac Trabeculae. *J.Physiol* **458**, 473
- Smith, G.L., Steele, D.S. and Crichton, C.A. (1992) Effects of inorganic phosphate on calcium tension. *Adv.Exp.Med.Biol.* **311**, 387-388.
- Smith, G.L. and Steele, D.S. (1998) Measurement of SR Ca²⁺ Content in the Presence of Caffeine in Permeabilised Rat Cardiac Trabeculae. *PflugersArch.-Eur.J.Physiol.* **623**, 1-9.
- Smith, G.L., Duncan, A.M., Neary, P., Bruce, L. and Burton, F.L. (2000) (Pi) inhibits the SR ca²⁺ pump and stimulates pump-mediated ca²⁺ leak in rabbit cardiac myocytes. *Am.J.Physiol.(Heart Circ.Physiol.)* **279**, H577-H585.
- Smith, J.B., Zheng, T. and Lyu, R.-M. (1989) Ionomycin Releases Calcium From The Sarcoplasmic Reticulum and Activates Na²⁺/Ca²⁺ exchange in Vascular Smooth Muscle Cells. *Cell Calcium* **10**, 125-134.
- Smith, J. S., Coronado, R. and Meissner, G. (1986) Single channel measurements of the calcium release channel from skeletal muscle sarcoplasmic reticulum. *J. Gen. Physiol.* **88**, 573-588.
- Smith, J.S., Imagawa, T., Ma, J., Fill, M., Campbell, K.P., Coronado, R. (1988) Purified ryanodine receptor from rabbit skeletal muscle is the calcium-release channel of sarcoplasmic reticulum. *J Gen Physiol.* **92**, 1-26.
- Snyder, S.H., Sabatini, D.M., Lai, M.M., Steiner, J.P., Hamilton, G.S. and Suzdak, P.D. (1998) Neural actions of immunophilin ligands. *Trends Pharmacol.Sci.* **19**, 21-26.
- Soler, F., Teruel, J.A., Fernandez-Belda, F. and Gomez-Fernandez, J.C. (1990) Characterization of the steady-state calcium fluxes in skeletal sarcoplasmic reticulum vesicles. Role of the Ca²⁺ pump. *Eur.J.Biochem.* **192**, 347-354.
- Spencer, C.M., Goa, K.L. and Gillis, J.C. (1997) Tacrolimus. An update of its pharmacology and clinical efficacy in the management of organ transplantation. *Drugs* **54**, 925-975.

- Steele, D.S. and Miller, D.J. (1992) Effects of cAMP and Forskolin on Caffeine-Induced Contractures and Myofilament Ca-Sensitivity in Saponin-Treated Rat Ventricular Trabeculae. *J.Muscle Res.Cell Mot.* **13**, 146-152.
- Steele, D.S., McAinsh, A.M. and Smith, G.L. (1995) Effects of Creatine Phosphate and Inorganic Phosphate on the Sarcoplasmic Reticulum of Saponin-Treated Rat Heart. *J.Physiol.* **483**, 155-166.
- Steele, D.S., McAinsh, A.M. and Smith, G.L. (1996) Comparative effects of inorganic phosphate and oxalate on uptake and release of Ca²⁺ by the sarcoplasmic reticulum in saponin skinned rat cardiac trabeculae. *J.Physiol.* **490.3**, 576
- Stern, M.D. (1992) Theory of Excitation-Contraction Coupling in Cardiac Muscle. *Biophys.J.* **63**, 497-517.
- Stern, M.D., Pizarro, G. and Rios, E. (1997) Local control model of excitation-contraction coupling in skeletal muscle. *J.Gen.Physiol.* **110**, 415-440.
- Stiles, M.K., Craig, M.E., Gunnell, S.L.N., Pfeiffer, D.R. and Taylor, R.W. (1991) The formation constants of Ionomycin with divalent cations in 80% methanol-water. *J.Biol.Chem.* **266**, 8336-8342.
- Stokes, D.L. and Wagenknecht, T. (2000) Calcium Transport Across the Sarcoplasmic Reticulum . *Eur.J.Biochem.* **267**, 5274-5279.
- Sun, X.H., Protasi, F., Takahashi, M., Takeshima, H., Ferguson, D.G. and Franzini-Armstrong, C. (1995) Molecular architecture of membranes involved in excitation-contraction coupling of cardiac muscle. *J.Cell Biology* **129**, 659-671.
- Sutko, J.L. and Airey, J.A. (1996) Ryanodine Receptors Ca²⁺ Release Channels: Does Diversity in Form Equal Diversity in Function? *Physiol.Rev.* **76** , 1027-1071.
- Sutko, J.L., Airey, J.A., Welch, W. and Ruest, L. (1997) The Pharmacology of Ryanodine and Related Compounds. *Pharmacol.Rev* **49**, 53-98.
- Szegedi, C., Sarkozi, S., Herzog, A., Jona, I. and Varsanyi, M. (1999) Calsequestrin: more than 'only' a luminal Ca²⁺ buffer inside the sarcoplasmic reticulum. *Biochem.J.* **337**, 19-22.
- Tada, M., Yamada, M., Ohmori, F., Kuzuya, T., Inui, M. and Abe, H. (1980) Transient State Kinetic Studies of Ca²⁺-dependent ATPase and Calcium Transport by Cardiac Sarcoplasmic

Reticulum: Effects of Cyclic AMP-dependent Protein Kinase-Catalysed Phosphorylation of Phospholamban. *J.Biol.Chem.* **255**, 1985-1992.

Takamatsu, T. and Wier, W.G. (1990) High temporal resolution video imaging of intracellular calcium. *Cell Calcium* **11**, 111-120.

Takasago, T., Imagawa, T., Furukawa, K., Ogurusu, T. and Shigekawa, M. (1991) Regulation of the cardiac ryanodine receptor by protein kinase-dependent phosphorylation. *J Biochem (Tokyo)*, **109**,163-70.

Takehisa H, Nishimura S, Matsumoto T, Ishida H, Kangawa K, Minamino N, Matsuo H, Ueda M, Hanaoka M, Hirose T, et al. (1989) Primary structure and expression from complementary DNA of skeletal muscle ryanodine receptor. *Nature*. **339**(6224), 439-45.

Tanaka, E., Kawai, M., Kurihara, S., Hotta, Y. and Soji, T. (1997) Effects of ruthenium red on the cellular functions and ultrastructure in intact ferret ventricular muscles. *Japanese J.Physiol.* **47**, 273-281.

Tanford, C. (1984) The Sarcoplasmic Reticulum Calcium Pump. *FEBS* **166**, 1-7.

Tanna, B., Welch, W., Ruest, L., Sutko, J.L. and Williams, A.J. (2000) The interaction of a neutral ryanoid with the ryanodine receptor channel provides insights into the mechanisms by which ryanoid binding is modulated by voltage. *J.Gen.Physiol.* **116**, 1-9.

Thastrup, O., Cullen, P.J., Drøbak, B.K., Hanley, M.R. and Dawson, A.P. (1990) Thapsigargin, a tumour promotor, discharges intracellular Ca²⁺ stores by specific inhibition of the endoplasmic reticulum Ca²⁺ -ATPase. *Proc.Natl.Acad.Sci.* **87**, 2466-2470.

Thomson, A.W., Bonham, C.A. and Zeevi, A. (1995) Mode of action of tacrolimus (FK506): molecular and cellular mechanisms. *Ther.Drug Monit.* **17**, 584-591.

Timerman, A.P., Ogunbunmi, E., Freund, E., Wiederrecht, G., Marks, A.R. and Fleischer, S. (1993) The calcium release channel of sarcoplasmic reticulum is modulated by FK-506-binding protein. Dissociation and reconstitution of FKBP-12 to the calcium release channel of skeletal muscle sarcoplasmic reticulum. *J.Biol.Chem.* **268**, 22992-22999.

Timerman, A.P., Jayaraman, T., Wiederrecht, G., Onoue, H., Marks, A.R. and Fleischer, S. (1994) The ryanodine receptor from canine heart sarcoplasmic reticulum is associated with a novel FK-506 binding protein. *Biochem Biophys Res Commun.* **198**, 701-706.

- Timmerman, A.P., Onoue, H., Xin, H.-B., Barg, S., Copello, J., Wiederrecht, G. and Fleischer, S. (1996) Selective Binding of FKBP12.6 by the Cardiac Ryanodine Receptor. *J.Biol.Chem.* **271**, 20385-20391.
- Tinker, A. and Williams, A. J. (1992) Divalent cation conduction in the ryanodine receptor-channel of sheep cardiac muscle sarcoplasmic reticulum. *J. Gen. Physiol.* **100**, 495-517.
- Toeplitz, B.K., Cohen, A.I., Funke, P.T., Parker, W.L. and Gougoutas, T.Z. (1979) Structure of ionomycin - a novel diacidic polyether antibiotic having high affinity for calcium ions. *J.Am.Chem.Soc.* **101**, 3344-3353.
- Tripathy, A., Xu, L., Mann, G. and Meissner, G. (1995) Calmodulin activation and inhibition of skeletal muscle Ca²⁺ release channel (ryanodine receptor). *Biophys.J.* **69**, 106-119.
- Tripathy, A. and Meissner, G. (1996) Sarcoplasmic reticulum luminal Ca²⁺ has access to cytosolic activation and inactivation sites of skeletal muscle Ca²⁺ release channel. *Biophys.J.* **70**, 2600-2615.
- Valdivia, H.H., Kaplan, J.H., Ellis-Davies, G.C.R. and Lederer, W.J. (1995) Rapid Adaptation of Cardiac Ryanodine Receptors: Modulation by Mg²⁺ and Phosphorylation. *Science* **267**, 1997-2000.
- Waas, W. and Hasselbach, W. (1981) Interference of Nucleoside Diphosphate and Inorganic Phosphate with Nucleoside-Trisphosphate-Dependent Calcium Fluxes and Calcium-Dependent Nucleoside-Trisphosphate Hydrolysis in Membranes of Sarcoplasmic-Reticulum Vesicles. *Eur.J.Biochem.* **116**, 601-608.
- Wagenknecht, T., Grassucci, R., Berkowitz, J., Wiederrecht, G.J., Xin, H.B. and Fleischer, S. (1996) Cryoelectron microscopy resolves FK506-binding protein sites on the skeletal muscle ryanodine receptor. *Biophys.J.* **70**, 1709-1715.
- Waku, K., Uda, Y. and Nakazawa, Y. (1971) Lipid composition in rabbit sarcoplasmic reticulum and occurrence of alkyl ether phospholipids. *J.Biochem.(Tokyo)* **69**, 483-491.
- Wang, E., Taylor, R.W. and Pfeiffer, D.R. (1998) Mechanism and specificity of lanthanide series cation transport by ionophores A23187, 4-BrA23187, and ionomycin. *Biophys.J.* **75**, 1244-1254.
- Wang, J.P., Needleman, D.H. and Hamilton, S.L. (1993) Relationship of low affinity [3]ryanodine binding sites to high affinity sites on the skeletal muscle Ca²⁺ release channel. *J.Biol.Chem.* **268**, 20974-20982.

- Weber, A. and Herz, R. (1968) The relationship between caffeine contracture of intact muscle and the effect of caffeine on reticulum. *J.Gen.Physiol.* **52**, 750-759.
- Weber, A. (1971) Regulatory mechanisms of the calcium transport system of fragmented rabbit sarcoplasmic reticulum. I. The effect of accumulated calcium on transport and adenosine triphosphate hydrolysis. *J.Gen.Physiol.* **57**, 50-63.
- Wendt, I.R. and Stephenson, D.G. (1983) Effects of caffeine on Ca-activated force production in skinned cardiac and skeletal muscle fibres of the rat. *Pflugers Arch.* **398**, 210-216.
- Wier, W.G., ter Keurs, H.E., Marban, E., Gao, W.D. and Balke, C.W. (1997) Ca²⁺ 'spatks' and waves in intact ventricular muscle resolved by confocal imaging. *Circ.Res.* **81**, 462-469.
- Wilkie, D.R. (1979) Generation of protons by metabolic process other than glycolysis in muscle cells. *J.Mol.Cell.Cardiol.* **11**, 325-330.
- Williams, A.J. and Ashley, R.H. (1989) Reconstitution of cardiac sarcoplasmic reticulum calcium channels. *Ann.NY Acad.Sci.* **560**, 163-173.
- Wimsatt, D.K., Hohi, C.M., Brierley, G.P. and Altschuld, R.A. (1990) Calcium Accumulation and Release by the Sarcoplasmic Reticulum of Digitonin-lysed Adult Mammalian Ventricular Cardiomyocytes. *J.Biol.Chem.* **265**, 14849-14857.
- Witcher, D. R., Kovacs, R.J., Schulman, H., Cefali, D.C. and Jones, L. R. (1991) Unique phosphorylation site on the cardiac ryanodine receptor regulates calcium channel activity. *J Biol Chem.* **266**, 11144-11152.
- Xu, A., Tripathy, A., Pasek, D.A. and Meissner, G. (1999) Ruthenium Red Modifies the Cardiac and Skeletal Muscle Ca²⁺ Release Channels (Ryanodine Receptors) By Multiple Mechanisms. *J.Biol.Chem.* **274**, 32680-32691.
- Yoshida, A., Takahashi, M., Imagawa, T., Shigekawa, M., Takisawa, H. and Nakamura, T. (1992) Phosphorylation of ryanodine receptors in rat myocytes during beta-adrenergic stimulation. *J Biochem (Tokyo)*. **111**, 186-90.
- Zacharova, D., Uhrík, B., Hencék, M., Lipskaja, E. and Pavelkova, J. (1990) Effects of ruthenium red on excitation and contraction in muscle fibres with Ca²⁺ electrogenesis. *Gen.Physiol.Biophys.* **9**, 545-568.

- Zhang, L., Kelley, J., Schmeisser, G., Kobayashi, Y.M. and Jones, L.R. (1997) Complex formation between junctin, triadin, calsequestrin, and the ryanodine receptor. Proteins of the cardiac junctional sarcoplasmic reticulum membrane. *J.Biol.Chem.* **272**, 23389-23397.
- Zhao, M., Li, P., Zhang, L., Winkfein, R.J. and Chen, S.R. (1999) Molecular identification of the ryanodine receptor pore-forming segment. *J.Biol.Chem.* **274**, 25971-25974.
- Zhong, L. and Inesi, G. (1998) Role of the S3 stalk segment in the thapsigargin concentration dependence of sarco-endoplasmic reticulum Ca^{2+} -ATPase inhibition. *J.Biol.Chem.* **273**, 12994-12998.
- Zhu, Y. and Nosek, T.M. (1992) Ruthenium red affects the contractile apparatus but not sarcoplasmic reticulum Ca^{2+} release of skinned papillary muscle. *Pflugers Arch.* **420**, 255-258.
- Zimanyi, I. and Pessah, I.N. (1991) Comparison of [3H]ryanodine receptors and Ca^{++} release from rat cardiac and rabbit skeletal muscle sarcoplasmic reticulum. *J Pharmacol Exp Ther.* **256**, 938-946.
- Zorzato, F., Fujii, J., Otsu, K., Phillips, M., Green, N. M., Lai, F. A., Meissner, G. and MacLennan, D. H. (1990) Molecular cloning of cDNA encoding human and rabbit forms of the Ca^{2+} release channel (ryanodine receptor) of skeletal muscle sarcoplasmic reticulum. *J Biol Chem.* **265**(4), 2244-56.
- Zorzato, F., Sacchetto, R. and Margreth, A. (1994) Identification of two ryanodine receptor transcripts in neonatal, slow-, and fast-twitch rabbit skeletal muscles. *Biochem Biophys Res Commun.* **203**, 1725-1730.
- Zucchi, R. and Ronca-Testoni, S. (1997) The Sarcoplasmic Reticulum Ca^{2+} Channel/Ryanodine Receptor: Modulation by Endogenous Effectors, Drugs and Diseased States. *Pharmacol.Rev* **49**, 1-51.

APPENDIX

P_i inhibits the SR Ca^{2+} pump and stimulates pump-mediated Ca^{2+} leak in rabbit cardiac myocytes

G. L. SMITH,¹ A. M. DUNCAN,¹ P. NEARY,² L. BRUCE,¹ AND F. L. BURTON²

¹Institute of Biomedical and Life Sciences, Glasgow University, Glasgow G12 8QQ; and

²Department of Medical Cardiology, Glasgow Royal Infirmary, Glasgow University, Glasgow G32 2ER, Scotland

Received 14 July 1999; accepted in final form 17 February 2000

Smith, G. L., A. M. Duncan, P. Neary, L. Bruce, and F. L. Burton. P_i inhibits the SR Ca^{2+} pump and stimulates pump-mediated Ca^{2+} leak in rabbit cardiac myocytes. *Am J Physiol Heart Circ Physiol* 279: H577-H585, 2000.—Measurements of sarcoplasmic reticulum (SR) Ca^{2+} uptake were made from aliquots of dissociated permeabilized ventricular myocytes using fura 2. Equilibration with 10 mM oxalate ensured a reproducible exponential decline of $[Ca^{2+}]$ from 600 nM to a steady state of 100–200 nM after addition of Ca^{2+} . In the presence of 5 μ M ruthenium red, which blocks the ryanodine receptor, the time course of the decline of $[Ca^{2+}]$ can be modeled by a Ca^{2+} -dependent uptake process and a fixed Ca^{2+} leak. Partial inhibition of the Ca^{2+} pump with 1 μ M cyclopiazonic acid or 50 nM thapsigargin reduced the time constant for Ca^{2+} uptake but did not affect the SR Ca^{2+} leak. Addition of 10 mM inorganic phosphate (P_i) decreased the rate of Ca^{2+} accumulation by the SR and increased the Ca^{2+} leak rate. This effect was reversed on addition of 10 mM phosphocreatine. 10 mM P_i had no effect on Ca^{2+} leak from the SR after complete inhibition of the Ca^{2+} pump. In conclusion, P_i decreases the Ca^{2+} uptake capacity of cardiac SR via a decrease in pump rate and an increase in Ca^{2+} pump-dependent Ca^{2+} leak.

cardiac; heart; sarcoplasmic reticulum; calcium; phosphate; calcium-adenosine 5'-triphosphatase; rabbit; inorganic phosphate

INTRACELLULAR INORGANIC PHOSPHATE concentration ($[P_i]$) increases to ~10 mM at the onset of hypoxia or ischemia in cardiac muscle (8, 26) and is accompanied by a rapid fall in contractility. Although other metabolic changes may occur at the same time (19, 33), the increased intracellular $[P_i]$ is thought to be a significant cause of reduced contractility within the first 1–2 min. P_i acts directly on the contractile proteins to reduce Ca^{2+} -activated force (13, 22). Furthermore, studies have shown that millimolar levels of P_i reduce the amount of Ca^{2+} available for release from the sarcoplasmic reticulum (SR) of cardiac muscle (37, 42), and these studies suggest that the inhibitory action of P_i on the SR may be an important

contributor to the rapid fall in contractility. P_i may inhibit SR function by actions within the SR lumen, on SR Ca^{2+} channels, or SR Ca^{2+} pumps. Fryer et al. (12) suggest that P_i may inhibit Ca^{2+} release from skeletal muscle SR by precipitating Ca^{2+} inside the SR lumen. But similar experiments on cardiac muscle failed to find evidence that precipitation limits SR Ca^{2+} release (39). It has been shown that P_i directly activates the cardiac ryanodine receptor and may increase Ca^{2+} efflux from the SR via this route (23). P_i may also activate a Ca^{2+} efflux pathway that is independent of the ryanodine receptor (39). Direct effects of P_i on the SR Ca^{2+} pump to reduce the Ca^{2+} sensitivity of Ca^{2+} uptake was suggested by work on cardiac SR vesicles (25), but that study demonstrated that P_i -induced increase of Ca^{2+} uptake was also possible. Alternatively, P_i may reduce only the maximum uptake capacity (41). That P_i can cause reversal of skeletal and cardiac SR Ca^{2+} pumps has been demonstrated amply in SR vesicle preparations (15, 40). Under these circumstances, Ca^{2+} efflux via the Ca^{2+} pump is linked to ATP synthesis from ADP and P_i . However, although evidence exists to suggest that Ca^{2+} pump reversal may limit the maximum Ca^{2+} content of cardiac muscle SR (35), P_i -induced pump reversal has not been demonstrated directly in native SR at concentrations of P_i , ATP, Mg, and pH normally observed in the early stages of hypoxia and ischemia.

The purpose of this study was to examine the effects of P_i on Ca^{2+} fluxes across cardiac SR membrane under conditions where both Ca^{2+} precipitation by P_i and Ca^{2+} leak via the ryanodine receptor are prevented. The actions of P_i are compared with those of specific Ca^{2+} pump inhibitors and a Ca^{2+} ionophore (ionomycin). The results show that P_i decreases the SR Ca^{2+} uptake rate and activates a Ca^{2+} leak from the SR. P_i -induced Ca^{2+} leak from the SR was not present when the SR Ca^{2+} pump was inhibited by thapsigargin. Possible mechanisms linking P_i -induced Ca^{2+} pump inhibition to activation of a Ca^{2+} leak are discussed.

Address for reprint requests and other correspondence: G.L. Smith, Institute of Biomedical and Life Sciences, West Medical Bldg., Univ. of Glasgow, Glasgow G12 8QQ, Scotland (E-mail: g.smith@bio.gla.ac.uk).

The costs of publication of this article were defrayed in part by the payment of page charges. The article must therefore be hereby marked "advertisement" in accordance with 18 U.S.C. Section 1734 solely to indicate this fact.

METHODS

Cell isolation. New Zealand White rabbits (2.5–3.0 kg) were given an intravenous injection of 500 U heparin together with an overdose of pentobarbital sodium (100 mg/kg). Isolated hearts were perfused retrogradely (25 ml/min, 37°C) with a nominally Ca^{2+} -free Krebs-Henseleit solution for 10 min. This was followed by perfusion for 10–17 min with recirculated Krebs-Henseleit solution supplemented with 0.6 mg/ml collagenase (type 1, Worthington Chemical), 0.1 mg/ml protease (type XIV, Sigma), and 80 μM CaCl_2 . The left ventricular free wall was isolated and incubated separately for 5 min in enzyme solution containing 80 μM CaCl_2 and 4% bovine serum albumin (BSA, fraction V, Sigma). The cell suspensions obtained at the end of the incubation period were filtered into Krebs-Henseleit solution without added Ca^{2+} . This procedure routinely produced a 80–90% yield of rod-shaped myocytes. Myocyte concentration was determined by use of a hemocytometer. Cells were lightly centrifuged (2 g for 1 min), and the supernatant was replaced with a mock intracellular solution. This procedure was repeated three times, and the cells were resuspended in a mock intracellular solution to give a final concentration of 5×10^6 cells/ml.

Cell permeabilization and fluorescence measurements. A 0.3-ml aliquot of cell suspension was exposed to 0.1 mg/ml β -escin (Sigma) and gently stirred for 1 min. The β -escin was removed by centrifuging and resuspending the cells in mock intracellular solution. The cells were then placed in a cuvette, and further solutions were added to give a final volume of 1.5 ml containing 5 mM ATP, the mitochondrial inhibitors carbonyl cyanide (20 μM) and oligomycin (20 μM , Calbiochem), 10 mM oxalate (Sigma), 5 μM ruthenium red (Sigma), and 10 μM fura 2 (Molecular Probes). Cells were maintained in suspension by gentle stirring, and the fura 2 fluorescence within the cuvette was recorded at 30 Hz with a spinning wheel spectrophotometer (Cairn Research). All experiments were done at room temperature (20–22°C).

Solution composition and calibration of fura 2 fluorescence signal. A mock intracellular solution was used to mimic the intracellular environment. It had the following composition (in mM): 130 K^+ , 10 Na^+ , 1 Mg^{2+} , 25 HEPES, 140 Cl^- , and 0.05 EGTA; pH 7.0. Solutions to measure the maximum and minimum fluorescence ratios (R_{max} and R_{min}) and the affinity constant of fura 2 contained 10 mM EGTA, 5 mM ATP, 5 μM ruthenium red, and permeabilized cells (at a concentration of 1×10^6 cells/ml). The presence of cells at this concentration did not affect these values. The equilibrium concentrations of metal ions in the calibration solutions were calculated by means of a computer program with the affinity constants for H^+ , Ca^{2+} , and Mg^{2+} for EGTA (taken from Ref. 36). The affinity constants used for ATP and creatine phosphate (CrP) were those quoted by Fabiato and Fabiato (9). Corrections for ionic strength, details of pH measurement, allowance for EGTA purity, and the principles of the calculations are detailed elsewhere (30). Free Mg^{2+} concentration was 0.9–1.0 mM in all solutions. Under the conditions used in this study, the apparent affinity constant of fura 2 for Ca^{2+} was 110 ± 20 nM, and the buffer value (β) was 14.0 ± 0.1 , values close to that measured by Grynkiewicz et al. (14) and as noted by Kargacin et al. (21). As described above, ruthenium red was used to block Ca^{2+} leak via the ryanodine receptor, and initial experiments determined that the block achieved with 5 μM was complete, and higher concentrations (20 μM) provided no further block. However, the 20 μM concentration was not used in this study, because previous work suggested that at this concentration, ruthenium red reduced cardiac SR

Ca^{2+} pump activity (2, 11, 20). Furthermore, ruthenium red quenches the fluorescence signal from fura 2 (20). However, at 5 μM ruthenium red, the quench appeared to affect the fluorescence at both excitation wavelengths equally, with no effect on the values of the dissociation constant K_d and β . Ca^{2+} uptake measurements were made by resuspending the cells in a solution of the following composition (in mM): 120 KCl, 5 Na_2ATP , 5.4 MgCl_2 , 25 HEPES, 0.05 K_2EGTA , 0.02 carbonyl cyanide *m*-chlorophenylhydrazone, 0.02 oligomycin, 10 K_2 -oxalate, 0.005 ruthenium red, and 0.01 fura 2; pH 7.0. Addition of 10 mM P_i was accompanied by 0.25 mM MgCl_2 . The added Mg ensured that free Mg^{2+} levels remained between 0.9 and 1.0 mM in the mock intracellular solution.

Data recording and analysis. The fluorescence ratio signal and the individual 340- and 380-nm wavelength signals were low-pass filtered (-3dB at 30 Hz) and digitized at 10 Hz for later analysis. Sections of the trace were converted to plots of $[\text{Ca}^{2+}]$ against time. Fitting of $[\text{Ca}^{2+}]$ decay curves to Eq. 3 (Fig. 1C) and linear increases were performed with Origin (Version 5.0, Microcal). SR uptake rate constant (k) and leak rate (l) are expressed with the asymptotic standard error-computed error of the parameter (a measure of the uncertainty of the parameter estimate). Where appropriate, curve fits were compared using an *F*-test, based on the sum-of-squares (SSQ) difference between the fitted curve and data values. Changes in k and l are calculated relative to the preceding control value. Changes in these parameters are expressed as means \pm SE. *t*-Tests were used to compare the relative changes; $P < 0.05$ was considered statistically significant.

RESULTS

Ca^{2+} uptake and release from oxalate-equilibrated permeabilized cardiac myocytes. Figure 1A shows a typical trace of $[\text{Ca}^{2+}]$ recorded from a cell suspension. Addition of an aliquot of CaCl_2 (10 μl of 10 mM) increases the total $[\text{Ca}^{2+}]$ within the cuvette by 67 μM and causes a rapid increase of the free $[\text{Ca}^{2+}]$ to ~ 0.8 μM . Over the next 10 min, the $[\text{Ca}^{2+}]$ decayed to below 100 nM. This procedure could be repeated up to five times before changes in the time course of the decay became detectable. Addition of thapsigargin (20 μM) caused an increase in the $[\text{Ca}^{2+}]$ within the cuvette, representing Ca^{2+} leak from the SR in the absence of an active Ca^{2+} uptake process. The rise of $[\text{Ca}^{2+}]$ after thapsigargin was approximately linear below 600 nM; above this value, the rate of leak decreased. On further addition of Ca^{2+} , there was no evidence for SR Ca^{2+} uptake (results not shown). High concentrations of thapsigargin (20 μM) were used to ensure effective inhibition of Ca^{2+} pump activity. This thapsigargin concentration was equivalent to 20 nmol/mg total cell protein. Previous work (17) has shown complete pump inhibition at 1–10 nM/mg total protein. A higher concentration of thapsigargin (50 μM) produced no further increase in the rate of Ca^{2+} leak from the SR (not shown). In all cases, the rise of $[\text{Ca}^{2+}]$ after high concentrations of thapsigargin (>1 μM ; $n = 11$) and cyclopiazonic acid (CPA) (>100 μM ; $n = 4$) was initially linear up to 650–700 nM. At 600 nM, the $[\text{Ca}^{2+}]$ was still within the standard error of the best-fit linear relationship in all 11 experiments. This remained the case in 9 of the 11 experiments at 650 nM and in 5 of

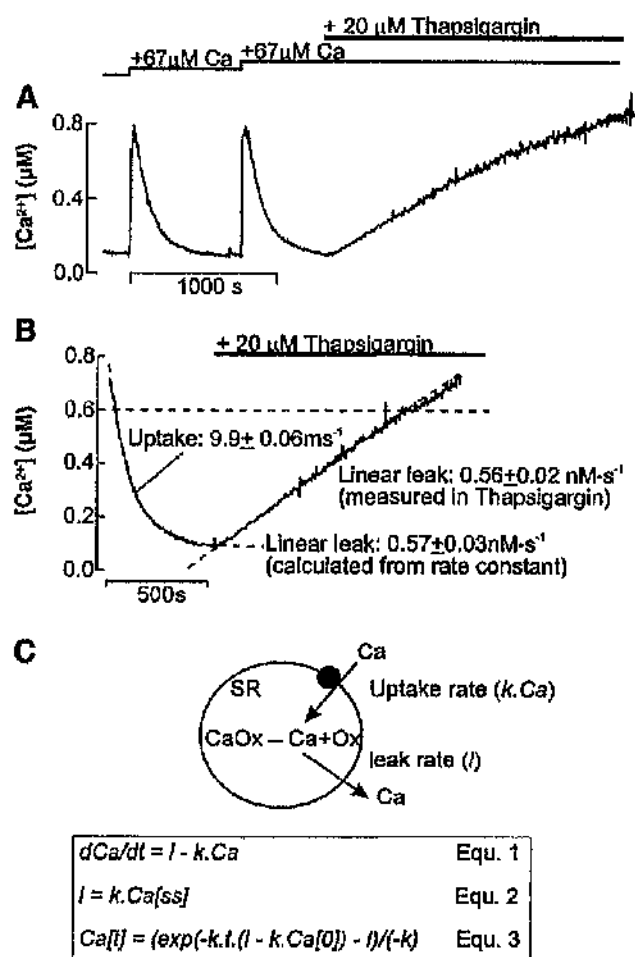


Fig. 1. A: records of $[Ca^{2+}]$ against time recorded from a cuvette containing 1.5 ml 1×10^6 /ml permeabilized myocytes suspended in mock intracellular solution by continuous stirring equilibrated with 10 mM oxalate. Additions of aliquots of $CaCl_2$ are indicated above the trace as increases in total $[Ca^{2+}]$ within the cuvette. Thapsigargin (20 μ M) was added at the point indicated. B: the record of $[Ca^{2+}]$ from a section of the trace shown in (A). The broken line through the decay phase indicates the best-fit single exponential curve to the record from 600 nM to the steady state. The broken line through the trace after addition of thapsigargin represents the best-fit straight line to the record \leq 600 nM. Values of rate constant and calculated and measured leak rate are shown on the record. C: a simplified model of the sarcoplasmic reticulum (SR) with Ca^{2+} pump and Ca^{2+} leak indicated. Ca^{2+} chelation/precipitation within the SR lumen is also indicated (CaOx). Below the diagram are equations describing the role of Ca^{2+} leak and uptake in determining the rate of change of cytosolic $[Ca^{2+}]$ (Eq. 1) and the time course of change in $[Ca^{2+}]$ from a starting $[Ca^{2+}]$ ($Ca[0]$). [SS], Steady state; t , time.

the 11 experiments at 700 nM. For this reason, 600 nM was taken as the maximum $[Ca^{2+}]$ for the subsequent pump leak modeling.

A section of the record in Fig. 1A is expanded in Fig. 1B to illustrate the time course of the decay of $[Ca^{2+}]$ and the increase of $[Ca^{2+}]$ on addition of thapsigargin. The broken line shown passing through the decay of $[Ca^{2+}]$ is the best-fit single exponential decay with a

rate constant of 9.9 ± 0.06 m/s (see figure legend) and a steady-state $[Ca^{2+}]$ of 105 nM. The addition of thapsigargin caused an immediate increase in $[Ca^{2+}]$ within the cuvette with an approximately linear time course (100–600 nM) at a rate of 0.56 nM/s. Figure 1C shows a schematic of the Ca^{2+} uptake and release pathways in a simplified model of cardiac SR, where the rate of Ca^{2+} uptake by the SR is determined by the cytosolic $[Ca^{2+}]$ alone ($k \times [Ca^{2+}]$). The leak of Ca^{2+} from the SR (in the absence of ryanodine receptor activity) is expressed as a constant value (l). Therefore, at any time, the rate of change of $[Ca^{2+}]$ outside the SR (dCa/dt) is determined by the relative rates of these two processes (Eq. 1). In the steady state, i.e., when $dCa/dt = 0$, the leak and uptake rates are equal (Eq. 2). Integrating Eq. 1 generates an expression that describes the variation of $[Ca^{2+}]$ with time (Eq. 3). Fitting the time course of the decay of $[Ca^{2+}]$ below 600 nM with Eq. 3, the values for SR Ca^{2+} uptake rate constant (k) and linear leak rate (l) can be calculated. The calculated leak rate (0.57 nM/s) was close to the values measured after addition of thapsigargin (0.56 nM/s). These measurements suggest that below 600 nM, the characteristics of Ca^{2+} uptake and release by cardiac SR is accurately modeled by the simplified model of SR Ca^{2+} fluxes shown in Fig. 1C. In this study, the average background leak rate varied between 0.5 and 1.5 nM/s (mean 1.03 ± 0.09 nM/s, $n = 15$). Despite this interexperiment variation, the leak rate-measured thapsigargin was not significantly different from the calculated values ($103 \pm 2\%$, $n = 7$). The reason for the variation in background leak is unknown, but factors such as percentage of rod-shaped cells within the aggregate preparation may be important. These measurements also strongly suggest that, under control conditions, there is no significant SR-dependent Ca^{2+} leak from the SR.

Pharmacological alterations of SR Ca^{2+} uptake and leak characteristics. Figure 2 shows the effects of partial inhibition of the pump on the calculated uptake and leak rate constants. Figure 2A shows two Ca^{2+} uptake curves superimposed, one before (control) and one after addition of a submaximal dose of thapsigargin (50 nM), a value that would be expected to approximately halve the rate of Ca^{2+} uptake by the SR Ca^{2+} pump (17). The rate of fall of $[Ca^{2+}]$ was slower, and the steady state $[Ca^{2+}]$ higher, in the presence of thapsigargin. Fitting this individual decay to Eq. 3 (Fig. 1C) indicates that the rate constant for Ca^{2+} uptake was approximately one-half of the control value. However, the calculated leak rate constant was not significantly different from control. Figure 2B shows curves and fitted model parameters to the decay of $[Ca^{2+}]$ before and after adding 1 μ M CPA. As with thapsigargin, partial inhibition of the pump reduced the Ca^{2+} uptake rate constant by $\sim 50\%$ but caused no significant change in the leak rate. Figure 2C shows the effects of addition of the Ca^{2+} ionophore ionomycin (1 μ M). The best-fit Ca^{2+} uptake rate constant was not altered, but the higher steady-state $[Ca^{2+}]$ was modeled by an increased leak rate. These results are consistent with

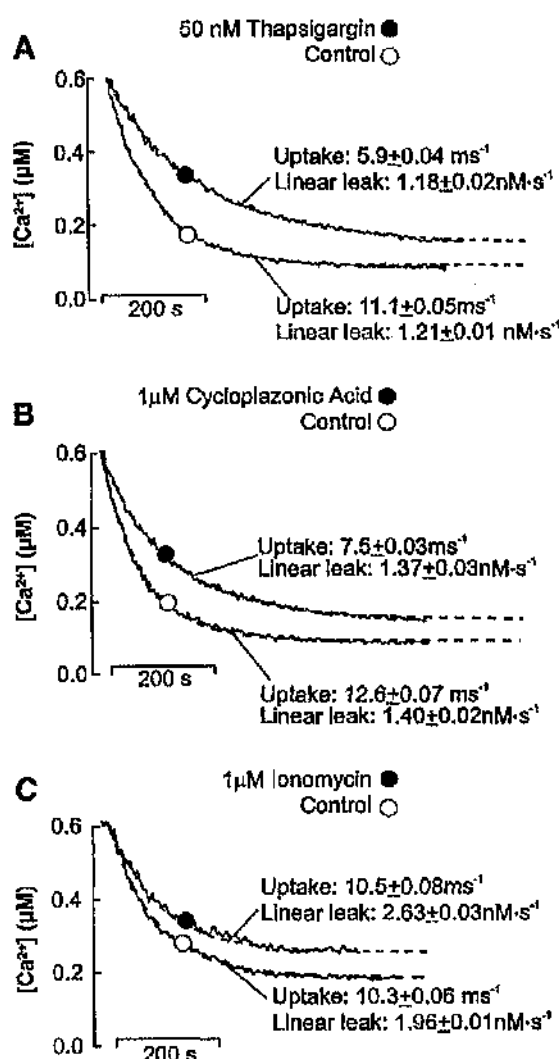


Fig. 2. Effects of thapsigargin (A), cyclopiazonic acid (B), and ionomycin (C) on the time course of decay of $[\text{Ca}^{2+}]$ in oxalate-equilibrated permeabilized cardiac myocytes. In each panel, the broken lines indicate the best fit to Eq. 3 (Fig. 1C) with a starting $[\text{Ca}^{2+}]$ ($[\text{Ca}(0)]$) of 600 nM. The uptake rate (k) and leak (l) associated with each curve are shown.

the simplified model for Ca^{2+} uptake and release proposed in this study and indicate that SR Ca^{2+} uptake is normally independent of Ca^{2+} leak.

Effects of P_i on Ca^{2+} uptake and leak rate constants. Figure 3A shows a continuous record of $[\text{Ca}^{2+}]$ from permeabilized cell aggregates during repetitive additions of Ca^{2+} . The addition of 10 mM P_i to the cuvette solution caused a small increase in steady-state $[\text{Ca}^{2+}]$. On subsequent addition of Ca^{2+} , the rate of decay was slower, and the steady-state $[\text{Ca}^{2+}]$ was increased. Addition of 10 mM CrP caused a fall in the steady-state $[\text{Ca}^{2+}]$, and upon subsequent addition of Ca^{2+} , the rate of Ca^{2+} uptake and the steady-state $[\text{Ca}^{2+}]$ were restored to values close to the control values. In Fig. 3B,

left, the Ca^{2+} decay curves before and after addition of P_i are superimposed. After addition of P_i , a decrease in the Ca^{2+} uptake rate constant and an increase in the leak are required to provide an accurate fit to the Ca^{2+} decay. The sensitivity of the decay curve to the fitted parameters is shown in Fig. 3B, right. The trace is the recorded time course of Ca^{2+} uptake in 10 mM P_i . The curve lying mainly above the trace is the best fit generated with the Ca^{2+} uptake rate fixed at the control value (i.e., only the leak rate was allowed to vary). The curve lying mainly below the trace is the best fit generated with the leak rate fixed at the control value (i.e., only the Ca^{2+} uptake rate was allowed to vary). Comparison of SSQ from these curves with that from the more complex model in which both uptake rate and leak were allowed to vary (Fig. 3B, left) indicated that the more complex model fit the data significantly better ($P < 0.001$). This suggests that both increased leak and uptake rates are necessary to explain the effects of 10 mM P_i . Experiments were done to examine the effects of 1 mM P_i . No significant effect of this lower concentration of P_i on either uptake rate or leak was observed; the mean values of these measurements are shown below.

Figure 3C shows the three uptake curves superimposed to illustrate the time course of Ca^{2+} uptake after addition of 10 mM CrP. The rate of Ca^{2+} uptake is greater and the steady-state $[\text{Ca}^{2+}]$ is lower than control and 10 mM P_i record. Furthermore, in the presence of CrP, the decay of $[\text{Ca}^{2+}]$ had more than one exponential component and was poorly fitted by a single exponential decay. Despite the poor fit, a similar leak-uptake analysis was performed in the presence of CrP. On average, the rate constant for uptake increased to $124 \pm 2\%$ ($n = 6$) and the steady-state $[\text{Ca}^{2+}]$ decreased to $89 \pm 5\%$ of control values on addition of 10 mM CrP, but calculated leak was unchanged ($102 \pm 0.4\%$).

Figure 4 shows the averaged relative change in uptake rate constant and leak rate after addition of CPA, thapsigargin, ionomycin, and P_i (1 and 10 mM). CPA and thapsigargin reduced the uptake rate constant to $\sim 60\%$ (Fig. 4A). Neither agent altered the leak significantly, although a small decrease was observed in both cases (Fig. 4B). The uptake rate constant was unaffected by ionomycin, but the leak rate was increased to $\sim 130\%$ of control values. As described above, 1 mM P_i had no significant effect on uptake or leak rate. 10 mM P_i caused a significant decrease in the uptake rate constant to $79 \pm 1.2\%$ ($P < 0.05$) and increased the leak rate to $117 \pm 0.6\%$ of control levels ($P < 0.05$).

P_i does not affect the rate of Ca^{2+} uptake in the presence of CrP. Figure 3, A and C, show that addition of CrP (10 mM) effectively reversed the effects of P_i on the SR. Another important aspect of this effect is shown in Fig. 5. Addition of 10 mM to the medium (in the absence of P_i) caused a significant increase in the rate constant and a decrease in steady-state $[\text{Ca}^{2+}]$, i.e., the effect of CrP was not dependent on the presence of 10 mM P_i . Of direct relevance to this study was the subsequent lack of effect of P_i on the rate of decay

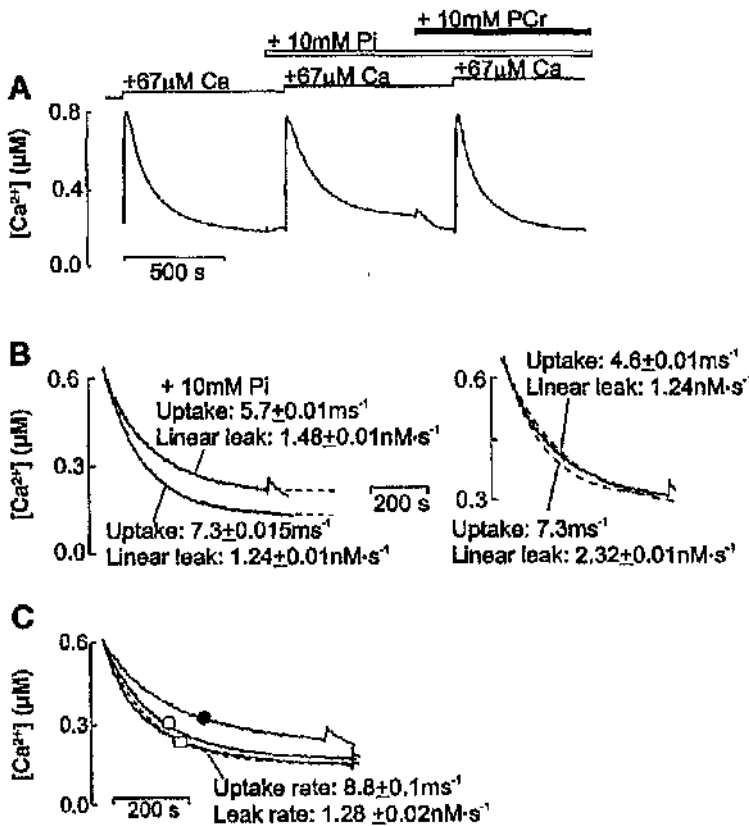


Fig. 3. *A*: records of $[Ca^{2+}]$ against time recorded from a cuvette containing 1.5 ml 1×10^9 /ml permeabilized myocytes suspended in mock intracellular solution (with 10 mM oxalate). Additions of aliquots of $CaCl_2$ are indicated above the trace as increases in total $[Ca^{2+}]$ within the cuvette. P_i (10 mM) and creatine phosphate (CrP, 10 mM) were added at the points indicated. *B*, left, shows the superimposed records of the decay of $[Ca^{2+}]$ from 600 nM. The broken line through each Ca^{2+} decay indicates the best-fit single exponential curve; the associated parameters of uptake rate and leak are shown beside each curve. Sum-of-squares (SSQ) values for the fit were the following: control, 4.20×10^{-16} ; 10 mM P_i , 5.12×10^{-15} . *B*, right, shows the decay of $[Ca^{2+}]$ recorded in the presence of 10 mM P_i . The two broken lines represent 1) a best-fit curve calculated by fixing the Ca^{2+} uptake rate at the control value (7.3 ms/s) and allowing the leak rate to be adjusted (SSQ = 3.2×10^{-15}) and 2) a best-fit curve calculated by fixing the leak rate at the control value (1.24 nM/s) and allowing the Ca^{2+} uptake rate to be adjusted (SSQ = 5.6×10^{-14}). *C*: superimposed records of the decay of $[Ca^{2+}]$ from 600 nM for the control (○), 10 mM P_i (●), and 10 mM P_i /10 mM CrP (□). The broken line is the best-fit curve to the latter curve; the uptake and leak rates are indicated.

of $[Ca^{2+}]$ in the continued presence of CrP. This is highlighted in Fig. 5*B*, where the decay curves before and after P_i are superimposable. Thus P_i had no discernible effects on SR Ca^{2+} fluxes in the presence of CrP.

Sensitivity of P_i -induced SR Ca^{2+} leak to thapsigargin. To test whether 10 mM P_i could increase the SR leak rate after Ca^{2+} pump inhibition, the effect of P_i was studied in the presence of a high concentration of thapsigargin. As shown in Fig. 6*A*, 10 mM P_i had no obvious effect on the background SR Ca^{2+} leak rate revealed by the addition of 20 µM thapsigargin. The best-fit straight lines through the record before and after addition of P_i have gradients that are not different. Addition of 1 µM ionomycin significantly increased the rate of loss of Ca^{2+} from the SR. On average, the background leak of Ca^{2+} in 10 mM P_i was $101 \pm 1.4\%$ ($n = 4$) of the control value in the presence of 20 µM thapsigargin. This suggests that 10 mM P_i induces a Ca^{2+} leak from the SR that is dependent on a functional Ca^{2+} pump. It follows that, in the continued presence of P_i , the SR pump serves as a route for Ca^{2+} leak and uptake; therefore, submaximal doses of thapsigargin should reduce leak and uptake rates (assuming the drug has equal ability to inhibit the SR Ca^{2+} pump in leak and uptake mode). To test this hypothesis, Ca^{2+} uptake and leak were assessed before and after partial pump inhibition by thapsigargin (50 nM)

in the continued presence of 10 mM P_i (Fig. 6*B*). Under these circumstances, 50 nM thapsigargin slowed the rate of Ca^{2+} uptake by the SR, but unlike in Fig. 2*A*, there was only a limited increase in steady-state $[Ca^{2+}]$. According to the model, 50 nM thapsigargin significantly decreased the rate of Ca^{2+} uptake and decreased the leak rate. On average, 50 nM thapsigargin did not change the steady-state $[Ca^{2+}]$ ($103 \pm 3\%$; $n = 6$), but it reduced the Ca^{2+} uptake rate constant to $68 \pm 4\%$ of the control value and leak rate to $72 \pm 3\%$ ($n = 6$) in the presence of 10 mM P_i .

DISCUSSION

Quantification of Ca^{2+} uptake and leak pathways in permeabilized cardiac myocytes. The experiments described in this study were designed to investigate the direct effects of P_i on SR Ca^{2+} pump function. For this reason, the experimental conditions were arranged to minimize any indirect effects that would complicate analysis. Modulation of SR pump activity via low-affinity Ca^{2+} binding sites within the SR has been previously demonstrated in SR vesicles from cardiac and skeletal muscle (18). P_i is known to enter the SR and, under some conditions, chelate and/or precipitate luminal Ca^{2+} , and in doing so, it may indirectly affect Ca^{2+} pump activity. To prevent this, these experiments were done in the presence of 10 mM oxalate.

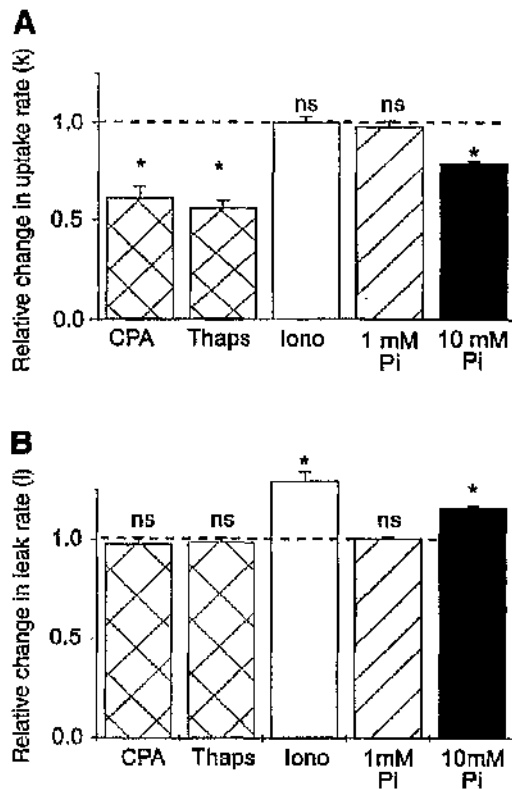


Fig. 4. Relative change in uptake rate (A) and leak rate (B) in 10 μ M cyclopiazonic acid (CPA), 50 nM thapsigargin (Thaps), 10 μ M ionomycin (Iono), and 1 mM and 10 mM P_i . Values are expressed as means \pm SE. *Significant difference from control ($P < 0.05$; $n = 6$); ns, no significant difference.

Previous studies (e.g., Ref. 5) have shown that in the presence of both oxalate and P_i , only Ca-oxalate precipitates are formed when the ratio of [oxalate] to [P_i] is < 2 . Ruthenium red (5 μ M) ensures that Ca^{2+} leak via the ryanodine receptor was inhibited (11, 28, 29). Under these conditions, the steady-state [Ca^{2+}] in this system (1.0×10^6 cells/ml) was normally between 100 and 150 nM, a value that represents a balance between a background Ca^{2+} leak from the SR and a maintained Ca^{2+} uptake. Addition of aliquots of the Ca^{2+} caused an initial increase in [Ca^{2+}], which decreased over the subsequent 5–10 min to the same steady state. The time course of the decrease in [Ca^{2+}] from 600 nM to the steady state followed a single exponential decay, suggesting that over this range of [Ca^{2+}] (between 600 and 100 nM), the rate of Ca^{2+} uptake is a function of [Ca^{2+}]. This is a simplification of the Ca^{2+} dependence of SR Ca^{2+} uptake anticipated on the basis of the known stoichiometry and affinity of the pump for Ca^{2+} in permeabilized rabbit myocytes [2 Ca^{2+} with an affinity of $\sim 0.3 \mu$ M (17, 21)]. The alteration in time course of Ca^{2+} uptake by CrP suggests that this metabolite may alter the affinity and/or the stoichiometry of the SR Ca^{2+} pump and is discussed in more detail below.

Inhibition of the SR Ca^{2+} pump by high concentrations of thapsigargin caused a gradual increase in [Ca^{2+}] within the cuvette, representing a background Ca^{2+} leak from the SR. When [Ca^{2+}] was below 600 nM, the increase in [Ca^{2+}] had an approximately linear time course, suggesting that luminal [Ca^{2+}] is considerably higher than the cytosolic values. Equilibration of the permeabilized myocytes with oxalate ensures a constant luminal [Ca^{2+}] determined by the solubility product of calcium oxalate (5, 27). Based on this, one would predict that the luminal [Ca^{2+}] would be unable to increase above $\sim 10 \mu$ M in the presence of 10 mM oxalate. The nature of the background Ca^{2+} leak from cardiac SR is unknown, but previous measurements suggest that the leak depends simply on the trans-SR [Ca^{2+}] gradient [reviewed in (10)]. Assuming that oxalate-equilibrated SR would act as a reservoir for Ca^{2+} , a constant background leak would generate a rise of [Ca^{2+}] that approached the SR luminal [Ca^{2+}] asymptotically. Over a sufficiently limited range of [Ca^{2+}] (between 100 and 600 nM), this Ca^{2+} leaks from the SR at a rate of ~ 1 nM/s (per 10^6 cells). This rate reflects a resting Ca^{2+} permeability of the SR (with a luminal [Ca^{2+}] of $\sim 10 \mu$ M). This leak is not limited by the dissociation of Ca^{2+} from oxalate, because increasing the Ca^{2+} permeability of the SR (with ionomycin) markedly increases the rate of Ca^{2+} leak.

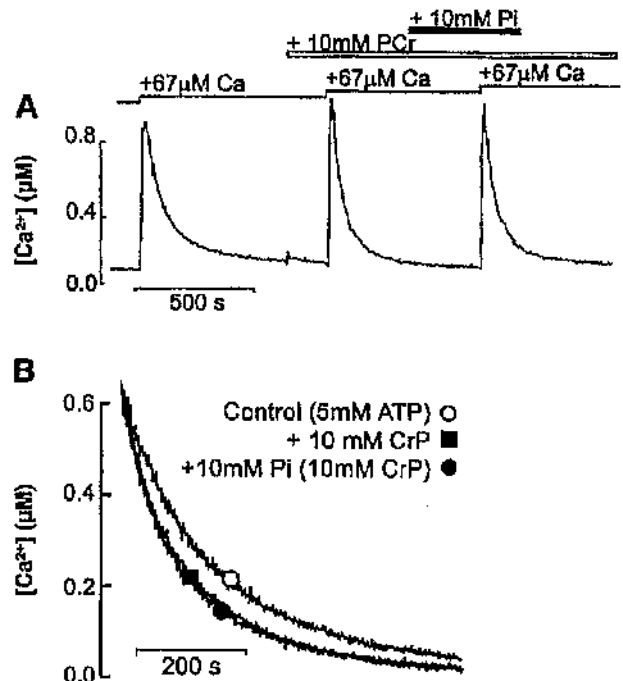


Fig. 5. A: records of [Ca^{2+}] against time recorded from a cuvette containing 1.5 ml 1×10^6 /ml permeabilized myocytes suspended in mock intracellular solution (with 10 mM oxalate). Additions of aliquots of $CaCl_2$ are indicated above the trace as increases in total [Ca^{2+}] within the cuvette. CrP (10 mM) and P_i (10 mM) were added at the points indicated. B: the superimposed records of the decay of [Ca^{2+}] from 600 nM.

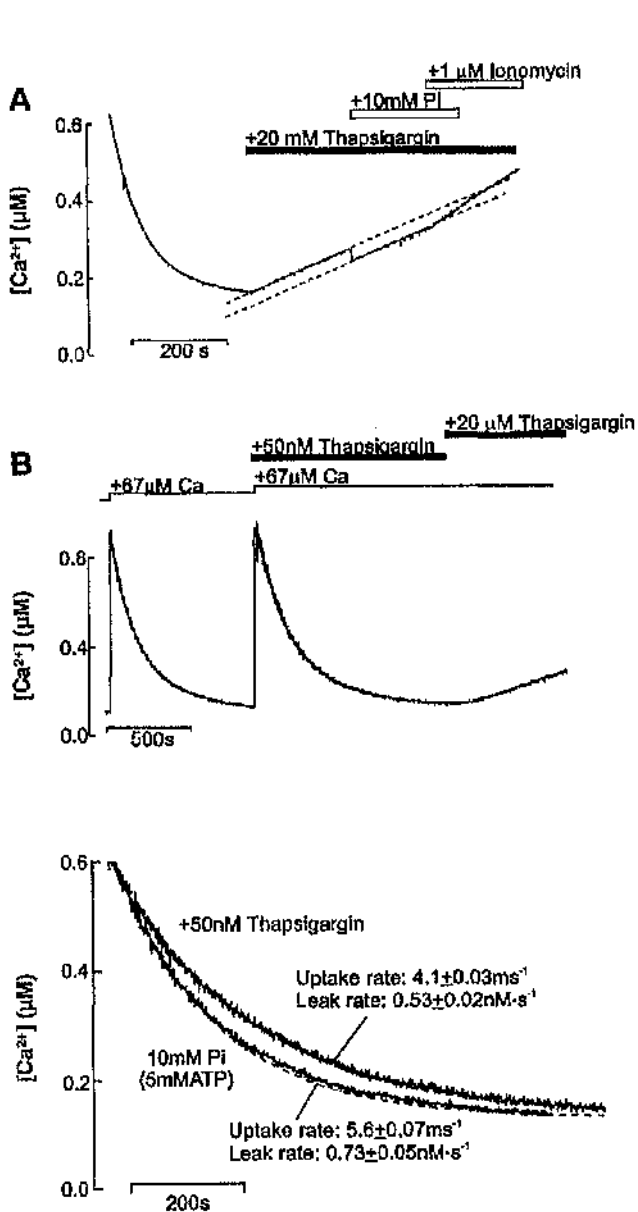


Fig. 6. A: records of $[Ca^{2+}]$ against time recorded from a cuvette containing 1.5 ml $1 \times 10^6/ml$ permeabilized myocytes suspended in mock intracellular solution (with 10 mM oxalate). Bars indicate when 20 μM thapsigargin, 10 mM P_i , and 1 μM ionomycin were added at the points indicated. The broken lines are the best-fit linear regression lines to the last 120 s before and the first 120 s after addition of P_i . B: top, records of $[Ca^{2+}]$ against time recorded from a cuvette containing 1.5 ml $1 \times 10^6/ml$ permeabilized myocytes suspended in mock intracellular solution (with 10 mM oxalate) in the continuous presence of 10 mM P_i . Additions of aliquots of $CaCl_2$ are indicated above the trace as increases in total $[Ca^{2+}]$ within the cuvette. Thapsigargin (50 nM and 20 μM) was added at the points indicated. Bottom, the superimposed records of the decay of $[Ca^{2+}]$ from 600 nM in 5 mM ATP/10 mM P_i and after addition of 50 nM thapsigargin. The broken lines are the best-fit curves to the individual decays with the associated uptake and leak rates.

Limitations of the method of analysis of SR Ca^{2+} flux. The model of the SR, expressed as equations in Fig. 1C, suggests that knowledge of the rate constant for Ca^{2+} uptake and the steady-state $[Ca^{2+}]$ is sufficient to estimate the Ca^{2+} leak rate. It should be emphasized that this method of analysis is valid only for the experimental conditions used in this study. The range of $[Ca^{2+}]$ studied must be in the range (between 200 and 600 nM) in which SR Ca^{2+} uptake is linear for forward transport via the SR Ca^{2+} pump. Furthermore, the $[Ca^{2+}]$ within the SR lumen must be constant; this ensures that the activity of the SR Ca^{2+} pump is not modulated by changes in $[Ca^{2+}]$ within the SR lumen. In addition to this, a constant SR $[Ca^{2+}]$ will ensure a constant passive leak, thus simplifying this aspect of the analysis. One further simplification inherent in this model is the neglect of Ca^{2+} buffering by the cells and constituents of the bathing solution. The Ca^{2+} binding properties of permeabilized cardiac myocytes have been studied in detail (16). These measurements suggest that the presence of myocytes ($10^6/ml$) would bind $\sim 0.1 \mu M$ Ca^{2+} at 600 nM $[Ca^{2+}]$. EGTA (50 μM) and fura 2 (10 μM) provide additional buffering with minor contributions from ATP and oxalate. Under the conditions of this study, these buffers would provide an approximately constant Ca^{2+} buffer within the range between 100 and 600 nM. In terms of the calculation of Ca^{2+} fluxes, buffering would have an identical scaling effect on both uptake and leak pathways and can therefore be ignored for the current purposes.

Pharmacological alterations of SR Ca^{2+} uptake and leak characteristics. The validity of this model was tested by selective inhibition of the Ca^{2+} pump with CPA and thapsigargin. Both agents are specific inhibitors of sarco(endo)plasmic reticulum Ca^{2+} pumps in muscle and nonmuscle cells (4, 34). At submaximal concentrations, these agents reduced the rate constant of Ca^{2+} uptake by the SR (17). Using the uptake-leak analysis shown in Fig. 1C, the calculated leak after partial inhibition of the pump was not significantly different from control values. This suggests that, in the absence of P_i , background Ca^{2+} leak was unaffected by an $\sim 50\%$ reduction of Ca^{2+} pump activity. Increased Ca^{2+} leak by addition of ionomycin increased the steady-state $[Ca^{2+}]$ but did not affect the rate constant for decay. This further validates the simple model of the SR described quantitatively in Fig. 1C and indicates that changes in SR Ca^{2+} efflux that are independent of the Ca^{2+} pump do not affect the SR Ca^{2+} uptake rate constant. Moreover, the results from Figs. 1 and 2 indicate that, under control conditions, Ca^{2+} leak from the SR is independent of SR Ca^{2+} pump activity, consistent with the absence of significant pump-mediated Ca^{2+} leak in the absence of P_i .

Effects of P_i on Ca^{2+} uptake and leak rate constants. Previous studies using permeabilized cardiac muscle have measured Ca^{2+} release on application of caffeine (37–39, 42). Results of these experiments are difficult to interpret in terms of actions on the SR, because chelation and/or precipitation of calcium phosphate within the SR and effects of P_i on the ryanodine recep-

tor cannot be excluded. However, these studies clearly showed that 10 mM P_i reduced the Ca^{2+} released by caffeine to ~60% of the control value. This action was accompanied by a transient release of Ca^{2+} from the SR (37, 38). The transient release was not blocked by ryanodine (39), suggesting that a release pathway other than the active ryanodine receptor was involved. However, a link between a functional Ca^{2+} pump and P_i -induced Ca^{2+} release was not established.

In the present study, addition of 10 mM P_i had two effects on cardiac SR: 1) it reduced the rate constant for Ca^{2+} uptake; and 2) it increased the rate of Ca^{2+} leak from the SR (Fig. 3). That P_i -induced increase in Ca^{2+} efflux from the SR is mediated by the Ca^{2+} pump is supported by the following. 1) On inhibition of the Ca^{2+} pump, P_i caused no significant increase in SR leak rate (Fig. 6A). 2) In the continued presence of 10 mM P_i , when pump-mediated Ca^{2+} leak exists, low concentrations of thapsigargin reduced Ca^{2+} leak from the SR and decreased the rate of Ca^{2+} uptake (Fig. 5B).

The effect of CrP on SR Ca^{2+} uptake. The effect of P_i could be reversed by the addition of 10 mM CrP (Fig. 3C). Furthermore, in the continued presence of CrP, 10 mM P_i had no significant effects on either flux process (Fig. 4). A similar dependence on CrP was described previously (38). This effect was attributed to the ability of CrP to rephosphorylate ADP via the enzyme creatine phosphokinase (CK), because inhibition of CK abolished the effect of CrP (38). There is good evidence that an SR-bound CK exists spatially close to the Ca^{2+} pump ATPase and preferentially rephosphorylates the ADP produced by the Ca^{2+} pump (32). These results suggest that the ability of P_i to affect the SR Ca^{2+} pumps requires high concentrations of ADP. The results from this study also support the view that CrP can significantly increase the Ca^{2+} uptake rate of the SR and may have significant effects on the Ca^{2+} affinity and/or stoichiometry of the pump (6, 24). In this study, background SR Ca^{2+} leak (in the absence of P_i) was unaffected by CrP, suggesting that, under control conditions, there was no pump-mediated leak from the SR.

Potential mechanism(s) of action of P_i on the SR Ca^{2+} pump. There are two mechanisms by which P_i may induce a Ca^{2+} pump-mediated SR Ca^{2+} leak, "pump reversal" and "pump-channel transition." It has been shown that, in SR vesicle preparations, millimolar levels of P_i can phosphorylate the SR Ca^{2+} pump directly (31). In the presence of ADP, this form of the pump can generate a Ca^{2+} efflux from the SR accompanied by the synthesis of ATP, i.e., pump reversal (15). In the present study, in the absence of CrP, ADP concentration within the cuvette would be expected to continuously increase during the experiment because of the cellular ATPases associated with permeabilized myocytes. Separate measurements of the cellular ATPase rate suggest that 1×10^6 cells/ml lower the ATP concentration at ~10 nM/s (A. Pagliocca and G. L. Smith, unpublished observation). This gives a predicted concentration range of ADP from ~60 to 120 μ M at the time of P_i addition. These values are similar to

the intracellular values measured during hypoxia and ischemia in cardiac muscle (1, 33) and are close to optimal for pump reversal (3). However, it is unclear from previous studies whether pump reversal occurs to a significant extent in the presence of millimolar concentrations of cytosolic ATP. Cytosolic ATP can also phosphorylate the SR Ca^{2+} pump as part of the normal sequence of events in Ca^{2+} transport. Pump reversal in the presence of ATP may be possible if the concentration of the phosphorylated intermediate of the pump increases above the level normally achieved by ATP. The ability of P_i to induce SR Ca^{2+} leak and decrease the uptake rate constant of the pump may be linked. While operating in the reverse mode, the pump would be unavailable for Ca^{2+} uptake, thereby reducing the number of active Ca^{2+} pumps. This could account for the decrease in the uptake rate constant. As mentioned earlier, the absence of CrP and increased levels of ADP may also alter the stoichiometry and Ca^{2+} affinity of the fraction of pumps operating in the normal mode (18). This effect could not be distinguished from a reduced maximal rate of pumping in these studies.

Alternatively, some studies suggest that under certain conditions, the SR Ca^{2+} pump can mediate a fast efflux of Ca^{2+} from the SR in an "uncoupled" or substrate-free state (7). Under these conditions, the SR Ca^{2+} pump acts as a channel and can mediate Ca^{2+} leak from the SR. It is unlikely that this is the mechanism for P_i -induced Ca^{2+} leak. This mode of the SR Ca^{2+} pump is seen only in substrate-free conditions or in the presence of agents that inhibit substrate binding (e.g., arsenate). Furthermore, P_i concentrations below 4 mM appear to block the uncoupled mode of the Ca^{2+} pump (7).

In summary, the results presented in this study suggest that, in the presence of 10 mM P_i and in the absence of CrP, a significant Ca^{2+} efflux from the SR occurs via the Ca^{2+} pump in cardiac muscle. The characteristics of the Ca^{2+} efflux suggest that it is caused by reversal of the SR Ca^{2+} pump.

This work was financially supported by the British Heart Foundation. P. Neary is a British Heart Foundation clinical lecturer, L. Bruce is funded by a Medical Research Council PhD studentship, and A. M. Duncan is funded by a British Heart Foundation PhD studentship.

REFERENCES

- Allen DG, Morris PG, Orchard CH, and Pirolo JS. A nuclear magnetic resonance study of metabolism in the ferret heart during hypoxia and inhibition of glycolysis. *J Physiol (Lond)* 361: 185-204, 1985.
- Alves EW and DeMeis L. Effect of compound 48/80 and ruthenium red on the Ca^{2+} -ATPase of sarcoplasmic reticulum. *J Biol Chem* 261: 18854-18859, 1986.
- Barlogie B, Hasselbach W, and Makinose M. Activation of calcium efflux by ADP and inorganic phosphate. *FEBS Lett* 12: 267-268, 1971.
- Baudet S, Shaoulian R, and Bers DM. Effects of thapsigargin and cyclopiazonic acid on twitch force and sarcoplasmic reticulum Ca^{2+} content of rabbit ventricular muscle. *Circ Res* 73: 813-819, 1993.
- Bell PU, Von Chak D, Hasselbach W, and Weber H-H. Competition between oxalate and phosphate during active cal-

- cium accumulation by sarcoplasmic vesicles. *Z. Naturforsch.* 32c: 281-287, 1977.
6. **Benech JC, Wolosker H, and DeMeis L.** Reversal of the Ca^{2+} pump of blood platelets. *Biochem J* 306: 35-38, 1995.
 7. **DeMeis L and Inesi G.** Functional evidence of a transmembrane channel within the Ca^{2+} transport ATPase of sarcoplasmic reticulum. *FEBS Lett* 299: 33-35, 1992.
 8. **Eisner DA, Elliott AC, and Smith GL.** The contribution of intracellular acidosis to the decline of developed pressure in ferret hearts exposed to cyanide. *J Physiol (Lond)* 391: 99-108, 1987.
 9. **Fabiato A and Fabiato F.** Calculator programs for computing the composition of the solutions containing multiple metals and ligands used for experiments in skinned muscle cells. *J Physiol (Paris)* 75: 463-505, 1979.
 10. **Feher JJ and Fabiato A.** Cardiac sarcoplasmic reticulum: Calcium uptake and release. In: *Calcium and the Heart*, edited by GA Langer. New York: Raven, 1990, p. 199-268.
 11. **Feher JJ, Manson NH, and Poland JL.** The rate and capacity of calcium uptake by sarcoplasmic reticulum in fast, slow, and cardiac muscle: effects of ryanodine and ruthenium. *Arch Biochem Biophys* 265: 171-182, 1988.
 12. **Fryer MW, Owen VJ, Lamb GD, and Stephenson DG.** Effects of creatine-phosphate and P_i on Ca^{2+} movements and tension development in rat skinned skeletal-muscle fibers. *J Physiol (Lond)* 482: 123-140, 1995.
 13. **Godt RE and Nosek TM.** Changes of intracellular milieu with fatigue or hypoxia depress contraction of skinned rabbit skeletal and cardiac muscle. *J Physiol (Lond)* 412: 155-180, 1989.
 14. **Grynkiowicz G, Poenie M, and Tsien RY.** A new generation of Ca indicators with greatly improved fluorescence properties. *J Biol Chem* 260: 3440-3450, 1985.
 15. **Hasselbach W.** The reversibility of the sarcoplasmic calcium pump. *Biochim Biophys Acta* 515: 23-53, 1978.
 16. **Hove-Madsen L and Bers DM.** Passive Ca buffering and SR Ca uptake in permeabilized rabbit ventricular myocytes. *Am J Physiol Cell Physiol* 264: C677-C686, 1993.
 17. **Hove-Madsen L and Bers DM.** Sarcoplasmic reticulum Ca^{2+} uptake and thapsigargin sensitivity in permeabilized rabbit and rat ventricular myocytes. *Circ Res* 73: 820-828, 1993a.
 18. **Inesi G and de Meis L.** Regulation and steady state filling in sarcoplasmic reticulum. *J Biol Chem* 264: 5926-5936, 1989.
 19. **Jennings RB and Steenbergen C.** Nucleotide metabolism and cellular damage in myocardial ischemia. *Annu Rev Physiol* 47: 727-749, 1985.
 20. **Kargacin GJ, Ali Z, and Kargacin ME.** Ruthenium red reduces the Ca^{2+} sensitivity of Ca^{2+} uptake into cardiac sarcoplasmic reticulum. *Pflügers Arch* 436: 328-342, 1998.
 21. **Kargacin GJ, Ali Z, and Kargacin ME.** Ruthenium red reduces the Ca^{2+} sensitivity of Ca^{2+} uptake into cardiac sarcoplasmic reticulum. *Pflügers Arch* 436: 328-342, 1998.
 22. **Kentish JC.** The effects of inorganic phosphate and creatine phosphate on force production in skinned muscles from rat ventricle. *J Physiol (Lond)* 370: 585-604, 1986.
 23. **Kermode H, Williams AJ, and Sitsapesan R.** The interactions of ATP, ADP and inorganic phosphate with the sheep cardiac ryanodine receptor. *Biophys J* 74: 1296-1304, 1998.
 24. **Korge P and Campbell KB.** Local ATP regeneration is important for sarcoplasmic reticulum Ca^{2+} pump function. *Am J Physiol Cell Physiol* 267: C357-C366, 1994.
 25. **Korge P and Campbell KB.** Regulation of calcium pump function in back inhibited vesicles by calcium-ATPase ligands. *Cardiovasc Res* 29: 512-519, 1995.
 26. **Kusuoka H, Weisfeldt ML, Zweier JL, Jacobus WE, and Marban E.** Mechanism of early contractile failure during hypoxia in intact ferret heart: evidence for modulation of maximal Ca^{2+} -activated force by inorganic phosphate. *Circ Res* 59: 270-282, 1986.
 27. **Lide DR.** *Handbook of Chemistry and Physics*. Boca Raton, LA: Chemical Rubber Company, 1994.
 28. **Ma J.** Block by ruthenium red of the ryanodine-activated calcium release channel of skeletal muscle. *J Gen Physiol* 102: 1031-1056, 1993.
 29. **Meissner G and Henderson JS.** Rapid calcium release from cardiac sarcoplasmic reticulum vesicles is dependent on Ca^{2+} and is modulated by Mg^{2+} , adenine nucleotide, and calmodulin. *J Biol Chem* 262: 3066-3073, 1987.
 30. **Miller DJ and Smith GL.** EGTA purity and the buffering of calcium ions in physiological solutions. *Am J Physiol Cell Physiol* 246: C160-C166, 1984.
 31. **Punzengruber C, Prager R, Kolassa N, Winkler F, and Suko J.** Calcium gradient-dependent and calcium gradient-independent phosphorylation of sarcoplasmic reticulum by orthophosphate. The role of magnesium. *Eur J Biochem* 92: 349-359, 1978.
 32. **Rossi AM, Eppenberger HM, Voipe P, Cotrufo R, and Walimann T.** Muscle-type MM creatine kinase is specifically bound to sarcoplasmic reticulum and can support Ca^{2+} uptake and regulate local ATP/ADP ratios. *J Biol Chem* 265: 5258-5266, 1990.
 33. **Rovetto MJ, Whitmer JT, and Neely JR.** Comparison of the effects of anoxia and whole heart ischemia on carbohydrate utilization in isolated working rat hearts. *Circ Res* 32: 699-711, 1973.
 34. **Seidler NW, Joan I, Vogh M, and Martonosi A.** Cyclopiazonic acid is a specific inhibitor of the Ca^{2+} -ATPase of the sarcoplasmic reticulum. *J Biol Chem* 264: 17816-17823, 1989.
 35. **Shannon TR, Ginsburg KS, and Bers DM.** Reverse mode of the sarcoplasmic reticulum Ca pump limits sarcoplasmic reticulum Ca uptake in permeabilized and voltage clamped myocytes. *Ann NY Acad Sci* 853: 350-352, 1998.
 36. **Smith GL and Miller DJ.** Potentiometric measurements of stoichiometric and apparent affinity constants of EGTA for protons and divalent ions including calcium. *Biochim Biophys Acta* 839: 287-299, 1985.
 37. **Smith GL and Steele DS.** Inorganic phosphate decreases the Ca^{2+} content of the sarcoplasmic reticulum in saponin-treated rat cardiac trabeculae. *J Physiol (Lond)* 458: 457-473, 1992.
 38. **Steele DS, McAinsh AM, and Smith GL.** Effects of creatine-phosphate and inorganic-phosphate on the sarcoplasmic-reticulum of saponin-treated rat-heart. *J Physiol (Lond)* 483: 155-166, 1995.
 39. **Steele DS, McAinsh AM, and Smith GL.** Comparative effects of inorganic phosphate and oxalate on uptake and release of Ca^{2+} by the sarcoplasmic reticulum in saponin skinned rat cardiac trabeculae. *J Physiol (Lond)* 490: 565-576, 1996.
 40. **Winkler F and Suko J.** Phosphorylation of the calcium-transport adenosine triphosphate of cardiac sarcoplasmic reticulum by orthophosphate. *Eur J Biochem* 77: 611-619, 1977.
 41. **Xiang J-Z and Kentish JC.** Effects of inorganic phosphate and ADP on calcium handling by the sarcoplasmic reticulum in rat skinned cardiac muscles. *Cardiovasc Res* 29: 391-400, 1995.
 42. **Zhu Y and Nosek TM.** Intracellular milieu changes associated with hypoxia impair sarcoplasmic reticulum Ca^{2+} transport in cardiac muscle. *Am J Physiol Heart Circ Physiol* 261: H620-H626, 1991.

Overexpression of FK506-Binding Protein FKBP12.6 in Cardiomyocytes Reduces Ryanodine Receptor-Mediated Ca^{2+} Leak From the Sarcoplasmic Reticulum and Increases Contractility

Jürgen Prestle, Paul M.L. Janssen, Anita P. Janssen, Oliver Zeitz, Stephan E. Lehnart, Lorraine Bruce, Godfrey L. Smith, Gerd Hasenfuss

Abstract—The FK506-binding protein FKBP12.6 is tightly associated with the cardiac sarcoplasmic reticulum (SR) Ca^{2+} -release channel (ryanodine receptor type 2 [RyR2]), but the physiological function of FKBP12.6 is unclear. We used adenovirus (Ad)-mediated gene transfer to overexpress FKBP12.6 in adult rabbit cardiomyocytes. Western immunoblot and reverse transcriptase-polymerase chain reaction analysis revealed specific overexpression of FKBP12.6, with unchanged expression of endogenous FKBP12. FKBP12.6-transfected myocytes displayed a significantly higher (21%) fractional shortening (FS) at 48 hours after transfection compared with Ad-GFP-infected control cells ($4.8 \pm 0.2\%$ FS versus $4 \pm 0.2\%$ FS, respectively; $n=79$ each; $P=0.001$). SR- Ca^{2+} uptake rates were monitored in β -escin-permeabilized myocytes using Fura-2. Ad-FKBP12.6-infected cells showed a statistically significant higher rate of Ca^{2+} uptake of 0.8 ± 0.09 nmol/s $^{-1}/10^6$ cells ($n=8$, $P<0.05$) compared with 0.52 ± 0.1 nmol/s $^{-1}/10^6$ cells in sham-infected cells ($n=8$) at a $[\text{Ca}^{2+}]$ of 1 $\mu\text{mol/L}$. In the presence of 5 $\mu\text{mol/L}$ ruthenium red to block Ca^{2+} efflux via RyR2, SR- Ca^{2+} uptake rates were not significantly different between groups. From these measurements, we calculate that SR- Ca^{2+} leak through RyR2 is reduced by 53% in FKBP12.6-overexpressing cells. Caffeine-induced contractures were significantly larger in Ad-FKBP12.6-infected myocytes compared with Ad-GFP-infected control cells, indicating a higher SR- Ca^{2+} load. Taken together, these data suggest that FKBP12.6 stabilizes the closed conformation state of RyR2. This may reduce diastolic SR- Ca^{2+} leak and consequently increase SR- Ca^{2+} release and myocyte shortening. (*Circ Res.* 2001;88:188-194.)

Key Words: cardiac myocytes ■ calcium ■ sarcoplasmic reticulum ■ adenovirus ■ gene transfer

In striated muscles, excitation-contraction (E-C) coupling involves depolarization of the plasma membrane to open voltage-gated calcium (Ca^{2+}) channels (known as dihydropyridine receptors [DHPRs]). This event in turn triggers the release of a larger amount of Ca^{2+} from the sarcoplasmic reticulum (SR) to initiate muscle contraction.¹ Ca^{2+} efflux from the SR is mediated by the SR- Ca^{2+} release channel (known as ryanodine receptor [RyR]), which is a tetramer comprised of 4 identical subunits. cDNA cloning revealed the existence of 3 different subtypes of RyRs: the skeletal muscle isoform RyR1, the heart muscle isoform RyR2, and the brain and smooth muscle isoform RyR3. The 3 isoforms share $\approx 66\%$ sequence homology at the amino acid level and are the largest ion channels presently known.

Ca^{2+} release from the SR is a finely regulated process that involves not only the RyR itself but also several accessory proteins modulating RyR activity. Among these proteins are

the FK506-binding protein FKBP12 and the orthologous protein FKBP12.6. The immunosuppressive drug FK506 binds to FKBP12 and FKBP12.6 and pentamerizes with calcineurin, calmodulin, and Ca^{2+} , resulting in the inhibition of cytokine induction and the subsequent immune response.² The physiological function of these proteins was unclear until the finding that FKBP12 associates with the RyR1 and modulates channel function.³⁻⁵ There is clear evidence from single-channel and lipid-bilayer studies that FKBP12 alters the kinetics of the channel activity and induces coupled gating of individual RyR1 channels in a junction.⁶⁻⁹ Although FKBP12 can bind to both RyR1 and RyR2, FKBP12.6 specifically associates with RyR2.¹⁰⁻¹² However, the data described so far regarding the putative physiological function of FKBP12.6 are conflicting. Single-channel recordings of RyR2 activity incorporated into planar-lipid bilayers suggested that removal of FKBP12.6 from the RyR2 by FK506

Original received July 27, 2000; revision received November 20, 2000; accepted November 22, 2000.

From the Department of Cardiology and Pneumology (J.P., P.M.L.J., A.P.J., O.Z., S.E.L., G.H.), Georg-August-University Göttingen, Göttingen, Germany, and Institute of Biomedical and Life Sciences (L.B., G.H.), Division of Neurosciences and Biomedical Systems, University of Glasgow, Glasgow, UK.

Correspondence to Jürgen Prestle, PhD, Georg-August-Universität Göttingen, Zentrum Innere Medizin, Abt. Kardiologie & Pneumologie, Robert-Koch-Strasse 40, 37075 Göttingen, Germany. E-mail prestle@med.uni-goettingen.de

© 2001 American Heart Association, Inc.

Circulation Research is available at <http://www.circresaha.org>

TABLE 1. DNA Primers Used for PCR

PCR Primer	Gene	Nucleotide Position/DNA Fragment Size	NIH GenBank Accession No.
Forward: 5'-CAGCAGCAGAGATCTCCAGAGGC-3'	Human FKBP12.6 (full length)	25-48	L37086
Reverse: 5'-TTCCTCAAGCAAGATCTCGCATGAACAC-3'		589-563; 564 bp	
Forward: 5'-TTCATCCAGAGACAGAAACAAACC-3'	FKBP12.6 (internal)	160-203	L37086
Reverse: 5'-ATTGGGAGGGATGACACC-3'		334-351; 172 bp	
Forward: 5'-CCGAGGCTGGGAGAAGG-3'	Rabbit FKBP12	171-188	M89928
Reverse: 5'-TCACCCAAAACGGAACAGA-3'		601-581; 421 bp	
Forward: 5'-ACCCTCGCCTGTTCCTAC-3'	Rabbit ryanodine receptor	3399-3418	U50465
Reverse: 5'-GGCCCATAGTGTCTCGTT-3'		3775-3758; 377 bp	
Forward: 5'-AGCCCACTCCATCCCAACA-3'	Rabbit calsequestrin	753-773	X55040
Reverse: 5'-GTCAGCGTCGTACATTCACCA-3'		1105-1083; 353 bp	
Forward: 5'-GGCCGCCAGAACATCATCC-3'	Rabbit GAPDH	671-690	L23961
Reverse: 5'-CTCTCGCTGGGGCGGTGTTG-3'		1106-1084; 436 bp	

NIH indicates National Institutes of Health.

PCR primers used to amplify the full-length cDNA of the human FKBP12.6 gene were modified to create an internal *BglII* site (underlined). Identity of all PCR fragments was verified by sequencing.

or rapamycin increases the open probability of the channel and induces the appearance of long-lasting subconductance states.^{13,14} In comparable in vitro studies, however, removal of FKBP12.6 from the RyR2 or addition of recombinant FKBP12.6 to stripped cardiac SR preparations did not alter channel behavior.^{11,15} Even more puzzling, FKBP12-deficient mice, which have unchanged FKBP12.6 levels, display a severe cardiac phenotype but have normal skeletal muscle.¹⁶ The majority of the FKBP12-knockout mice died between embryonic day 14 and birth because of severe dilated cardiomyopathy. Both the skeletal and the cardiac-muscle RyRs from these mice showed similar alterations in single-channel behavior compared with RyRs from wild-type mice, ie, an increased open probability of the channel and the appearance of subconductance states.

Binding of FKBP12.6 to the RyR2 was shown to be regulated by phosphorylation of the channel subunits. Phosphorylation by protein kinase A, which is associated with the RyR2 via the anchoring protein mAKAP, dissociates FKBP12.6 from the channel, resulting in destabilization of the channel complex. Hyperphosphorylation of RyR2 in the failing human heart results in defective channel function and may thus account for dysregulated SR-Ca²⁺ handling during heart failure.¹⁷

In the present study, single-cell shortening, SR-Ca²⁺ uptake rates, and caffeine-evoked contractions reflecting SR-Ca²⁺ content were measured in rabbit cardiomyocytes overexpressing FKBP12.6 on adenovirus-mediated gene transfer. The results suggest that FKBP12.6 overexpression can modulate E-C coupling in cardiomyocytes.

Material and Methods

Recombinant Adenovirus Vector Construction

Full-length cDNA of the human FKBP12.6 gene was cloned by polymerase chain reaction (PCR) from a human heart-muscle-specific cDNA sample by the use of PCR primers that span the whole coding region of FKBP12.6 cDNA (see Table 1). Recombinant adenoviruses were generated by standard procedures.

Primary Culture of Rabbit Ventricular Myocytes and Adenoviral Gene Transfer

Female Chinchilla bastard rabbits (Charles River, Sulzfeld, Germany; 2.5 to 3 kg, n=9) were heparinized and anesthetized with sodium thiopental (50 mg/kg IV). Outlines of this study were designed and carried out in accordance with institutional guidelines regarding care and use of animals. Ventricular myocytes were isolated by the enzymatic method as described.¹⁸ Myocytes were counted, and adenoviral infection with indicated multiplicity of infection (MOI) was performed during plating of the myocytes at a density of 0.5x10⁵ rod-shaped cells/cm² onto laminin (20 µg/mL)-coated tissue-culture dishes. After 3 hours, unattached cells were removed by 3 wash steps, and myocytes were cultured in supplemented M199 medium (Sigma).

Verification of Transgene Expression and Virus Transfection Efficiency

Reverse transcriptase-PCR (RT-PCR) analysis of transfected myocytes was performed with gene-specific primer pairs (see Table 1) by the use of a hot-start Taq polymerase (Perkin Elmer) with 33 cycles each.

Western immunoblot analysis was performed with a polyclonal anti-FKBP12 (C-19) antibody (Santa Cruz Biotechnology) and an enhanced chemoluminescence detection system (Amersham) according to the manufacturer's instructions.

Single-Cell Shortening Measurements

Myocyte shortening was measured by an edge-detection system (Crecent Electronics) at a stimulation frequency of 1 Hz and a sampling rate of 240 Hz. Online and offline analysis was performed with custom-designed Labview software (National Instruments).

Caffeine-induced contractions reflecting SR-Ca²⁺ load were measured after a stimulation train at 1 Hz by rapidly switching the superfusing solution to one containing 10 mmol/L caffeine for 5 to 6 seconds.

Measurements of SR-Ca²⁺ Uptake Rates

Isolated rabbit cardiomyocytes were infected with Ad-FKBP12.6 or Ad-LacZ at an MOI of 10 and were harvested after 48-hour culture time by gentle scraping off the culture dish. An aliquot of 0.1 mL of cell suspension (1.5x10⁶ cells/mL) was exposed to 0.1 mg/mL β-escin (Sigma) and gently stirred for 30 seconds. β-Escin was removed by centrifuging and resuspending the cells in mock intracellular solution (see the online data supplement available at http://

www.circresaha.org). Cells were then placed in a cuvette, and additional solutions were added to give a final volume of 0.15 mL, containing 50 $\mu\text{mol/L}$ EGTA, 5 mmol/L ATP, 10 mmol/L CrP (Sigma), the mitochondrial inhibitors carbonyl cyanide (20 $\mu\text{mol/L}$) and oligomycin (20 $\mu\text{mol/L}$) (Calbiochem), 10 mmol/L oxalate (Sigma), and 10 $\mu\text{mol/L}$ Fura-2 (Molecular Probes). Cells were maintained in suspension by gentle stirring, and the Fura-2 fluorescence within the cuvette was recorded at 100 Hz using a dual-wavelength spectrophotometer (IonOptix). All experiments were done at room temperature (20°C to 22°C).

Statistics

All data are presented as mean \pm SEM. Myocyte-shortening data were analyzed by Student's *t* test for unpaired data. Ca^{2+} uptake rates were tested for statistically significant differences between experimental groups by 2-way repeated-measure ANOVA followed by Student-Newman-Keuls test. $P < 0.05$ was accepted as statistically significant.

An expanded Materials and Methods section can be found in an online data supplement available at <http://www.circresaha.org>.

Results

Adenoviral Gene Transfer of FKBP12.6 in Isolated Rabbit Ventricular Myocytes

Two different recombinant adenoviruses expressing human FKBP12.6, Ad-FKBP12.6, and Ad-FKBP12.6-GFP and 2 control adenoviruses, Ad-LacZ and Ad-GFP, were used in this study. Efficiency of adenoviral gene transfer in isolated rabbit ventricular myocytes was initially verified using the green fluorescent protein (GFP) and LacZ viruses. The transfection protocol resulted in transfection efficiencies of typically more than 95% at an MOI of 10 (data not shown).

Western immunoblot analysis using an antibody that cross-reacts with both FKBP12 and FKBP12.6 was used to verify transgene protein expression in the transfected myocytes. Although both proteins consist of 108 amino acid residues, FKBP12.6 migrates slower during denaturing electrophoresis than FKBP12.¹⁰ Interestingly, as shown in Figure 1A, FKBP12 is the prominent isoform in rabbit cardiomyocytes. FKBP12.6 can be detected only with the RT-PCR analysis (Figure 1B). Endogenous mRNA expression of FKBP12.6 in control cells was found to be much lower than endogenous FKBP12 expression. Adenovirus-mediated overexpression of FKBP12.6 resulted in a 5-fold increase in relative FKBP12.6 mRNA levels at 24 hours after transfection and a 6-fold increase at 48 hours after transfection compared with control. FKBP12 mRNA expression was unchanged on FKBP12.6 overexpression, as was mRNA expression of RyR2.

The DNA sequence of the 172-bp PCR fragment amplified by primers. FKBP12.6 internal (see Table 1) in rabbit cardiomyocytes was found to be 94.2% homologous to rat FKBP12.6 cDNA and 97.6% homologous to human FKBP12.6 cDNA.

Contractile Parameters of Isolated Cardiomyocytes

Single-cell shortening of Ad-FKBP12.6-GFP-infected and Ad-GFP-infected myocytes was measured at 24 and 48 hours after adenoviral transfection by a video-edge detection system (Figure 2). At 48 hours after transfection, myocyte fractional shortening (FS, expressed in percentage of diastolic cell length) was 21% higher in Ad-FKBP12.6-GFP-infected

cells compared with Ad-GFP-infected cells ($4.8 \pm 0.2\%$ FS versus $4 \pm 0.2\%$ FS, respectively; $n = 79$ cells each, $P = 0.001$). At 24 hours after transfection, at a lower level of FKBP12.6 overexpression (see Figure 1B), FS was 15% higher in FKBP12.6 cells compared with GFP control cells ($5.3 \pm 0.2\%$ FS versus $4.6 \pm 0.3\%$ FS, respectively; $n = 55$ cells each, $P = 0.034$). Shortening-time characteristics of both groups of myocytes are given in Table 2. FKBP12.6 overexpression slightly but statistically significantly prolonged time to peak shortening after 2 days of culture time. Time to 50% relengthening was unchanged in both groups of myocytes at both time points.

SR- Ca^{2+} Uptake Rates in Permeabilized Cardiomyocytes

SR- Ca^{2+} uptake rates were monitored in β -escin-permeabilized cardiomyocytes with the use of the fluorescent dye Fura-2 (Figure 3). The measurements of SR- Ca^{2+} uptake rates

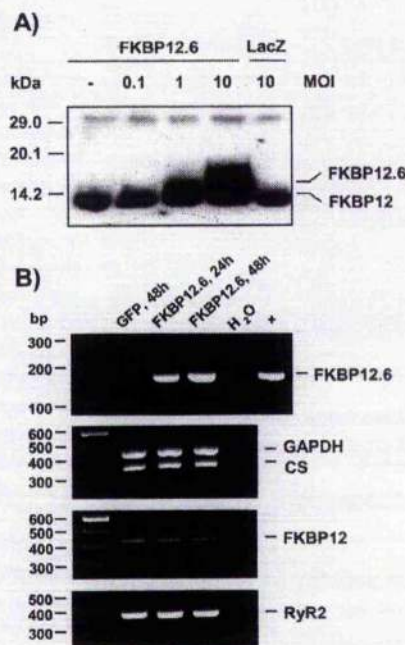


Figure 1. A, Western immunoblot analysis of Ad-LacZ (LacZ)-infected and Ad-FKBP12.6-GFP (FKBP12.6)-infected myocytes. Cells were infected with indicated MOI and harvested after 48 hours of culture time. FKBP12.6 protein expression increases with increasing virus titers. The fact that FKBP12.6 migrates as a broad band during electrophoresis and could not be clearly separated from endogenous FKBP12 is most likely attributable to the lysis procedure of the cells under high-salt conditions. B, RT-PCR analysis of Ad-GFP (GFP)-infected and Ad-FKBP12.6-GFP (FKBP12.6)-infected myocytes. Cells were infected at an MOI of 10 and were harvested for RT-PCR analysis with gene-specific primers (see Table 1) after 24 and 48 hours of culture time. Size of DNA markers are indicated on the left. + indicates positive control with FKBP12.6 plasmid DNA as template. Duplex RT-PCR with GAPDH- and calsequestrin-specific primers using the same probes indicates equal cDNA load in each PCR. FKBP12.6 mRNA expression in Ad-FKBP12.6-GFP-infected cells increases with culture time, whereas endogenous FKBP12 and RyR2 mRNA expression remains unchanged. A representative of $n = 3$ experiments is shown.

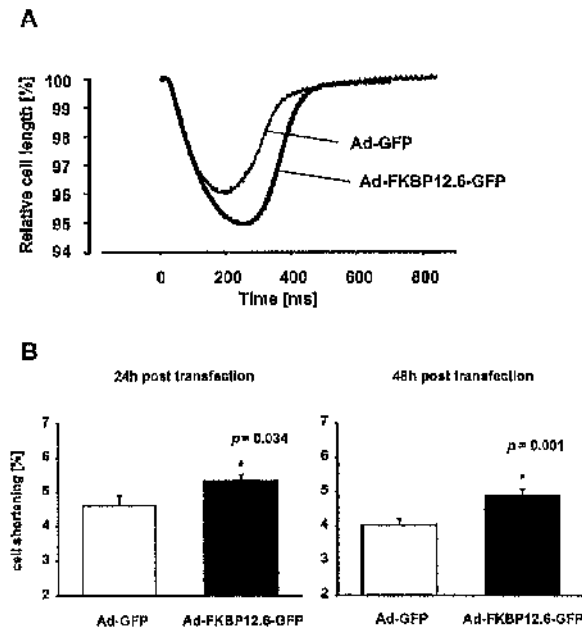


Figure 2. Single-cell shortening of Ad-GFP-infected and Ad-FKBP12.6-GFP-infected rabbit ventricular myocytes (MOI 10 each). **A**, Representative tracings of shortening experiments with Ad-GFP-infected and Ad-FKBP12.6-GFP-infected myocytes. Cells were electrically stimulated at 1 Hz at 37°C in M199 medium. **B**, Statistical analysis of FS in Ad-GFP-infected and Ad-FKBP12.6-GFP-infected myocytes after 24 hours ($n=55$ each) and after 48 hours of culture time ($n=79$ each). FS in FKBP12.6-overexpressing cells was 15% higher ($P=0.034$, Student's *t* test) compared with GFP control cells at 1 day after transfection and 21% higher ($P=0.001$, Student's *t* test) at 2 days after transfection.

were done in the presence of 10 mmol/L oxalate. Oxalate enters the SR and acts as a Ca^{2+} sink, maintaining a constant $[Ca^{2+}]$ in the SR. A typical fluorescence signal is shown in Figure 3A. Addition of aliquots of Ca^{2+} at the times indicated increased the $[Ca^{2+}]$ within the cuvette to $\approx 3 \mu\text{mol/L}$. The time course of the decay of $[Ca^{2+}]$ represents a balance between Ca^{2+} uptake by the SR- Ca^{2+} -ATPase pump and SR- Ca^{2+} leak. Addition of 5 $\mu\text{mol/L}$ ruthenium red (RuR) caused the subsequent decay of $[Ca^{2+}]$ to be faster because of

TABLE 2. Shortening-Time Parameters of Ad-FKBP12.6-GFP-Infected and Ad-GFP-Infected Rabbit Ventricular Myocytes

	24 Hours After Transfection		48 Hours After Transfection	
	GFP	FKBP12.6	GFP	FKBP12.6
n	55	55	79	79
TTPS, ms	205 \pm 6	212 \pm 6	229 \pm 6	246 \pm 6*
RT ₅₀ , ms	90 \pm 4	86 \pm 4	128 \pm 12	128 \pm 11

Rabbit cardiomyocytes were infected with either Ad-FKBP12.6 or Ad-GFP at an MOI of 10. Cells were paced at a stimulation frequency of 1 Hz at 37°C. Values represent mean \pm SEM of *n* myocytes. TTPS indicates time to peak shortening; RT₅₀, time to 50% relengthening.

* $P=0.049$ vs GFP.

block of Ca^{2+} leak through SR- Ca^{2+} release channels. In a series of experiments, we observed no differences in SR- Ca^{2+} uptake characteristics between noninfected (control) and Ad-LacZ-infected cells (summarized in Table 3). Myocytes overexpressing FKBP12.6 showed a significant higher rate of Ca^{2+} uptake at 1 $\mu\text{mol/L}$ Ca^{2+} than LacZ-infected myocytes. Figures 3B (i) and 3C (i) show superimposed traces of $[Ca^{2+}]$ arranged to intersect at 1 $\mu\text{mol/L}$ Ca^{2+} to illustrate the difference in the rate of Ca^{2+} uptake. These differences in Ca^{2+} uptake rates are more clearly distinguished when expressed as the rate of change of $[Ca^{2+}]$ ($d[Ca^{2+}]/dt$) plotted against the associated $[Ca^{2+}]$ (Figure 3B (ii) and 3C (ii)). From these plots, it is evident that comparable rates of Ca^{2+} uptake were achieved at $<0.5 \mu\text{mol/L}$ Ca^{2+} in both cell types and in the presence of RuR. However, at $[Ca^{2+}] >0.5 \mu\text{mol/L}$, $d[Ca^{2+}]/dt$ values were lower in the absence of RuR, consistent with activation of a significant RyR2-mediated leak. As described in Materials and Methods, the values of $d[Ca^{2+}]/dt$ that were measured at 1 $\mu\text{mol/L}$ Ca^{2+} were converted to a net Ca^{2+} flux using the Ca^{2+} buffer power, and the mean values of Ca^{2+} uptake are shown in Table 3. In the presence of RuR, Ca^{2+} uptake rates in the 3 experimental groups were not significantly different. This result indicates that the 3 groups of myocytes have comparable rates of Ca^{2+} pump activity and background Ca^{2+} leak. The markedly different uptake rates in the absence of RuR (ie, in the presence of RyR2 activity) indicate that SR- Ca^{2+} leak through RyR2 is $\approx 50\%$ lower in FKBP12.6-overexpressing cardiomyocytes at 1 $\mu\text{mol/L}$ Ca^{2+} . This difference between experimental groups is most clearly seen when the change in Ca^{2+} efflux rate is expressed relative to the control rate. Addition of RuR increased the rate of Ca^{2+} uptake ≈ 2 -fold in noninfected and Ad-LacZ-infected cells (1.79 \pm 0.14-fold and 2.02 \pm 0.11-fold, respectively). The relative increase in Ca^{2+} uptake rate was significantly less in Ad-FKBP12.6-infected cells (1.3 \pm 0.16-fold, $P<0.05$) compared with control cells.

The effects of rapamycin on RyR-mediated Ca^{2+} leak from the SR was studied in noninfected myocytes (control) and FKBP12.6-overexpressing cells. In the noninfected control group, rapamycin (5 $\mu\text{mol/L}$) had no significant effect on the magnitude of the RuR-sensitive leak (Table 4). When normalized to control conditions, Ca^{2+} uptake rate was not significantly altered in the presence of rapamycin (1.11 \pm 0.07-fold increase, not significant). However, when rapamycin was applied to myocytes overexpressing FKBP12.6, there was a statistically significant slowing of the rate of Ca^{2+} uptake to 0.74 \pm 0.1 of the value under control conditions. This was significantly different from the effect of rapamycin on noninfected cells ($P=0.021$). Because comparable rates of Ca^{2+} uptake are achieved in the presence of RuR, these results suggest that rapamycin increased the RuR-sensitive leak in rabbit myocytes overexpressing FKBP12.6.

Caffeine-Induced Contractures in Isolated Cardiomyocytes

To investigate whether the differences in shortening amplitude and SR- Ca^{2+} uptake rates between FKBP12.6-overexpressing myocytes and control myocytes were associ-

TABLE 3. Oxalate Facilitated Ca^{2+} Uptake Rates Measured From β -Escin-Permeabilized Rabbit Ventricular Myocytes

	Noninfected (n=4) (nmol/ 10^6 cells/s $^{-1}$)	Ad-LacZ (n=8) (nmol/ 10^6 cells/s $^{-1}$)	Ad-FKBP12.6 (n=8) (nmol/ 10^6 cells/s $^{-1}$)
(A) Ca^{2+} uptake rate (1 $\mu\text{mol/L}$ Ca^{2+})	0.59 \pm 0.07*	0.52 \pm 0.1*	0.8 \pm 0.09
(B) Ca^{2+} uptake rate (1 $\mu\text{mol/L}$ Ca^{2+} , 5 $\mu\text{mol/L}$ RuR) (5 $\mu\text{mol/L}$ RuR)	1.06 \pm 0.27†	1.05 \pm 0.13†	1.04 \pm 0.37
(C) Calculated RuR-sensitive, Ca^{2+} efflux (1 $\mu\text{mol/L}$ Ca^{2+}) (B-A)	0.47	0.53	0.24

Rabbit cardiomyocytes were infected with Ad-LacZ or Ad-FKBP12.6 at an MOI of 10. Cells were analyzed at 20°C after 48 hours of culture time, as described in Materials and Methods. Values in row C are calculated by subtracting mean values in row B and A; positive values represent net SR- Ca^{2+} efflux. Values represent mean \pm SEM.

*Significantly different value from the Ad-FKBP12.6 group ($P<0.05$).

†Significantly different value from the corresponding values in the absence of RuR (row A, $P<0.05$).

ated with differences in SR- Ca^{2+} load, we analyzed caffeine-induced contractures in Ad-GFP-infected and Ad-FKBP12.6-GFP-infected cardiomyocytes during steady-state shortening at a stimulation frequency of 1 Hz in a separate set of experiments. The amplitude of caffeine-induced contractures

provides an index of the SR- Ca^{2+} content.²⁴ As shown in Figure 4, caffeine-evoked contractures were statistically significantly larger in FKBP12.6-overexpressing myocytes compared with control myocytes (18.8 \pm 1.2% FS, n=23, versus 15.2 \pm 1.1% FS, n=26, respectively, $P=0.037$) at 48 hours after transfection. Overexpression of FKBP12.6 increased Ca^{2+} load of the SR by 20% compared with control cells.

Discussion

Role of FKBP12.6 in Modulation of E-C Coupling in Cardiac Muscle

The present study, using adenoviral gene transfer to specifically overexpress FKBP12.6 in rabbit myocytes, indicates 3 significant effects of FKBP12.6 overexpression: (1) reduction of RyR2-mediated Ca^{2+} efflux from cardiac muscle SR; (2) higher SR- Ca^{2+} load; and (3) increased amplitude of twitch shortening in single myocytes.

The relationship between modulation of RyR2 activity and contractility is an active area of research.^{19,20} Contradictory evidence exists concerning the steady-state effects of changes in RyR activity. Cyclic ADP ribose is thought to increase the open probability of RyR, increase peak systolic $[\text{Ca}^{2+}]_i$, and increase twitch shortening in guinea pig myocytes.²¹ In contrast, tetracaine, a drug that decreases Ca^{2+} sensitivity of RyR2, had no effects on rat-myocyte shortening in the steady state.²² Furthermore, caffeine, a drug that increases the Ca^{2+} sensitivity of the RyR2, can decrease the peak systolic $[\text{Ca}^{2+}]_i$.^{22,23} Therefore, it is difficult to extrapolate directly from the effects of FKBP12.6 overexpression to the increased twitch shortening observed in this study. Yet our data strongly suggest that overexpression of FKBP12.6 reduces Ca^{2+} leak from the SR during diastole, thereby increasing SR- Ca^{2+} content, and thus increases the amount of Ca^{2+} available for release, which in turn increases twitch shortening amplitude. In a way analogous to that described recently for FKBP12 and RyR1, FKBP12.6 overexpression may alter not only the Ca^{2+} efflux through RyR2 but also the degree of cooperative activity of the RyR2 cluster.⁹

Effects of FKBP12.6 Ligands on Cardiac E-C Coupling

A range of effects of rapamycin and FKS06 have been reported. McCall et al²⁵ observed increased Ca^{2+} transient

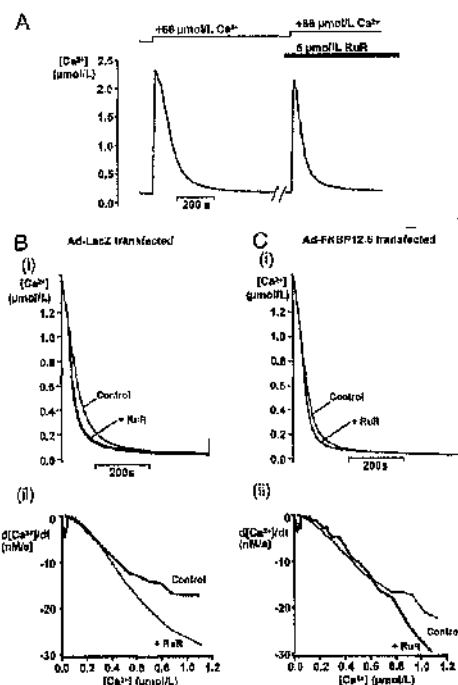


Figure 3. SR- Ca^{2+} uptake rates in permeabilized rabbit ventricular myocytes at 48 hours after transfection. A, Representative records of $[\text{Ca}^{2+}]$ against time recorded from a cuvette containing 1.5×10^6 /mL permeabilized myocytes suspended in a mock intracellular solution by continuous stirring (initial total volume 150 μL). Addition of aliquots of CaCl_2 are indicated above the trace as increases in total $[\text{Ca}^{2+}]$ within the cuvette. RuR (5 $\mu\text{mol/L}$) was added at the point indicated. Panels B (i) and C (i) show superimposed sections of records (intersecting at 1 $\mu\text{mol/L}$ Ca^{2+}) of the decline of $[\text{Ca}^{2+}]$ taken after the addition of CaCl_2 from 2 separate experiments: panel B from cells infected with Ad-LacZ (MOI 10) and panel C with cells infected with Ad-FKBP12.6 (MOI 10). Panels B (ii) and C (ii) show plots of rate of change of $[\text{Ca}^{2+}]$ ($d[\text{Ca}^{2+}]/dt$) against $[\text{Ca}^{2+}]$ for the records shown in panel B (i) and C (i).

TABLE 4. Oxalate-Facilitated Ca²⁺ Uptake Rates Measured From β-Escin-Permeabilized Rabbit Ventricular Myocytes in the Presence of Rapamycin

	Noninfected (n=6) (nmol/10 ⁶ cells/s ⁻¹)	Ad-FKBP12.6 (n=3) (nmol/10 ⁶ cells/s ⁻¹)
(A) Ca ²⁺ uptake rate (1 μmol/L Ca ²⁺)	0.55±0.12	0.74±0.13*
(B) Ca ²⁺ uptake rate (1 μmol/L Ca ²⁺ , 5 μmol/L Rap)	0.61±0.2	0.55±0.16
(C) Calculated Rap-sensitive Ca ²⁺ efflux (1 μmol/L Ca ²⁺) (A-B)	-0.06	0.19
(D) Ca ²⁺ uptake rate (1 μmol/L Ca ²⁺ , 5 μmol/L RuR)	0.98±0.2†	1.09±0.24†

Rabbit cardiomyocytes were infected with Ad-FKBP12.6 at an MOI of 10. Cells were analyzed at 20°C after 48 hours of culture time, as described in Materials and Methods. Values in row C are calculated by subtracting mean values in row A and B; positive values represent net SR-Ca²⁺ efflux. Values represent mean±SEM. Rap indicates rapamycin.

*Significantly different value from the nontransfected group (P<0.05).

†Significantly different value from the corresponding values in the absence of RuR (row A, P<0.05).

amplitude in isolated rat myocytes exposed to FK506, with no obvious change in SR-Ca²⁺ content. High concentrations (50 μmol/L) of FK506 caused prolonged openings of RyR2 and prolongation of the Ca²⁺ transient in rat myocytes.¹⁴ Yet similar concentrations of FK506 had no dramatic effect on the Ca²⁺ transient in voltage-clamped rat cardiac myocytes.²⁶

To date, there seems to be no information available concerning the effect of either of these ligands on the E-C coupling of isolated rabbit ventricular myocytes. In the present study, 5 μmol/L rapamycin had no significant effect on the SR of noninfected myocytes. In contrast, rapamycin significantly decreased the rate of Ca²⁺ uptake at 1 μmol/L in myocytes overexpressing FKBP12.6. These results suggest that the decreased Ca²⁺ flux through RyR2 observed on overexpression of FKBP12.6 could be reversed by rapamycin. This is consistent with the interpretation that increased cytosolic levels of FKBP12.6 are the cause of altered RyR2 properties with reduced Ca²⁺ leakage through RyR2.

Molecular Studies of RyR2 and FKBP12.6

Each RyR subunit contains only one FKBP-binding site, resulting in the structural formulas (RyR1 protomer)₄-(FKBP12)₄ and (RyR2 protomer)₄-(FKBP12.6)₄, respectively.^{4,10} However, from in vitro binding studies using ³⁵S-labeled FKBP12.6 and purified SR vesicles, Timmerman et al¹¹ calculated that ≈17% of the total FKBP12.6-binding sites in dog SR vesicles seem to be unoccupied. Marx et al¹⁷ recently showed that association of FKBP12.6 to RyR2 depends on phosphorylation state of RyR2 subunits.

Previous studies regarding the functional relevance of FKBP12.6 for RyR2 function are inconsistent. Single-channel analyses of RyR2 activity in planar-lipid bilayers are conflicting. In some studies, neither FKBP12 nor FKBP12.6 affects channel behavior,^{11,15} whereas other studies show marked changes in channel activity on dissociation of FKBP.^{13,14} In contrast, our data indicate that FKBP12.6 plays an important role in cardiac SR-Ca²⁺ release, which in turn depends on RyR2 function. This discrepancy may be explained by differences in the complexity of E-C-coupling mechanisms between cardiac and skeletal muscle in vivo. In cardiac myocytes, SR-Ca²⁺ release via RyR2 is triggered by depolarization-dependent Ca²⁺-influx through DHPRs, a phenomenon referred to as Ca²⁺-induced Ca²⁺ release.¹ In skeletal muscle cells, a voltage-induced change in DHPR conformation directly initiates RyR1 receptor opening without a requirement for Ca²⁺ influx.²⁷ Moreover, there is a functional diversity among the RyR subtypes despite their structural homology of ≈66%.

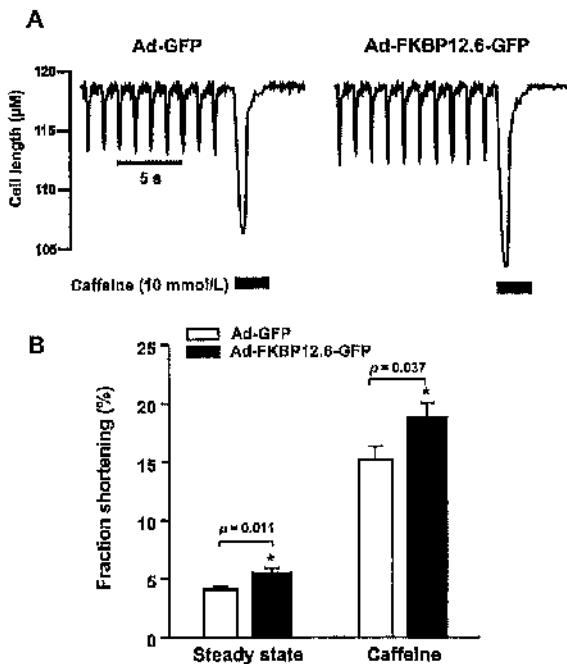


Figure 4. Caffeine-induced contractures in isolated rabbit ventricular myocytes. A, Representative twitch contractions of myocytes infected with Ad-GFP (n=23) and Ad-FKBP12.6-GFP (n=26) after 48 hours of culture time during steady-state electrical stimulation at 1 Hz and after caffeine application (10 mmol/L). B, Statistical analyses of fractional shortening (FS) in Ad-GFP-infected and Ad-FKBP12.6-GFP-infected myocytes. Shortening amplitude after caffeine application increased by 20% in Ad-FKBP12.6-infected cells compared with control cells (18.8±1.2% FS versus 15.2±1.1% FS, respectively, P=0.037, Student's t test). During steady-state shortening without caffeine, FS was 4.1±0.2 in Ad-GFP control cells and 5.5±0.3 in FKBP12.6-overexpressing cells (P=0.011, Student's t test).

RyR2 is not capable of supporting skeletal muscle-type E-C coupling in RyR1 knockout mice.²⁸ Furthermore, keeping in mind that several other accessory proteins besides FKBP12 or FKBP12.6, such as sorcin, calmodulin, and calsequestrin, and phosphorylation of the RyR itself may be involved in proper RyR function, it is reasonable to speculate that the complex nature of the SR-Ca²⁺ release process in cardiac and skeletal muscle cells is difficult to reconstitute in vitro.

It is still an open question as to whether FKBP12 and FKBP12.6 are exchangeable with respect to function. Although a physical and functional association of FKBP12 and RyR1 has been demonstrated for animal species from all 5 classes of vertebrates,²⁹ RyR2 can bind both FKBP12.6 and FKBP12, and both are expressed in myocardial tissue from different species, including humans (unpublished data, May 2000). Our data support the hypothesis that FKBP12.6 can modulate rabbit RyR2 in a similar manner as FKBP12 modulates RyR1 activity.

Acknowledgments

This study was supported in part by the Deutsche Stiftung Volkswagenwerk. G.L.S. was a recipient of a traveling grant from the Physiological Society. L.B. is funded by the Medical Research Council (UK). The authors thank Dr S. Dieterich for help with the cloning of human FKBP12.6 and S. Ott-Gebauer and M. Kothe for excellent technical assistance.

References

- Fabiato A. Time and calcium dependence of activation and inactivation of calcium-induced release of calcium from the sarcoplasmic reticulum of a skinned canine Purkinje cell. *J Gen Physiol*. 1985;85:247-289.
- Thomson AW, Bonham CA, Zeevi A. Mode of action of tetracaine (FK506): molecular and cellular mechanisms. *Ther Drug Monit*. 1995;17:584-591.
- Collins JH. Sequence analysis of the ryanodine receptor: possible association with a 12 kDa, FK506-binding immunophilin/protein kinase C inhibitor. *Biochem Biophys Res Commun*. 1991;178:1288-1290.
- Jayaraman T, Brillantes A-M, Timerman AP, Fleischer S, Erdjument-Bromage H, Tempst P, Marks AR. FK506 binding protein associated with the calcium release channel (ryanodine receptor). *J Biol Chem*. 1992;267:9474-9477.
- Brillantes A-MB, Ondrias K, Scott A, Kobrinsky E, Ondriasová E, Moschella MC, Jayaraman T, Landers M, Ehrlich BE, Marks AR. Stabilization of calcium release channel (ryanodine receptor) function by FK506-binding protein. *Cell*. 1994;77:513-523.
- Ahern GP, Junankar PR, Dulhunty AF. Subconductance states in single-channel activity of skeletal muscle ryanodine receptors after removal of FKBP12. *Biophys J*. 1997;72:146-162.
- Marks AR. Intracellular calcium-release channels: regulators of life and death. *Am J Physiol*. 1997;272:H597-H605.
- Valdivia HH. Modulation of intracellular Ca²⁺ levels in the heart by sorcin and FKBP12, two accessory proteins of ryanodine receptors. *Trends Pharmacol Sci*. 1998;19:479-482.
- Marx SO, Ondrias K, Marks AR. Coupled gating between individual skeletal muscle Ca²⁺ release channels (ryanodine receptors). *Science*. 1998;281:818-821.
- Lam E, Martin MM, Timerman AP, Sabers C, Fleischer S, Lukas T, Abraham RT, O'Keefe SJ, O'Neill EA, Wiederrecht GJ. A novel FK506 binding protein can mediate the immunosuppressive effects of FK506 and is associated with the cardiac ryanodine receptor. *J Biol Chem*. 1995;270:26511-26522.
- Timerman AP, Onoue H, Xin H-B, Barg S, Copello J, Wiederrecht G, Fleischer S. Selective binding of FKBP12.6 by the cardiac ryanodine receptor. *J Biol Chem*. 1996;271:20385-20391.
- Xin H-B, Rogers K, Qi Y, Kanematsu T, Fleischer S. Three amino acid residues determine selective binding of FK506-binding protein 12.6 to the cardiac ryanodine receptor. *J Biol Chem*. 1999;274:15315-15319.
- Kaftan E, Marks AR, Ehrlich BE. Effects of rapamycin on ryanodine receptor/Ca²⁺-release channels from cardiac muscle. *Circ Res*. 1996;78:990-997.
- Xiao R-P, Valdivia HH, Bogdanov K, Valdivia C, Lakatta EG, Cheng H. The immunophilin FK506-binding protein modulates Ca²⁺ release channel closure in rat heart. *J Physiol (Lond)*. 1997;500:343-354.
- Barg S, Copello JA, Fleischer S. Different interactions of cardiac and skeletal muscle ryanodine receptors with FK-506 binding protein isoforms. *Am J Physiol*. 1997;272:C1726-C1733.
- Shou W, Aghdasi B, Armstrong DL, Guo Q, Bao S, Charng M-J, Mathews LM, Schneider MD, Hamilton SL, Matzuk MM. Cardiac defects and altered ryanodine receptor function in mice lacking FKBP12. *Nature*. 1998;391:489-492.
- Marx SO, Reiken S, Hisamatsu Y, Jajaraman T, Burkhoff D, Roseblit N, Marks AR. PKA phosphorylation dissociates FKBP12.6 from the calcium release channel (ryanodine receptor): defective regulation in failing hearts. *Cell*. 2000;101:365-376.
- Donahue JK, Kikkawa K, Johns DC, Marbán E, Lawrence JH. Ultrarapid, highly efficient viral gene transfer to the heart. *Proc Natl Acad Sci U S A*. 1997;94:4664-4668.
- Eisner DA, Trafford AW, Diaz ME, Overend CL, O'Neill SC. The control of Ca release from the cardiac sarcoplasmic reticulum: regulation versus autoregulation. *Cardiovasc Res*. 1998;38:589-604.
- Meissner G. Ryanodine receptor/Ca²⁺ release channels and their regulation by endogenous effectors. *Annu Rev Physiol*. 1994;56:485-508.
- Iino S, Cui Y, Galione A, Terrar DA. Actions of cADP-ribose and its antagonists on contraction in guinea-pig isolated ventricular myocytes: influence of temperature. *Circ Res*. 1997;81:875-884.
- Overend CL, O'Neill SC, Eisner DA. The effect of tetracaine on stimulated contractions, sarcoplasmic reticulum Ca²⁺ content and membrane current in isolated rat ventricular myocytes. *J Physiol (Lond)*. 1998;507:759-769.
- Konishi M, Kurihara S, Sakai T. The effects of caffeine on tension development and intracellular calcium transients in rat ventricular muscle. *J Physiol (Lond)*. 1984;355:605-618.
- O'Neill SC, Eisner DA. A mechanism for the effects of caffeine on Ca²⁺ release during diastole and systole in isolated rat ventricular myocytes. *J Physiol (Lond)*. 1990;430:519-536.
- McCall E, Li L, Satoh H, Shannon TR, Blatter LA, Bers DM. Effects of FK-506 on contraction and Ca²⁺ transients in rat cardiac myocytes. *Circ Res*. 1996;79:1110-1121.
- DuBell WH, Wright PA, Lederer WJ, Rogers TB. Effect of immunosuppressant FK506 on excitation contraction coupling and outward K⁺ currents in rat ventricular myocytes. *J Physiol (Lond)*. 1997;501:509-516.
- Schneider M, Schandler W. Voltage dependent charge movement in skeletal muscle: a possible step in excitation-contraction coupling. *Nature*. 1973;242:244-246.
- Yamazawa T, Takeshima H, Sakurai T, Endo M, Iino M. Subtype specificity of the ryanodine receptor for Ca²⁺ signal amplification in excitation-contraction coupling. *EMBO J*. 1996;15:6172-6177.
- Qi Y, Ogunbunmi EM, Freund EA, Timerman AP, Fleischer S. FK-binding protein is associated with the ryanodine receptor of skeletal muscle in vertebrate animals. *J Biol Chem*. 1998;273:34813-34819.

